

UCLA

UCLA Electronic Theses and Dissertations

Title

Applications of Boron in Iridium, Copper, and Nickel Catalysis; Synthesis and Design of Gene-Expression Dependent CO-Releasing Molecules

Permalink

<https://escholarship.org/uc/item/8bb5249p>

Author

Tobolowsky, Robert

Publication Date

2018

Peer reviewed|Thesis/dissertation

UNIVERSITY OF CALIFORNIA

Los Angeles

Applications of Boron in Iridium, Copper, and Nickel Catalysis; Synthesis and Design of Gene-
Expression Dependent CO-Releasing Molecules

A dissertation submitted in partial satisfaction of the
requirements for the degree of Doctor of Philosophy
in Chemistry

by

Robert Tobolowsky

2018

© Copyright by

Robert Tobolowsky

2018

ABSTRACT OF THE DISSERTATION

Applications of Boron in Iridium, Copper, and Nickel Catalysis; Synthesis and Design of Gene-Expression Dependent CO-Releasing Molecules

by

Robert Tobolowsky

Doctor of Philosophy in Chemistry

University of California, Los Angeles, 2018

Professor Craig A. Merlic, Chair

A method is reported for synthesis of synthetically-valuable borylated pyridines via a Lewis acid promoted C-H activation approach. The transformation involves BF_3 or BH_3 Lewis-acid precomplexation followed by Ir-catalyzed borylation. The method's development was guided by computational studies, culminating in the development of a reaction with several advantages over existing methods, including enhanced reactivity, improved regioselectivity, novel formation of trifluoroborate salts and an operationally simple purification procedure. During the reaction discovery process, we also devised a convenient and rapid synthesis of isotopically enriched ^{10}B -pinacolborane, which was used to probe the reaction mechanism.

The synthesis and screening of various π -base ligands for use in a copper-promoted coupling reaction of alcohols and vinyl boronates are also highlighted. While alkenes and alkynes are frequently used as π -bond ligands in transition-metal promoted reactions, allenes have long been underutilized for this purpose despite possessing excellent π -bond donor

characteristics. Several alkynes and allenes were synthesized and tested as π -bond ligands in a copper-mediated oxidative vinyl ether synthesis. Cyclonona-1,2-diene was identified as an ideal allene additive for the reaction.

Next, building upon our previous work on palladium-catalyzed oxidative couplings of vinyl boronates, we describe our efforts towards translating this chemistry to a nickel-catalyzed manifold. Central to the success of this new method was the serendipitous discovery that nitroarenes act as a terminal oxidant for nickel, enabling the synthesis of biaryls and butadienes. To the best of our knowledge, this is the first example of nitroarenes used as oxidants in a nickel-catalyzed coupling reaction.

The final part of this work chronicles the design and synthesis of a new class of carbon-monoxide releasing molecules. While carbon monoxide is a pervasive environmental toxin, it's also an endogenously-produced, essential signaling molecule in all vertebrates. In order to better study the physiological effects of CO, we synthesized molecules which are activated by the presence of genetically programmable β -galactosidase enzyme. This chapter represents an important first step towards the realization of a useful biochemical tool and perhaps even a unique therapeutic compound.

The dissertation of Robert Tobolowsky is approved.

Kendall N. Houk

Jacob J. Schmidt

Craig A. Merlic, Committee Chair

University of California, Los Angeles

2018

TABLE OF CONTENTS

Abstract of Dissertation	ii
List of Schemes.....	viii
List of Tables	xii
List of Figures.....	xiii
Abbreviations.....	xv
Acknowledgements.....	xix
Vita.....	xx
Publications and Presentations.....	xxi
Chapter I. Controlling Reactivity and Selectivity of Iridium-Catalyzed C-H Borylation of Pyridines with Lewis Acids	
1.1. Introduction.....	1
1.2. Review of Aryl Boronate Synthesis and C-H Borylation.....	2
1.3. Review of Methods to Control Regioselectivity in Ir-Catalyzed C-H Borylation Reactions...9	
1.4. Introduction to C-H Borylation of Heterocyclic Lewis Acid-Base Complexes	15
1.5. DFT Calculations Predict a Major Lewis Acid Effect.....	17
1.6. C-H Borylation of Pyridine-BF ₃ and Isolation of Pyridinium Trifluoroborate	20
1.7. Development of H ¹⁰ Bpin Synthesis for Mechanistic Investigation.....	24
1.8. C-H Borylation of Other Heterocycle-BF ₃ Complexes	29
1.9. Investigation of Other Lewis Acids for C-H Borylation	32
1.10. Conclusion	35
1.11. Experimental Procedures	36
1.12. Computational Methods.....	53
1.13. X-Ray Diffraction Analysis for 1-16 and 1-52	54
1.14. References.....	57
1.15. NMR Spectra	62
Chapter II. Synthesis of Alkyne and Allene Ligands for Copper-Promoted Vinyl Ether Synthesis	
2.1. Background and Introduction	91

2.2. Synthesis of Alkyne and Allene Ligands for Copper-Promoted Vinyl Ether Synthesis	95
2.3. Effects of Alkyne and Allene Ligands on Coupling Yield	105
2.4. Conclusion	110
2.5. Experimental Methods	110
2.6. References	129
2.7. NMR Spectra	132

Chapter III. Nickel-Catalyzed Oxidative Coupling of Aryl- and Vinylboronates

3.1. Introduction.....	163
3.2. Initial Screening Results	166
3.3. A Serendipitous Discovery	168
3.4. Optimization of the Nitroarene-Mediated Nickel-Catalyzed Oxidative Coupling of Boronate Esters.....	170
3.5. Reaction Scope.....	173
3.6. Summary and Outlook	177
3.7. Experimental Methods	178
3.8. References	189
3.9 NMR Spectra	192

Chapter IV. Design and Synthesis of a Gene-Expression Dependent CO-Releasing Molecule

4.1. Introduction.....	205
4.2. Nitric Oxide as a Gasotransmitter.....	206
4.3. Hydrogen Sulfide as a Gasotransmitter	209
4.4. Carbon Monoxide as a Gasotransmitter.....	212
4.5. Triggered CO-Releasing Molecules	214
4.6. Enzyme Triggered CO-Releasing Molecules	215
4.7. Designing a Gene Expression-Dependent CO-Releasing Molecule.....	216
4.8. Synthesis of Galactose-Linked Iron-Diene Complexes.....	219
4.9. Progress towards Detection of CO Release	223
4.10. Conclusion	227
4.11. Experimental Methods	228

4.12. References	236
4.13. NMR Spectra	240

Appendix

Computational Data for Figures 1-3 and 1-4	252
--	-----

LIST OF SCHEMES

Chapter I

Scheme 1.1. Examples of enzymatic C-H activation reactions demonstrating exquisite selectivity.	1
Scheme 1.2. Generalized methods for the synthesis of aryl boronate esters.	2
Scheme 1.3. Borylation of toluene via irradiation of iron-boryl complex 1-1	3
Scheme 1.4. Catalytic borylation of benzene with an Ir-boryl complex.	3
Scheme 1.5. Borylation of octane with a Rh-catalyst.	4
Scheme 1.6. Borylation of cumene and anisole revealing steric and electronic effects on regioselectivity.	5
Scheme 1.7. Iridium and bipyridine system gives statistical mixtures of borylated arenes.	6
Scheme 1.8. C-H borylation of various heterocycles in octane.	7
Scheme 1.9. Directed- <i>ortho</i> borylation using an electron-poor phosphine ligand.	10
Scheme 1.10. Silyl-phosphine ligand enabling directed- <i>ortho</i> metalation of aryl ester.	10
Scheme 1.11. Relay-directed <i>ortho</i> metalation using silyl-bearing substrate.	11
Scheme 1.12. Activation of C-H bond <i>ortho</i> to carbamate via proposed outer shell hydrogen bonding.	12
Scheme 1.13. Kanai's <i>meta</i> -selective borylation using a ligand with hydrogen-bonding urea functionality (line 1) and <i>ortho</i> -selective ligand with Lewis acidic boronate functionality (line 2).	13
Scheme 1.14. Bpin as a traceless directing group for the borylation of indole.	14
Scheme 1.15. Bulky Lewis acids direct borylation far from basic functionalities.	14
Scheme 1.16. B ₂ pin ₂ does not form a stable complex with pyridine (line 1), unlike BF ₃ (line 2).	16
Scheme 1.17. Key experiments highlighting the different outcomes of the C-H borylation reaction with pyridine or pyridine-BF ₃ complex.	21
Scheme 1.18. Suzuki Coupling reactions of pyridinium trifluoroborate 1-16	22
Scheme 1.19. Comparison of reactions of 4-pyridyl-Bpin 1-14 and phenyl-Bpin 1-19 with BF ₃ ·OEt ₂	24
Scheme 1.20. Initial synthetic route to HBpin.	25

Scheme 1.21. Alternative routes to HBpin explored by attempting rapid synthesis of useful amine-boranes from tributylborate.	26
Scheme 1.22. Synthesis of HBpin (1-24) and <i>N,N</i> -diethylaniline-borane complex (1-23) by borane gas transfer.	27
Scheme 1.23. Rapid 2-step synthesis of H ¹⁰ Bpin.	28
Scheme 1.24. Isotopically-enriched HBpin gives isotopically-enriched borylation products after the iridium-catalyzed reaction.....	28
Scheme 1.25. Proposed sequence of transformations for the conversion of 1-13 to 1-16	29
Scheme 1.26. Borylation of 2-picoline.	29
Scheme 1.27. Borylation of 3-picoline.	30
Scheme 1.28. Borylation of 1-methylimidazole with and without BF ₃	32
Scheme 1.29. Reaction sequence demonstrating borylation of 1-58 , decomplexation, and Suzuki reaction for net replacement of C-H bond with a biaryl linkage.	34
Scheme 1.30. Borane-promoted borylation of substituted pyridines.....	35

Chapter II

Scheme 2.1. Examples of alkynes used as additives in a Ni- and Cu-catalyzed reaction.	93
Scheme 2.2. Allene additive improves the yield of Ni-catalyzed addition of boronates to α,β -unsaturated carbonyls.....	94
Scheme 2.3. Example of allene-phosphine ligand AllenePhos involved in Rh-catalyzed asymmetric addition of boronic acids to α -keto esters.	95
Scheme 2.4. Serendipitous discovery of vinyl-ether formation during a Pd-catalyzed oxidative coupling of vinyl boronates with a Cu(II) oxidant.....	96
Scheme 2.5. Synthesis of cyclonona-1,2-diene via Skattebøl rearrangement.	99
Scheme 2.6. Synthesis of cyclononyne from cyclonona-1,2-diene via lead(IV) acetate-promoted oxidation and LiAlH ₄ -reduction sequence.....	99
Scheme 2.7. Synthesis of cyclooctyne via bromination-elimination.....	100
Scheme 2.8. Synthesis of 4-methoxycyclonona-1,2-diene via silver-promoted solvolysis and elimination.	101
Scheme 2.9. Lead-promoted transformation of allene 2-2 into 3-methoxycyclonon-1-yne.....	101
Scheme 2.10. Synthesis of 2-7 from 1,2-bis(chlorodimethylsilyl)ethane.....	103
Scheme 2.11. Alkylation of 1,4-butyne diol with methyl iodide.....	103

Scheme 2.12. Failed dibromocyclopropanation of 2-25	104
Scheme 2.13. Reworked synthesis of 2-9 , using a cyclic acetonide to facilitate dibromocyclopropane formation.....	104
Scheme 2.14. Generation of side products during the synthesis of 2-9 in ethereal solvents.....	105
Scheme 2.15. Significant yield improvements observed for <i>n</i> -octanol and 2-propanol with 2-2 ligand.....	108

Chapter III

Scheme 3.1. One of the first examples of a transition-metal catalyzed cross-coupling reaction, reported by Corriu in 1972.....	163
Scheme 3.2. Our group has developed both palladium (line 1) and nickel (line 2) catalyzed oxidative coupling reactions of vinyl boronates.	164
Scheme 3.3. Depiction of the outcomes of intermolecular (homocoupling) vs. intramolecular (ring closure) oxidative coupling reactions.....	165
Scheme 3.4. Liu's reported conditions for Ni-catalyzed homocoupling of aryl boronic acids in refluxing pyridine.....	167
Scheme 3.5. Serendipitous discovery of conditions for oxidative coupling of vinyl boronates with Ni-catalysis.	168
Scheme 3.6. Reaction of 3-13 under nickel (top) and palladium (bottom) conditions.	174

Chapter IV

Scheme 4.1. Oxidation of L-arginine to L-citrulline and NO by NOS.....	207
Scheme 4.2. NO-mediated signaling pathway depicting role of sildenafil for the treatment of sexual dysfunction in men.	208
Scheme 4.3. Biosynthesis of H ₂ S by the action of CAT and MPST on cysteine.	209
Scheme 4.4. Release of H ₂ S via reduction of diallyl disulfide by glutathione.	210
Scheme 4.5. Photocaged <i>gem</i> -dithiol (4-5) as H ₂ S-releasing compound.	211
Scheme 4.6. Mechanism of H ₂ S release from pronucleophilic ester/thiocarboxylate 4-6 upon hydrolysis by esterase enzyme.....	212
Scheme 4.7. Mechanism of CO-release by ET-CORMs.	215
Scheme 4.8. Control experiment demonstrating that CO release is enzyme-dependent.	216
Scheme 4.9. Planned synthesis of gene expression dependent CO-releasing molecules 4-17 and 4-18	219
Scheme 4.10. Synthesis of 4-16 starting from cyclohexenone.	219

Scheme 4.11. Full synthesis of gene expression-dependent CO-releasing molecules.	223
Scheme 4.12. Chang and Coworker's Pd-Based Probe for CO.....	225

LIST OF TABLES

Chapter I

Table 1.1. Yield of 1-16 with various changes to the reaction conditions.	23
Table 1.2. Unsuitable BF ₃ complexes for Ir-catalyzed C-H borylation.	31
Table 1.3. Screen of alternative Lewis acid complexes.	33

Chapter II

Table 2.1. Binding affinities of various alkenes with a Ni-complex.	92
Table 2.2. Alcohol substrate screen in copper-promoted vinyl ether synthesis.	97
Table 2.3. Optimization of Grubb's metathesis conditions for the synthesis of 2-21	102
Table 2.4. Alkyne ligand performance in a Cu-promoted vinyl ether synthesis.	106
Table 2.5. Allene ligand performance in a Cu-promoted vinyl ether synthesis.	107

Chapter III

Table 3.1. Initial screening results.	166
Table 3.2. Selected variations on Liu's conditions to minimize pyridine solvent requirements.	167
Table 3.3. Ligand screening results.	171
Table 3.4. Concentration study results.	171
Table 3.5. Effect of added PPh ₃ on coupling yield.	173
Table 3.6. Vinyl boronate substrate scope.	175
Table 3.7. Aryl boronic acid and ester screening results.	176
Table 3.8. Aryl boronate substrate scope.	177

Chapter IV

Table 4.1. Glycosylation of phenol as a test reaction.	220
Table 4.2. Optimization of deprotection/glycosylation sequence.	221

LIST OF FIGURES

Chapter I

- Figure 1.1. Proposed catalytic cycle for the borylation of benzene with an Ir-catalyst.....8
- Figure 1.2. Selected examples of Ir-catalyzed borylation regioselectivity demonstrating no clear trend.15
- Figure 1.3. Free energy profile for Ir-catalyzed borylation of pyridine. Structures for borylation at the meta-position of pyridine are shown. Energy levels for *ortho*-, *meta*- and *para*-activation are denoted by red, blue and green lines, respectively.18
- Figure 1.4. Free energy profile for Ir-borylation of pyridine-BF₃. Structures for borylation at the meta-position of pyridine are shown. Results for *ortho*-, *meta*- and *para*-activation are denoted by red, blue and green lines, respectively.19
- Figure 1.5. Crystal structure of **1-16** obtained by X-ray diffraction analysis.22

Chapter II

- Figure 2.1. Structure of Zeise's salt, first prepared in 1827.91
- Figure 2.2. Synthetic overview of ligand syntheses indicating step count.98
- Figure 2.3. Proposed mechanism of Cu-promoted vinyl ether synthesis.109

Chapter III

- Figure 3.1. Comparison of cross coupling (left) and oxidative coupling (right) mechanisms. ...165
- Figure 3.2. Mechanism accounting for formation of triphenylphosphine oxide and azoxybenzene when a nickel(0) source reacts with nitrobenzene.174

Chapter IV

- Figure 4.1. Schematic representing the differences between traditional signal transmission involving small molecules (top) versus enzymatic gasotransmitter production and delivery (bottom).206
- Figure 4.2. Organic nitrites/nitrates with vasodilatory effects.....208
- Figure 4.3. Structure of Flu-DNB, a photoactivated NO-releasing compound.209
- Figure 4.4. DTT-modified ibuprofen, an example of an H₂S prodrug that exhibits improved pharmacological properties.210
- Figure 4.5. Mechanism of endogenous CO production by oxidation of heme by heme oxygenase (HO-1).....213
- Figure 4.6. Structure of CORM-3.214

Figure 4.7. Examples of pH, oxidation, and light triggered CORMs.	214
Figure 4.8. Gene-expression dependent CO-releasing molecule can be used to target specific cells with CO.....	217
Figure 4.9. LacZ reporter gene could be used alongside a galactosidase activated CORM to selectively dose transgenic colonies with CO.....	218
Figure 4.10. UV-VIS spectra of myoglobin before and after addition of β -galactosidase and diastereomer 1 of 4-17/4-18	219

ABBREVIATIONS

~	Approximately
o	Degree
*	Star
α	Alpha
β	Beta
δ	Delta
η	Eta
μ	Micro
π	Pi
σ	Sigma
ω	Omega
Ac	Acetyl
ATR	Attenuated total reflection
aq	Aqueous
Ar	Any aryl
atm	Atmosphere
b	Broadened
Bn	Benzyl
Boc	<i>tert</i> -Butyloxycarbonyl
Bu	Butyl
C	Celsius
cal	Calorie
cm ⁻¹	Inverse centimeters
CO	Carbon Monoxide
CORM	CO-Releasing Molecule
CTAB	Cetyltrimethylammonium bromide
Cy	Cyclohexyl
d	Doublet
DA	Diels-Alder
DCE	1,2-Dichloroethane

DCM	Dichloromethane
DEG	Diethylene glycol
DFT	Density functional theory
DMAP	4-Dimethylamino pyridine
DMF	<i>N,N</i> -Dimethylformamide
DMSO	Dimethyl sulfoxide
DoM	Directed- <i>ortho</i> metallation
dppb	1,3-Bis(diphenylphosphino)butane
dppe	1,3-Bis(diphenylphosphino)ethane
dppp	1,3-Bis(diphenylphosphino)propane
<i>dr</i>	Diastereomeric ratio
dtbpy	4,4'-di- <i>tert</i> -butyl-2,2'-bipyridine
<i>E</i>	Entgegen
E ₂	Bimolecular elimination
<i>ee</i>	Enantiomeric excess
eg	Ethylene glycol
equiv	Equivalents
Et	Ethyl
Et ₂ O	Diethyl Ether
EtOAc	Ethyl Acetate
EtOH	Ethanol
FG	Functional group
g	Gram
<i>gem</i>	Geminal
Grubbs 1	Grubbs' first generation catalyst
Grubbs 2	Grubbs' second generation catalyst
h	Hour
HMPA	Hexamethylphosphoramide
HRMS	High resolution mass spectroscopy
HO	Heme oxygenase
hν	Light

Hz	Hertz
<i>i</i>	Iso
IR	Infrared
J	joule
kcal	Kilocalorie
L	Ligand
LAH	Lithium aluminum hydride
<i>m</i>	meta
m	Milli
M	Molar
Me	Methyl
MeOH	Methanol
MHz	Megahertz
mol	Mole
mmol	Millimole
Ms	Mesyl
<i>n</i>	Normal
NMR	Nuclear magnetic resonance
<i>o</i>	Ortho
Ox	Oxidant
<i>p</i>	Para
p	Pentet
Ph	Phenyl
pin	Pinacol
ppm	Parts per million
Pr	Propyl
q	Quartet
R	Any alkyl group
<i>R</i>	Rectus
rt	Room temperature
s	Singlet

<i>S</i>	Sinister
S_N2	Bimolecular substitution
<i>t</i>	Triplet
TADA	Transannular Diels-Alder
TBAB	Tetrabutylammonium bromide
TBAF	Tetrabutylammonium fluoride
TBDPS	<i>tert</i> -Butyldiphenylsilyl
TBS	<i>tert</i> -Butyldimethylsilyl
Tf	Triflate
TFA	Trifluoroacetic acid
THF	Tetrahydrofuran
TIPS	Triisopropylsilyl
TLC	Thin layer chromatography
Tol	Tolyl
Ts	Tosyl
UV	Ultraviolet
<i>vic</i>	Vicinal
<i>Z</i>	Zusammen

ACKNOWLEDGEMENTS

First and foremost, I would like to thank my research advisor, Professor Craig Merlic. From the outset, it was clear that his unmatched intellect and perhaps harsh wit would no doubt be conducive to my development as an organic chemist and scientist. Thank you, Craig, for always keeping your door open.

I also wish to acknowledge the helpful conversations with all my coworkers in the Merlic group. A special thanks to Byron Boon, Brett Cory, Tioga Martin, and Aaron Green for your assistance in my research endeavors and your friendship.

If I had to trace the spark that ignited my passion for organic chemistry, I'd need to acknowledge Professor Suzanne Blum at UC Irvine who challenged and inspired me during my undergraduate years. Without your guidance and teaching, I never would have achieved this degree.

I would also like to thank the NIH/CBI Fellowship and the UCLA Graduate Division for the financial support I received during my degree. Also, a big thank you to Professor Heather Maynard, director of the CBI program, who was a great mentor and from whom I learned so much.

This thesis would not be possible without the editing and critique of my committee; thank you very much Professor Ken Houk and Professor Bill Gelbart for taking the time out of your busy schedule to attend my oral examination and to read this thesis.

Lastly, I am forever grateful and indebted to the ceaseless support from my family: Ann, Stephen, Barbie, and William. There's no chance I could have done this without you.

VITA

- 2011
B.A., Chemistry
University of California, Irvine
Irvine, CA
- 2013
M.S., Chemistry
University of California, Los Angeles
Los Angeles, CA
- 2011-2012
Teaching Assistant
University of California, Los Angeles
- 2012-2015
Chemistry-Biology Interface Training Grant Awardee
University of California, Los Angeles
- 2015-2018
Teaching Fellow
University of California, Los Angeles

PUBLICATIONS AND PRESENTATIONS

Tobolowsky, Robert A.; Green, Aaron G.; Merlic, Craig A. 248th ACS National Meeting & Exposition, San Francisco, CA, United States, August 10-14, 2014.

Tobolowsky, Robert A.; Green, Aaron; Merlic, Craig A. 251st ACS National Meeting & Exposition, San Diego, CA, United States, March 13-17, 2016.

Nickel-Catalyzed Oxidative Coupling of Aryl and Vinyl-Boronates in the Presence of Nitrobenzene. Tobolowsky, R.A.; Merlic, C.A. In preparation.

Boron-Based Lewis Acids Control Reactivity and Selectivity in Iridium-Catalyzed Heteroarene Borylation Reactions. Tobolowsky, R.A.; Green, A.G.; Merlic, C.A. *Org Lett*. Manuscript in preparation.

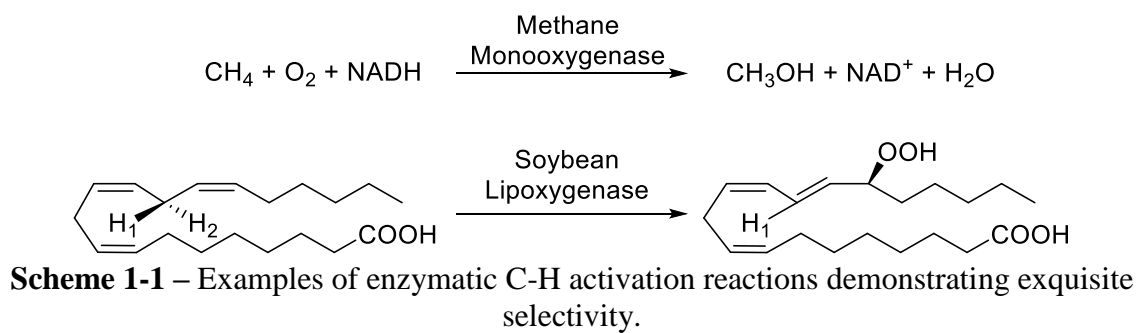
Synthesis and Design of Gene Expression-Dependent CO-Releasing Molecules. Tobolowsky, R.A.; Teuthorn, A.; Merlic, C.A. In preparation.

Allenes as π -Ligands for Copper-Promoted Synthesis of Vinyl Ethers. Martin, T.J.; Cory, B.H.; Tobolowsky, R. A.; Korch, K. M.; Merlic, C.A. *Org Lett*. **2018** Submitted.

Chapter I – Controlling Reactivity and Selectivity of Iridium-Catalyzed C-H Borylation of Pyridines with Lewis Acids

1.1 – Introduction

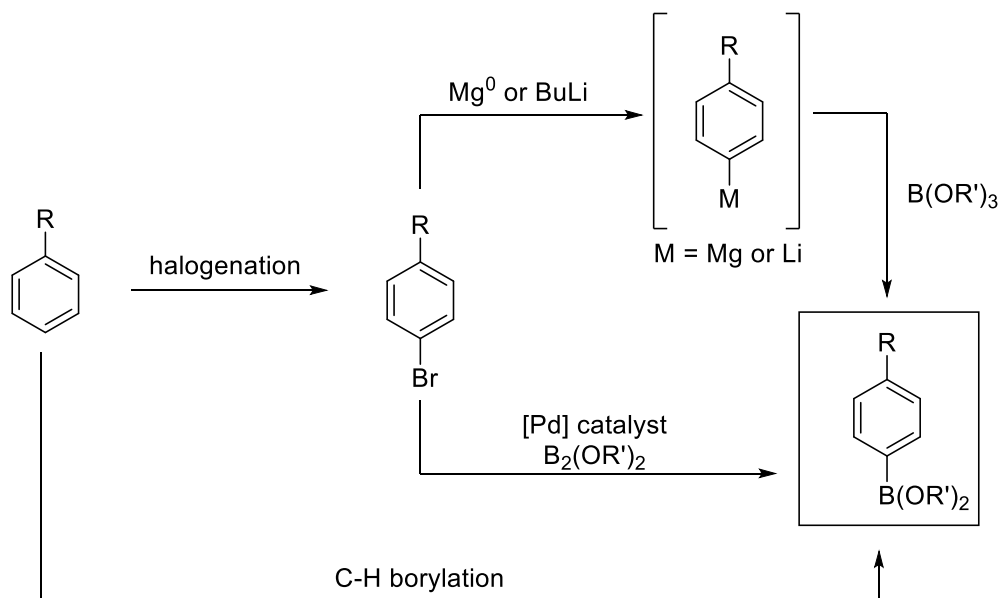
Selective cleavage and replacement of the ubiquitous carbon-hydrogen bond with new functionality has been described as a holy grail of organic chemistry.¹ Given this class of reactions' inherent high efficiency and atom economy, it's not surprising that natural enzymes have evolved to use C-H activation to perform remarkable feats of selective bond formation. For example, methane monooxygenase² is capable of oxidizing methane to methanol by replacing a single methyl C-H bond with an C-O bond. Soybean lipoxygenase³ activates a C-H bond with incredible regio- and stereochemical control to oxidize a fatty acid (Scheme 1-1).



Although Mother Nature leverages the well-defined geometry of enzyme active sites to pinpoint reactivity, this level of control is usually impossible for the organic chemist. A persistent challenge of C-H activations is controlling regioselectivity when multiple chemically similar C-H bonds exist in a substrate.⁴ In this chapter, I provide a review of an important type of C-H activation, the C-H borylation of arenes. Next, I discuss the methods and strategies used to control regioselectivity in this reaction. Finally, I describe my endeavor to improve the regioselectivity of the reaction using Lewis-acid additives.

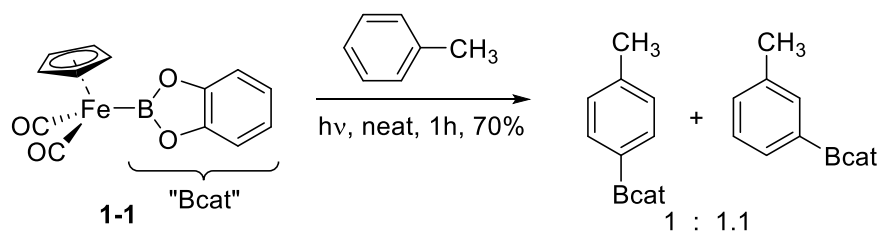
1.2 – Review of Aryl Boronate Synthesis and C-H Borylation

Organoboranes are versatile molecules that can be used as nucleophiles in Suzuki-type cross coupling reactions⁵ or converted into countless other functional groups, including alcohols,⁶ amines,^{7–10} ethers,^{11,12} ketones,¹³ halides,¹⁴ or azides.¹⁵ This “wild card” character of organoboranes makes them useful in organic synthesis, since a single organoboron compound can be transformed into a diverse array of products. Aryl boronate esters, prized for their stability and ease of purification, are traditionally made via one of two methods. In the first method, an aryl halide is metallated with either lithium or magnesium, then trapped with an electrophilic boron source such as trimethylborate or isopropyl pinacolborate (PinBOP).¹⁶ In the second method, aryl halides are reacted with palladium and a diboron compound such as bis(pinacolato)diboron (B_2pin_2) to furnish boronate esters.¹⁷ Transition-metal catalyzed C-H borylation represents an important evolution of these stalwart reactions: it allows for direct and mild installation of boron, without the need for prefunctionalization to the organohalide (Scheme 1-2).



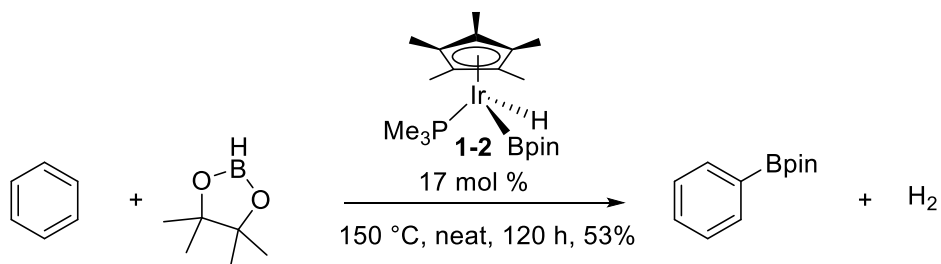
Scheme 1-2 – Generalized methods for the synthesis of aryl boronate esters.

The history of the C-H borylation reaction chronicles the transformation of an organometallic curiosity into a powerful synthetic method. In 1995, Hartwig et al. reported that irradiation of boryl-metal carbonyl complexes (M = Fe, Re, Mn) provided borylated hydrocarbons in good yield.¹⁸ For example, toluene could be borylated using the iron complex **1-1** to furnish a mixture of 3- and 4-boryl isomers (Scheme 1-3). This result underscores several key shortcomings with early C-H borylation reactions that would be solved in the decade to follow. First, the reaction required a stoichiometric amount of the organometallic reagent. Second, the transformation was restricted to simple hydrocarbons, such as benzene, toluene, or hexene. Finally, the reaction was performed neat with excess substrate, precluding the borylation of exotic or expensive molecules via this method.



Scheme 1-3 – Borylation of toluene via irradiation of iron-boryl complex **1-1**.

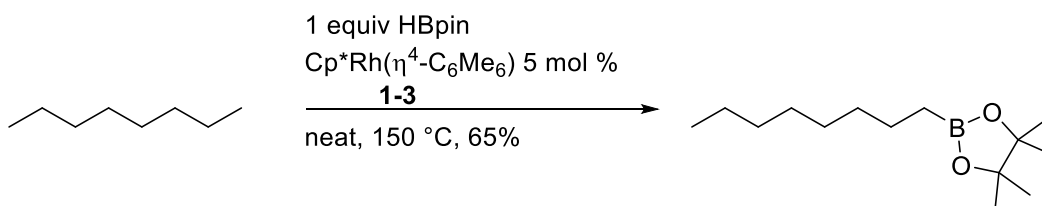
Major progress in the field was reported by Smith et al. in 1999, with the discovery that *catalytic* C-H borylation was possible using iridium.¹⁹



Scheme 1-4 – Catalytic borylation of benzene with an Ir-boryl complex.

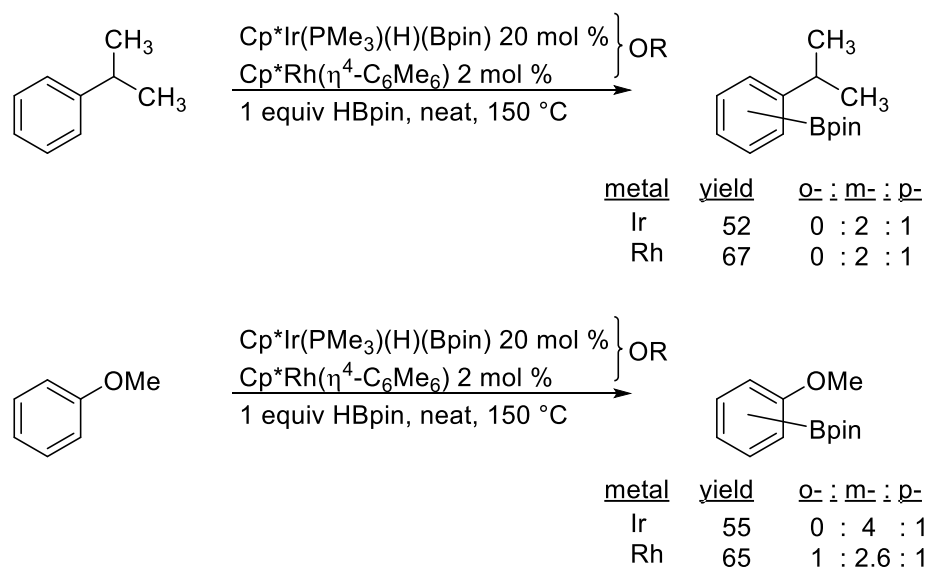
The Cp*Ir(PMe₃)(H)(Bpin) catalyst (**1-2**), prepared by reaction of Cp*Ir(PMe₃)(H)(Ph) and HBpin, was found to borylate benzene (solvent) in 53% yield with 17 mol % catalyst loading

(Scheme 1-4). Although the high metal loading and requirement to run the reaction neat wasn't ideal, achieving a catalytic system was a critical milestone towards practicality. Iridium wasn't the only metal investigated for catalytic C-H borylation: In 2000, Hartwig et al. reported a highly active rhodium catalyst **1-3** for the borylation of alkanes (Scheme 1-5).²⁰



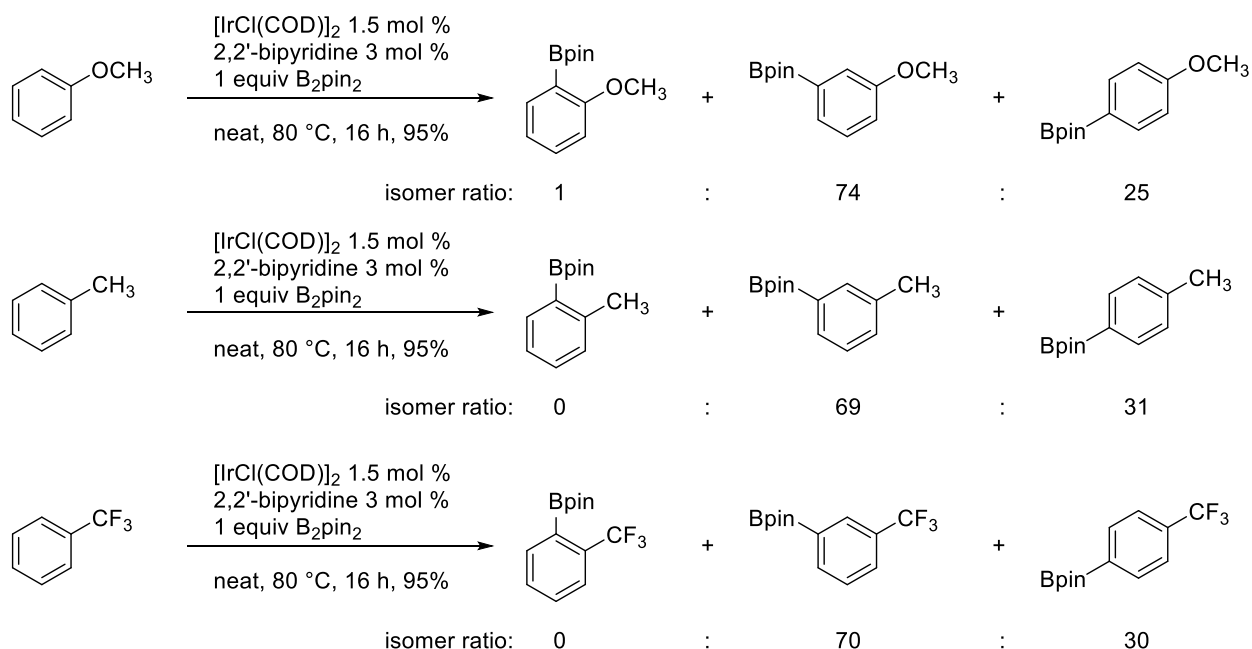
Scheme 1-5 – Borylation of octane with a Rh-catalyst.

Although **1-3** would prove not to be very popular for arene borylation, Smith investigated it alongside an iridium catalyst (**1-2**) in such a reaction.²¹ This report marks the beginning of investigations into the regioselectivity of C-H borylations. Smith found the reaction of cumene to be sterically controlled, with no *ortho* borylation but statistical amounts (2:1) of *meta* and *para* borylation. However, anisole exhibited an increased preference for *meta* borylation, suggesting electronic factors played at least some role in the regiochemical outcome (Scheme 1-6).



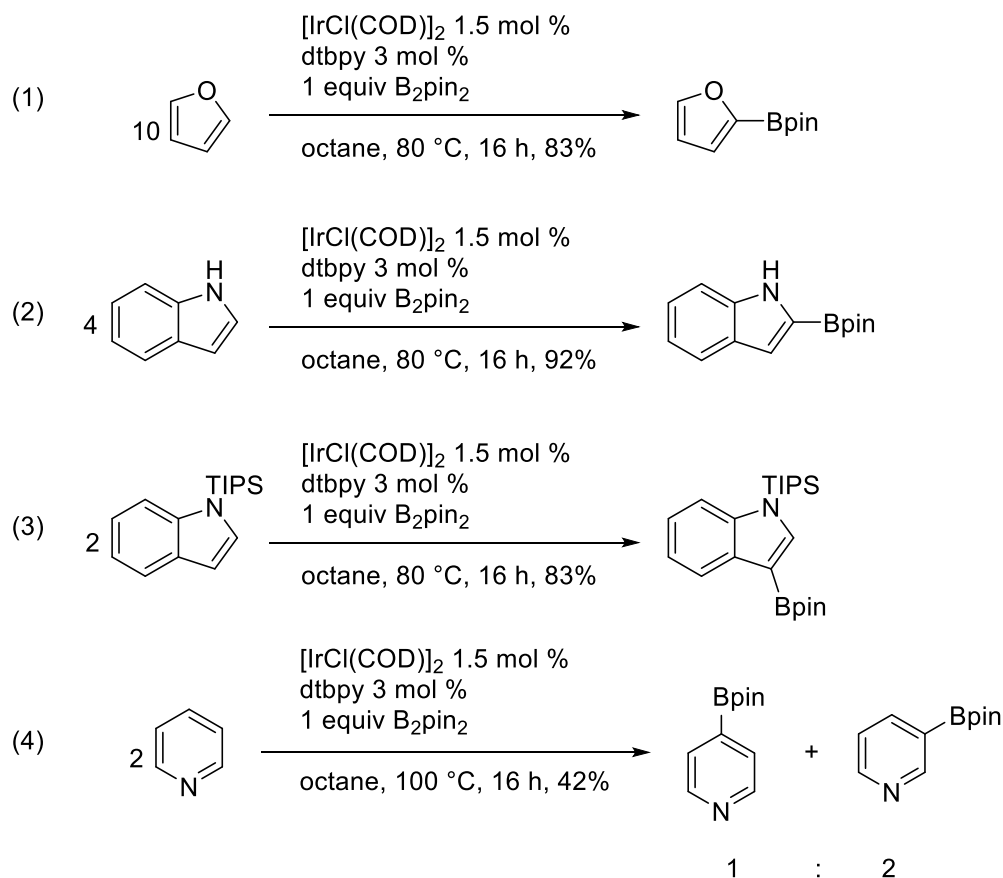
Scheme 1-6 –Borylation of cumene and anisole revealing steric and electronic effects on regioselectivity.

In 2001, the Hartwig and Miyaura groups identified the highly competent $[\text{IrCl}(\text{COD})]_2$ precatalyst with a 2,2'-bipyridyl ligand system, which allowed for catalyst loadings as low as 3 mol % iridium and borylation yields as high as 95%.²² This report provides another glimpse into C-H borylation regiochemistry. For example, anisole gave three borylated products: *ortho*, *meta*, and *para* in a 1:74:25 ratio. Similar product distributions were observed for toluene and benzotrifluoride as shown in Scheme 1-7. The authors commented that the lack of *ortho* borylation was likely due to steric effects of the substituents, while the essentially statistical selectivity of *meta* and *para* positions in both electron-rich and electron-poor arenes suggested regiochemistry was only marginally influenced by electronic factors. Furthermore, this paper marks the first isolation and characterization of the active tris-boryl iridium catalyst that is generated by the reaction of $[\text{IrCl}(\text{COD})]_2$ with B_2pin_2 (See Figure 1-1, B for structure).



Scheme 1-7 – Iridium and bipyridine system gives statistical mixtures of borylated arenes.

In 2002, the same groups described C-H borylation of heterocycles in octane using $[\text{IrCl}(\text{COD})]_2$ with bulkier 4,4'-di-*tert*-butyl-2,2'-bipyridine (dtbpy) as ligand.²³ The heterocycles tested included thiophene, furan, pyrrole, indole, pyridine, and quinoline, as shown in Scheme 1-8. While previous C-H borylation reactions were typically conducted neat, octane solvent was critical to prevent coordinative-saturation of the iridium complex by the nucleophilic heterocyclic substrates. In nearly all cases, the reaction exhibited very good regioselectivity for the 2-position, which was suggested to be a consequence of a more acidic C-H bond rather than the steric argument usually invoked. However, the authors noted that a silyl-protected indole was borylated at the 3-position instead, which they did ascribe to a steric effect (Scheme 1-8, line 3). Pyridine was a notable outlier and poorly performing substrate, giving a mixture of mono- and diboryl pyridine isomers in low yield (Scheme 1-8, line 4). Interestingly, 2-boryl pyridine isomers were completely absent.



Scheme 1-8 – C-H borylation of various heterocycles in octane.

Following a computational study by Sakaki,²⁴ a corroborating experimental kinetic and mechanistic study of the Ir-catalyzed C-H borylation was conducted by the Hartwig group in 2005. The investigation into the active catalytic species was performed using variable temperature NMR alongside isotope labelling studies. In addition to proposing a mechanism, the authors also determined that $[\text{IrCl}(\text{COD})]_2$ led to the formation of ClBpin, which formed problematic insoluble adducts with the dtbpy ligand. This problem could be solved by using $[\text{Ir}(\text{OMe})(\text{COE})_2]_2$. The experimental and computational work of Hartwig and Sakaki led to the proposal of the reaction mechanism shown in Figure 1-1.

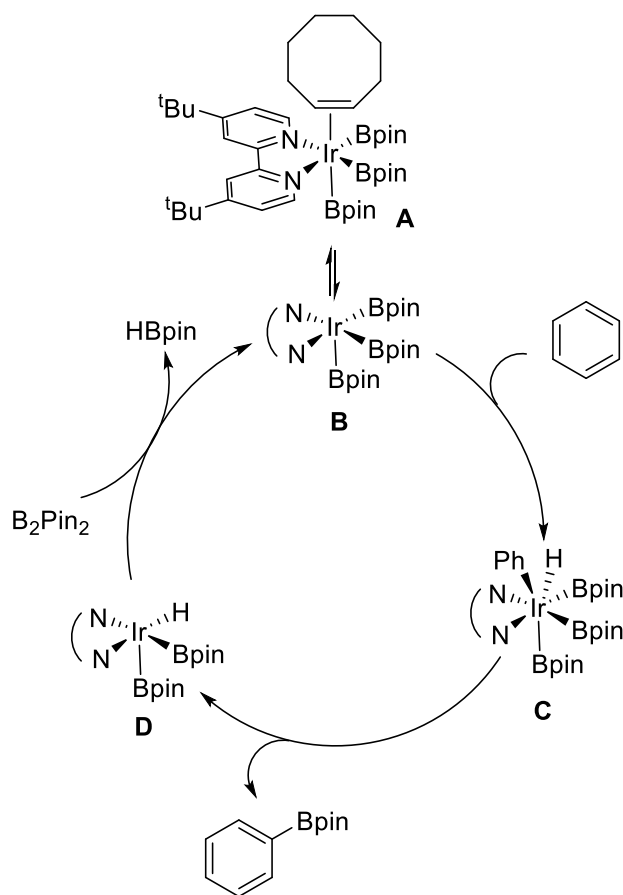


Figure 1-1 – Proposed catalytic cycle for the borylation of benzene with an Ir-catalyst.

The mechanism begins with generation of the trisboryl iridium complex **A** from the $[\text{Ir}(\text{OMe})(\text{COE})_2]_2$ precatalyst and B_2pin_2 . Dissociation of the COE ligand to give **B** opens a coordination site allowing for sigma C-H bond activation to give Ir(V) complex **C**. Reductive elimination produces the borylated arene and Ir(III) hydride **D**, which transmetalates with B_2Pin_2 to complete the cycle and generate an equivalent of HBpin. It's known that HBpin can also enter the catalytic cycle reacting with **D** to generate **B** and H_2 , which can sometimes lead to yields greater than 100% relative to the B_2pin_2 stoichiometry.

Over the next decade, the Ishiyama-Miyaura-Hartwig (IMH) $[\text{Ir}(\text{OMe})(\text{COD})]_2$ catalyst with dtbpy ligand would become the gold standard for the C-H borylation reaction. Although this

chapter focuses on Ir-catalyzed C-H borylation, related reactions have been achieved with iron,¹⁸ rhodium,^{20,25,26} cobalt,²⁷ nickel,²⁸ and platinum,²⁹ in addition to transition-metal free organocatalyzed methods.³⁰ While all the references mentioned thus far take an undirected approach to C-H activation, there has been considerable progress in the field of directed, regioselective C-H borylation.

1.3 -- Review of Methods to Control Regioselectivity in Ir-Catalyzed C-H Borylation Reactions

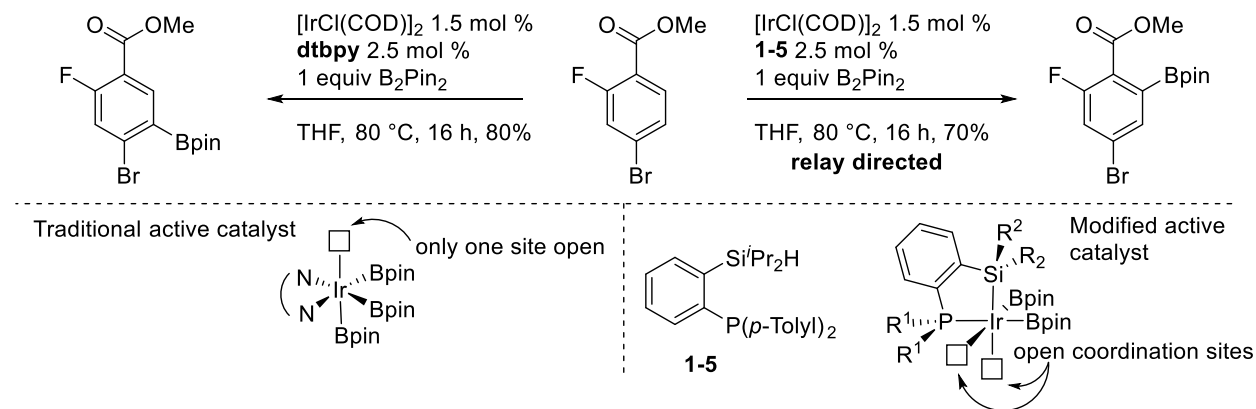
Unlocking the incredible potential of a site-specific C-H borylation has been of great interest in the synthetic community. As discussed previously, many substrates have innate selectivity based on electronic or steric factors. However, directed methods exist that can improve or overpower these native preferences, as well as increase the local concentration of the catalyst and facilitate bond cleavage of C-H bonds that are normally unreactive. One common strategy of this type is directed ortho-metalation (DoM), whereby the borylation catalyst is guided to a C-H bond vicinal to a heteroatom.^{31,32} With respect to the scope of directing groups, esters, ketones, amines, carbonates, carbamates, and sulfonates have been used. One complication with this method is that the coordinatively-saturated active iridium catalyst, [Ir(dtbpv)(Bpin)₃], is found to be only weakly susceptible to chelation by basic functionality. This problem has been addressed by changing the ligands. For example, the very electron poor P[3,5-(CF₃)₂C₆H₃]₃ ligand in conjunction with the IMH catalyst enables good *ortho* selectivity as shown in Scheme 1-9.³³



Scheme 1-9 – Directed-*ortho* borylation using an electron-poor phosphine ligand.

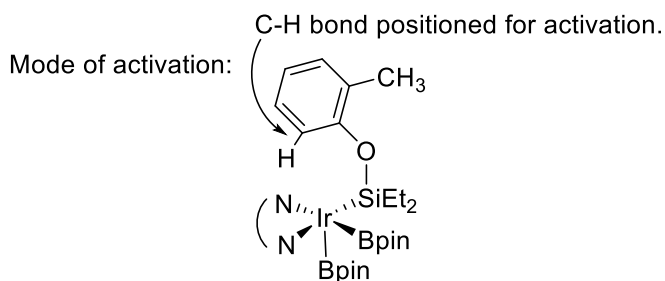
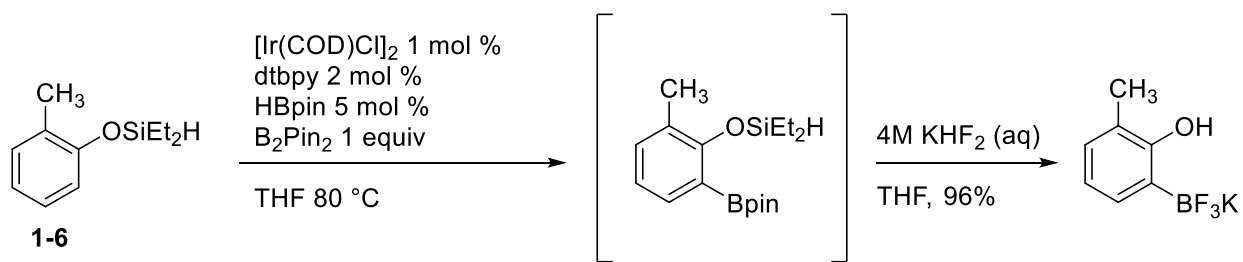
In the same vein, a weakly binding and hemilabile bidentate hydrazone ligand in place of dtbpy was also reported to enable borylation *ortho* to a 2-pyridyl directing group.³⁴

Relay-directed metalation entails replacing one of the boryl groups of the trisboryl iridium catalyst with silicon. Smith et al. reported the use of an aryl phosphine ligand bearing a 2-silyl substituent (**1-5**).³⁵ The phosphine binds the iridium as an L-type ligand, while the silyl group transmetalates with a boryl ligand to form an X-type covalent linkage. The result is two vacant coordination sites on Ir allowing for *ortho* borylation of arenes with a variety of directing groups. The effect is quite dramatic: As shown in Scheme 1-10, the ester-directed reaction conducted with ligand **1-5** has a completely different regiochemical outcome than the reaction conducted with IMH catalyst and dtbpy ligand.



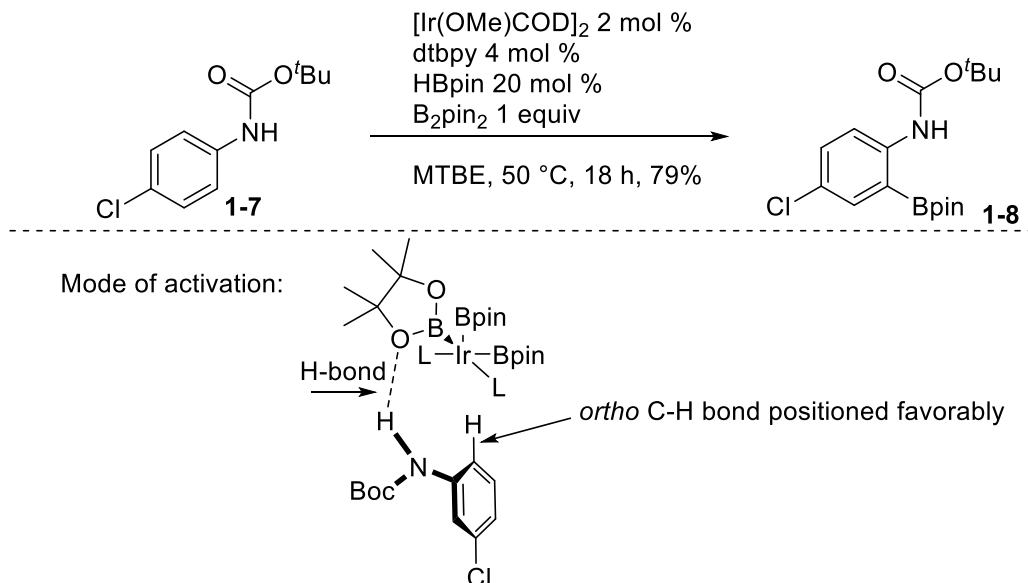
Scheme 1-10 – Silyl-phosphine ligand enabling directed-*ortho* metalation of aryl ester.

In a conceptually similar approach, a silyloxy-directing group on the substrate (**1-6**) (rather than ligand) can undergo transmetalation with a boryl group on the catalyst and thus accomplish both the necessary open coordination site and proper positioning of the *ortho* C-H bond (Scheme 1-11).³⁶ However, these DoM strategies do have drawbacks: (1) The directing functionality must be laboriously installed and removed, (2) selectivity is exclusively *ortho*, and (3) in some cases, excess of the arene is necessary to prevent di-*ortho* borylation.



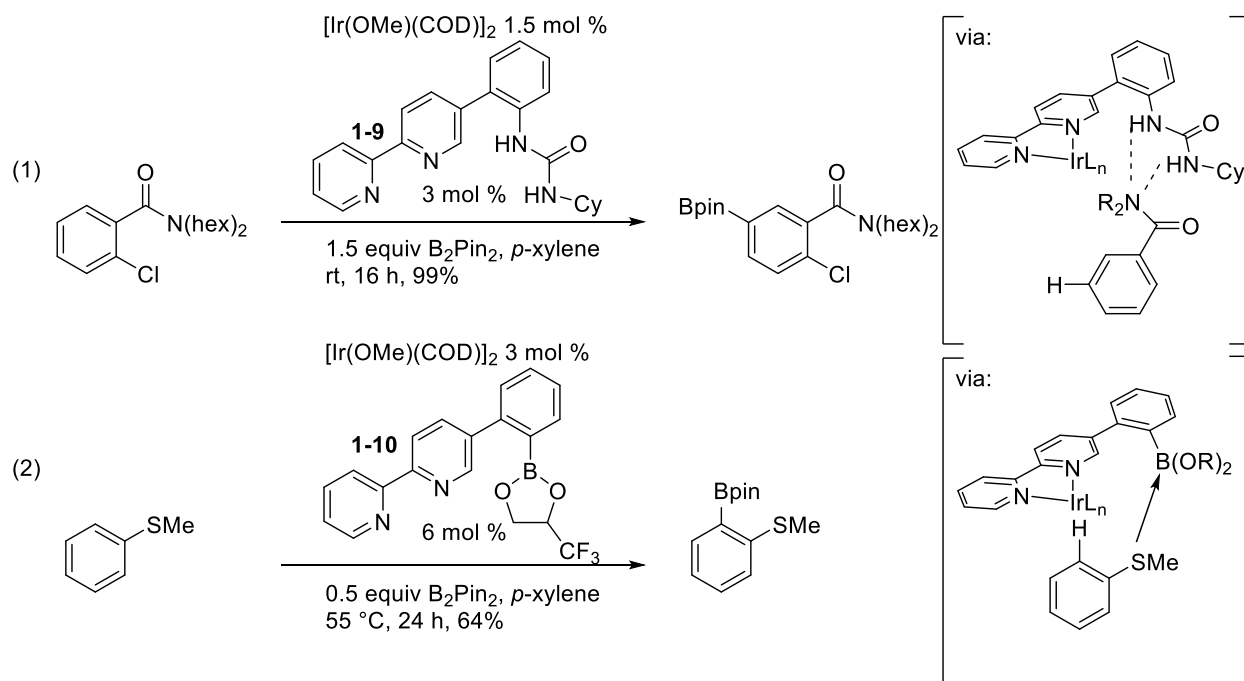
Scheme 1-11 – Relay-directed *ortho* metalation using silyl-bearing substrate.

A distinct DoM-like strategy sidesteps the issue of coordinative-saturation of the iridium entirely by capitalizing on outer sphere interactions instead. Singleton, Maleczka, and Smith demonstrated that *Boc*-protected aryl amines such as **1-7** could participate in hydrogen bonding with the boryl ligands on iridium, thereby activating the *ortho* position to give **1-8** as shown in Scheme 1-12.³⁷

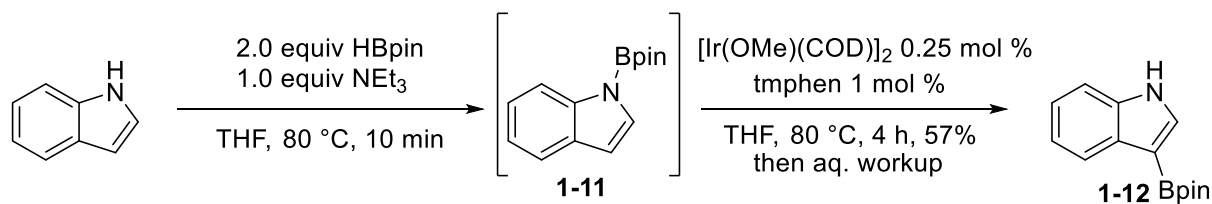


Scheme 1-12 – Activation of C-H bond *ortho* to carbamate via proposed outer shell hydrogen bonding.

Likewise, modification of the bipyridine scaffold could be used to direct the catalyst via ligand-substrate secondary interactions. The Kanai group developed a system that uses a bipyridyl ligand with a pendant urea moiety (**1-9**).³⁸ This design results in organizing hydrogen bond interactions between the metal-bound ligand and aromatic amides, esters, phosphonates, phosphonic diamide or phosphine oxides present in substrates to give preferentially *meta* borylation products (Scheme 1-13, line 1). In a subsequent report, the Kanai group developed a ligand with a pendant Lewis acidic boronate (**1-10**) which participated in a secondary Lewis acid-base interaction with the sulfur atom of thioanisole to direct borylation to the *ortho* position (Scheme 1-13, line 2).³⁹

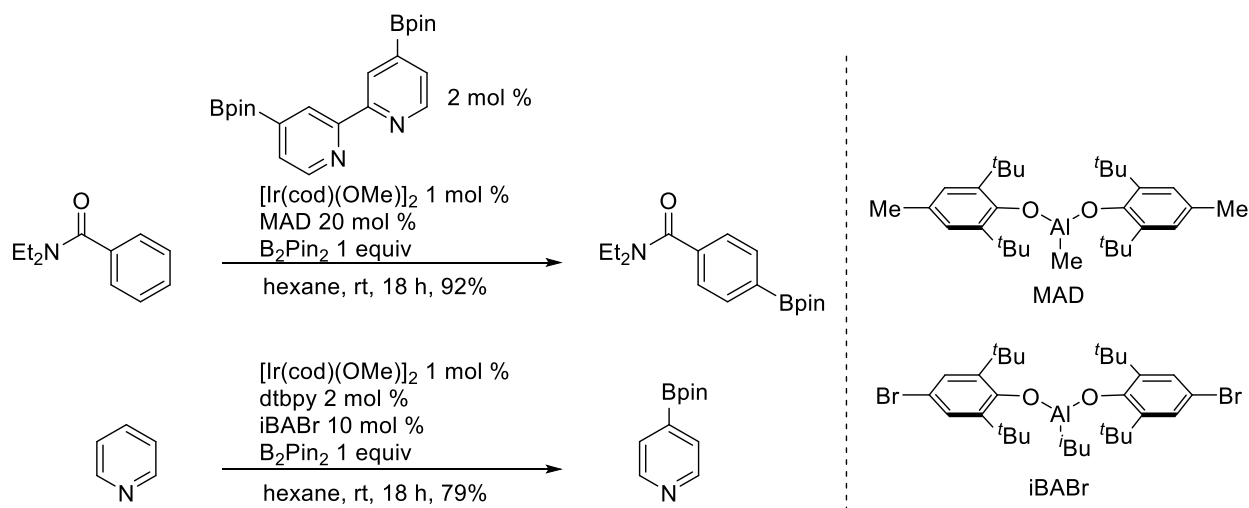


Because C-H borylations are very sensitive to the steric environment, installing large blocking groups that temporarily bulk up the substrate is an effective strategy for controlling regioselectivity. As previously mentioned, a silyl protected indole exhibited preference for 3-borylation rather than 2-borylation observed for the parent indole (Scheme 1-8, line 3). Later, *Boc* groups were also shown to be effective for this purpose.⁴⁰ A more subtle method developed by Maleczka and Smith used Bpin as a traceless directing group to accomplish this goal.⁴¹ As shown in Scheme 1-14, aryl amines and indoles were found to react with HBpin when tertiary amines were present to form a bulky N-Bpin complex (**1-11**) that was borylated at sites distal to nitrogen to give product **1-12**. The entire protection-borylation-deprotection process took place in a single pot, with the only differences from the standard borylation protocol being addition of a tertiary amine and an aqueous workup to hydrolyze the azaborate product.



Scheme 1-14 – Bpin as a traceless directing group for the borylation of indole.

A 2017 report by Nakao et al. describes addition of a catalytic amount of an extremely bulky aluminum Lewis acid that sterically modulates arenes with Lewis basic functions.⁴² As shown in Scheme 1-15, MAD promoted the selective *para*-borylation of *N,N*-diethylbenzamide, while iBABr promoted the 4-borylation of pyridine.



Scheme 1-15 – Bulky Lewis acids direct borylation far from basic functionalities.

In this brief review, it should be apparent that there is a great deal of interest in perfecting the C-H borylation of arenes. While once a reaction at the mercy of its innate selectivity, iridium-catalyzed C-H borylation is now bolstered by various methods that direct the activation of specific bonds. Strategies to guide regioselectivity have included directed *ortho*-metallation, templating secondary interactions between substrate and ligand, and modulation of substrates' steric demands. Despite all these advancements, there still exist challenges. For example, late

stage functionalization of complex molecules using C-H borylation is a method still in its infancy, with the potential to enable efficient syntheses of complex natural products and drugs.⁴³ Thus, future work should aim to identify conditions that allow universal directed C-H borylation with more directing functionalities (particularly those relevant to pharmaceuticals and natural products) and exhibit delicate and tunable selectivity when multiple potential directing groups are present.

1.4 – Introduction to C-H Borylation of Heterocyclic Lewis Acid-Base Complexes

Our group began investigating the mechanism of iridium-catalyzed C-H borylation because we found the regioselectivity differences between pyridine and other heterocycles puzzling. For example, while pyridine gave a statistical mixture of 3- and 4-borylation products, indole gave exclusively 2-borylation and quinoline gave exclusively 3-borylation (Figure 1-2).

Borylation site selectivity with $[\text{Ir}(\text{OMe})(\text{COD})]_2$ catalyst:

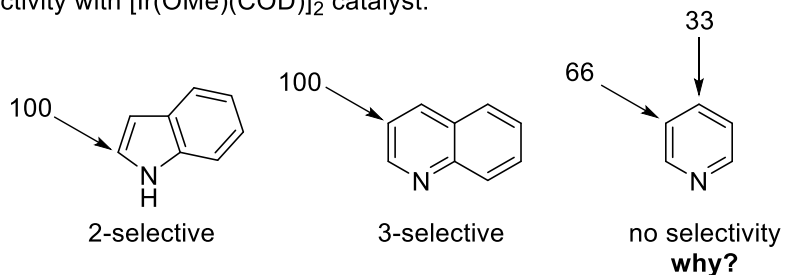
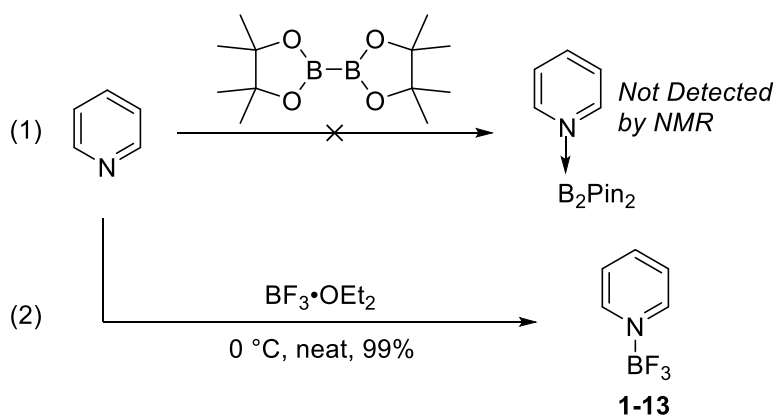


Figure 1-2 – Selected examples of Ir-catalyzed borylation regioselectivity demonstrating no clear trend.

Computations by Dr. Aaron Green probed the reaction mechanism to compute the energy differences between different bond activations for various heterocycles. After all calculations failed for pyridine, he considered the possibility that Lewis acid-base interactions between the pyridine and the electrophilic iridium complex or boron reagents were affecting the transition state energy levels throughout the mechanism. Indeed, incorporating these interactions into the calculations showed a large benefit for pyridine. This inspired the experimental question: Would

adding an external Lewis acid improve reactivity and selectivity in iridium-catalyzed C-H borylation reactions of nucleophilic heterocycles? Importantly, we hypothesized that such a Lewis acid would not exert effects solely by altering the steric environment, but also by preventing other detrimental interactions such as catalyst poisoning.^{43,44}

The experimental study began by examining the behavior of pyridine in the Ir-catalyzed C-H borylation reaction. Pyridine was chosen as the model substrate for two reasons: (1) Pyridine is a nucleophilic nitrogenous heterocycle that is known to readily react with Lewis acids⁴⁵ and (2) Pyridine exhibits poor regioselectivity in the C-H borylation reaction, thus it was a reaction in serious need of improvement. Early computational work suggested that B₂pin₂, the boron source most frequently used in the C-H borylation reaction, could complex with pyridine during the reaction. However, variable temperature NMR studies could not detect such an interaction (Scheme 1-16, line 1). Moving forward, we opted to investigate the effect of adding a much stronger Lewis acid to the reaction, BF₃. Boron trifluoride-etherate proved to be a very convenient source of BF₃ since it instantly reacts with pyridine to form the stable and isolable 1:1 complex **1-13** as shown in Scheme 1-16, line 2. In addition, the small size of BF₃ had the benefit of computational tractability and a minimal steric influence on the substrate.



Scheme 1-16 – B₂pin₂ does not form a stable complex with pyridine (line 1), unlike BF₃ (line 2).

1.5 – DFT Calculations Predict a Major Lewis Acid Effect

Dr. Aaron Green performed calculations to compare the energetics of pyridine borylation with and without BF_3 in the reaction. B_2eg_2 (eg = ethylene glycol) was used in place of B_2pin_2 for computational simplicity since that would remove twelve methyl groups from the catalyst. The calculated pathway for pyridine borylation in absence of BF_3 is shown in Figure 1-3. The computed mechanism begins with iridium-pyridine complex **A**, which isomerizes to the η^2 complex **B** before reaching the first transition state **C** leading to oxidative addition intermediate **D**. Note that the energy levels for the *ortho*, *meta*, and *para* borylation are shown, but only structures for a *meta* reaction are shown. Borylative reductive elimination via transition state **E** produces iridium-coordinated intermediate **F**, which releases product **G**. Resultant iridium hydride **H** is regenerated to active starting complex **A** via reaction with B_2eg_2 and pyridine.

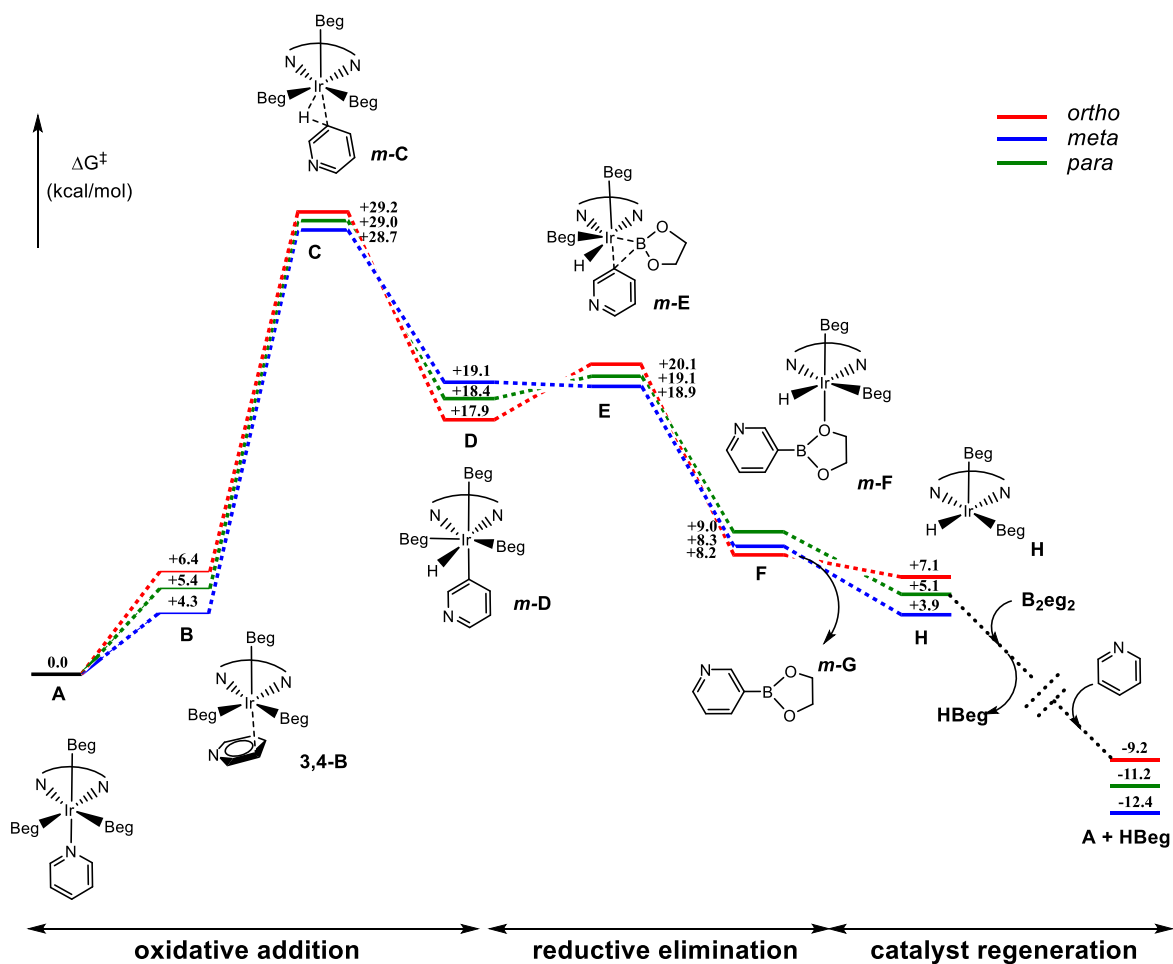


Figure 1-3 –Free energy profile for Ir-catalyzed borylation of pyridine. Structures for borylation at the meta-position of pyridine are shown. Energy levels for *ortho*-, *meta*- and *para*-activation are denoted by red, blue and green lines, respectively.

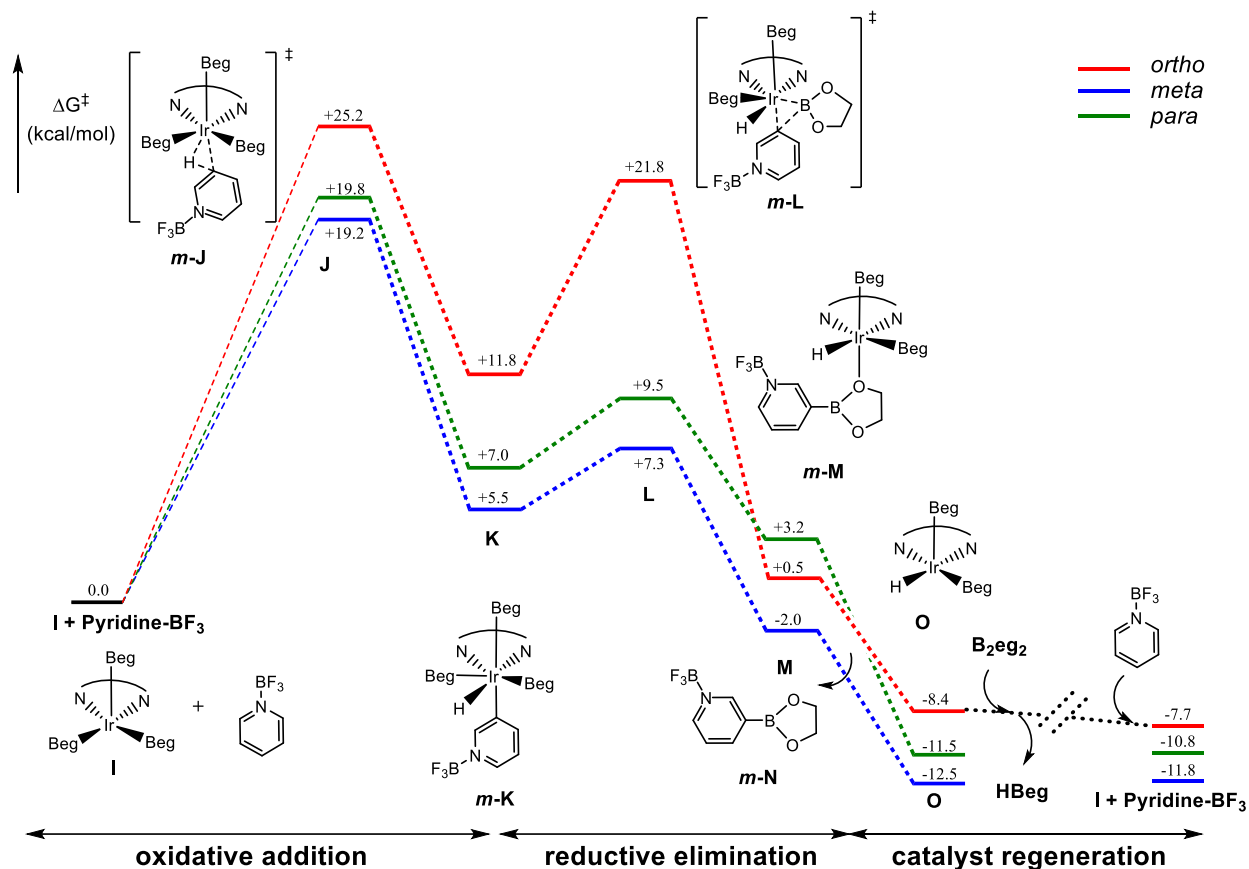


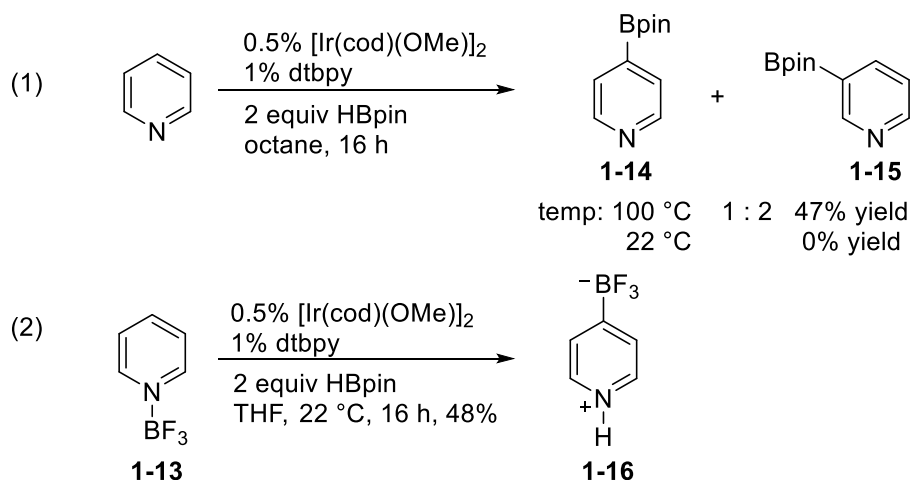
Figure 1-4 - Free energy profile for Ir-borylation of pyridine-BF₃. Structures for borylation at the meta-position of pyridine are shown. Results for *ortho*-, *meta*- and *para*-activation are denoted by red, blue and green lines, respectively.

The calculated pathway for borylation of pyridine complexed with BF₃ Lewis acid is shown in Figure 1-4. The mechanism begins with interaction of iridium complex **I** and pyridine-BF₃, which directly proceeds to oxidative addition intermediate **K** via transition state **J**. Unlike the mechanism shown in Figure 1-3, no local minimum for the η^2 complex was found towards transition state **J**. After reductive elimination to complex **M** through TS **L**, ejection of product **N** is associated with concomitant formation of hydride **O**. Finally, regeneration of catalyst **I** is achieved in the presence of B₂eg₂. These results reveal that the activation energy of the rate limiting step of the reaction is reduced substantially when BF₃ is present (19.2 vs 28.7 kcal/mol). Furthermore, the energy differences between the regioisomeric transition states are exaggerated

in the presence of the BF₃, suggesting that the added Lewis acid may not merely lower the barrier of the reaction, but also improve its site selectivity. Our rationale for the observed energy differences with added BF₃ can be explained by two effects: (1) The Lewis acid inductively withdraws electron density from the aromatic system, weakening the C-H bonds and facilitating bond activation; and (2) The presence of the blocking BF₃ group prevents deleterious Lewis acid/base interactions between the iridium catalyst and pyridine.

1.6 – C-H Borylation of Pyridine-BF₃ and Isolation of Pyridinium Trifluoroborate

With these promising computational predictions now guiding the experimental design, we first conducted the control reaction. Congruent with literature reports,^{23,46} borylation of free pyridine required heating to 100 °C and gave a mélange of *para*- and *meta*-boryl products **1-14** and **1-15** in a 1 to 2 ratio (Scheme 1-17, line 1). Preparation of pyridine-BF₃ (**1-13**) was accomplished in 99% yield by added BF₃•OEt₂ directly to pyridine at 0 °C. Pyridine-BF₃ was then subjected to the Ir-catalyzed borylation reaction. To our delight, the pyridine complex reacted at room temperature to give a 4-boryl pyridine as the sole product (Scheme 1-17, line 2). The result represents a significant improvement over the reaction of pyridine without Lewis acid additive, since the reaction can now be conducted at room temperature and gives a single product instead of an inseparable mixture of isomers. However, the most intriguing result was that we obtained a pyridinium trifluoroborate **1-16**, not the expected pinacol boronate.



Scheme 1-17 – Key experiments highlighting the different outcomes of the C-H borylation reaction with pyridine or pyridine-BF₃ complex.

It should be mentioned that for some time we did not know the structure of **1-16**. The extremely simple proton and carbon NMR spectra of **1-16** are mostly noninformative. In addition, quadrupolar relaxation of the boron nucleus caused one of the carbon peaks in the ¹³C NMR to be invisible, greatly complicating our structural analysis. Eventually, out of frustration, I performed benchtop pyrolysis of the compound using a Bunsen burner, which produced a brilliant green flame confirming the presence of boron. After this observation, we opted to perform X-ray crystallographic analysis, which ultimately confirmed the structure (Figure 1-5). The analysis revealed the compound forms monoclinic crystals with a space group of P2₁/c and contains a B-C bond length of 1.627 Å.

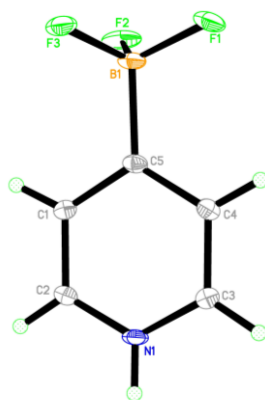
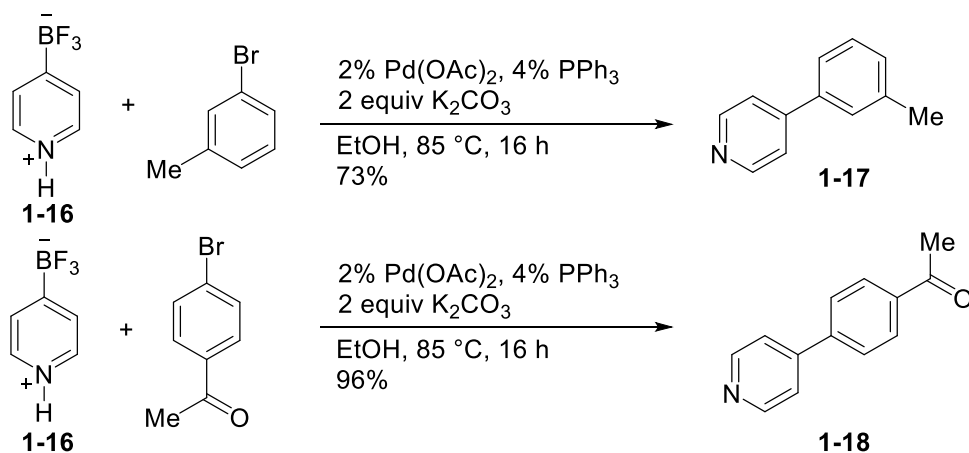


Figure 1-5 – Crystal structure of **1-16** obtained by X-ray diffraction analysis.

While potassium trifluoroborates are convenient, crystalline compounds popularized for use in cross-coupling reactions by Gary Molander, pyridinium trifluoroborate **1-16** had not been previously characterized.^{47,48} A major advantage of the pyridinium trifluoroborate compared to the pinacol boronate is it can be rapidly isolated from the reaction mixture and obtained pure by simple precipitation from acetone. By comparison, pyridyl pinacol boronates are more difficult to purify, requiring either laborious flash column chromatography or distillation. In addition, we verified that **1-16** is a great substrate in Suzuki coupling reactions, providing convenient access to substituted pyridines **1-17** and **1-18** in good yield as shown in Scheme 1-18.



Scheme 1-18 – Suzuki Coupling reactions of pyridinium trifluoroborate **1-16**.

Although this project was initially inspired by computational predictions on pyridine as a substrate, the unexpected isolation of the trifluoroborate product marked our foray into new uncharted territory. We began our investigation into the reaction with various changes to the standard reaction conditions (Table 1-1). Without ligand, catalyst, or HBpin, the reaction failed completely. When B₂pin₂ was used, the reaction did not proceed, though product formation could be restored when B₂pin₂ was used alongside a catalytic amount of HBpin. This phenomenon has been observed in other C-H borylation reports.⁴⁹

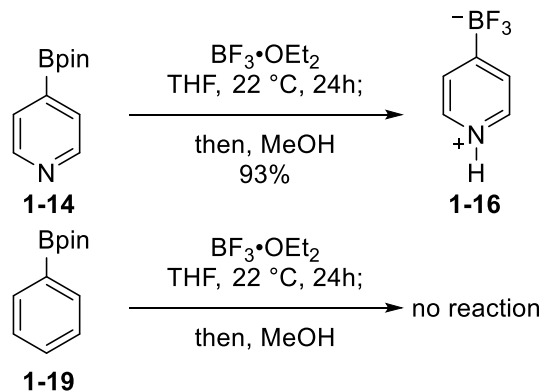
Reaction scheme showing the conversion of 4-(trifluoromethyl)pyridine (**1-13**) to 4-(trifluoromethyl)pyridinium trifluoroborate (**1-16**). The reaction conditions are: 0.5% [Ir(cod)(OMe)₂], 1% dtbpy, 2 equiv HBpin, THF, 22 °C, 16 h.

Deviation from Baseline	Isolated Yield
none	48
0 °C	0
no [Ir(cod)(OMe) ₂]	0
no dtbpy	0
no HBpin	0
0.5 equiv HBpin	0
1 equiv HBpin	0
3 equiv HBpin	12
B ₂ pin ₂ instead of HBpin	0
1 equiv B ₂ pin ₂ with 10% HBpin	0
1.5 equiv B ₂ pin ₂ with 10% HBpin	35
2 equiv B ₂ pin ₂ with 10% HBpin	33

Table 1-1 – Yield of **1-16** with various changes to the reaction conditions.

We hypothesized the pyridinium trifluoroborate **1-16** was formed through the intermediacy of a pinacol boronate ester, as evidenced by the experiment described in Scheme 1-19. An authentic sample of 4-pyridine boronic acid pinacol ester (**1-14**) was synthesized using the Miyaura protocol, then subjected to BF₃•OEt₂.¹⁷ The boronate ester was completely consumed and pyridinium trifluoroborate **1-16** formed. Interestingly, BF₃•OEt₂ is apparently not

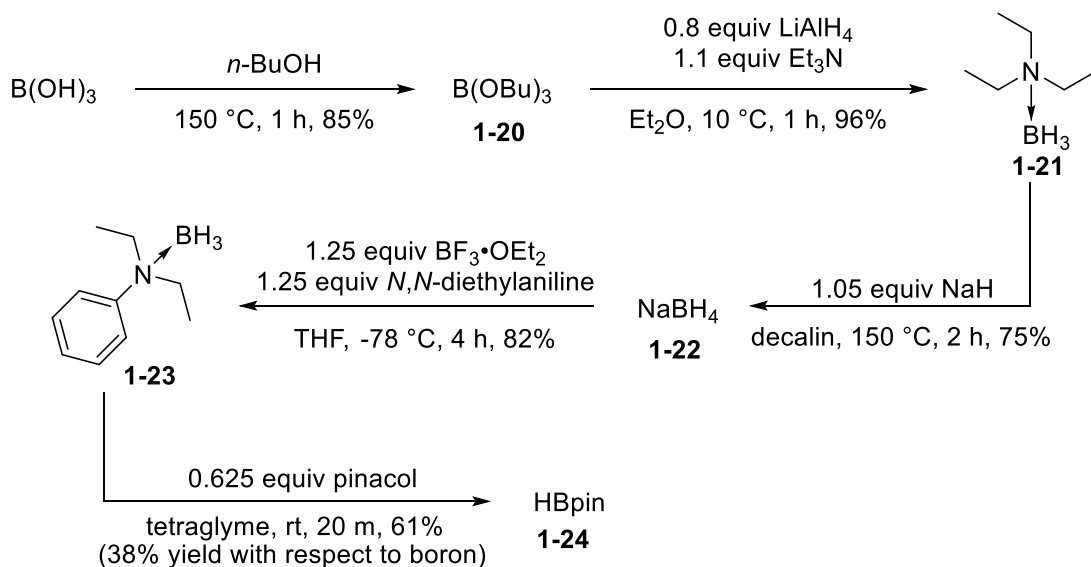
a general reagent for this purpose, since 4-phenyl boronic acid pinacol ester **1-19** exhibited no reaction under the same conditions.



Scheme 1-19 – Comparison of reactions of 4-pyridyl-Bpin **1-14** and phenyl-Bpin **1-19** with $\text{BF}_3 \cdot \text{OEt}_2$.

1.7 – Development of H^{10}Bpin Synthesis for Mechanistic Investigation

To obtain even more information about the reaction mechanism, we decided to synthesize ^{10}B -labelled HBpin to determine if the boron in the product was from HBpin or BF_3 . Thanks to a generous gift of $^{10}\text{B}(\text{OH})_3$ from the laboratory of Professor Alex Spokoyny, we hoped to synthesize pinacolborane using this material as a starting point. Unfortunately, there was no direct synthesis of HBpin from boric acid reported in the literature, however by bridging known syntheses together, access to HBpin from boric acid seemed possible as shown in Scheme 1-20.^{50,51}

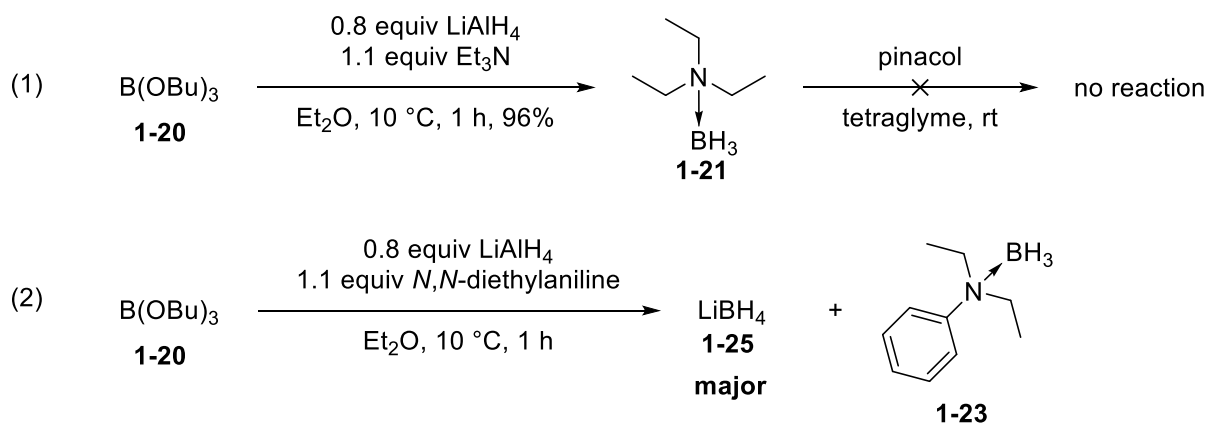


Scheme 1-20 – Initial synthetic route to HBpin

Before attempting to synthesize the isotopically-enriched HBpin, we tested the route using natural abundance boric acid. Starting from boric acid, esterification with butanol gave tributylborate (**1-20**) in 85% yield. Reduction of the borate with LiAlH_4 in the presence of triethylamine produced the amine-BH₃ complex **1-21** in 96% yield, which was complexed with NaH to form NaBH₄ (**1-22**) in 75% yield. The sodium borohydride was reacted with $\text{BF}_3\cdot\text{OEt}_2$, generating B₂H₆ gas in situ which is trapped by *N,N*-diethylaniline to form **1-23**, the aniline-borane complex in 82% yield. Finally, **1-23** was reacted with pinacol to generate HBpin (**1-24**). Unfortunately, the reaction was very sensitive to the stoichiometry of amine-borane **1-23** to pinacol, with the best results obtained when 0.625 equivalents of pinacol was used. This caused the final step to deliver HBpin in, at best, 38% yield with respect to **1-23**. Furthermore, since the HBpin was to be purified by distillation, the low yield made the distillation process very loss intensive. Using this method, we were able to obtain a roughly 15% overall yield of HBpin starting from boric acid. Although the synthesis was possible using completely known chemistry, the route was circuitous and low yielding. Worse yet, the reaction of BF_3 and $\text{Na}^{10}\text{BH}_4$ to give **1-**

23 would cause significant erosion of the isotopic purity, since a balanced equation indicates that a portion of the borane gas produced is derived from the boron of BF_3 . For these reasons, we decided to go back to the drawing board and develop an improved route.

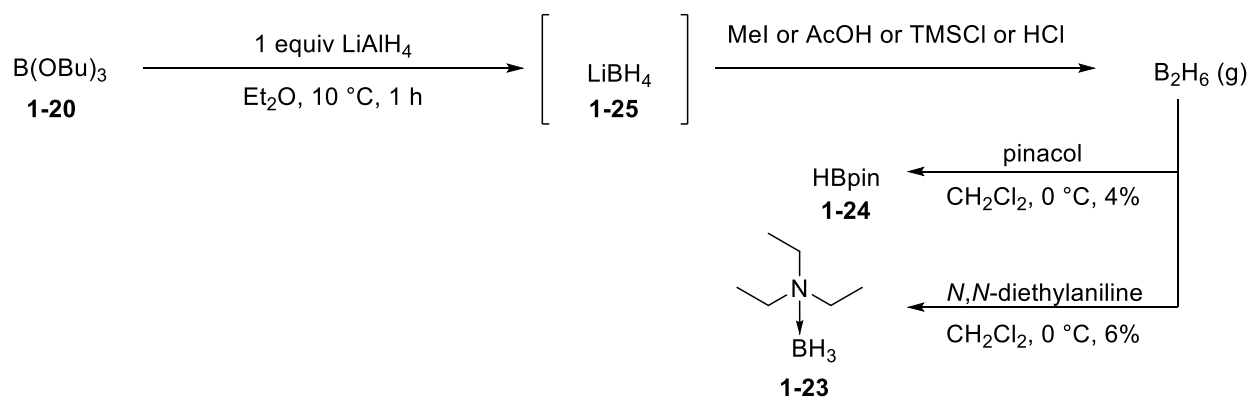
Developing an efficient synthesis of HBpin from boric acid would require eliminating as many synthetic steps as possible. First, we attempted to react the triethylamine-borane complex **1-21** with pinacol to form HBpin, but no reaction occurred (Scheme 1-21, line 1). We suspected that the electron-rich triethylamine-borane complex **1-21** was less reactive towards displacement by pinacol than the electron-poor aniline-borane complex **1-23**. Second, we attempted to intercept the late stage **1-23** in a rapid fashion by reacting tributylborate with LiAlH_4 in the presence of *N,N*-diethylaniline. Unfortunately, the reaction gave very little of the desired aniline-borane complex, and we obtained mostly LiBH_4 (**1-25**) instead (Scheme 1-21, line 2). Clearly, the identity of the amine can drastically change the reactivity of their corresponding borane complexes.



Scheme 1-21 – Alternative routes to HBpin explored by attempting rapid synthesis of useful amine-boranes from tributylborate.

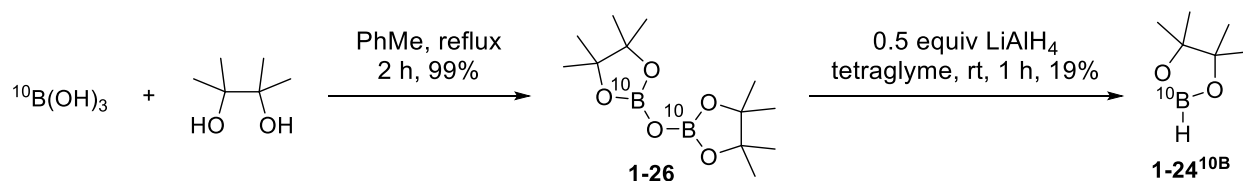
A report by Brown⁵² indicated that LiBH_4 could be decomposed to borane by various reagents, including methyl iodide, hydrogen chloride, chlorotrimethylsilane, and acetic acid. Since we knew that we could make LiBH_4 via the reaction of $\text{B}(\text{OBu})_3$ and LiAlH_4 , we tried

using these reagents in reactions in the hope of generating borane gas and bubbling it through a solution of the amine or pinacol. Although we did observe formation of the **1-23** and **1-24** using this method, the yield of desired products was extremely low, indicative of poor capture of the borane gas (Scheme 1-22).



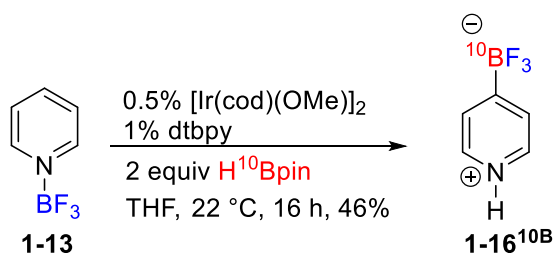
Scheme 1-22 – Synthesis of HBpin (**1-24**) and *N,N*-diethylaniline-borane complex (**1-23**) by borane gas transfer.

We were inspired by the observation that tributylborate could be reduced by excess lithium aluminum hydride to lithium borohydride and wondered if LiAlH₄ could reduce a pinacolborate as well. If so, a highly efficient synthesis of HBpin could be realized. To test this idea, we refluxed boric acid with an equimolar amount of pinacol in toluene solvent under a Dean-Stark apparatus with Merlic modification for the removal of water. To our delight, the resulting BpinOBpin (**1-26**) could be treated with LiAlH₄ in tetraglyme to furnish pinacolborane and lithium borohydride as a side product. Isolating the pinacolborane from this mixture by distillation gave a 20% yield and thus we had developed a simple, two-step procedure to synthesize HBpin from B(OH)₃. We repeated the synthesis with isotopically enriched (>96%) boric acid, which gave a 19% yield of H¹⁰Bpin (Scheme 1-23).



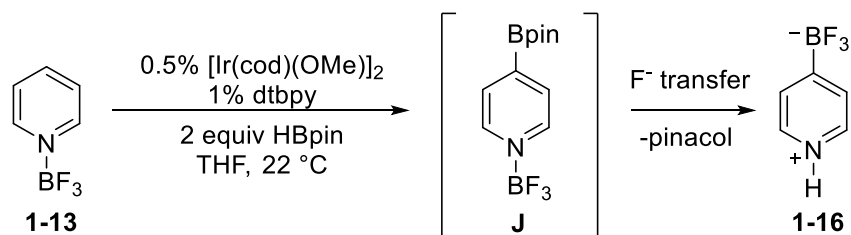
Scheme 1-23 – Rapid 2-step synthesis of H^{10}Bpin .

With isotopically-enriched H^{10}Bpin (**1-24**) in hand, we applied it to the iridium reaction and isolated the borylated product. This product was analyzed by high-resolution mass spectrometry to determine its isotopic ratio. The results indicated the borylated product was 96% ^{10}B enriched, matching the level of enrichment of the $^{10}\text{B}(\text{OH})_3$. This proves definitively that the boron present in the borylated pyridine is from HBpin and not BF_3 (Scheme 1-24).



Scheme 1-24 – Isotopically-enriched HBpin gives isotopically-enriched borylation products after the iridium-catalyzed reaction.

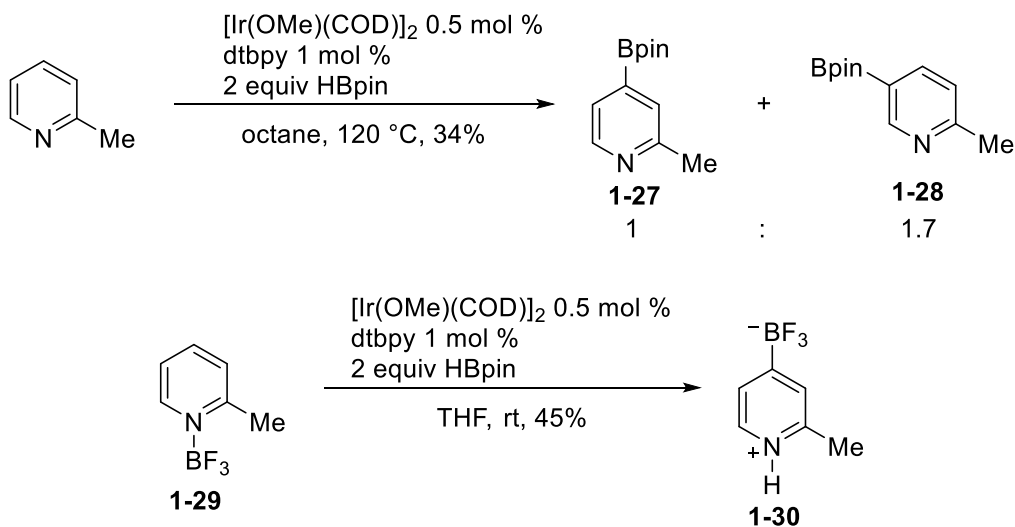
With this information, we propose the following sequence for the formation of **1-16**. In the first step, **1-13** undergoes C-H borylation according to the mechanism calculated by Dr. Green in Figure 1-4. However, although the computed mechanism predicts 3- and 4-borylation transition states are similar in energy, only 4-borylation occurs. Borylation leads to diboryl intermediate **J**, which could not be isolated. Next, displacement of pinacol with fluoride occurs to give the trifluoroboryl species via an unknown mechanism to furnish **1-16** (Scheme 1-25). The fluoride exchange is all the more unusual given the stability of **1-13**.



Scheme 1-25 – Proposed sequence of transformations for the conversion of **1-13** to **1-16**.

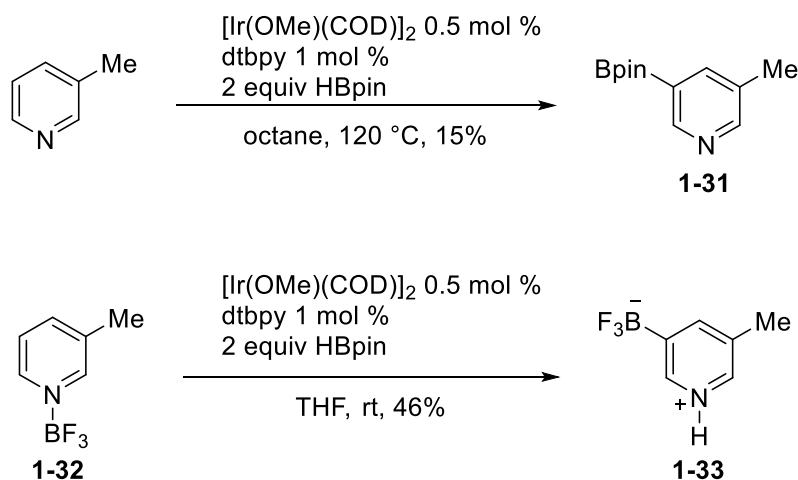
1.8 – C-H Borylation of Other Heterocycle-BF₃ Complexes

The Ir-catalyzed borylations of 2- and 3-picoline were investigated to determine the influence of steric effects on product formation. 2-Picoline was reacted under two sets of conditions: First, without Lewis acid at elevated temperatures in octane, and then as the BF₃ complex (prepared as before) at room temperature in THF. 2-Picoline is borylated without Lewis acid to a nearly equal mixture of 4- and 5- boryl products (**1-27** and **1-28**), with 5-boryl **1-28** formed as the major component. On the other hand, 2-picoline-BF₃ complex **1-29** is borylated solely at the 4-position to give **1-30**, indicating the presence of BF₃ can overpower the native steric bias of the substrate (Scheme 1-26).



Scheme 1-26 – Borylation of 2-picoline.

On the other hand, 3-picoline is a cleaner substrate for Ir-catalyzed borylation even without Lewis acid. It is reported in the literature to react exclusively to give 5-boryl pyridine **3-31**, though in our hands it did so in only 15% yield.⁴³ 3-Picoline-BF₃ (**1-32**) still underwent borylation at exclusively at the 5-position to give **3-33**, but we did obtain a higher yield (Scheme 1-27) at a significantly reduced temperature.



Scheme 1-27 – Borylation of 3-picoline.

In both cases, reactions conducted with BF₃ Lewis acid gave the trifluoroboryl products instead of pinacol boronates. These results demonstrate that BF₃ can improve this class of reactions by increasing yields, improving regioselectivity, allowing reduced reaction temperatures, and facilitating simple purification of products by precipitation.

Unfortunately, the scope of other heterocycles that benefit from added BF₃ for the iridium-catalyzed borylation was determined to be very limited. A collection of heteroaromatic-BF₃ complexes were prepared (**1-34** – **1-51**) and subjected to the iridium-catalyzed C-H borylation reaction, but none reacted to give borylated compounds as desired as shown in Table 1-2. Most of the heterocyclic complexes simply failed to react at all and were recovered unchanged. Some of the BF₃ complexes, namely those derived from 2-methylbenzoxazole (**1-37**), 2-

methoxypyridine (**1-46**), 3-methoxypyridine (**1-47**), and 3-phenylpyridine (**1-49**) decomposed to give complex mixtures of products after the borylation reaction. The quinoline- and isoquinoline- BF_3 complexes **1-34** and **1-35** instead underwent reduction to give tetrahydroquinoline and dihydroisoquinoline, respectively. Although the limited scope was disappointing, many of these heterocycles are competent substrates without Lewis acid, typically reacting to give single regioisomers. Therefore, the beneficial Lewis acid effects we observe represent a complementary method for the borylation of the most challenging substrate, pyridine. Although 2- and 3-picoline also showed a substantial benefit.

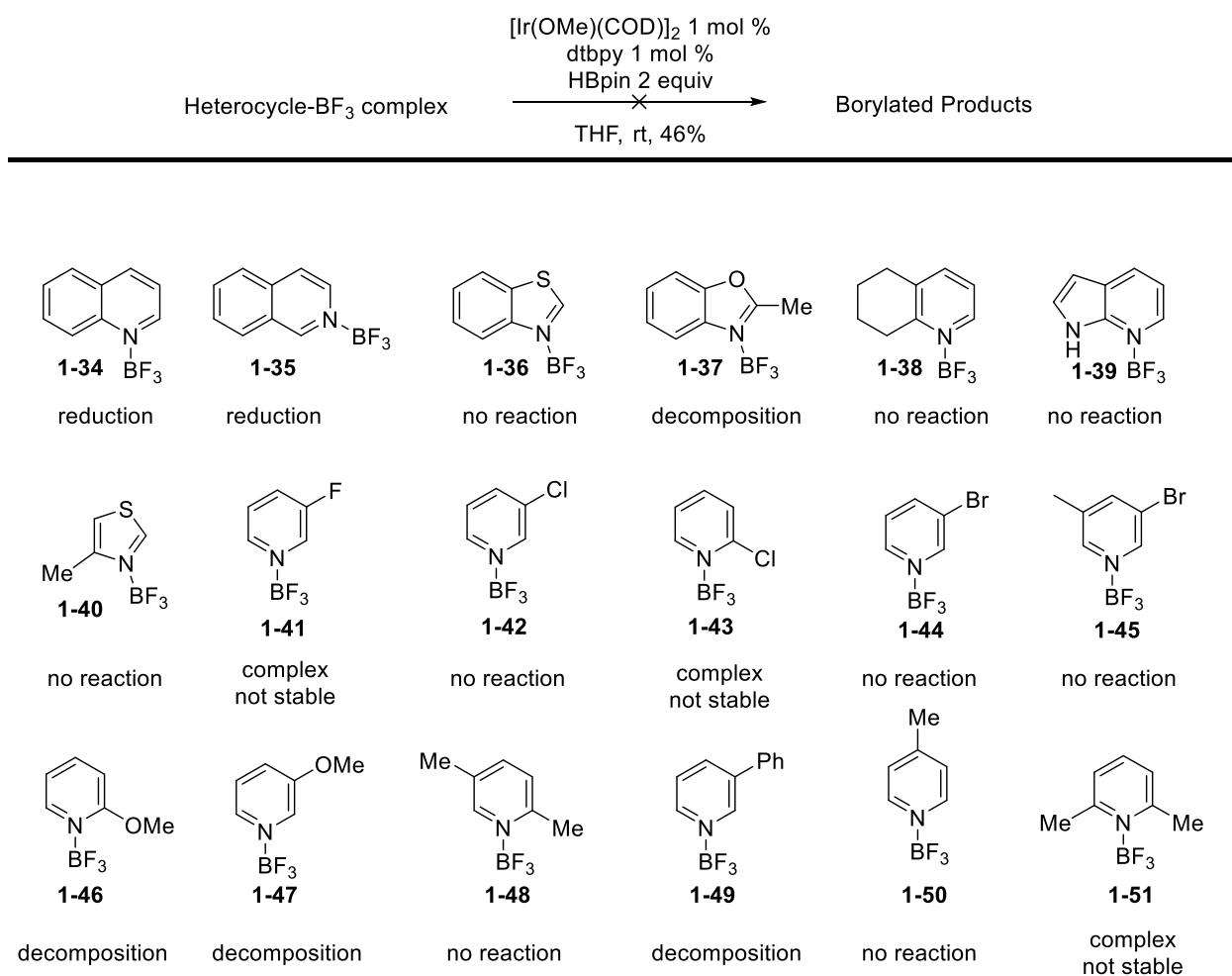
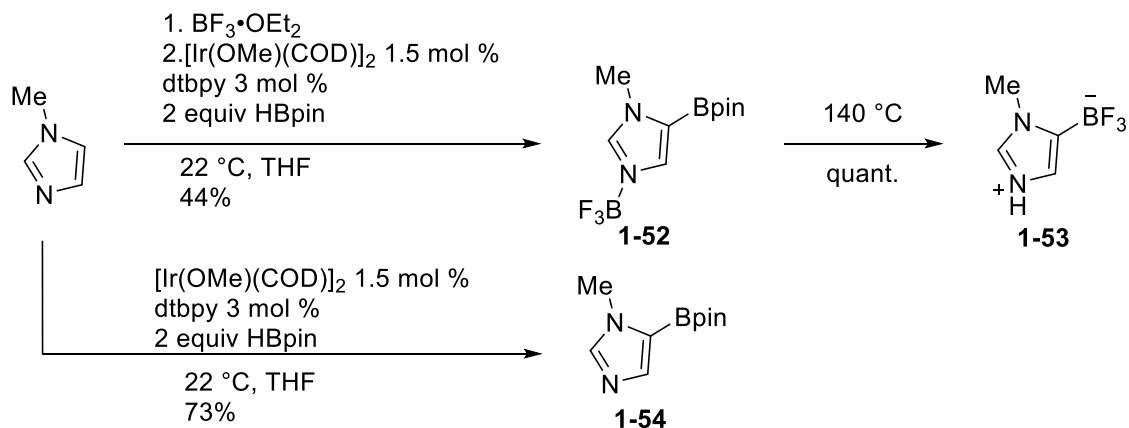


Table 1-2 – Unsuitable BF_3 complexes for Ir-catalyzed C-H borylation.

Contrasting the lackluster results of the alternative heterocycle screen, interesting behavior was observed with the 1-methylimidazole- BF_3 complex. As shown in Scheme 1-28, the compound was borylated exclusively at the 5-position as the pinacol boronate, but the BF_3 group remained bound to nitrogen (**1-52**). The structure of **1-52** was confirmed by X-ray diffraction analysis. This result is an outlier from previous products obtained because it's the only case of a Bpin group remaining intact with BF_3 present. As a control reaction, the borylation of 1-methylimidazole was performed without any Lewis acid additives and we found the reaction is quite facile at room temperature, giving **1-54** in good yield.⁵³ Although BF_3 didn't improve the borylation yield or selectivity of this heterocycle, the reaction did provide mechanistic information. When the diboryl imidazole compound **1-52** was heated to 140 °C, it rearranged to give the trifluoroboryl species **1-53**. The conversion could be monitored by ^{19}F NMR and confirmed by high resolution mass spectrometry. This provides further evidence that the reaction of pyridine proceeds via a similar diboryl species as shown in Scheme 1-25.

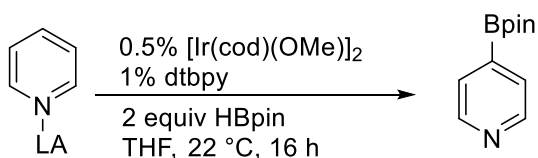


Scheme 1-28 – Borylation of 1-methylimidazole with and without BF_3

1.9 – Investigation of Other Lewis Acids for C-H Borylation

In addition to testing other heterocycles, we also investigated alternative Lewis acids. As shown in Table 1-3, a variety of pyridine complexes were prepared and screened for reactivity.

Preparation of the pyridine complexes **1-55**, **1-56**, and **1-57** was performed by adding the corresponding Lewis Acids to pyridine at 0 °C, just as we had done for the synthesis of pyridine-BF₃ complex **1-13**. None of these other haloborane-pyridine complexes gave any product whatsoever, perhaps a result of poor solubility or the tendency for these compounds to release acidic decomposition products that destroy HBpin. Commercially-available pyridine-SO₃ complex **1-59** was found to be unreactive as well. We also examined the molybdenum complex of bipyridine **1-60**,⁵⁴ with the hope that a facile borylation would prove useful towards the synthesis of substituted bpy ligands.

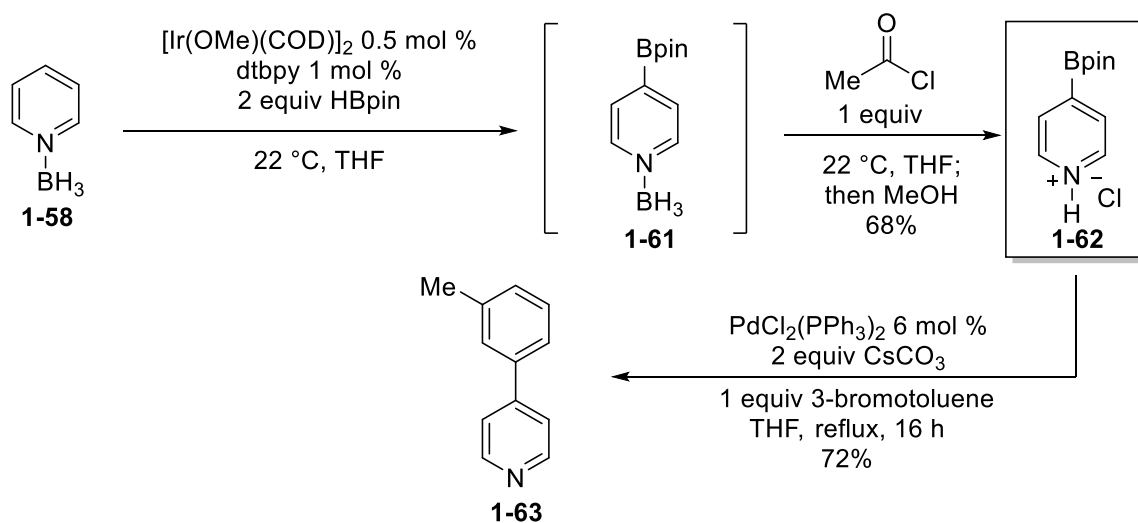


Substrate	Product (Yield)	Substrate	Product (Yield %)
	n.r. (0)		(68)
	n.r. (0)		n.r. (0)
	n.r. (0)		n.r. (0)

Table 1-3 – Screen of alternative Lewis acid complexes.

Among these alternative Lewis acids tested, only the commercially-available pyridine-BH₃ complex **1-58** proved to be a viable substrate in the C-H borylation reaction, giving clean borylation at the 4-position (**1-61**) by ¹H NMR analysis of the crude reaction mixture. We found

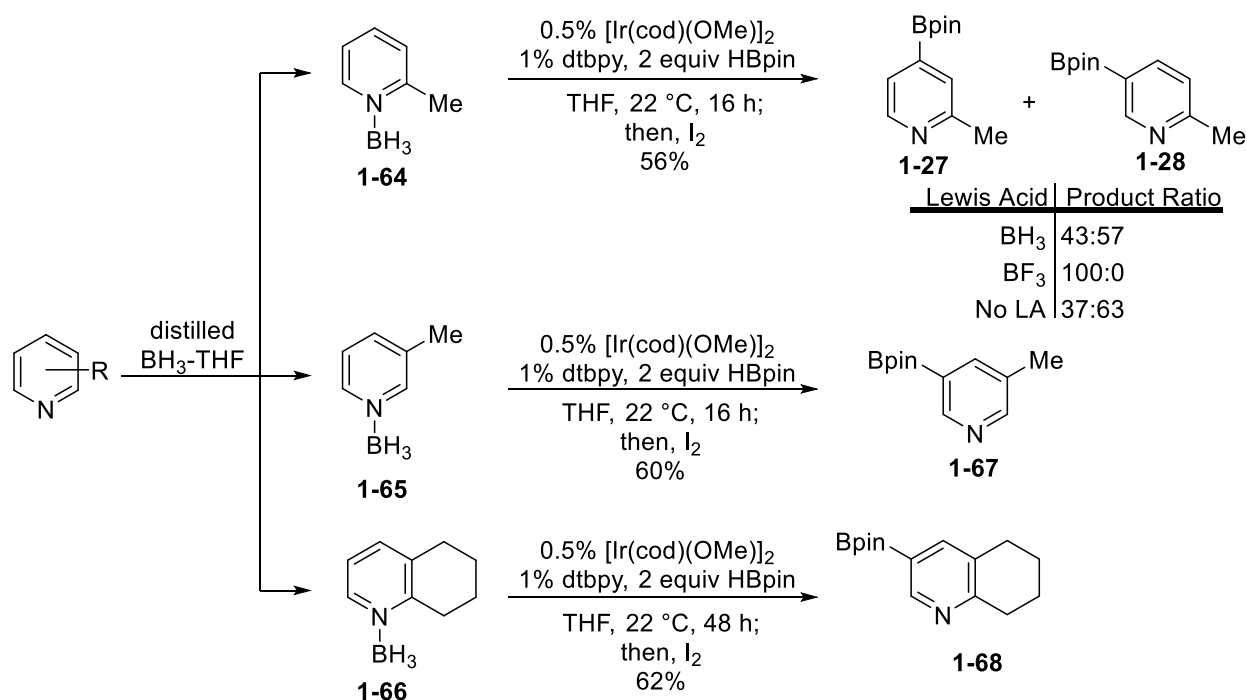
borane remained complexed to pyridine at the end of the reaction, complicating the workup and isolation. To remove the borane, we tried various techniques, including heating, oxidation with I_2 , reaction with strong Lewis bases (guanidine), and treatment with Bronsted acids (HBr), but none of these strategies were effective. Ultimately, we discovered that acetyl chloride was highly competent at effecting decomplexation, giving pure 4-pyridyl Bpin in 68% yield as the hydrochloride salt (**1-62**) after trituration from hexane. Acetyl chloride was chosen after recognizing that amine-borane complexes are mild reducing agents and that the boryl pyridine is a very weak donor, so a reactive, electrophilic carbonyl group was necessary. To confirm the utility of the product, the salt was subjected to a Suzuki coupling reaction to give a good yield of substituted pyridine **1-63** (Scheme 1-29).



Scheme 1-29 – Reaction sequence demonstrating borylation of **1-58**, decomplexation, and Suzuki reaction for net replacement of C-H bond with a biaryl linkage.

We next prepared the borane complexes of 2- and 3-picoline but were surprised to find they did not react. The problem was traced to our commercial source of borane, BH_3 -THF, which contained tertiary amine stabilizers that carried over into the next step, disrupting the borylation reaction. To solve this problem, we removed the stabilizers by distillation of the BH_3 -THF. The

2-picoline-BH₃ (**1-64**), 3-picoline-BH₃ (**1-65**), and 2,3-cyclohexenopyridine-BH₃ (**1-66**) complexes were made by addition of the heterocycles to a solution of the distilled BH₃-THF. After removal of volatiles in vacuo, these complexes were borylated at room temperature (Scheme 1-30). For these products, we found I₂ was more effective than acetyl chloride at removing the complexed borane at the end of the reactions. Intriguingly, **1-64** borylated to a mixture of regioisomers **1-27** and **1-28**. Because BF₃ and BH₃ have similar steric profiles, the differences in borylation selectivity between the two Lewis acids demonstrate that electronic, rather than steric effects, are likely responsible for the changes in regioselectivity.



Scheme 1-30 – Borane-promoted borylation of substituted pyridines.

1.10 – Conclusion

In summary, we were inspired by DFT calculations to examine Ir-catalyzed C-H borylation reactions of Lewis acid-pyridine complexes. The experiments showed that addition of BF₃ could dramatically improve the reaction of pyridine, allowing room temperature borylation

of the compound to give a single regioisomer. BF_3 was also found to override the native site selectivity of 2-picoline, an effect we ascribe to electronic rather than steric reasons. Furthermore, the presence of BF_3 assisted not only the reaction, but also the workup: the products were unexpectedly isolated as conveniently-purified pyridinium trifluoroborate zwitterions. Mechanistic studies, including development of a convenient synthesis of isotopically-enriched HBpin, suggested these unusual products were formed via the intermediacy of a diboryl intermediate. Although the scope of the Lewis acid effect was limited, the study led us to identify BH_3 as another viable Lewis acid for room temperature, *para*-selective borylation of pyridine. Depending on the selection of Lewis acid, one can dial in the type of boryl product obtained: BF_3 for the trifluoroborate or BH_3 for the pinacol boronate. Future work will aim to clearly ascertain the mechanism of BF_3 transfer, as well as the full scope of the Lewis acid effect.

1.11 – Experimental Procedures

General Methods: All commercial compounds were used as received unless otherwise noted. Methanol was distilled over Mg^0 . Tetrahydrofuran and ether were distilled prior to use from sodium-benzophenone ketyl. Pyridine, 2-picoline, 3-picoline, and 2,3-cyclohexenopyridine were distilled from KOH. 1-methylimidazole was distilled from sodium. BH_3 -THF was vacuum distilled immediately before use. Di- μ -methoxobis(1,5-cyclooctadiene)diiridium(I) (Strem, 98%), 4,4'-di-*tert*-butyl-2,2'-dipyridyl (Aldrich, 98%), and bis(pinacolatodiboron) (Oakwood, 98%) were stored in a glovebox and used as received. 4,4,5,5-Tetramethyl-1,3,2-dioxaborolane (Oakwood, 97%) and pyridine-borane complex (Sigma, 95%) were stored in a freezer and dispensed as received under nitrogen. ^{10}B -boric acid was purchased from Ceradyne (a 3M subsidiary) and was certified to min. 96% ^{10}B by weight. NMR data obtained with Bruker ARX-400 or AV-500 instrument and calibrated to the solvent signal (^1H NMR: CDCl_3 $\delta = 7.26$ ppm,

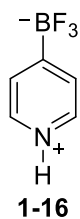
DMSO-*d*₆ δ = 2.50 ppm, D₂O δ = 4.80 ppm, CD₃OD δ = 4.87 ppm and ¹³C NMR: CDCl₃ δ = 77.0 ppm, DMSO-*d*₆ δ = 39.5 ppm, CD₃OD δ = 49.2 ppm). Multiplicities are indicated by s (singlet), d (doublet), t (triplet), q (quartet), p (pentet), m (multiplet), or b (broadened). Carbons bearing boron atoms were not observed in ¹³C NMR spectra due to quadripolar relaxation. ¹⁹F NMR was obtained on a Bruker ARX-400. ¹¹B NMR was on a Bruker ARX-400. ¹⁰B NMR was obtained on a DRX-500. IR spectra were recorded with an ATR attachment and selected peaks are reported in cm⁻¹. High resolution mass spectral data was recorded with ESI LC-TOF Micromass LCT.

Safety. Experiments contained in this experimental section were conducted with proper personal protective equipment (gloves, lab coat, safety glasses) and engineering controls (fume hood). Hazardous substances used in this experimental include pinacolborane (pyrophoric), BH₃-THF (pyrophoric), LiAlH₄ (pyrophoric), tetrahydrofuran (acute toxin), boron trifluoride etherate (acute toxin), and iodine (oxidizer).

Complexation of BF₃ (or BCl₃, BBr₃, HBBR₂) to Heterocycles⁵⁵ A 50 mL Schlenk tube was flame-dried under vacuum and backfilled with a nitrogen atmosphere. After cooling, the vacuum inlet adaptor was replaced with a rubber septum and purged with nitrogen. Then, 10 mmol (1 equiv) of the freshly distilled heterocycle of choice were added via syringe. The apparatus was chilled to 0 °C, followed by dropwise addition of 1.23 mL (10 mmol, 1 equiv) boron trifluoride etherate (or equivalent molar amounts of BCl₃, BBr₃, or HBBR₂). Petroleum ether (approx. 4 mL) was added via syringe and swirled to ensure complete mixing of the reagents. Within one minute, the product precipitated as a flocculent white solid. The flask was placed under strong vacuum for several hours to remove all volatiles. The resulting complexes were used without further purification.

General Procedure for Borylation of Pyridine BF₃ Complexes (Method A) To a 25 mL flame dried round bottom flask equipped with a stirbar in a glovebox was added Di- μ -methoxobis(1,5-cyclooctadiene)diiridium(I) (3.3 mg, 0.005 mmol), 4,4'-Di-tert-butyl-2,2'-dipyridyl (2.7 mg, 0.01 mmol), and heterocycle-BF₃ complex (1 mmol). The flask was sealed with a rubber septum and connected to a N₂-filled Schlenk line via needle. THF (0.5 mL) was added followed by HBpin (0.29 mL, 2 mmol). The resulting orange mixture stirred for 16 h at rt. Workup was accomplished by quenching the crude mixture with MeOH, followed by removal of solvent in vacuo. The crude product was treated with acetone (or 3-methyl-2-butanone) to give a white precipitate that was triturated 2x with acetone (or 3-methyl-2-butanone). The precipitate was dried under vacuum to give product that could be further purified by recrystallization from methanol.

trifluoro(pyridinium-4-yl)borate



Procedure: Prepared via **Method A** using 865 mg (5.8 mmol) of pyridine-BF₃ complex. The product was purified by trituration with acetone to give 415 mg (48%) of trifluoro(pyridin-1-ium-4-yl)borate as a white solid. The structure was confirmed by single crystal X-Ray crystallography.

MP: 258 °C

¹H NMR (400 MHz, D₂O) δ : 8.57 (d, *J* = 6.0 Hz, 2H), 8.08 (d, *J* = 5.6 Hz, 2H);

^{13}C NMR (100 MHz, D_2O) δ : 138.4 , 129.2 (Boron-containing carbon not observed);

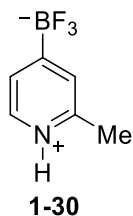
^{19}F NMR (271 MHz, D_2O) δ : -143.9;

^{11}B NMR (148 MHz, D_2O) δ : -2.08 (q, $J = 47.0$ Hz);

IR (neat, ATR): 2979, 2931, 1622, 1452, 1372, 1336, 1272, 1218, 1145, 1009, 982, 959, 887, 850, 698, 673, 620 cm^{-1} ;

HRMS (ESI) m/z : $[\text{M-F}]^+$ Calcd for $\text{C}_5\text{H}_5\text{BF}_2\text{N}$ 127.0519; Found 127.0520.

trifluoro(2-methylpyridinium-4-yl)borate



Procedure: Prepared via **Method A** using 322 mg (2 mmol) of 2-picoline- BF_3 complex. The product was purified by trituration with 3-methyl-2-butanone to give 144 mg (45%) of trifluoro(2-methylpyridinium-4-yl)borate as a white solid.

MP: 223 $^{\circ}\text{C}$

^1H NMR (400 MHz, D_2O) δ : 8.39 (d, $J = 5.6$ Hz, 1H), 7.88 (s, 1H), 7.85 (d, $J = 6.0$ Hz, 1 H), 2.74 (s, 3H);

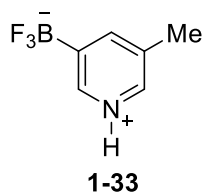
^{13}C NMR (100 MHz, D_2O) δ : 150.9, 137.7, 129.8, 126.3, 18.6 (Boron-containing carbon not observed);

^{19}F NMR (271 MHz, D_2O) δ : -140.2;

IR (neat, ATR): 3286, 3191, 1636, 1620, 1495, 1400, 1271, 1164, 968, 907, 838, 793. 734, 706, 627, 612 cm^{-1} ;

HRMS (ESI) m/z : $[M-F]^+$ Calcd for $\text{C}_6\text{H}_7\text{BF}_2\text{N}$ 142.0641; Found 142.0651.

trifluoro(5-methylpyridinium-3-yl)borate



Procedure: Prepared via **Method A** using 161 mg (1 mmol) of 3-picoline- BF_3 complex. The product was purified by trituration with 3-methyl-2-butanone to give 73 mg (46%) of trifluoro(5-methylpyridinium-3-yl)borate as a white solid.

MP: 249 $^{\circ}\text{C}$

^1H NMR (400 MHz, $\text{DMSO}-d_6$) δ : 8.47 (s, 1H), 8.32 (s, 1H), 8.24 (s, 1H), 2.40 (s, 3H);

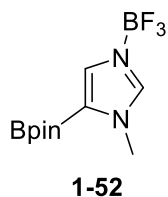
^{13}C NMR (100 MHz, D_2O) δ : 150.2, 139.6, 138.5, 137.3, 17.4 (Boron-containing carbon not observed);

^{19}F NMR (271 MHz, D_2O) δ : -140.5;

IR (neat, ATR): 3238, 3110, 1618, 1562, 1263, 1171, 986, 823, 681, 608, 583, 561, 525 cm^{-1} ;

HRMS (ESI) m/z : $[M-F]^+$ Calcd for $\text{C}_6\text{H}_7\text{BF}_2\text{N}$ 142.0641; Found 142.0649.

1-methyl-5-(4,4,5,5-tetramethyl-1,3,2-dioxaborolan-2-yl)imidazole-BF₃



Procedure: Prepared via **Method A** using 300 mg (2 mmol) of 1-methylimidazole-BF₃ complex. The product was purified by trituration with hexane and 3-methyl-2-butanone. The remaining solids were recrystallized from 3-methyl-2-butanone and 240 mg (44%) of 1-methyl-5-(4,4,5,5-tetramethyl-1,3,2-dioxaborolan-2-yl)imidazole-BF₃ complex was isolated and the structure confirmed by X-ray crystallography.

MP: 66 °C

¹H NMR (400 MHz, CDCl₃) δ: 8.08 (s, 1H), 7.70 (s, 1H), 3.94 (s, 3H), 1.34 (s, 12H)

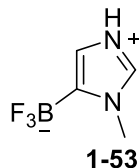
¹³C NMR (100 MHz, CDCl₃) δ: 138.1, 134.0, 83.2, 35.7, 24.6 (Boron-containing carbon not observed);

¹⁹F NMR (271 MHz, CD₃OD) δ: -150.3;

IR (neat, ATR): 3346, 3162, 3075, 2984, 2899, 2873, 2832, 1620, 1558, 1508, 1475, 1237, 1208, 1139, 1056, 978 cm⁻¹;

HRMS (ESI) m/z: [M-BF₃+H]⁺ Calcd for C₁₀H₁₈BN₂O₂ 209.1463; Found 209.1468.

trifluoro(1-methyl-1H-imidazol-3-ium-5-yl)borate



A 50 mg sample of **1-52** was dissolved in a 1:1 mixture of 3-methyl-2-butanone and methanol in a pressure tube and heated at 140 °C for 16 h. The solvents were removed and the resulting solid was rinsed 2x with 3-methyl-2-butanone to remove pinacol to give 28 mg (100%) of **1-53**.

MP: >260 °C

¹H NMR (400 MHz, CD₃OD) δ: 8.54 (s, 1H), 7.05 (s, 1H), 3.87 (s, 3H)

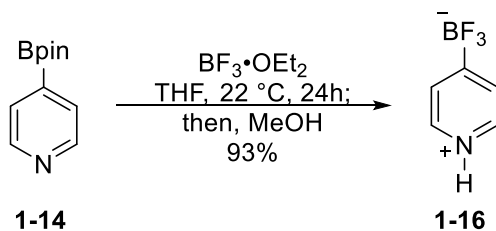
¹³C NMR (100 MHz, CD₃OD) δ: 134.4, 120.3, 34.1 (Boron-containing carbon not observed);

¹⁹F NMR (271 MHz, CD₃OD) δ: -143.1;

IR (ATR, neat): 3710, 3697, 3681, 2981, 2967, 2938, 2923, 2965, 2844, 2826, 1455, 1356, 1346, 1308, 1238, 1201, 1055, 1033, 1014, 952, 913 cm⁻¹;

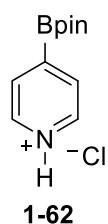
HRMS (ESI) m/z: [M-F]⁺ Calcd for C₄H₆BF₂N₂ 130.0628; Found 130.0622.

Conversion of 4-(4,4,5,5-tetramethyl-1,3,2-dioxaborolan-2-yl)pyridine 1-14 to Trifluoro(2-methylpyridin-1-ium-4-yl)borate 1-16 with BF₃•OEt₂



4-(4,4,5,5-tetramethyl-1,3,2-dioxaborolan-2-yl)pyridine (103 mg, 0.5 mmol) was dissolved in 1.5 mL of THF. To this solution 0.61 mL of $\text{BF}_3 \cdot \text{OEt}_2$ was added and the reaction allowed to stir for 24 h. 1 mL of MeOH was added, then all the solvent was evaporated and the residual solids washed 3x with 1 mL portions of acetone to give 68 mg (93%) of trifluoro(2-methylpyridinium-4-yl)borate.

4-(4,4,5,5-tetramethyl-1,3,2-dioxaborolan-2-yl)pyridin-1-ium chloride



Procedure: Using a syringe, 0.25 mL (2 mmol) of commercially-obtained pyridine- BH_3 (~8M BH_3 in pyridine) was added to a solution of di- μ -methoxobis(1,5-cyclooctadiene)diiridium(I) (6.6 mg, 0.01 mmol) and 4,4'-di-tert-butyl-2,2'-dipyridyl (5.4 mg, 0.02 mmol) in 1.5 mL of THF. The resulting brown solution was stirred under nitrogen and 0.58 mL (4 mmol) of HBpin was added. The mixture was stirred for 16 h at rt. For workup, 5 mL of hexane was added and the mixture was stirred for 15 min until a cream-colored precipitate formed. The orange supernatant was decanted and discarded and the precipitate (the BH_3 complex of the desired borylation product) collected and placed under vacuum to remove volatiles. To remove complexed borane, these solids were dissolved in 5 mL of THF and 0.14 mL (2 mmol) of acetyl chloride was added. After stirring for 4 h at rt, 1 mL of methanol was added (warning: gas evolves) and the reaction stirred for an additional 1 h. The volatiles were removed in vacuo, then acetone was added to precipitate 4-(4,4,5,5-tetramethyl-1,3,2-dioxaborolan-2-yl)pyridine hydrochloride. The supernatant was decanted and the product isolated as a white solid (328 mg, 68%).

^1H NMR (400 MHz, D_2O) δ : 8.70 (d, $J = 6.4$ Hz, 2H), 8.26 (d, $J = 6.4$ Hz, 2H), 1.23 (s, 12H);

^{13}C NMR (100 MHz, CDCl_3) δ : 146.4, 130.5, 85.6, 24.9 (Boron-containing carbon not observed);

IR (neat, ATR): 2988, 2981, 1978, 1628, 1604, 1492, 1455, 1373, 1201, 1147, 1065, 1039, 961, 937, 805, 772;

HRMS (ESI) m/z : $[\text{M}-\text{HCl}]^+$ Calcd for $\text{C}_{11}\text{H}_{16}\text{BNO}_2$ 205.1389; Found 205.1382.

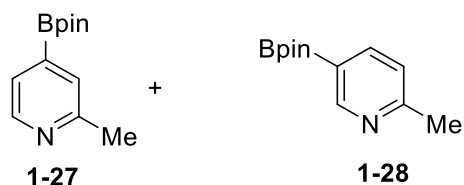
Complexation of Heterocycles to BH_3 1.1 equivalents of a commercially obtained 1M solution of BH_3 in THF (stabilized with *N*-isopropyl-*N*-methyl-*tert*-butylamine) was distilled at rt under vacuum (1 mm Hg) and collected in a receiving flask equipped with a stir bar and chilled to -78 $^\circ\text{C}$. The cold distillate was then treated with the appropriate heterocycle (1 equiv) and placed under strong vacuum and allowed to warm to rt. Once the volatiles were removed, the remaining BH_3 complex was used immediately in the borylation reactions without further purification as described below.

Borylation of 2-picoline- BH_3 , 3-picoline- BH_3 , and 2,3-cyclohexenopyridine- BH_3 (Method B)

A solution of di- μ -methoxobis(1,5-cyclooctadiene)diiridium(I) (6.6 mg, 0.01 mmol) and 4,4'-di-*tert*-butyl-2,2'-dipyridyl (5.4 mg, 0.02 mmol) in 1.5 mL of THF was added to a flask containing 2 mmol of heterocycle- BH_3 complex. The resulting solution was stirred under nitrogen and 0.58 mL (4 mmol) of HBpin was added. The reaction was stirred for 16 h at rt (48 h for 2,3-cyclohexenopyridine- BH_3 complex). Next, the THF was *completely* removed in vacuo and the remaining residue dissolved in 6 mL of CHCl_3 (THF is reactive during the subsequent iodine workup, so it must be removed). 254 mg I_2 crystals (1 mmol, 2 equiv) were added to this solution, which immediately underwent vigorous bubbling (the flask was left open to air to allow

the gases to escape). After stirring for 1 h, the reaction mixture was partitioned between 100 mL saturated aq. sodium thiosulfate and 200 mL of diethyl ether in a separatory funnel. After extracting the aqueous phase 2x additional times with 100 mL portions of ether, the combined ether extracts were dried over magnesium sulfate, filtered, and concentrated to give the borylated products.

2-methyl-4-(4,4,5,5-tetramethyl-1,3,2-dioxaborolan-2-yl)pyridine 8 and 2-methyl-5-(4,4,5,5-tetramethyl-1,3,2-dioxaborolan-2-yl)pyridine



Procedure: Prepared via **Method B** using 186 mg (2 mmol) of 2-picoline and 2.2 mL of a 1 M solution of BH₃ complex in THF. We obtained 245 mg (56%) of a 1.3:1 mixture of 2-methyl-4-(4,4,5,5-tetramethyl-1,3,2-dioxaborolan-2-yl)pyridine (**1-27**) and 2-methyl-5-(4,4,5,5-tetramethyl-1,3,2-dioxaborolan-2-yl)pyridine (**1-28**) as an orange oil (ratio determined by ¹H NMR).

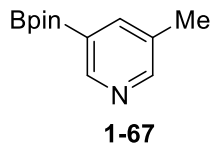
¹H-NMR (400 MHz, CDCl₃) δ: 4-boryl isomer 8.49 (dd, *J* = 4.8, 0.9 Hz, 1H), 7.50 (d, *J* = 0.9 Hz, 1H), 7.42 (d, *J* = 4.8 Hz, 1H), 2.55 (s, 3H), 1.33 (s, 12H); 5-boryl isomer 8.82 (d, *J* = 1.8 Hz, 1H), 7.94 (dd, *J* = 7.7, 1.8 Hz, 1H), 7.13 (d, *J* = 7.7 Hz, 1H), 2.56 (s, 3H), 1.32 (s, 12H) Note: inseparable impurities of pinacol and O(Bpin)₂ were present in the product mixture;

¹³C-NMR (100 MHz, CDCl₃) δ mixture: 160.7, 157.4, 154.5, 147.9, 143.0, 128.7, 125.8, 123.0, 84.5, 84.1, 24.8, 24.5, 24.2, 24.1 (Boron-containing carbon not observed);

IR (neat, ATR): 2944, 2768, 2713, 2675, 2479, 1615, 1471, 1397, 1220, 1159, 1060, 1035, 770, 753 cm^{-1} ;

HRMS (ESI) m/z : $[M+H]^+$ Calcd for $\text{C}_{12}\text{H}_{19}\text{BNO}_2$ 220.1511; Found 220.1506.

3-methyl-5-(4,4,5,5-tetramethyl-1,3,2-dioxaborolan-2-yl)pyridine



Procedure: Prepared via **Method B** using 186 mg (2 mmol) of 3-picoline and 2.2 mL of a 1 M solution of BH_3 complex in THF. We obtained 263 mg (60%) of 3-methyl-5-(4,4,5,5-tetramethyl-1,3,2-dioxaborolan-2-yl)pyridine as a white solid.

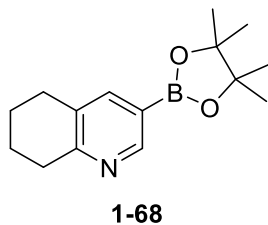
$^1\text{H-NMR}$ (400 MHz, CDCl_3) δ : 8.74 (s, 1H), 8.49 (s, 1H), 8.48 (s, 1H), 2.31 (s, 3H), 1.34 (s, 12H);

$^{13}\text{C-NMR}$ (100 MHz, CDCl_3) δ : 152.1, 152.0, 142.9, 132.5, 84.2, 24.9, 18.3 (Boron-containing carbon not observed);

IR (neat, ATR): 2980, 2937, 2360, 1602, 1367, 1143, 913, 852, 739, 676 cm^{-1} ;

HRMS (ESI) m/z : $[M+H]^+$ Calcd for $\text{C}_{12}\text{H}_{19}\text{BNO}_2$ 220.1511; Found 220.1509.

3-(4,4,5,5-tetramethyl-1,3,2-dioxaborolan-2-yl)-5,6,7,8-tetrahydroquinoline



Procedure: Prepared via **Method B** (48 h reaction time) using 266 mg (2 mmol) of

2,3-cyclohexenopyridine and 2.2 mL of a 1 M solution of BH_3 complex in THF. We obtained 321 mg (62%) of 3-(4,4,5,5-tetramethyl-1,3,2-dioxaborolan-2-yl)-5,6,7,8-tetrahydroquinoline as a white solid.

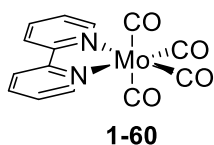
^1H NMR (400 MHz, CDCl_3) δ : 8.67 (s, 1H), 7.75 (s, 1H), 2.95 (t, $J = 6.0$ Hz, 2H), 2.76 (t, $J = 6.0$ Hz, 2H), 1.90-1.86 (m, 2H), 1.81-1.78 (m, 2H), 1.34 (s, 12H);

^{13}C NMR (100 MHz, CDCl_3) δ : 159.4, 151.3, 144.2, 132.3, 84.2, 32.0, 28.4, 24.8, 22.7, 22.5 (Boron-containing carbon not observed);

IR (neat, ATR): 2978, 2934, 1612, 1457, 1418, 1396, 1369, 1274, 1218, 1182, 1137, 1111, 1013, 962, 915, 851, 712, 676, 601 cm^{-1} ;

HRMS (ESI) m/z : $[\text{M}+\text{H}]^+$ Calcd for $\text{C}_{15}\text{H}_{23}\text{BNO}_2$ 260.1825; Found 260.1846.

Synthesis of $\text{Mo}(\text{bpy})(\text{CO})_4$

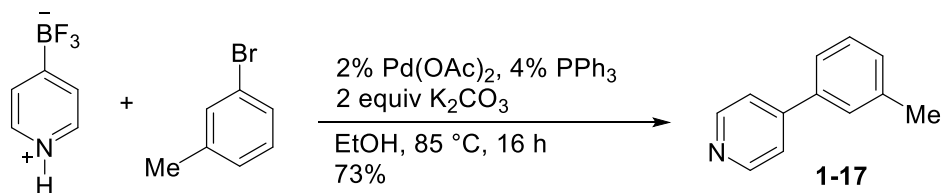


Prepared according to a protocol described by Stiddard.⁵⁴ In a 50 mL round bottom flask equipped with a stirbar and reflux condenser, $\text{Mo}(\text{CO})_6$ (2.640 g, 10 mmol) and 2,2'-bipyridine (1.562 g, 10 mmol) were combined and stirred in toluene and brought to a gentle reflux for 1.5 h. The mixture was refluxed and the brilliant red product was filtered and washed with toluene and hexane sequentially. The red crystals were dried under vacuum, providing 3.3145 g (91%) of $\text{Mo}(\text{bpy})(\text{CO})_4$.

^1H NMR (400 MHz, CDCl_3) δ : 9.09 (ddd, $J = 5.5, 1.5, 0.8$ Hz, 2H), 8.57 (dt, $J = 8.22, 0.8$ Hz, 2H), 8.17 (td, $J = 8.2, 1.5$ Hz, 2H), 7.63 (ddd, $J = 5.5, 1.54, 0.85$ Hz, 2H);

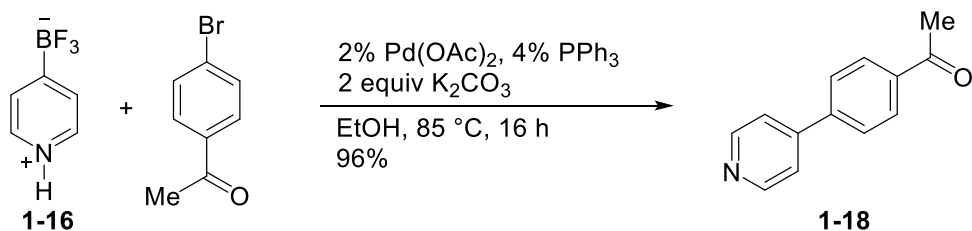
^{13}C NMR (100 MHz, CDCl_3) δ : 222.4, 205.3, 154.7, 152.7, 138.3, 125.8, 123.0.

Palladium Coupling Reaction of Trifluoro(pyridin-1-ium-4-yl)borate and 3-Bromotoluene



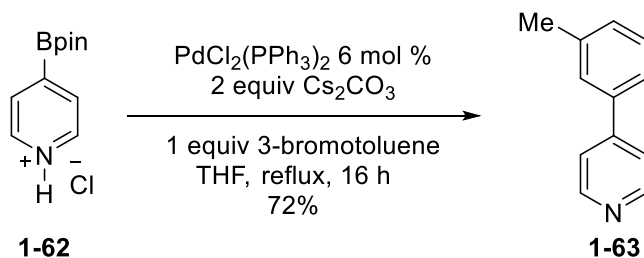
Trifluoro(pyridin-1-ium-4-yl)borate (147 mg, 1 mmol), $\text{Pd}(\text{OAc})_2$ (4.5 mg, 0.02 mmol), PPh_3 (10.5 mg, 0.04 mmol), K_2CO_3 (276 mg, 2 mmol), and 3-bromotoluene (0.121 mL, 1 mmol) were combined with 3 mL of EtOH in a sealed pressure tube. The reaction was heated at 85 °C and stirred under a N_2 atmosphere for 16 h. The mixture cooled to rt, then diluted with EtOAc and passed through a short silica plug, which was then washed with additional EtOAc. The filtrate was concentrated and the residue chromatographed (2:1 EtOAc/Hex + 1% TEA) to give 124 mg (73%) of 4-(m-tolyl)pyridine with spectra data matching literature values.⁵⁶

Palladium Coupling Reaction of Trifluoro(pyridin-1-ium-4-yl)borate and 4-Bromoacetophenone



Trifluoro(pyridin-1-ium-4-yl)borate (147 mg, 1 mmol), Pd(OAc)₂ (4.5 mg, 0.02 mmol), PPh₃ (10.5 mg, 0.04 mmol), K₂CO₃ (276 mg, 2 mmol), and 4-bromoacetophenone (239 mg, 1.2 mmol) were combined with 3 mL of EtOH in a sealed pressure tube. The reaction was heated at 85 °C and stirred under a N₂ atmosphere for 16 h. The mixture was cooled to rt, then diluted with EtOAc and passed through a short silica plug, which was then washed with additional EtOAc. The filtrate was concentrated and the residue chromatographed (3:1 EtOAc/Hex + 1% TEA) to give 189 mg (96%) of 1-(4-(pyridin-4-yl)phenyl)ethan-1-one with spectra data matching literature values.⁵⁶

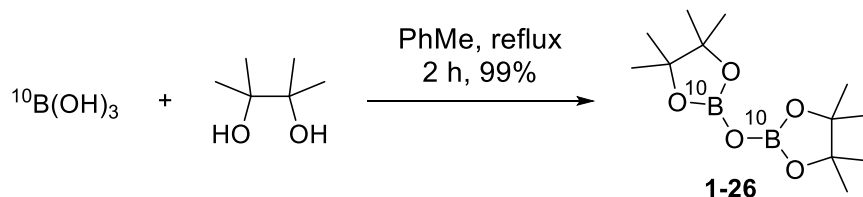
Palladium Coupling Reaction of 4-(4,4,5,5-tetramethyl-1,3,2-dioxaborolan-2-yl)pyridin-1-ium chloride and 3-Bromotoluene



To a flask containing 483 mg (2 mmol) of 4-(4,4,5,5-tetramethyl-1,3,2-dioxaborolan-2-yl)pyridin-1-ium chloride was added Cs₂CO₃ (1.3 g, 4 mmol), PdCl₂(PPh₃)₂ (138 mg, 0.12 mmol), and 20 mL of THF. After purging with nitrogen, 3-bromotoluene (0.243 mL, 2 mmol) was added via syringe and the reaction was refluxed for 16 h. The mixture was cooled to rt, filtered through a silica plug (EtOAc wash), and concentrated to give 440 mg of a crude oil. The crude product was purified by silica gel flash column chromatography (2:1 EtOAc:Hexanes +

1% TEA) to give 243 mg (72%) of 4-(m-tolyl)pyridine with spectra data matching literature values.⁵⁶

Synthesis of $^{10}\text{BpinO}^{10}\text{Bpin}$



A round bottom flask was charged with 2.017 g (33 mmol) of $^{10}\text{B}(\text{OH})_3$ min. 96% ^{10}B by wt., 3.9063 g (33 mmol) of pinacol, and 20 mL of toluene. The mixture was heated at reflux with a Dean-Stark trap for 1 h to remove water. The resulting clear solution was allowed to cool, and then concentrated to give 4.1953g (95%) of the bis-boryloxide $\text{O}(^{10}\text{Bpin})_2$ as a white solid.

Spectral data matched literature values.⁵⁷

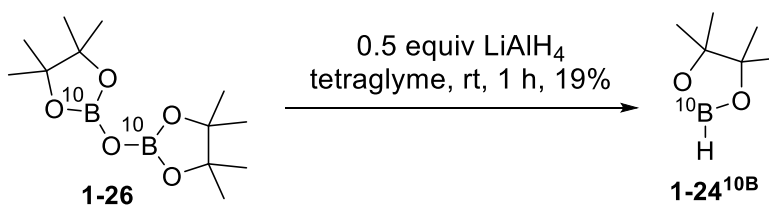
^1H NMR (400 MHz, CDCl_3) δ : 1.01 (s, 24H);

^{13}C NMR (100 MHz, CDCl_3) δ : 83.2, 25.0.

IR (neat, ATR): 3347, 3004, 2982, 2942, 1519, 1360, 1266, 1215, 1165, 1140 cm^{-1} ;

HRMS (DART) m/z : $[\text{M}]^+$ Calcd for $\text{C}_{12}\text{H}_{24}^{10}\text{B}_2\text{O}_5$ 268.1882; Found 268.1881.

Synthesis of H^{10}Bpin



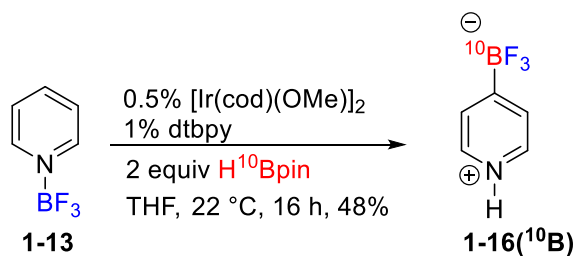
In a round bottom flask, 4.0514 g (15 mmol) of O(¹⁰Bpin)₂ was dissolved in 5 mL of tetraglyme (some heating was necessary to ensure complete dissolution of the solid). In another round bottom flask, 286 mg (7.5 mmol) of LiAlH₄ was dissolved in 5 mL of tetraglyme. The LAH solution was then added dropwise to the O(¹⁰Bpin)₂ solution at rt. After 1h, the resulting gray solution was distilled at 55 °C (40 mm Hg) and collected in a chilled (-78 °C) receiving bulb to give 721 mg (19 %) of H¹⁰Bpin. Mass spectrum not obtained due to instability of pinacolborane in ionization conditions.

¹H NMR (400 MHz, CDCl₃) δ: 4.21-3.36 (m, 1H) 1.25 (s, 12H);

¹³C NMR (100 MHz, CDCl₃) δ: 83.2, 24.9;

¹¹B NMR (148 MHz, CDCl₃) δ: 28.1 (d, *J* = 177.6 Hz). (from trace ¹¹B);

¹⁰B NMR (160 MHz, CDCl₃) δ: 28.1 (d, *J* = 177.6 Hz).



Synthesis of 1-16(¹⁰B)

Prepared via **Method A** using 147 mg (1 mmol) of pyridine-BF₃ complex and 0.29 mL (2 mmol) of H¹⁰Bpin. After reaction, the purification was accomplished by trituration with acetone to give 68 mg (46%) of ¹⁰B-trifluoro(pyridin-1-ium-4-yl)borate as a white solid. MS analysis shows 97:3 (¹⁰B:¹¹B) enrichment. For reference, natural abundance boron is present in 1:4 (¹⁰B:¹¹B) ratio.

¹H NMR (400 MHz, D₂O) δ: 8.57 (d, *J* = 6.0 Hz, 2H), 8.08 (d, *J* = 5.6 Hz, 2H);

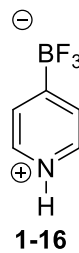
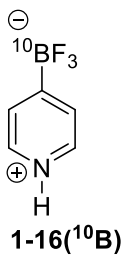
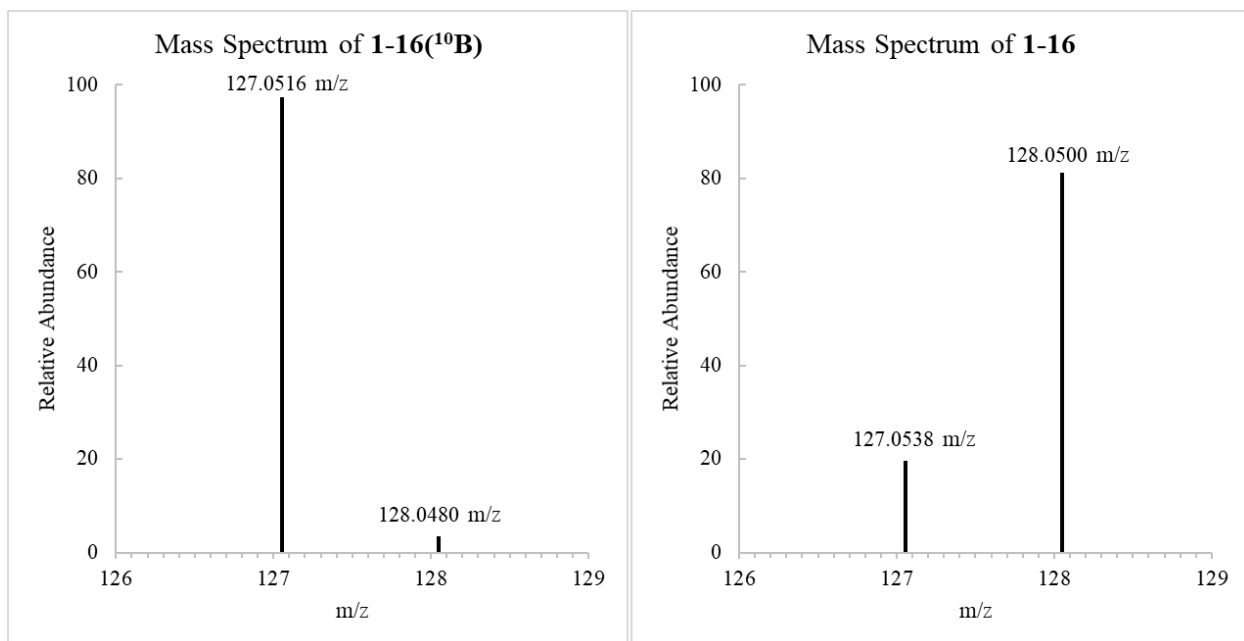
^{13}C NMR (125 MHz, D_2O) δ : 138.4, 129.2 (Boron-containing carbon not observed);

^{19}F NMR (271 MHz, D_2O) δ : -143.9;

^{11}B NMR (148 MHz, D_2O) δ : 2.14 (q, $J = 49.2$ Hz) (from trace ^{11}B);

IR (neat, ATR): 2979, 2941, 1598, 1490, 1371, 1351, 1219, 1197, 1139, 981, 908, 768 cm^{-1} ;

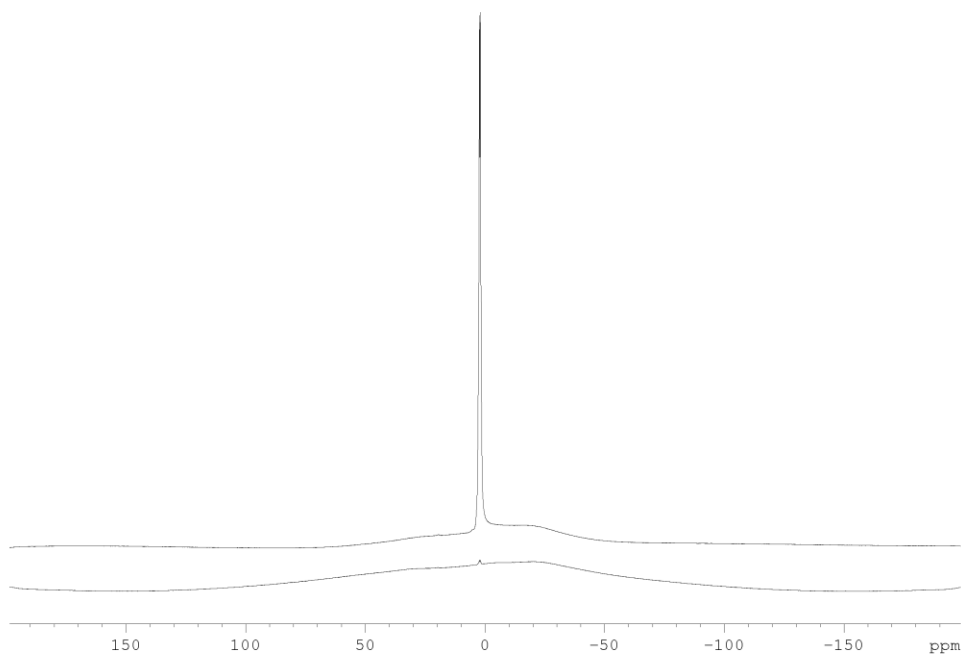
HRMS (DART) m/z : $[\text{M}-\text{F}]^+$ Calcd for $\text{C}_5\text{H}_5^{10}\text{BF}_2\text{N}$ 127.0519; Found 127.0516.



Isotope enrichment determined by mass spectrometry:

1-16(^{10}B): 97.0 atom % ^{10}B ; 3 atom % ^{11}B

1-16: 19.1 atom % ^{10}B ; 80.9% atom % ^{11}B



Comparison of ¹¹B NMR of **1-16** (top) and **1-16**(¹⁰B) (bottom) as qualitative representation of relative isotope abundance.

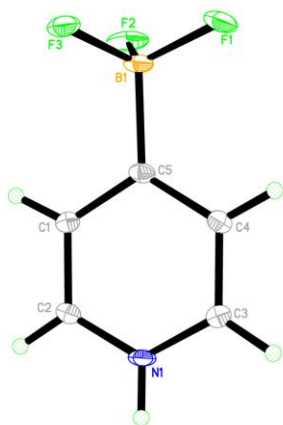
1.12 – Computational Methods

Geometry optimizations were performed using B3LYP/6-31G(d) with tight convergence criteria. Thermal corrections were calculated from unscaled vibrational frequencies at the same level of theory for a standard state of 1 atm and 298.15 K. All stationary points were characterized and confirmed by vibrational analysis. Electronic energies were obtained from single points on the B3LYP/6-31(G) geometries using the M06 meta-hybrid functional with a 6-311g** basis set. Solvation was accounted for by employing the SMD solvation model with n-octane as the solvent.

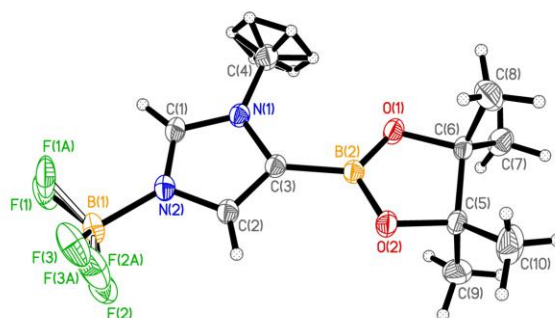
For complete computational coefficients, see Appendix I.

1.13 – X-Ray Diffraction Analysis for 1-16 and 1-52

Data of **1-16** were collected on a Bruker APEX-II CCD diffractometer using Sealed Mo X-Ray Tube monochromated MoK α radiation with $\lambda = 0.71073$ at 100 K. Data of **1-52** were collected on a Bruker APEX-II CCD diffractometer using I μ S micro-focus source monochromated CuK α radiation with $\lambda = 1.54178$ at 298 K. The structures were solved and refined using the SHELXL-2014/6 program.



1-16



1-52

Selected Bond Lengths (Å) for **1-16**:

B(1)-F(1)	1.411
B(1)-C(5)	1.627
N(1)-C(2)	1.334
N(1)-C(3)	1.335
C(1)-C(2)	1.379
C(1)-C(5)	1.391
C(3)-C(4)	1.380
C(4)-C(5)	1.388

Selected Bond Lengths (Å) for **1-52**:

F(1)-B(1)	1.355
B(1)-N(2)	1.591
B(2)-C(3)	1.552
N(1)-C(1)	1.326
N(1)-C(3)	1.390
N(1)-C(4)	1.464
N(2)-C(1)	1.322
N(2)-C(2)	1.370
C(2)-C(3)	1.35

Crystallographic Data for **1-16** and **1-52**.

Compound	1-16	1-52
Empirical formula	C ₅ H ₃ BF ₃ N	C ₁₀ H ₁₇ B ₂ F ₃ N ₂ O ₂
Formula weight	146.91	275.88
Temperature	100(2) K	298(2) K
Wavelength	0.71073 Å	1.54178 Å
Crystal system	Monoclinic	Monoclinic
Space group	P2 ₁ /c	P2 ₁ /c
Unit cell dimensions	a = 8.763(2) Å b = 4.9191(12) Å c = 14.144(3) Å α = 90° β = 91.998(4)° γ = 90°	a = 10.5770(9) Å b = 11.1030(9) Å c = 12.3371(10) Å α = 90° β = 106.459(4)° γ = 90°
Volume	609.3(3) Å ³	1389.5(2) Å ³
Z	4	4
Density (calculated)	1.601 Mg/m ³	1.319 Mg/m ³
Absorption coefficient	0.158 mm ⁻¹	0.991 mm ⁻¹
F(000)	296	576
Crystal size	0.500 x 0.030 x 0.030 mm ³	0.400 x 0.400 x 0.200 mm ³
Theta range for data collection	2.326 to 26.370°.	4.359 to 68.234°.
Index ranges	-10 <= h <= 10, -6 <= k <= 6, -17 <= l <= 17	-12 <= h <= 10, -13 <= k <= 13, -14 <= l <= 14
Reflections collected	6003	9359
Independent reflections	1240 [R(int) = 0.0343]	2526 [R(int) = 0.0302]
Completeness to theta = 25.242°	99.8 %	99.2 %
Absorption correction	Semi-empirical from equivalents	Semi-empirical from equivalents
Max. and min. transmission	0.74 and 0.56	0.75 and 0.60
Refinement method	Full-matrix least-squares on F ²	Full-matrix least-squares on F ²
Data / restraints / parameters	1240 / 0 / 106	2526 / 36 / 204
Goodness-of-fit on F ²	1.151	1.072
Final R indices [I > 2σ(I)]	R1 = 0.0388, wR2 = 0.0914	R1 = 0.0619, wR2 = 0.1561
R indices (all data)	R1 = 0.0451, wR2 = 0.0940	R1 = 0.0650, wR2 = 0.1609
Largest diff. peak and hole	0.312 and -0.182 e.Å ⁻³	0.275 and -0.519 e.Å ⁻³

Atomic coordinates (x10⁴) and equivalent isotropic displacement parameters (Å²x10³) for **1-16**. U(eq) is defined as one third of the trace of the orthogonalized U_{ij} tensor.

	x	y	z	U(eq)
B(1)	2376(3)	888(4)	6381(1)	24(1)
F(1)	3506(1)	-566(2)	5905(1)	32(1)
F(3)	2653(2)	3674(2)	6252(1)	34(1)
F(2)	964(1)	244(3)	5962(1)	40(1)
N(1)	2540(2)	-820(3)	9416(1)	23(1)
C(1)	1522(2)	1607(4)	8118(1)	23(1)
C(2)	1590(2)	1091(4)	9076(1)	24(1)
C(3)	3439(2)	-2270(4)	8864(1)	25(1)
C(4)	3391(2)	-1797(4)	7902(1)	23(1)
C(5)	2438(2)	182(4)	7505(1)	20(1)

Atomic coordinates ($\times 10^4$) and equivalent isotropic displacement parameters ($\text{\AA}^2 \times 10^3$) for **1-52**. $U(eq)$ is defined as one third of the trace of the orthogonalized U_{ij} tensor.

	<i>x</i>	<i>y</i>	<i>z</i>	<i>U(eq)</i>
<i>F(1)</i>	9599(10)	8353(5)	4700(5)	105(2)
<i>F(2)</i>	7694(4)	7939(7)	5076(7)	104(2)
<i>F(3)</i>	9572(8)	7201(8)	6172(6)	92(2)
<i>F(1A)</i>	10110(8)	7941(11)	5038(11)	112(3)
<i>F(2A)</i>	8007(14)	8220(8)	4691(9)	113(4)
<i>F(3A)</i>	9020(17)	7100(13)	6121(10)	108(4)
<i>B(1)</i>	8925(2)	7503(2)	5096(2)	56(1)
<i>B(2)</i>	7224(2)	3370(2)	3230(2)	40(1)
<i>O(1)</i>	7036(1)	2781(1)	2240(1)	55(1)
<i>O(2)</i>	6641(1)	2855(1)	3956(1)	53(1)
<i>N(1)</i>	8675(1)	5169(1)	2884(1)	41(1)
<i>N(2)</i>	8724(1)	6347(1)	4303(1)	44(1)
<i>C(1)</i>	9102(2)	6212(2)	3376(2)	46(1)
<i>C(2)</i>	8019(2)	5337(2)	4400(1)	43(1)
<i>C(3)</i>	7965(2)	4586(1)	3520(1)	40(1)
<i>C(4)</i>	8942(2)	4714(2)	1857(2)	59(1)
<i>C(5)</i>	5809(2)	1885(2)	3340(1)	46(1)
<i>C(6)</i>	6429(2)	1622(2)	2361(1)	44(1)
<i>C(7)</i>	5466(2)	1291(2)	1244(2)	65(1)
<i>C(8)</i>	7550(2)	726(2)	2658(2)	79(1)
<i>C(9)</i>	4424(2)	2400(3)	2937(2)	78(1)
<i>C(10)</i>	5841(4)	848(2)	4132(2)	91(1)

1.14 – References

- (1) Arndtsen, B. A.; Bergman, R. G.; Mobley, T. A.; Peterson, T. H. *Acc. Chem. Res* **1995**, 28, 154.
- (2) Wallar, B. J.; Lipscomb, J. D. *Chem. Rev.* **1996**, 96, 2625.
- (3) Hamberg, M.; Samuelsson, B. *J. Biol. Chem.* **1967**, 242, 5329.
- (4) Hartwig, J. F.; Larsen, M. A. *ACS Cent. Sci.* **2016**, 2, 281.
- (5) Lennox, A. J. J.; Lloyd-Jones, G. C. *Chem. Soc. Rev.* **2014**, 43, 412.
- (6) Brown, H. C.; Zweifel, G. *J. Am. Chem. Soc.* **1959**, 81, 247.
- (7) Chan, D. M. T.; Monaco, K. L.; Wang, R.-P.; Winters, M. P. *Tetrahedron Lett.* **1998**, 39, 2933.
- (8) Vantourout, J. C.; Law, R. P.; Isidro-Llobet, A.; Atkinson, S. J.; Watson, A. J. B. *J. Org. Chem.* **2016**, 81, 3942.
- (9) Chattopadhyay, B.; Dannatt, J. E.; Andujar-De Sanctis, I. L.; Gore, K. A.; Maleczka, R. E.; Singleton, D. A.; Smith, M. R. *J. Am. Chem. Soc.* **2017**, 139, 7864.
- (10) Lam, P.; Clark, C.; Saubern, S.; Adams, J.; Winters, M.; Chan, D.; Combs, A. *Tetrahedron Lett.* **1998**, 39, 2941.
- (11) Evans, D. A.; Katz, J. L.; West, T. R. *Tetrahedron Lett.* **1998**, 39, 2937.
- (12) Shade, R. E.; Hyde, A. M.; Olsen, J.-C.; Merlic, C. A. *J. Am. Chem. Soc.* **2010**, 132, 1202.
- (13) Negishi, E. ichi; Abramovitch, A.; Merrill, R. E. *J. Chem. Soc. Chem. Commun.* **1975**, 138.

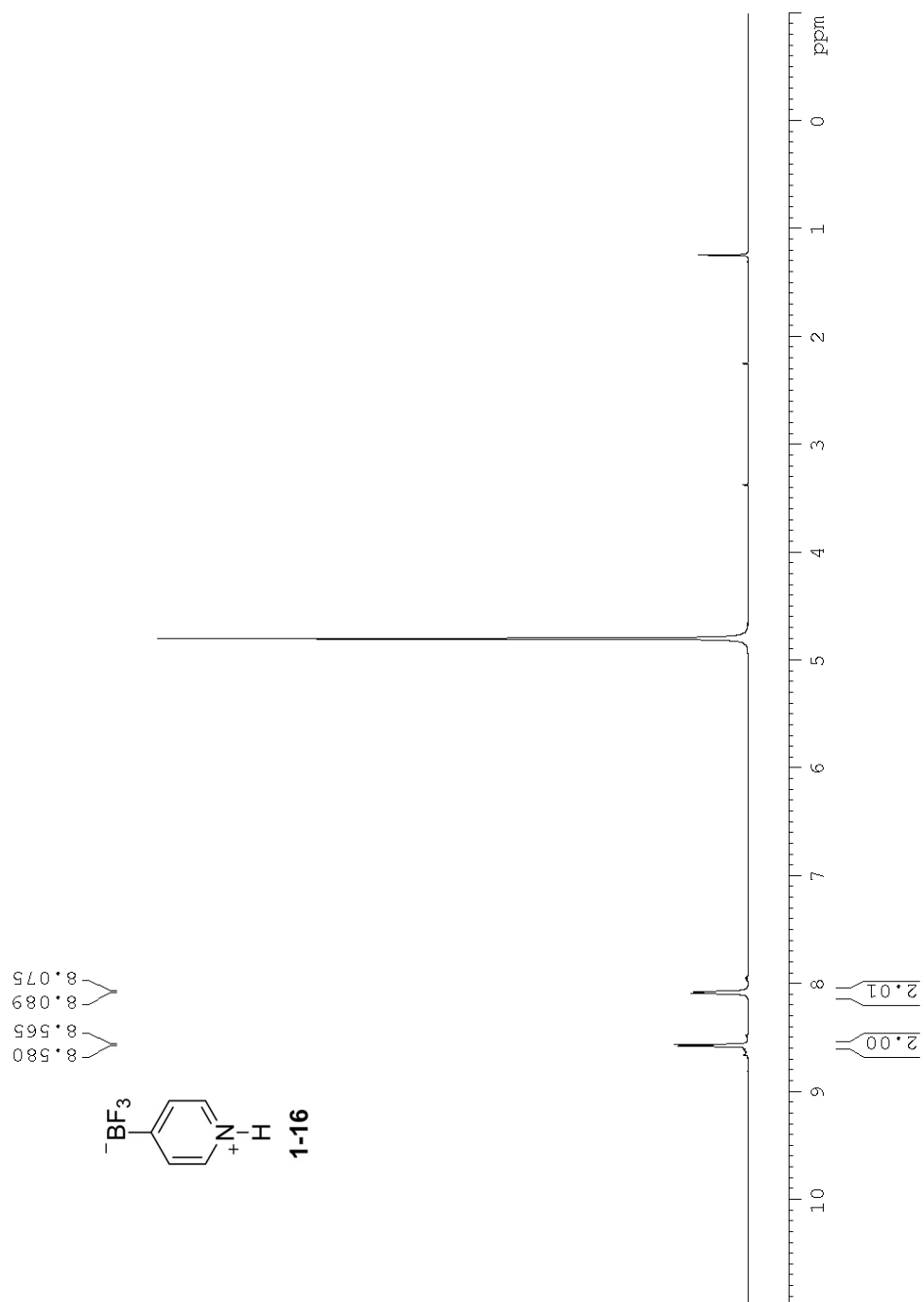
- (14) Szumigala, R. H.; Devine, P. N.; Gauthier, D. R.; Volante, R. P. *J. Org. Chem.* **2004**, *69*, 566.
- (15) Grimes, K.; Gupte, A.; Aldrich, C. *Synthesis* **2010**, *2010*, 1441.
- (16) Pelter, A.; Smith, K.; Brown, H. C. *Borane Reagents*; Academic Press, 1988.
- (17) Ishiyama, T.; Murata, M.; Miyaura, N. *J. Org. Chem.* **1995**, *60*, 7508.
- (18) Waltz, K. M.; He, X.; Muhoro, C.; Hartwig, J. F. *J. Am. Chem. Soc.* **1995**, *117*, 11357.
- (19) Iverson, C. N.; Smith, M. R. *J. Am. Chem. Soc.* **1999**, *121*, 7696.
- (20) Chen, H.; Schlecht, S.; Semple, T. C.; Hartwig, J. F. *Science* **2000**, *287*, 1995.
- (21) Cho, J. Y.; Iverson, C. N.; Smith, M. R. *J. Am. Chem. Soc.* **2000**, *122*, 12868.
- (22) Ishiyama, T.; Takagi, J.; Ishida, K.; Miyaura, N.; Anastasi, N. R.; Hartwig, J. F. *J. Am. Chem. Soc.* **2002**, *124*, 390.
- (23) Takagi, J.; Sato, K.; Hartwig, J. F.; Ishiyama, T.; Miyaura, N. *Tetrahedron Lett.* **2002**, *43*, 5649.
- (24) Tamura, H.; Yamazaki, H.; Sato, H.; Sakaki, S. *J. Am. Chem. Soc.* **2003**, *125*, 16114.
- (25) Shimada, S.; Batsanov, A. S.; Howard, J. A. K.; Marder, T. B. *Angew. Chem. Int. Ed.* **2001**, *40*, 2168.
- (26) Mertins, K.; Zapf, A.; Beller, M. *J. Mol. Catal. A Chem.* **2004**, *207*, 21.
- (27) Obligacion, J. V.; Semproni, S. P.; Chirik, P. J. *J. Am. Chem. Soc.* **2014**, *136*, 4133.
- (28) Furukawa, T.; Tobisu, M.; Chatani, N. *Chem. Commun.* **2015**, *51*, 6508.

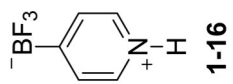
- (29) Furukawa, T.; Tobisu, M.; Chatani, N. *J. Am. Chem. Soc.* **2015**, *137*, 12211.
- (30) Légaré, M.-A.; Courtemanche, M.-A.; Rochette, É.; Fontaine, F.-G. *Science* **2015**, *349*, 513.
- (31) Gilman, H.; Bebb, R. L. *J. Am. Chem. Soc.* **1939**, *61*, 109.
- (32) Wittig, G.; Fuhrmann, G. *Chem. Ber.* **1940**, *73*, 1197.
- (33) Ishiyama, T.; Isou, H.; Kikuchi, T.; Miyaura, N. *Chem. Commun.* **2010**, *46*, 159.
- (34) Ros, A.; Estepa, B.; López-Rodríguez, R.; Álvarez, E.; Fernández, R.; Lassaletta, J. M. *Angew. Chem. Int. Ed.* **2011**, *50*, 11724.
- (35) Ghaffari, B.; Preshlock, S. M.; Plattner, D. L.; Staples, R. J.; Maligres, P. E.; Krska, S. W.; Maleczka, R. E.; Smith, M. R. *J. Am. Chem. Soc.* **2014**, *136*, 14345.
- (36) Boebel, T. A.; Hartwig, J. F. *J. Am. Chem. Soc.* **2008**, *130*, 7534.
- (37) Roosen, P. C.; Kallepalli, V. A.; Chattopadhyay, B.; Singleton, D. A.; Maleczka, R. E.; Smith, M. R. *J. Am. Chem. Soc.* **2012**, *134*, 11350.
- (38) Kuninobu, Y.; Ida, H.; Nishi, M.; Kanai, M. *Nat Chem* **2015**, *7*, 712.
- (39) Li, H. L.; Kuninobu, Y.; Kanai, M. *Angew. Chem. Int. Ed.* **2016**, *56*, 1495.
- (40) Kallepalli, V. A.; Shi, F.; Paul, S.; Onyeozili, E. N.; Maleczka, R. E.; Smith, M. R. *J. Org. Chem.* **2009**, *74*, 9199.
- (41) Preshlock, S. M.; Plattner, D. L.; Maligres, P. E.; Krska, S. W.; Maleczka, R. E.; Smith, M. R. *Angew. Chem. Int. Ed. Engl.* **2013**, *52*, 12915.
- (42) Yang, L.; Semba, K.; Nakao, Y. *Angew. Chem. Int. Ed.* **2017**, *56*, 4853.

- (43) Larsen, M. A.; Hartwig, J. F. *J. Am. Chem. Soc.* **2014**, *136*, 4287.
- (44) Green, A. G.; Liu, P.; Merlic, C. A.; Houk, K. N. *J. Am. Chem. Soc.* **2014**, *136*, 4575.
- (45) Lokhov, R. E.; Lokhova, S. S.; Gaidarova, N. M.; Belen'kii, L. I. *Chem. Heterocycl. Compd.* **1981**, *17*, 923.
- (46) Ishiyama, T.; Miyaura, N. *Pure Appl. Chem.* **2006**, *78*, 1369.
- (47) Molander, G. A.; Sandrock, D. L. *Curr. Opin. Drug Discov. Devel.* **2009**, *12*, 811.
- (48) Darses, S.; Genet, J.-P. *Chem. Rev.* **2008**, *108*, 288.
- (49) Smith, Milton R., Maleczka, Robert E., Sabasovs, Dmitrijs, Oppenheimer, J. Methods for Producing Borylated Arenes. 20150361109, 2015.
- (50) Safronov, A. V.; Jalisatgi, S. S.; Hawthorne, M. F. *Inorg. Chem.* **2016**, *55*, 5116.
- (51) Kikuchi, T.; Nobuta, Y.; Umeda, J.; Yamamoto, Y.; Ishiyama, T.; Miyaura, N. *Tetrahedron* **2008**, *64*, 4967.
- (52) Brown, H. C.; Murray, K. J.; Murray, L. J.; Snover, J. A.; Zweifel, G. *J. Am. Chem. Soc.* **1960**, *82*, 4233.
- (53) Smith, Milton R. III; Malecza, Robert E. Jr; Kallepalli, Venkata A.; Onyeozili, E. Process for producing oxazole, imidazole, pyrazole boryl compounds. US2008091027, 2008.
- (54) Stiddard, M. H. B. *J. Chem. Soc.* **1962**, 4712.
- (55) Chénard, E.; Sutrisno, A.; Zhu, L.; Assary, R. S.; Kowalski, J. A.; Barton, J. L.; Bertke, J. A.; Gray, D. L.; Brushett, F. R.; Curtiss, L. A.; Moore, J. S. *J. Phys. Chem. C* **2016**, *120*, 8461.

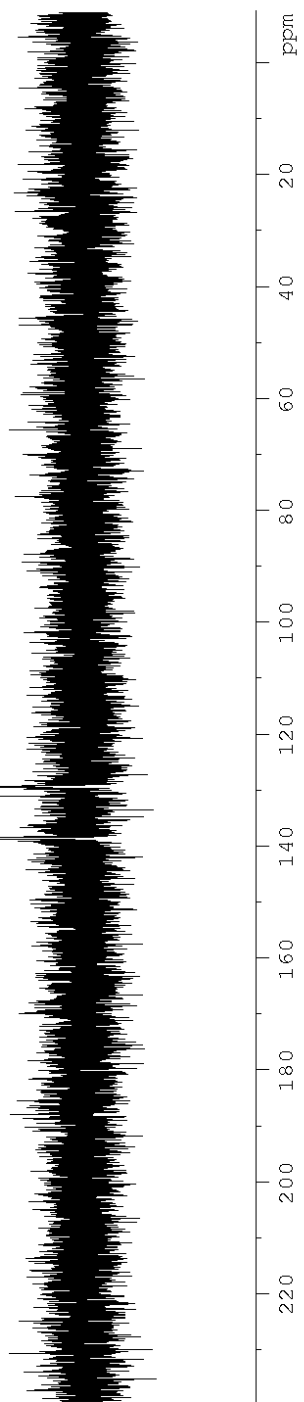
- (56) Chennamaneni, L. R.; William, A. D.; Johannes, C. W. *Tetrahedron Lett.* **2015**, 56, 1293.
- (57) Hawkeswood, S.; Stephan, D. W. *Dalt. Trans.* **2005**, 2182.

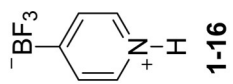
1.15 – NMR Spectra



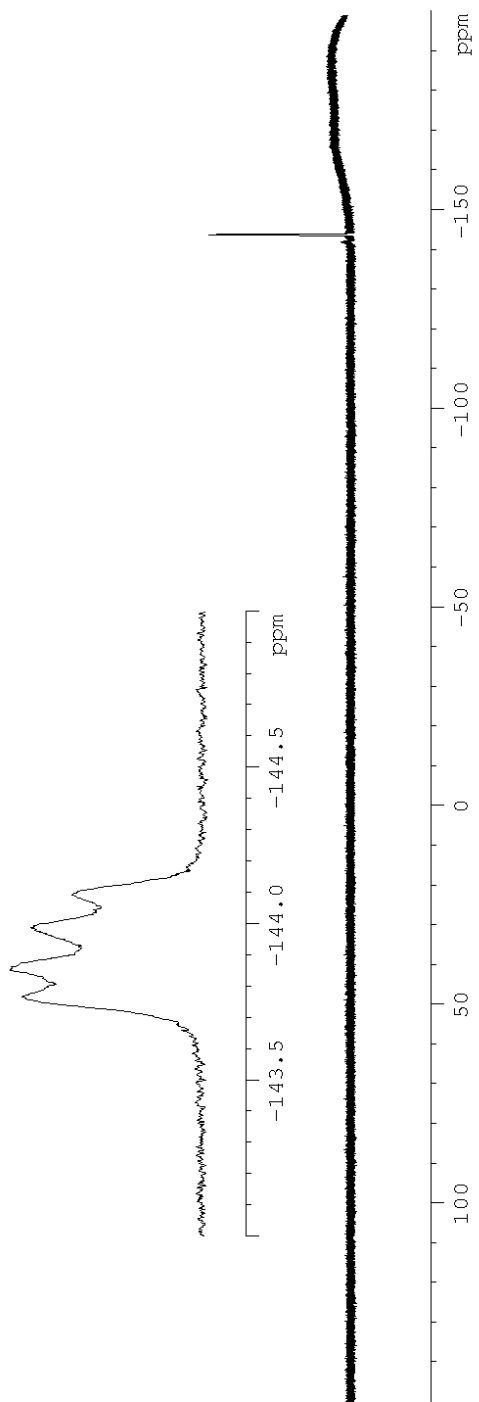


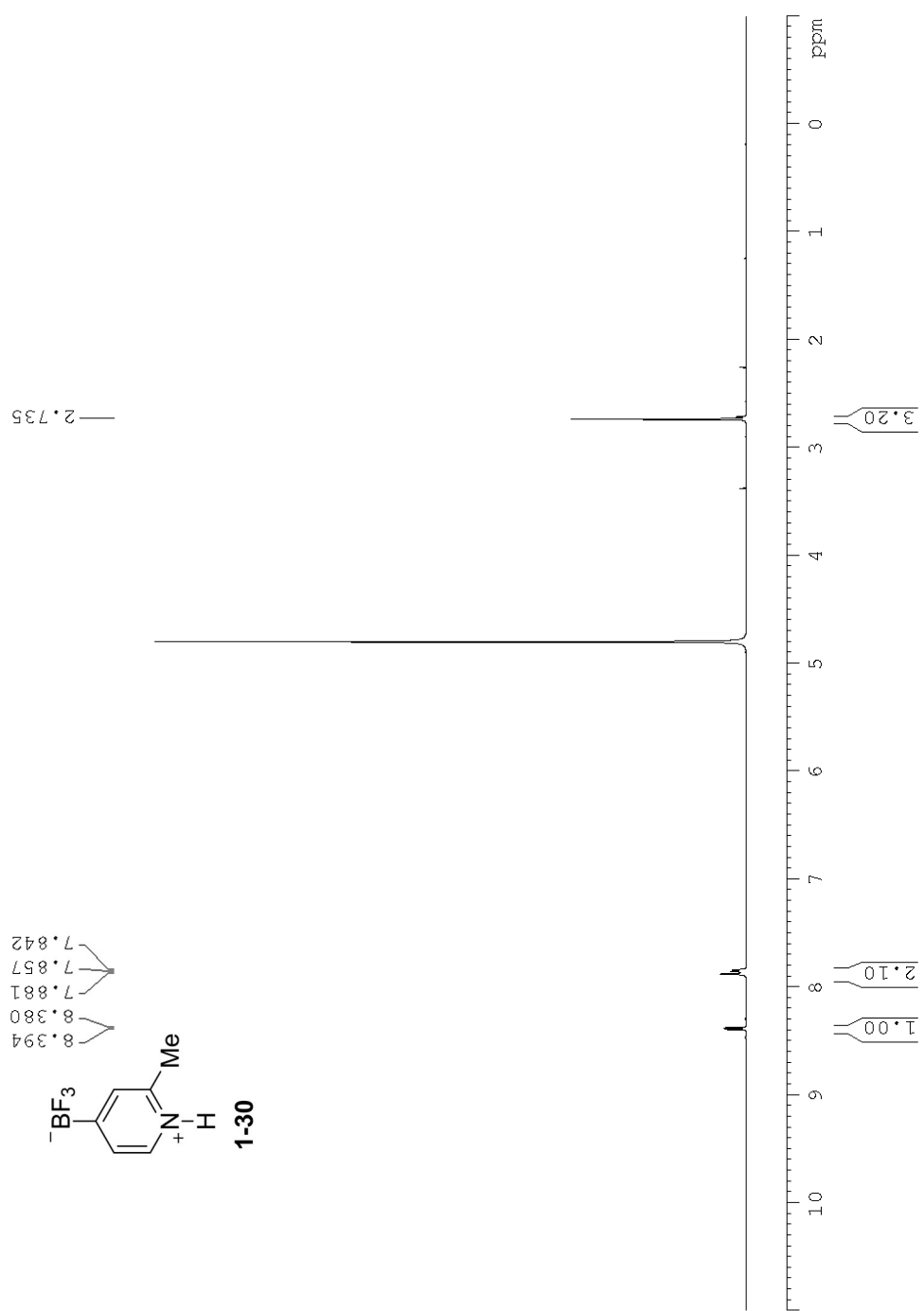
— 129.25
— 138.44

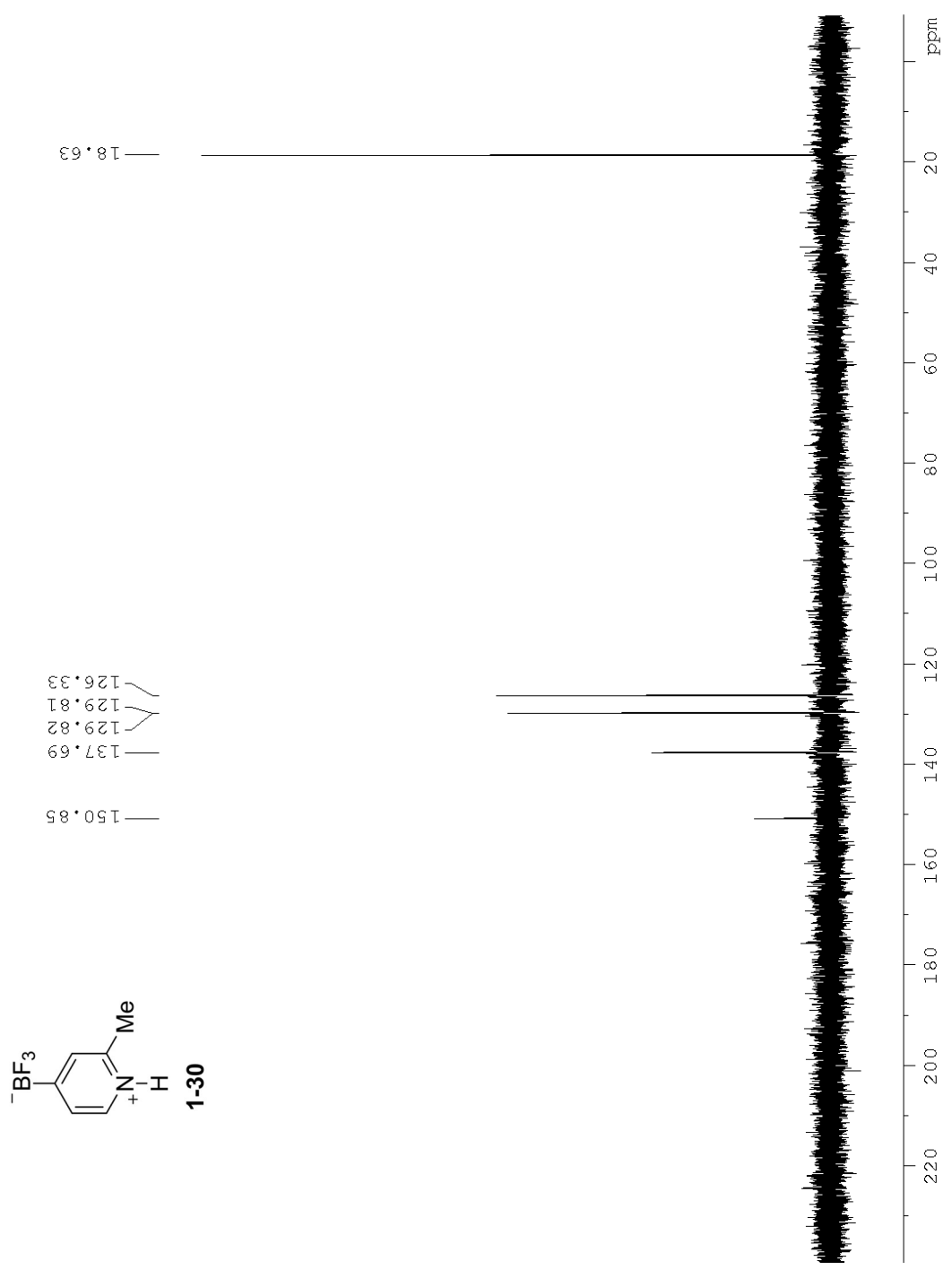


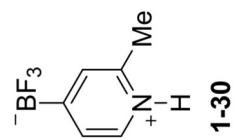


-143.77
-143.85
-143.99
-144.09

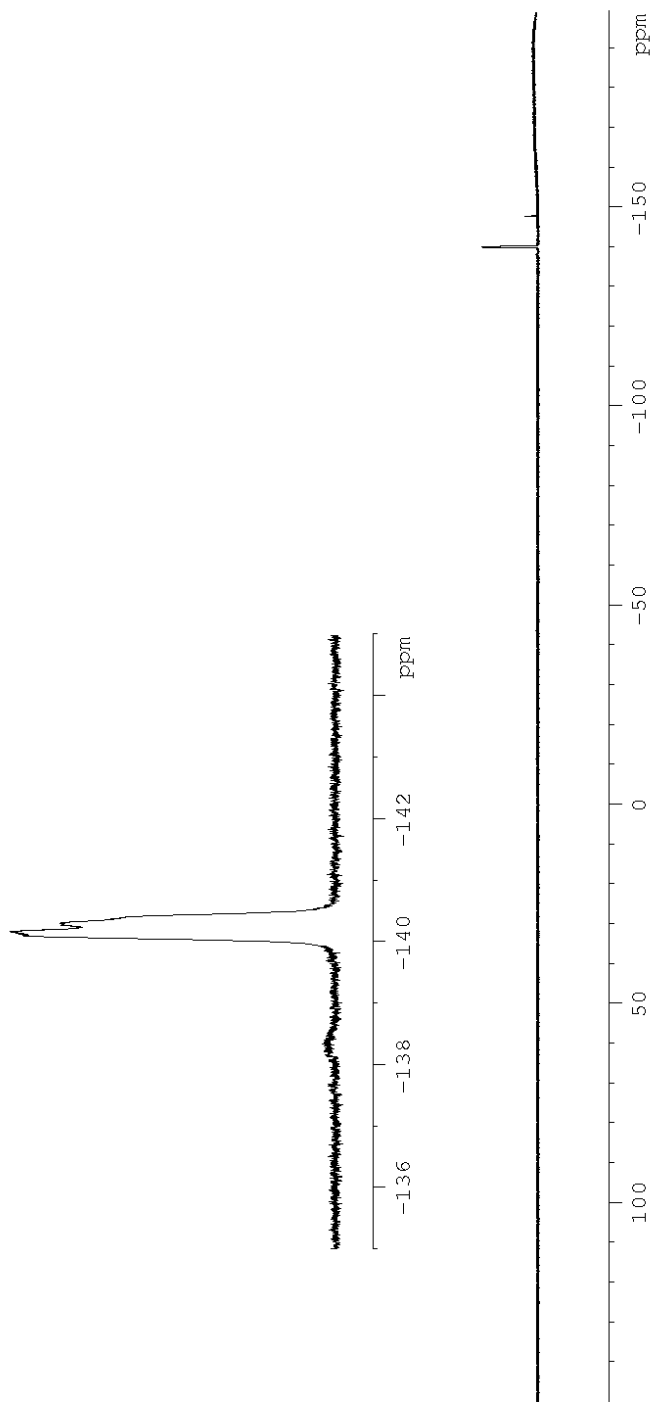


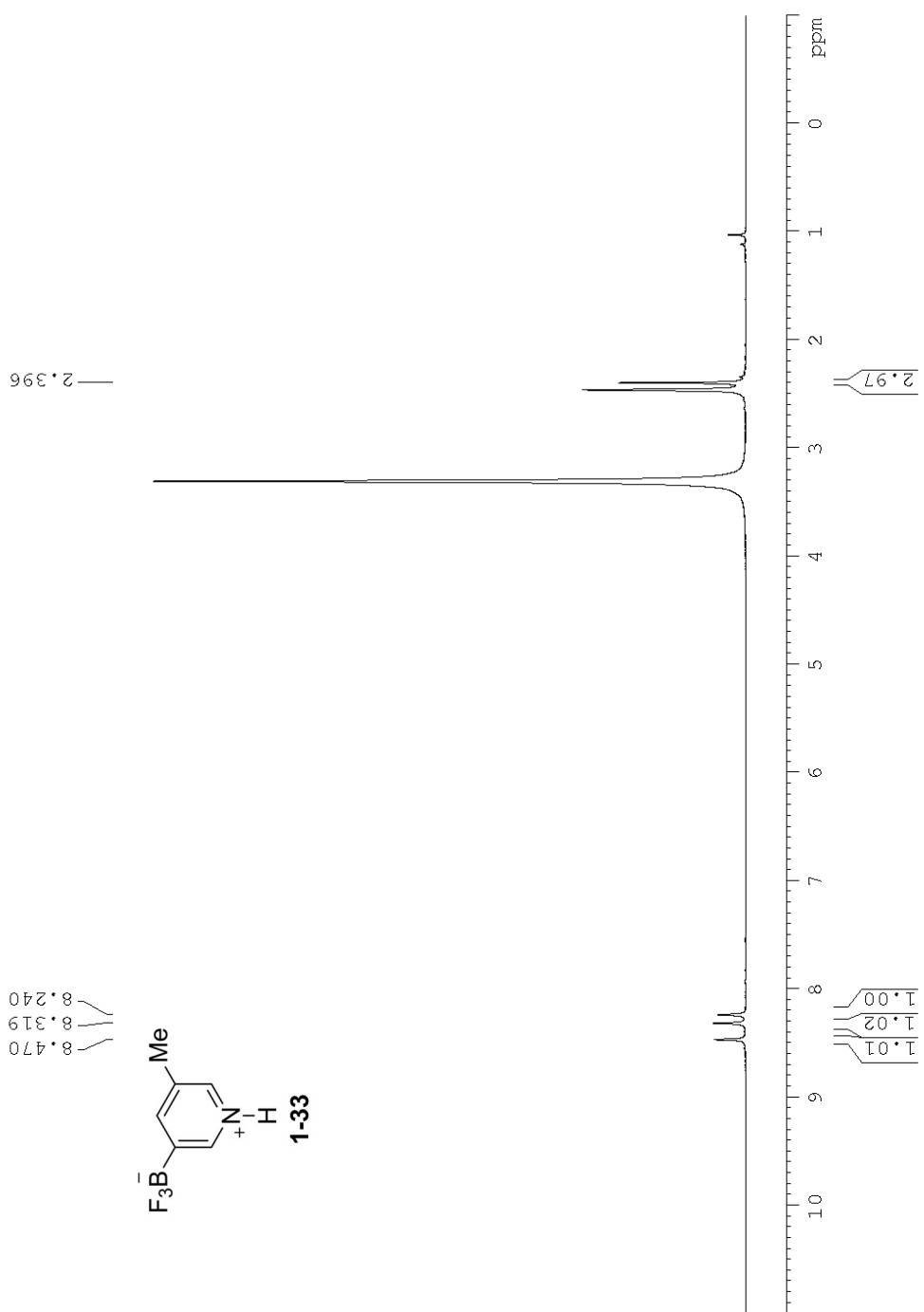


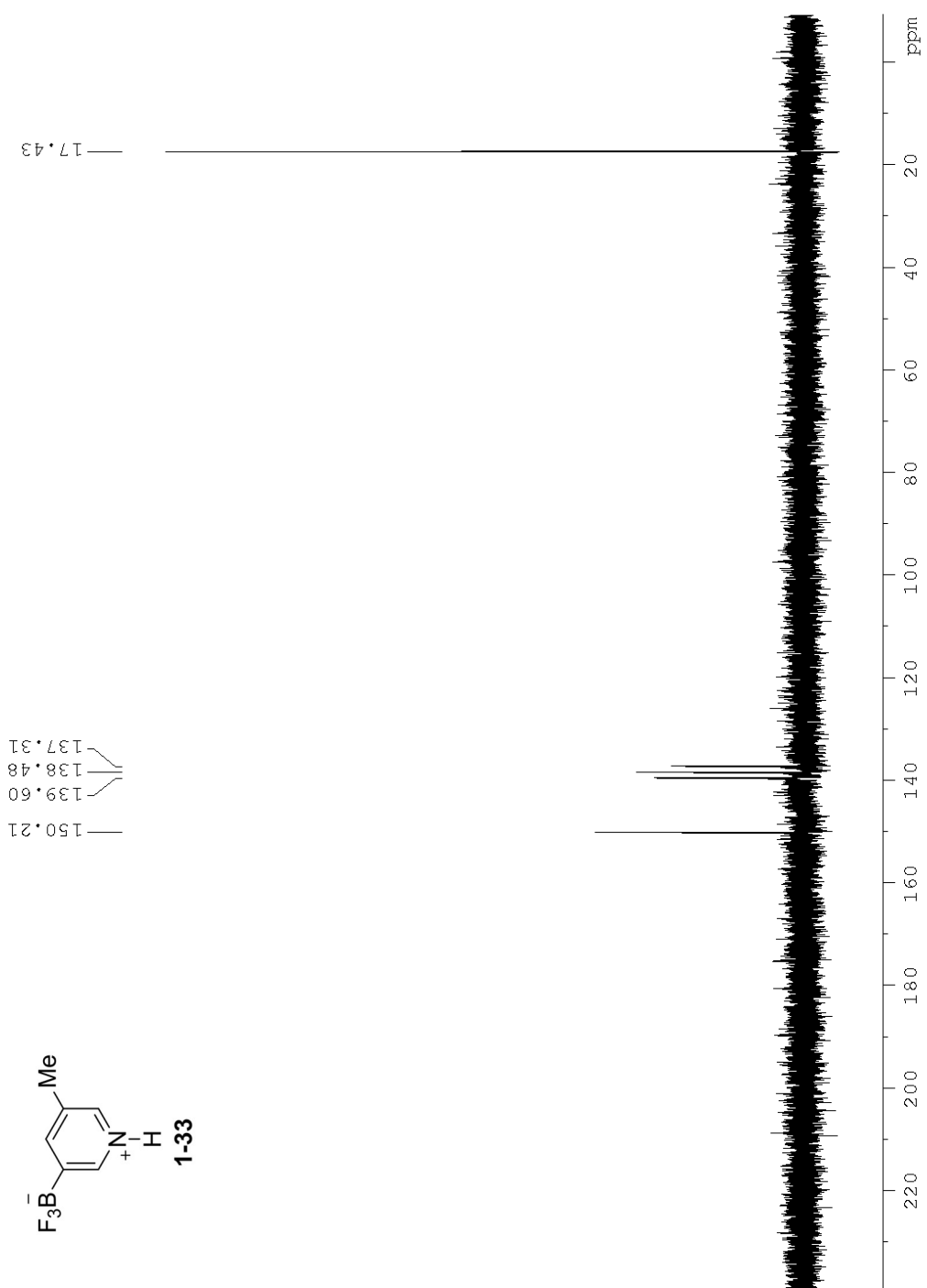


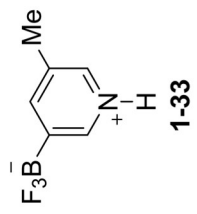


-140.17
-140.31

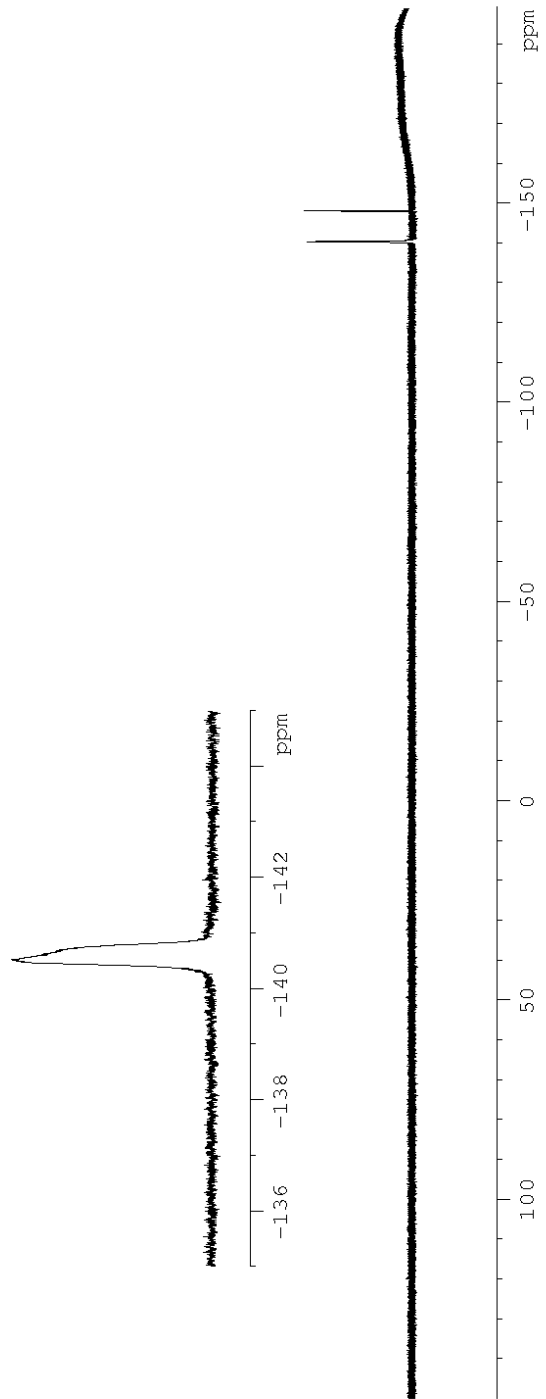


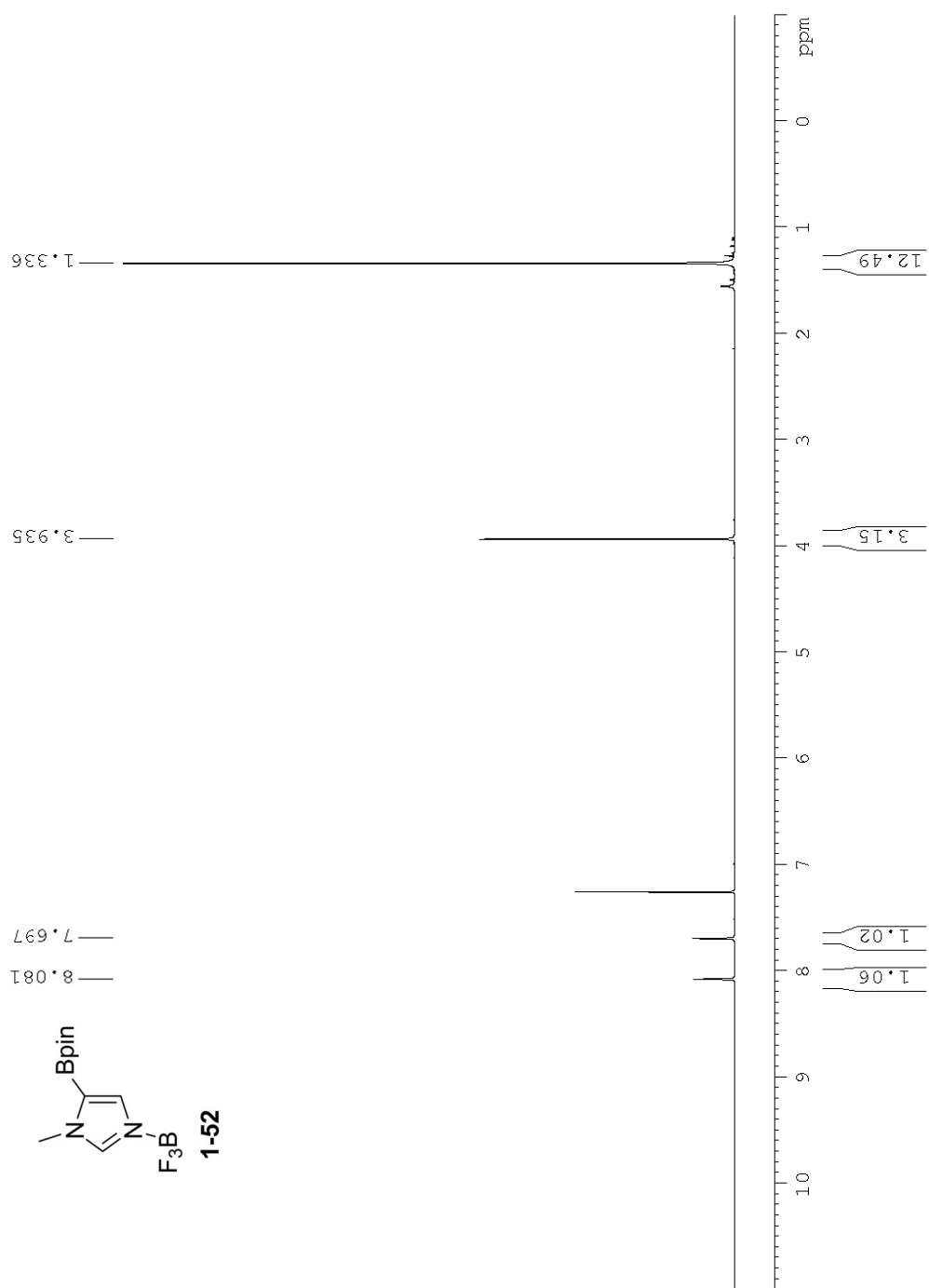


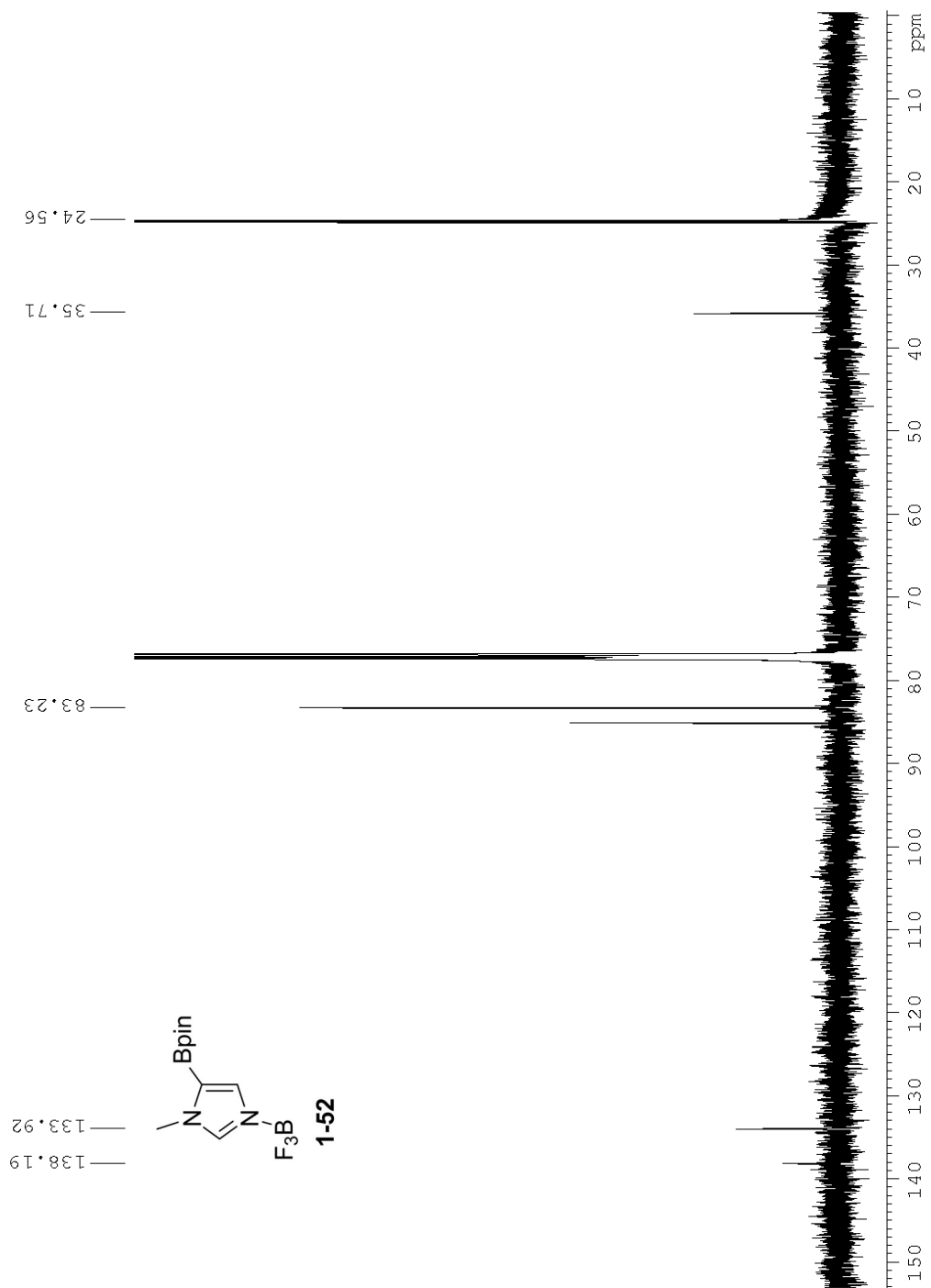


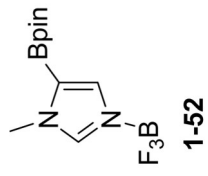


—140.52

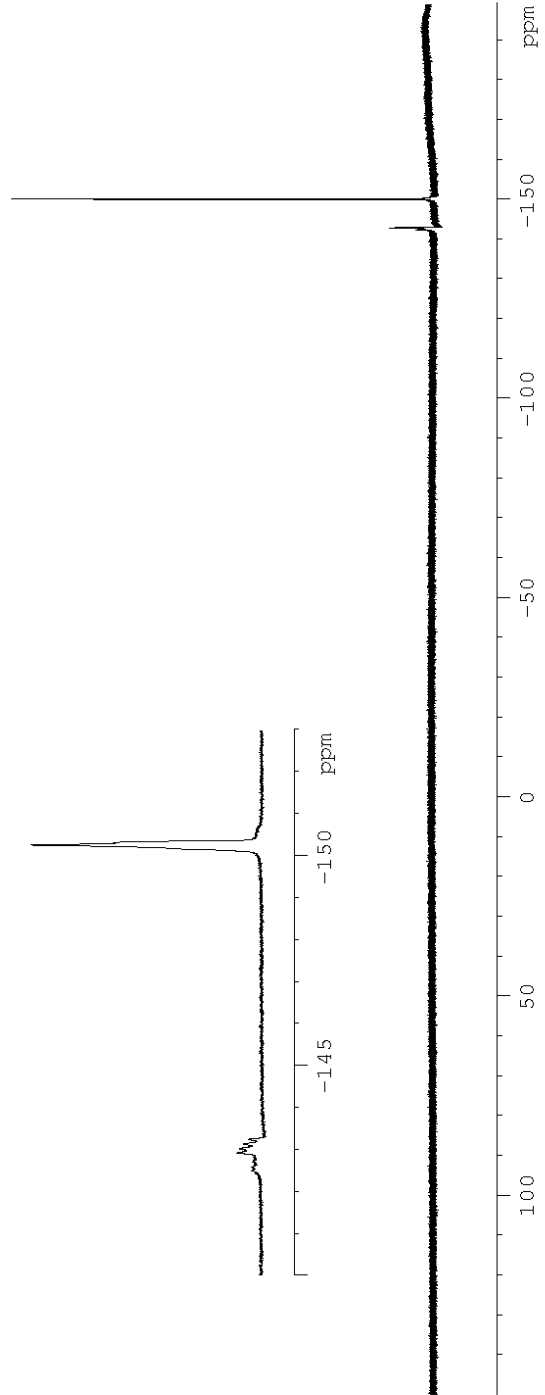


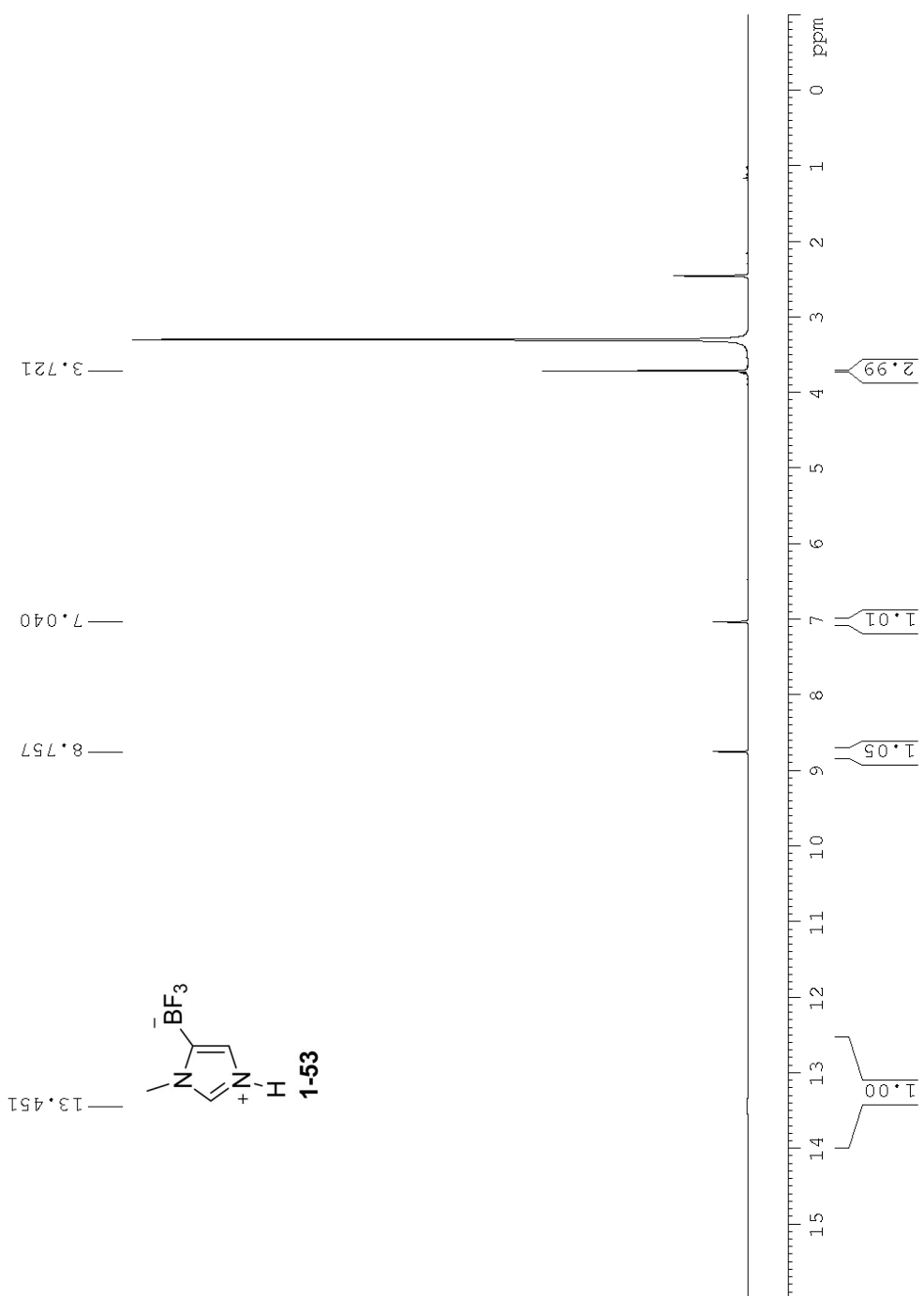


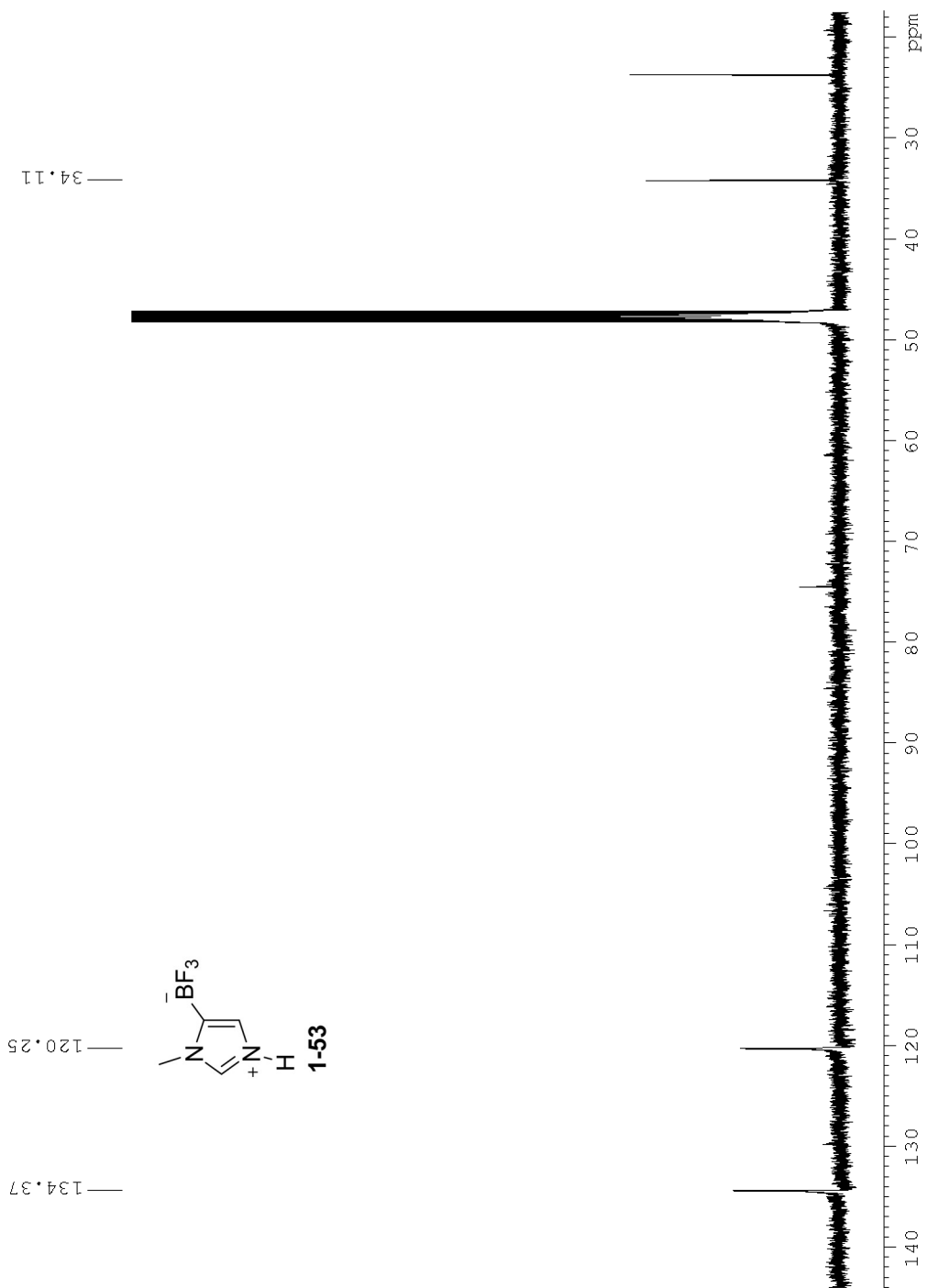


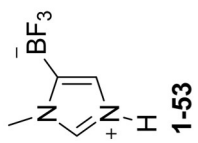


—150.27

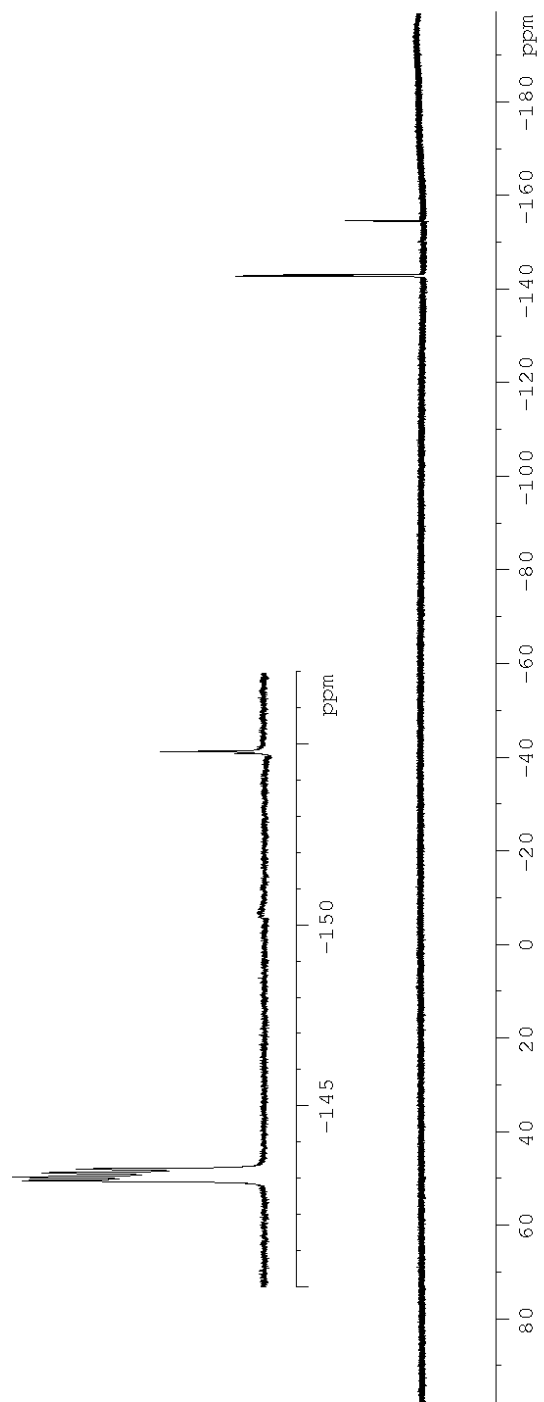


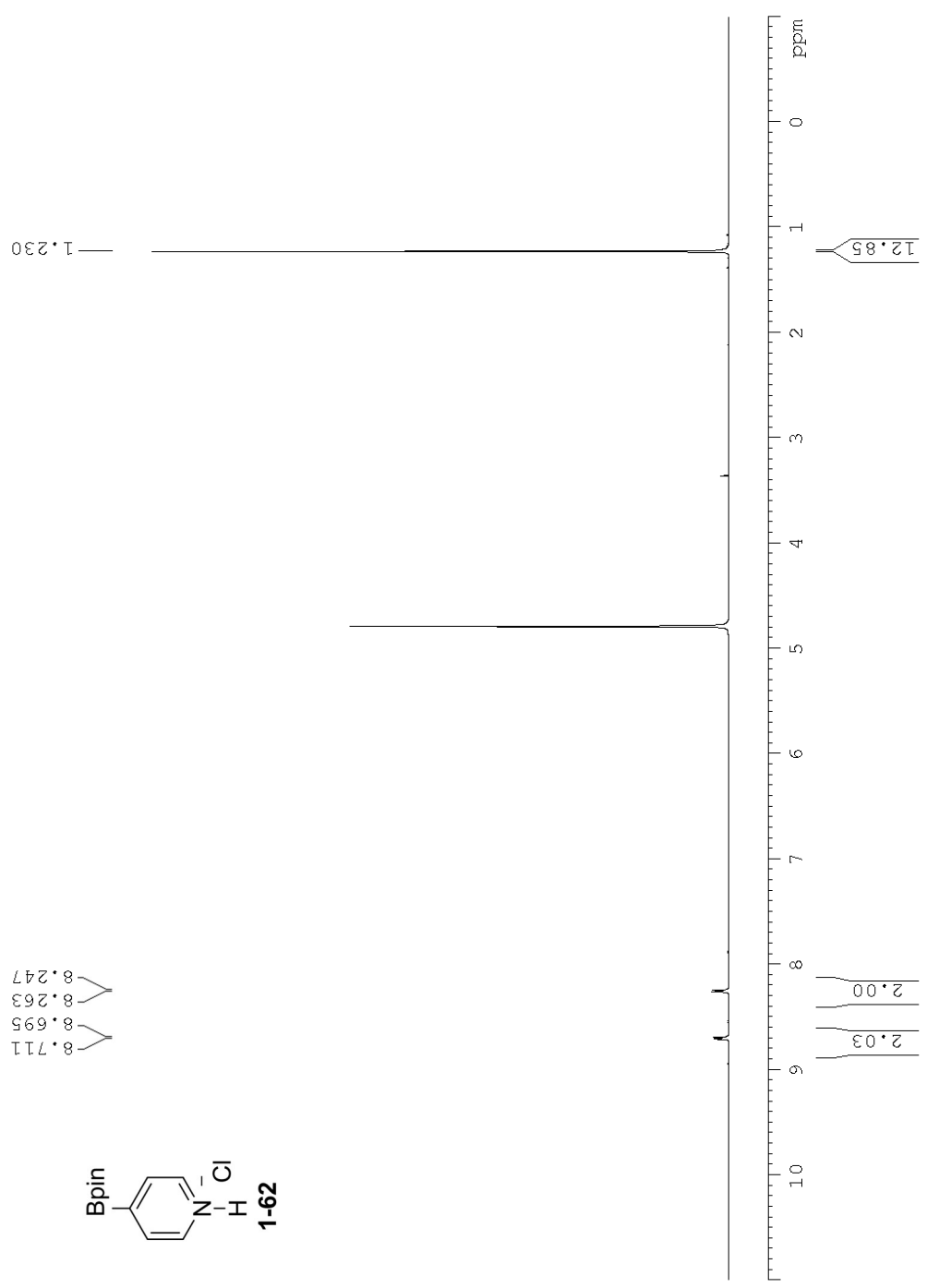


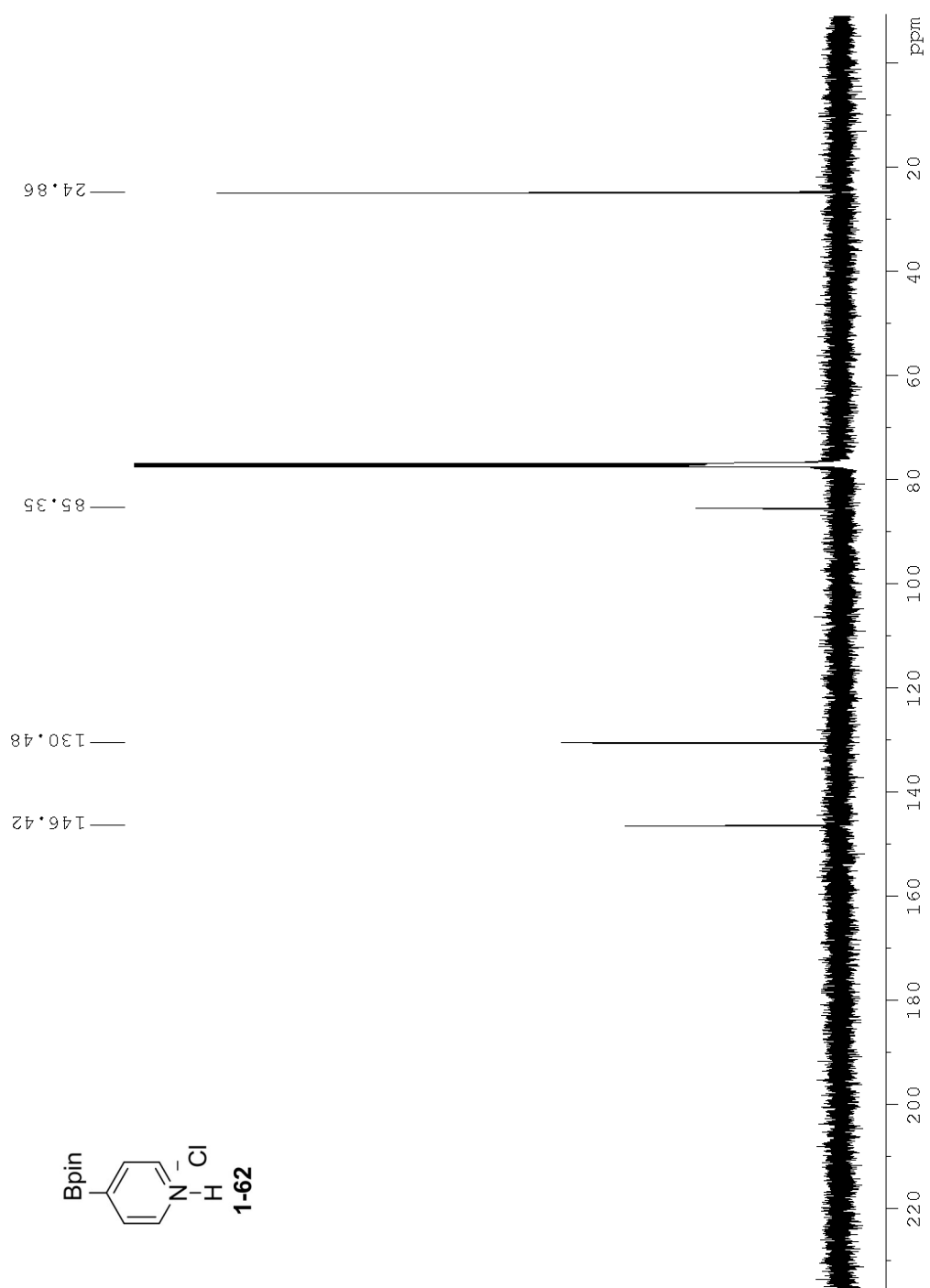


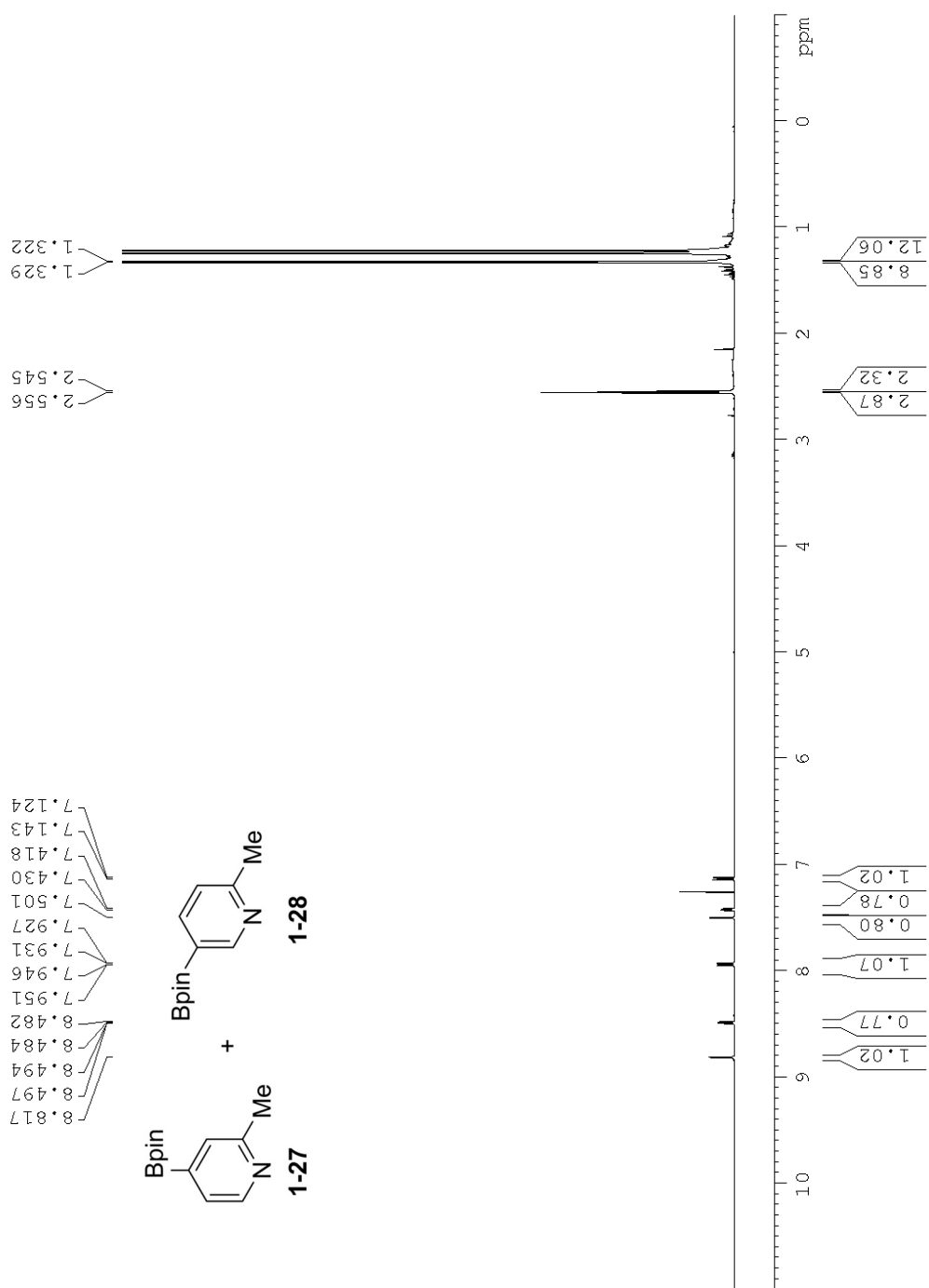


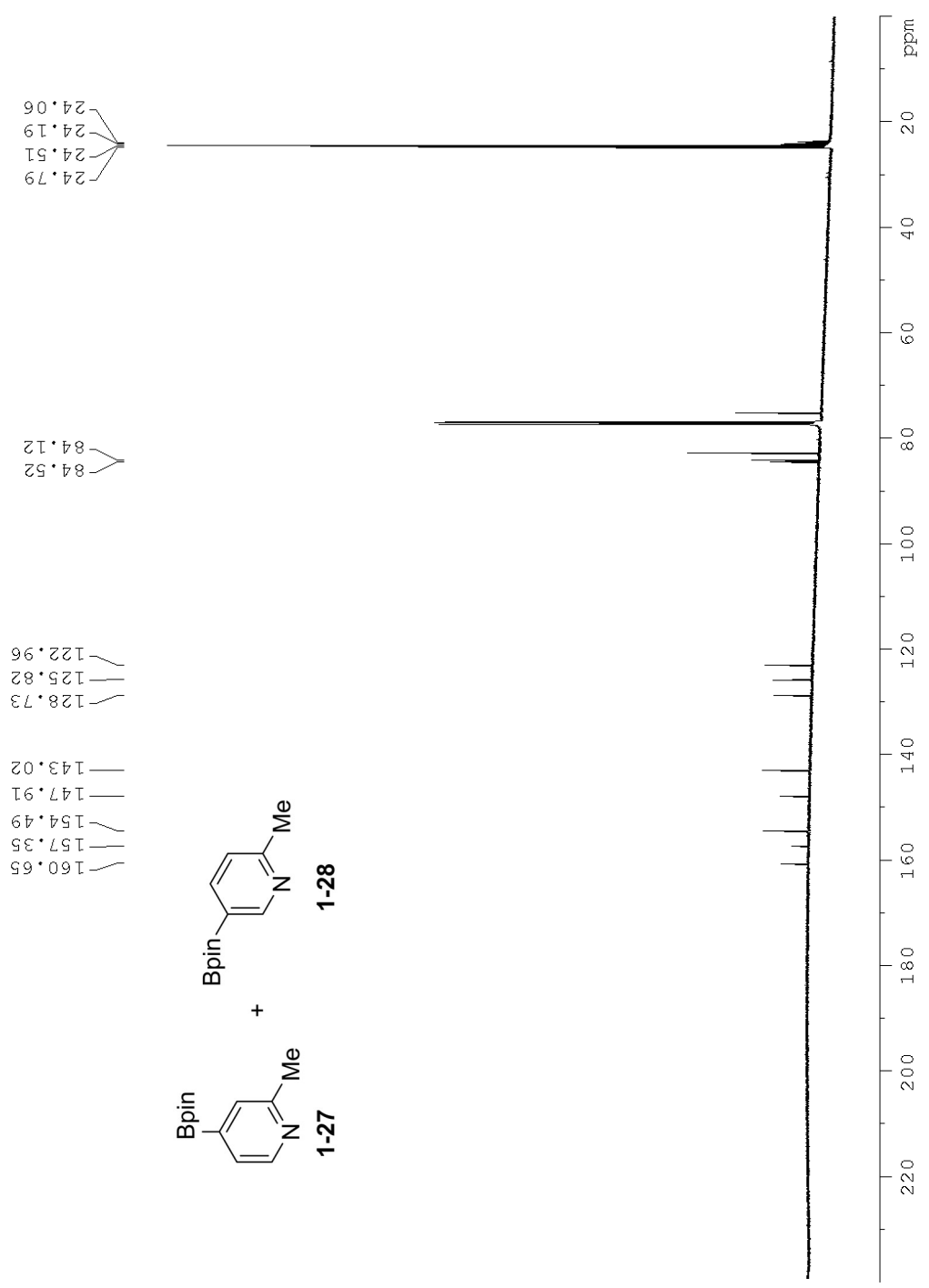
-142.95
-143.05
-143.16
-143.27

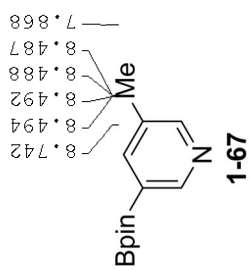
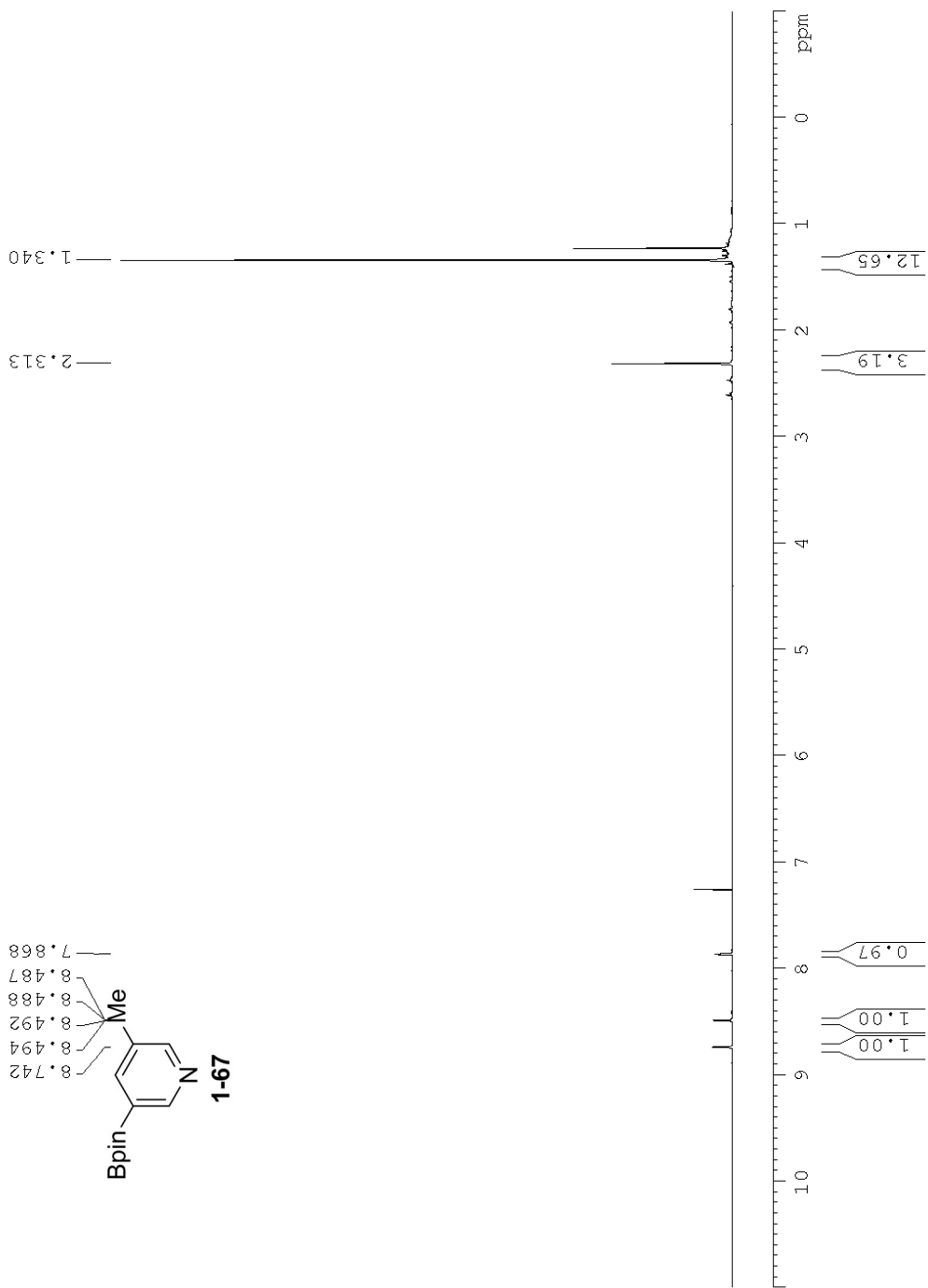


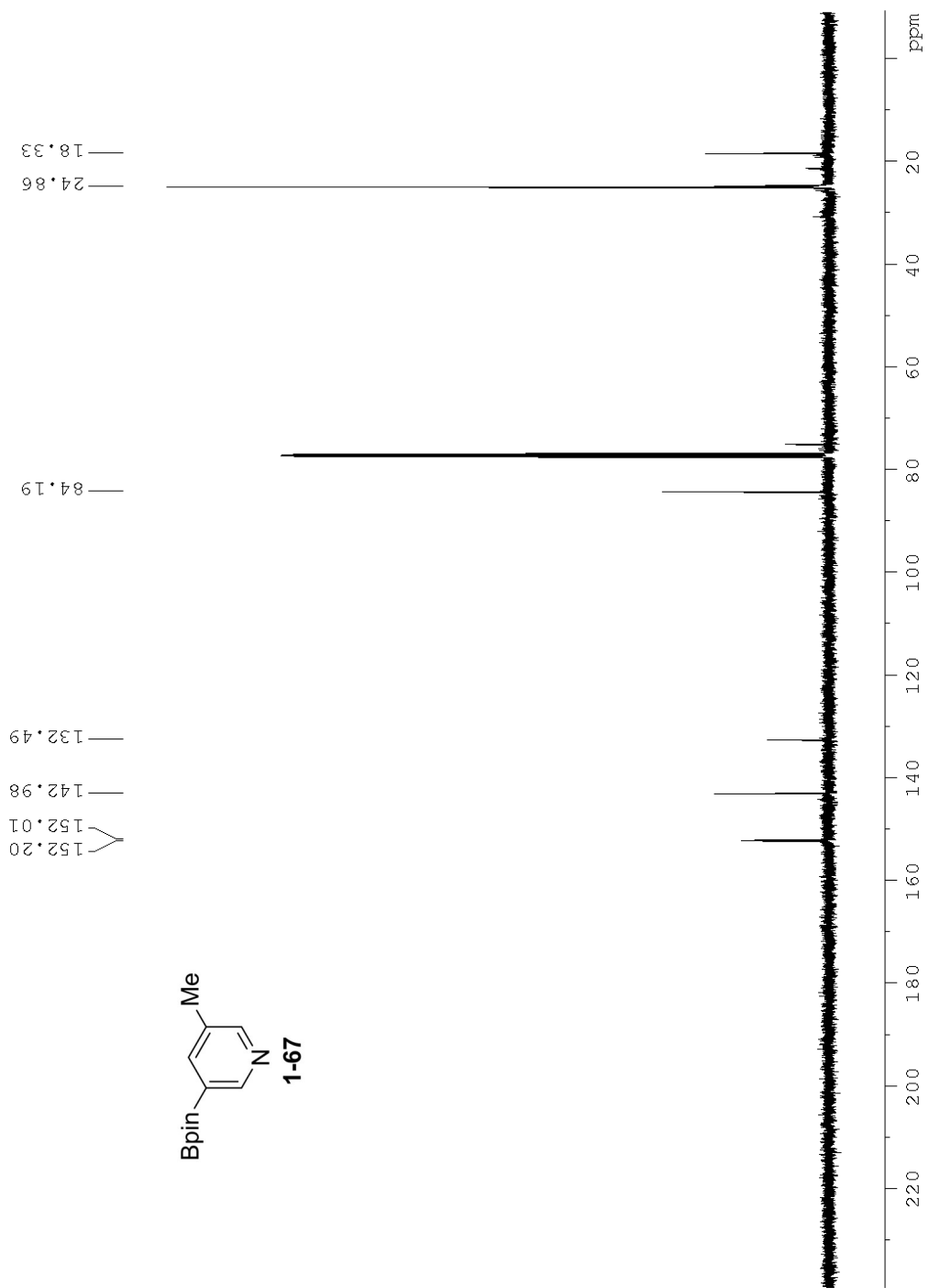


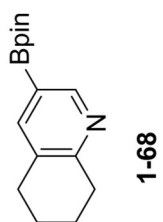
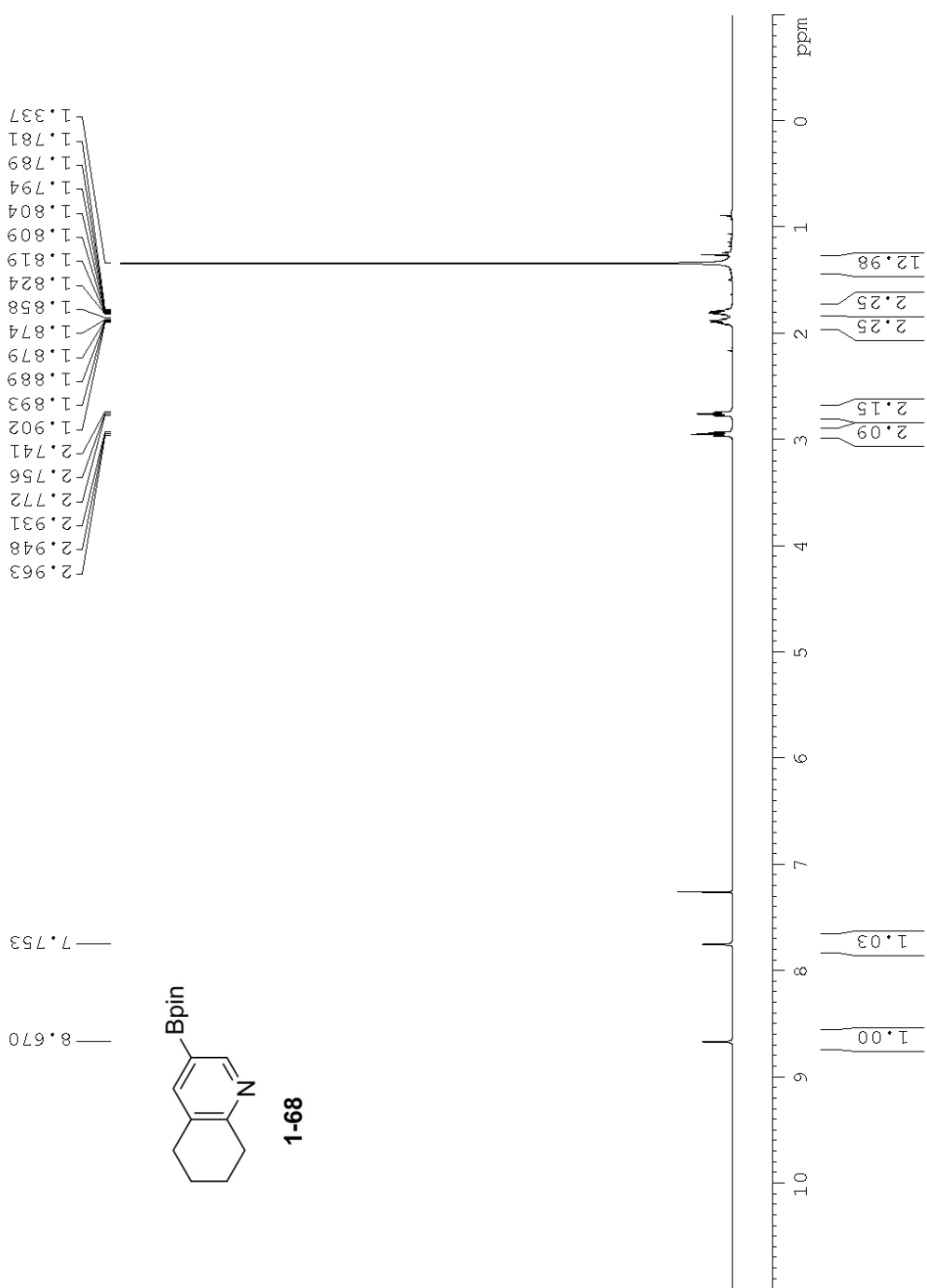


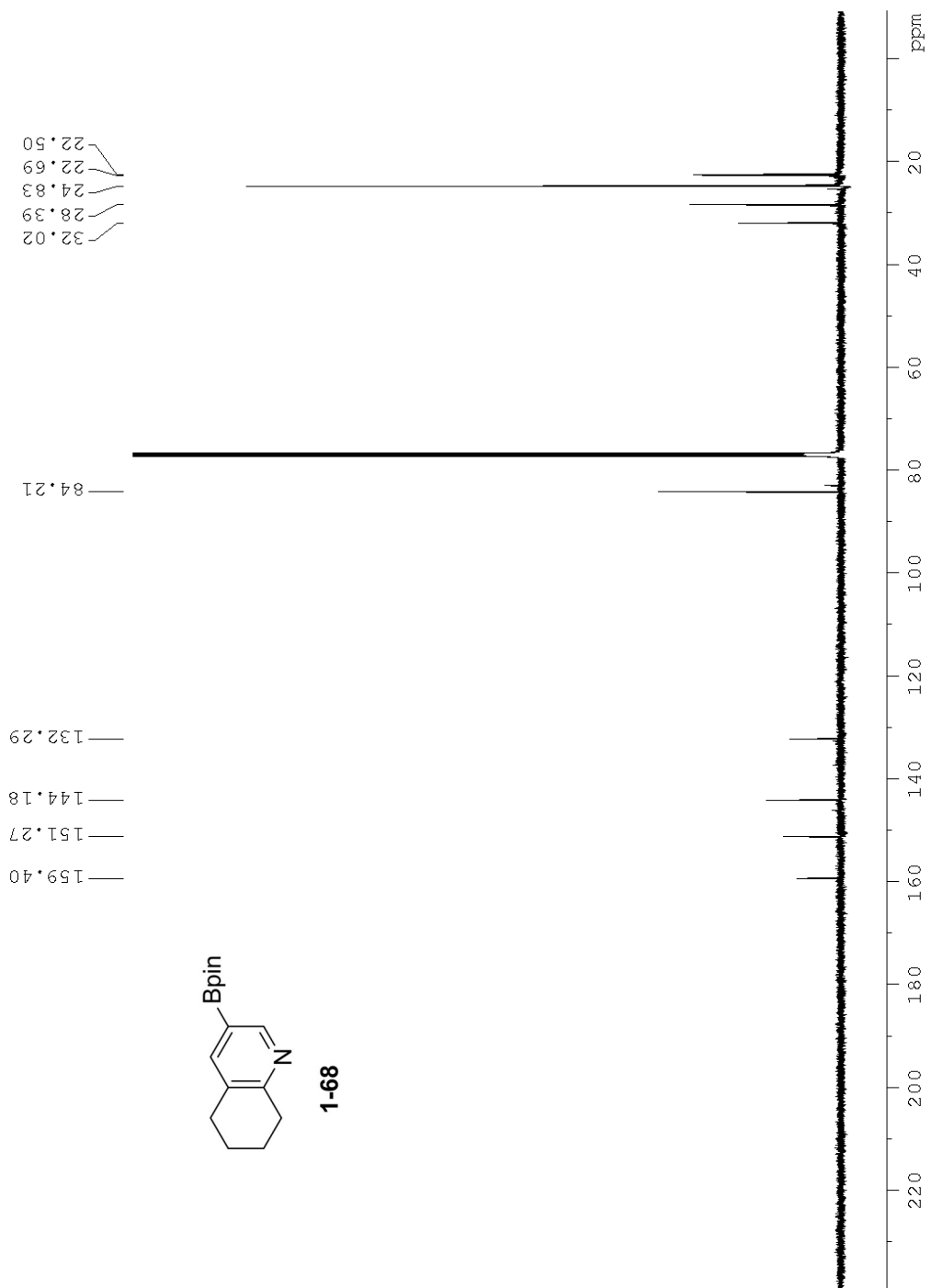


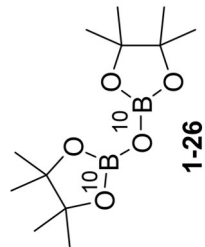




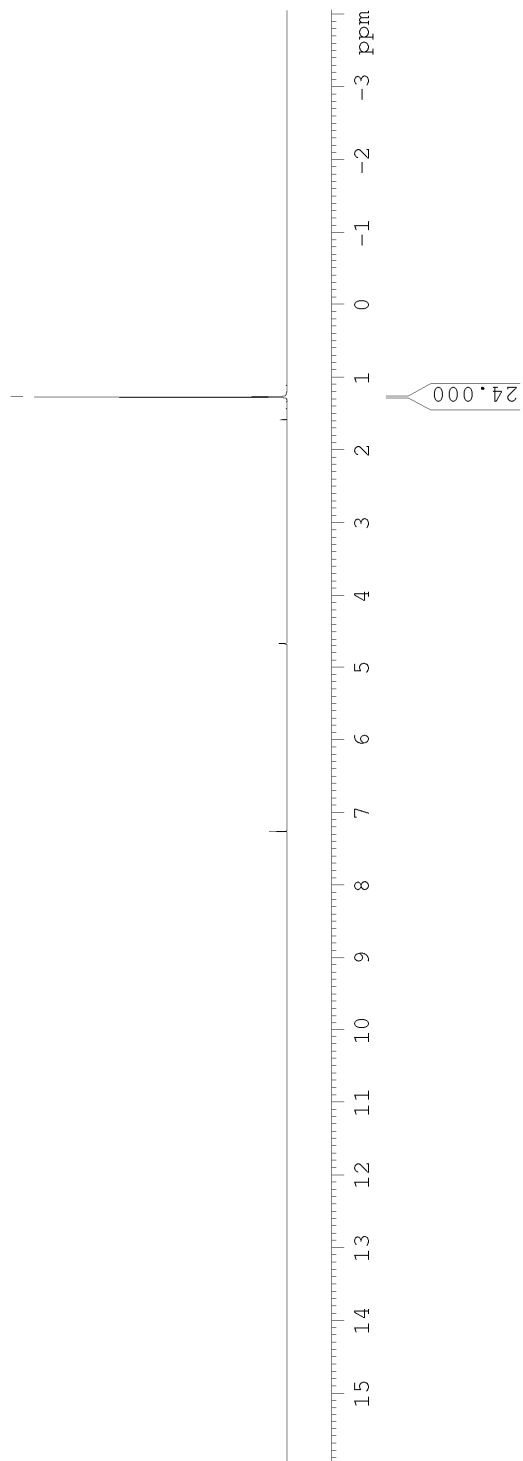


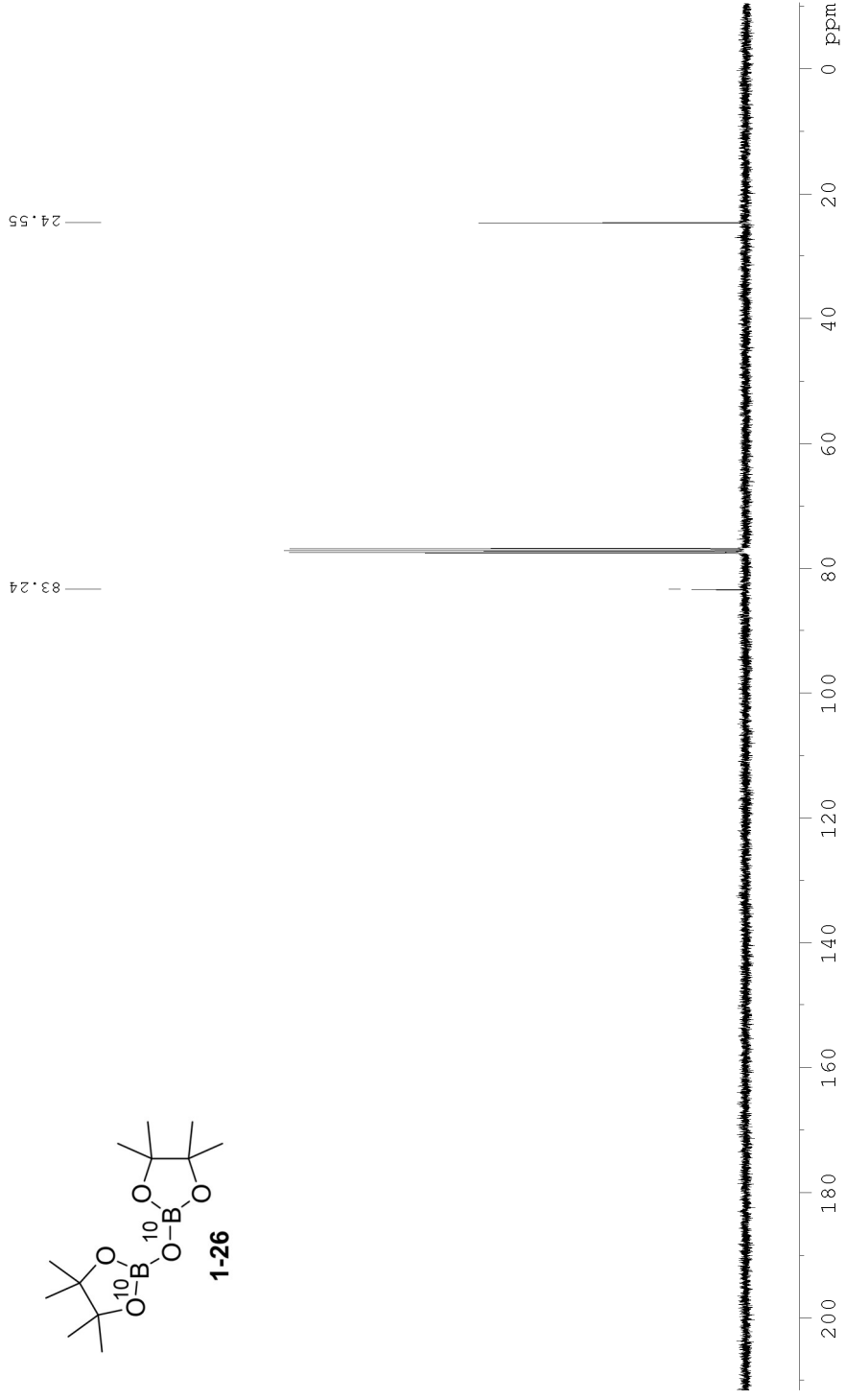
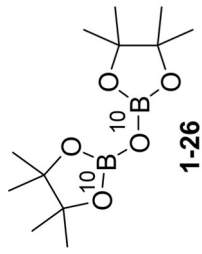


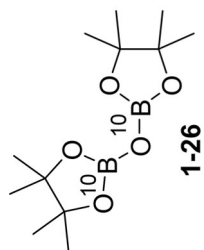




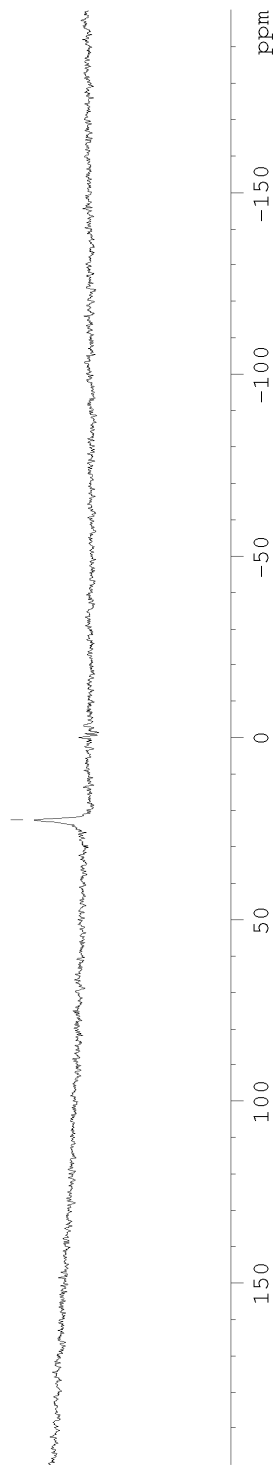
1.27

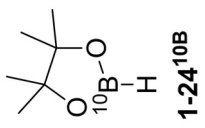
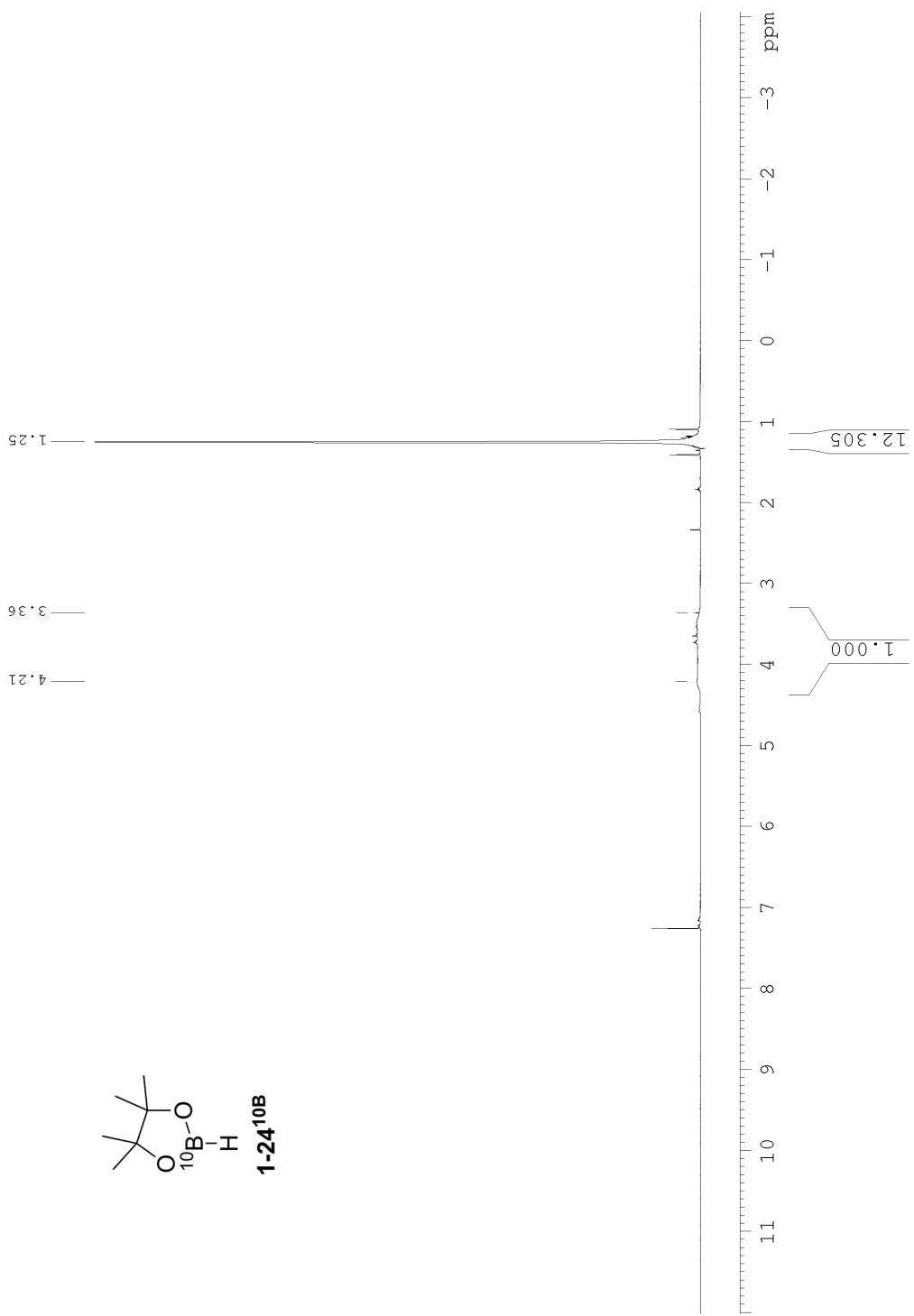


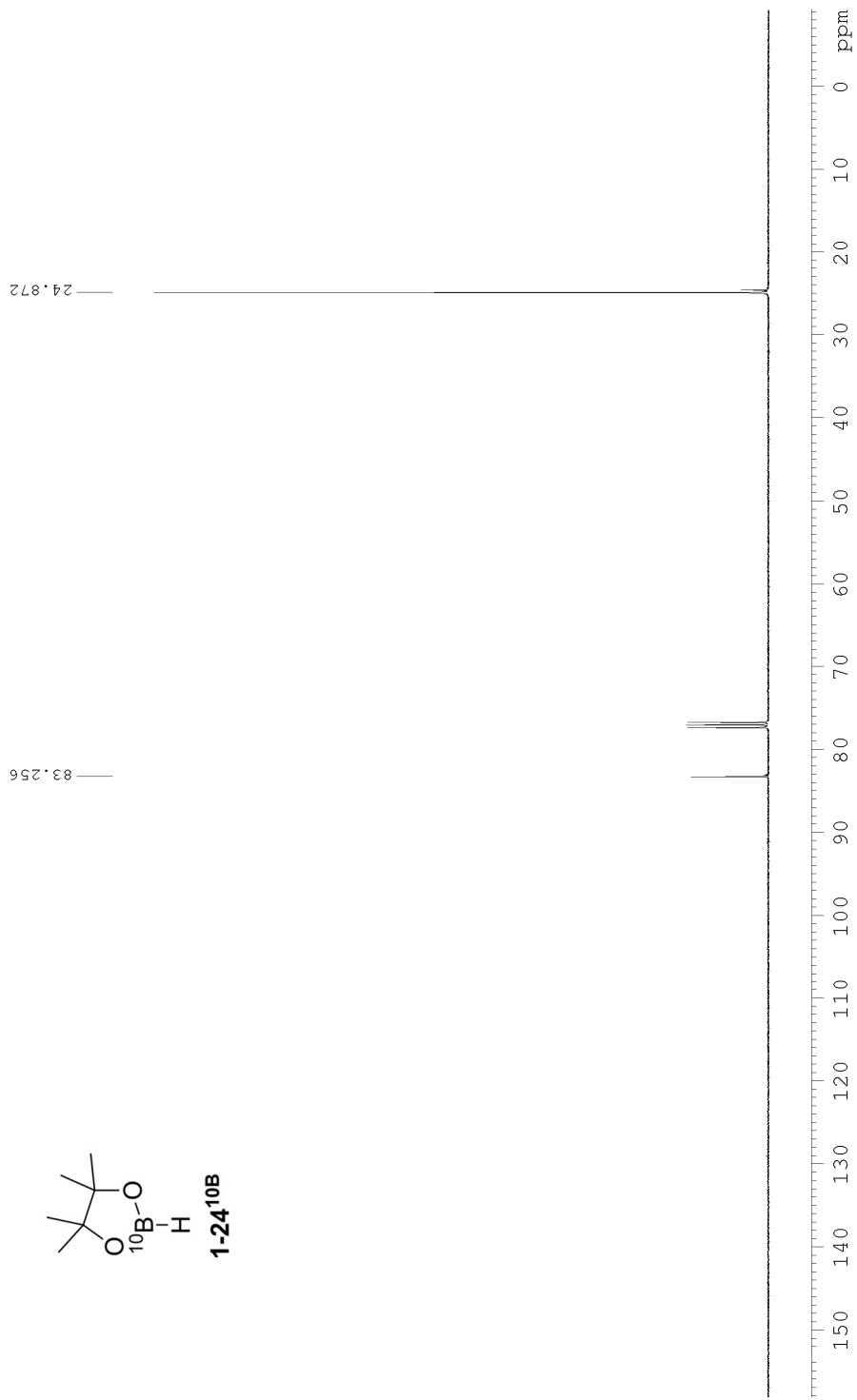
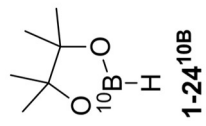


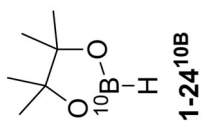


22.63

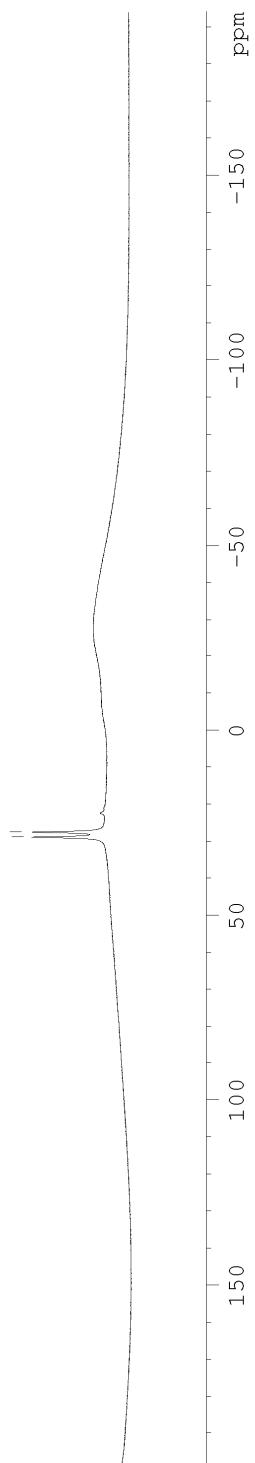








28.82
27.45



Chapter II – Synthesis of Alkyne and Allene Ligands for Copper-Promoted Vinyl Ether Synthesis

2.1 – Background and Introduction

A key advantage of transition-metal catalyzed reactions is the ability to choose from a vast collection of ligands to pair with the metal. Subtle changes to ligand structure can have a dramatic impact on the reaction outcome, making the choice of ligand equally as important as the choice of metal. This fact is perhaps best demonstrated by the wide array of phosphine ligands that are commercially available. As of June 2018, over 200 phosphine ligands were for sale in Sigma Aldrich's catalog alone. Despite perhaps being thought of as “non-traditional” ligands, π -base ligands, such as alkenes and alkynes, have a rich and robust history. In fact, one of the first organometallic complexes ever prepared, Zeise's salt, is an alkene-platinum complex (Figure 2-1).¹

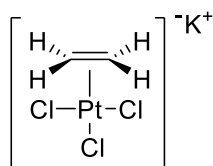


Figure 2-1 – Structure of Zeise's salt, first prepared in 1827.

A well-recognized explanation of the geometry and energetics of the binding of olefins to metals was proposed in the 1950s by Dewar, Chatt, and Duncanson.²⁻⁴ The model describes two simultaneous orbital interactions that enable association of a π -bond to the metal center: (1) sigma-donation from the olefin's HOMO to the metal and (2) π -donation (backbonding) from the metal to the olefin's LUMO. Because of these interactions, the bound olefin experiences a disruption from its native geometry. Namely, the π -ligand will partially rehybridize to an increased amount of p-character. This model predicts that the factors controlling the binding

affinity of a given π -bond can be quite varied. In 1973, Tolman undertook a detailed study of the effects of ring strain, steric environment, and electronic nature of various olefins on binding equilibrium constants between a π -ligand and a nickel(0)-phosphine complex (Table 2-1).⁵ The author showed that electron-deficient olefins bound more tightly, likely a consequence of their lowered LUMO and increased backbonding. Cyclic maleic anhydride was an especially strong ligand. Among the simple cyclic alkenes, norbornene was the only compound to exhibit a favorable equilibrium to the metal-olefin complex, a consequence of relieved ring strain upon binding.

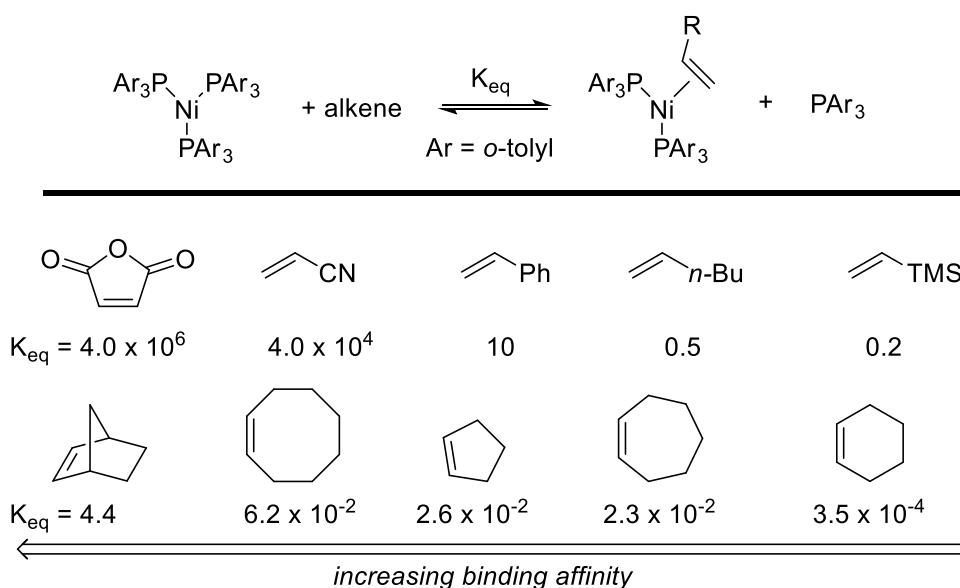
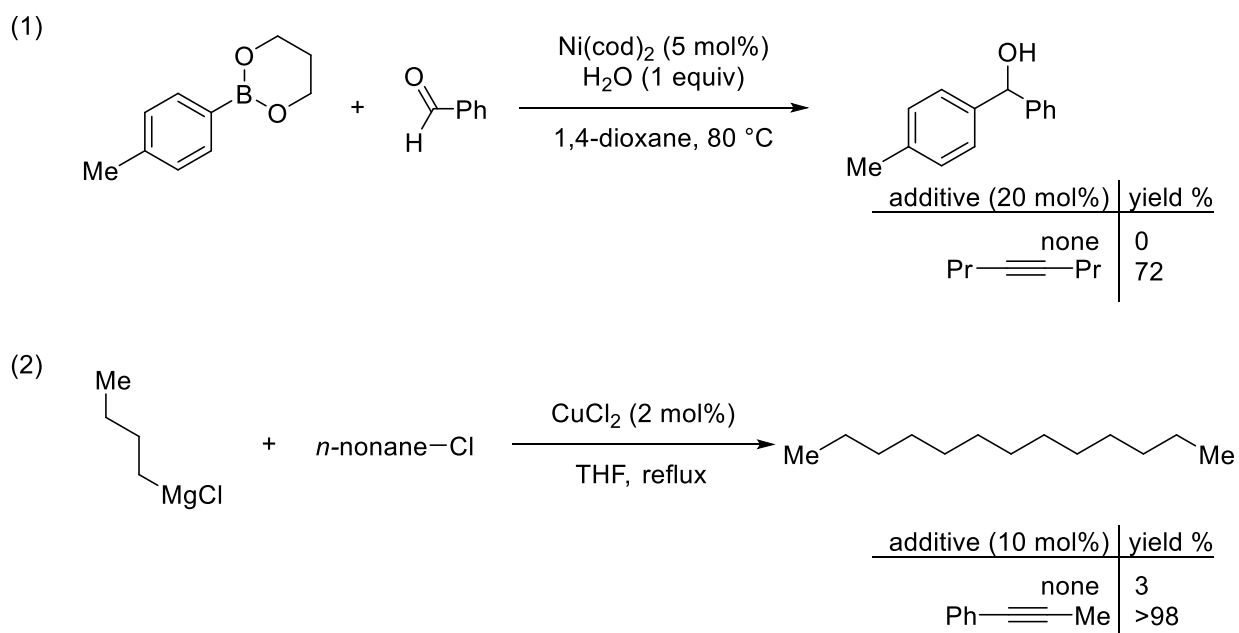


Table 2-1 – Binding affinities of various alkenes with a Ni-complex.

There are many transition-metal catalyzed transformations that possess altered reactivity or selectivity in the presence of π -bonds. A 2008 review by Rovis⁶ provides many examples of the effects of added π -bases to transition-metal mediated reactions. Among the examples reviewed, it's clear that while alkenes are well-studied as ligands, there is a relative dearth of examples of reactions benefitting from added alkynes and especially allenes.

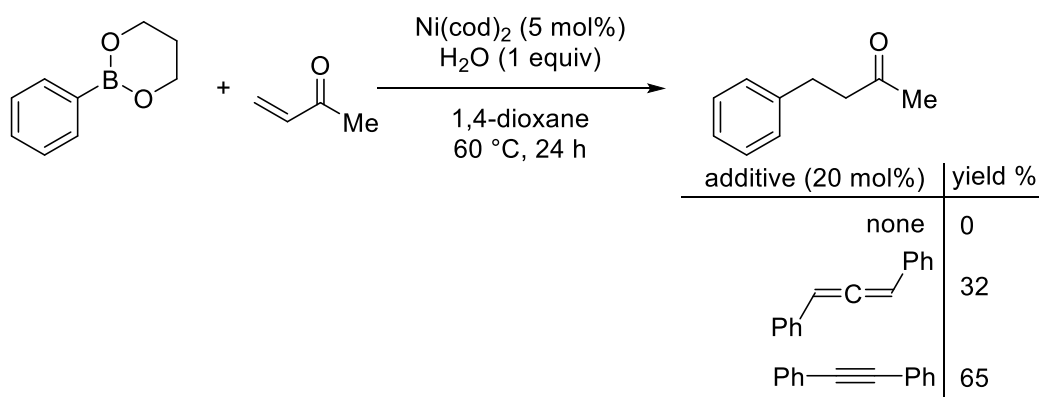
Examples of alkynes being used as additives to improve transition metal-catalyzed reactions are rare. In 2005, Eiji et al. reported that Ni-catalyzed addition of boronates to aldehydes was facilitated by addition of diphenylacetylene (Scheme 2-1, line 1).⁷ When the reaction was attempted in the absence of alkyne, no product was formed. However, with alkyne additive, the authors were able to achieve a 72% isolated yield. The authors noted that other commonly used ligands, such as phosphines, failed to produce products. A 2007 report by Kambe demonstrated a remarkable effect of 1-phenylpropyne on a copper-promoted coupling reaction of alkyl halides and Grignard reagents (Scheme 2-1, line 2).⁸ Without the π -base additive, the reaction only gave a 3% coupling yield, but with the additive, yields were greater than 98%. Mechanistically, the authors suggested that the alkyne may act to bind and prevent decomposition of an unstable Cu(I) intermediate.



Scheme 2-1 – Examples of alkynes used as additives in a Ni- and Cu-catalyzed reaction.

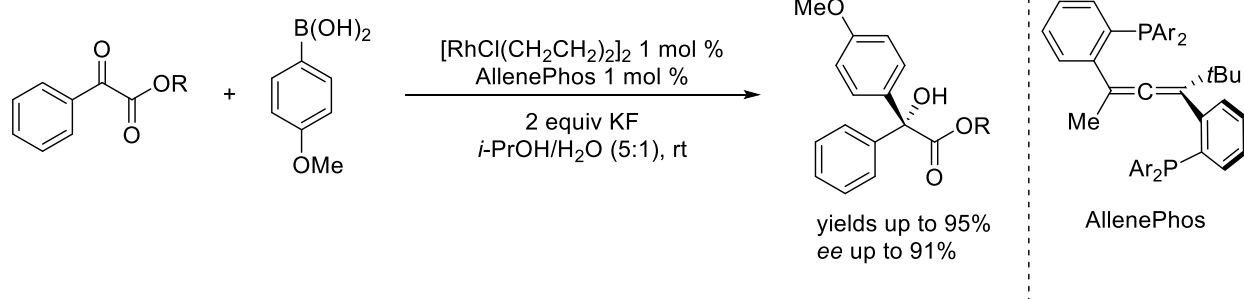
Examples of allenes as beneficial additives to transition-metal mediated reactions are extremely rare. One such example was reported as a follow-up to Eiji et al.'s Ni-catalyzed

addition of boronates to aldehydes. In this 2006 report, the conditions were extended to enable boronate additions to α,β -unsaturated carbonyl compounds.⁹ Although ultimately an alkyne ligand proved most effective, the authors did demonstrate a significant improvement in yield using an allene ligand (Scheme 2-2).



Scheme 2-2 – Allene additive improving the yield of Ni-catalyzed addition of boronates to α,β -unsaturated carbonyls

In 2011, Ready et al. synthesized and used a chiral allene-phosphine ligand, AllenePhos, in a Rh-catalyzed addition of boronic acids to α -keto esters (Scheme 2-3).¹⁰ Although the allene was designed as an axially-chiral scaffold to facilitate asymmetric induction by the ligand, the authors discovered it was not an innocent bystander. Platinum was found to react with the allene and destroy it, forming a Pt-C bond. In the case of rhodium, the authors suggested the metal's interaction with the allene was important for both catalysis and asymmetric induction. Specifically, crystal structure data showed the Rh-catalyst engaging the less hindered olefin of the allene (methyl over *tert*-butyl) in a L-type linkage. This suggests the allene in AllenePhos not only provided the chiral backbone, but also assisted in creating a deep chiral pocket for the catalyst via chelation.

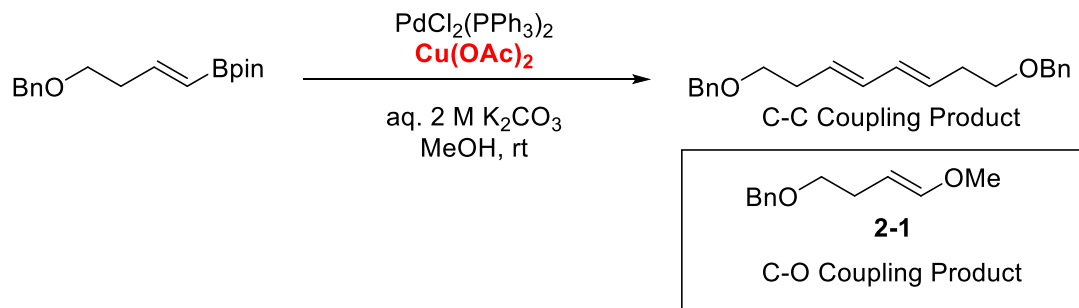


Scheme 2-3 – Example of allene-phosphine ligand AllenePhos involved in Rh-catalyzed asymmetric addition of boronic acids to α -keto esters.

Because of the critical role that ligands play in transition-metal mediated reactions, use of non-traditional π -bases as ligands provides a new path to discovery. Alkynes, and especially allenes, represent an underutilized class of ligands with a bright outlook. Moving forward, organometallic chemists should continue to be cognizant of the often-beneficial effects of π -bonds, both when present within their substrates or as ligands.

2.2 – Synthesis of Alkyne and Allene Ligands for Copper-Promoted Vinyl Ether Synthesis

While studying palladium-catalyzed oxidative couplings¹¹ of vinylboronates, our group observed a fascinating vinyl ether side-product **2-1** upon screening copper(II) acetate as a stoichiometric oxidant (Scheme 2-4). This product, the result of C-O coupling of the vinyl boronate with methanol solvent, was believed to have been formed via a Chan–Evans–Lam type copper-promoted oxidative coupling.^{12–14} Because vinyl ethers are valuable synthetic targets, the group developed and optimized Cu-promoted conditions to accomplish the transformation in good yield.^{15,16}



Scheme 2-4 – Serendipitous discovery of vinyl-ether formation during a Pd-catalyzed oxidative coupling of vinyl boronates with a Cu(II) oxidant.

A curious early finding was made during a substrate screen: allyl alcohol coupled in significantly higher yield than propanol (Table 2-2).¹⁷ Since the size and electronic nature of the substrates are very similar, we ascribed the improved performance of allyl alcohol to a self-ligation effect via its π -bond. We envisioned that adding external π -ligands might lead to improved yields across the board. Indeed, after screening a variety of additives, we reported that addition of alkenes and alkynes could improve the yield of the transformation. As studies continued, a key observation was made: Cyclic alkenes, such as norbornadiene, outperformed their acyclic counterparts. This finding was attributed to increased strain energy, which is relieved upon coordination by copper due to the geometry-altering effects of π -backbonding. By analogy, we hypothesized that cyclic alkynes and allenes would bind copper tightly and provide an increase to reaction yield. To test this hypothesis, a family of allene and alkyne ligands were synthesized and screened for their effects on yield of a vinyl ether in a copper-promoted coupling reaction.

entry	R	yield (%)
1	Me	89
2	Et	93
3	<i>n</i> -Pr	60
4	<i>n</i> -Bu	62
5	<i>n</i> -Hex	42
6	<i>n</i> -Oct	37
7	<i>i</i> -Pr	18
8	<i>tert</i> -Bu	0
9	allyl	87

large difference in yield suggests π -ligand effect

Table 2-2 – Alcohol substrate screen in copper-promoted vinyl ether synthesis.

As shown in Figure 2-2, a total of eight π -bond ligands were synthesized for screening. Starting from cyclooctene, a total of five ligands were prepared: cyclonona-1,2-diene (**2-2**), cyclononyne (**2-3**), cyclooctyne (**2-4**), 4-methoxycyclonona-1,2-diene (**2-5**), and 3-methoxycyclonon-1-yne (**2-6**). Silicon-containing cyclic allene 1,1,4,4-tetramethyl-1,4-disilacyclonona-6,7-diene (**2-7**) was synthesized via ring-closing metathesis of a bis-allyl bearing open-chain precursor. Methylation of but-2-yne-1,4-diol gave 1,4-dimethoxybut-2-yne (**2-8**). Finally, deceptively difficult-to-obtain 1,5-dimethoxypenta-2,3-diene (**2-9**) was circuitously prepared from *cis*-1,4-butanediol. Details of each compound's synthesis are described below.

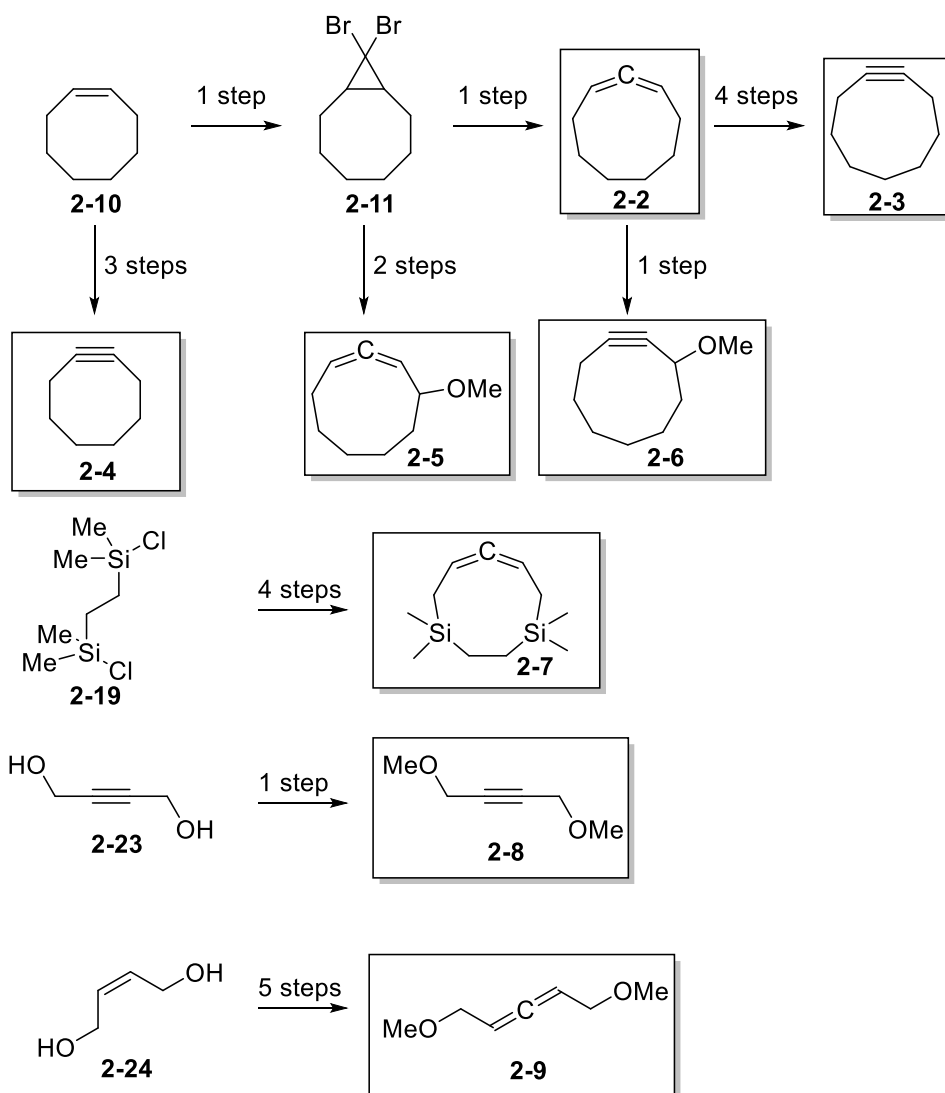
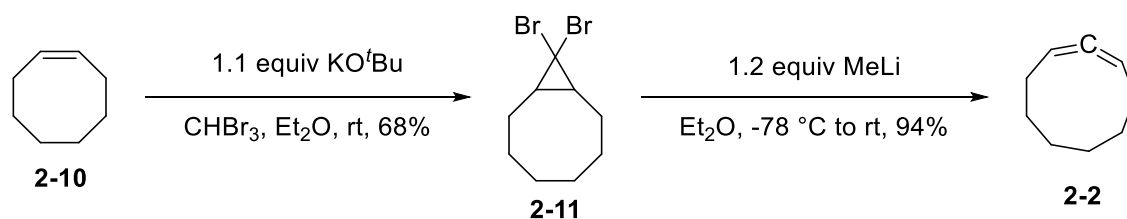


Figure 2-2 – Synthetic overview of ligand syntheses indicating step count.

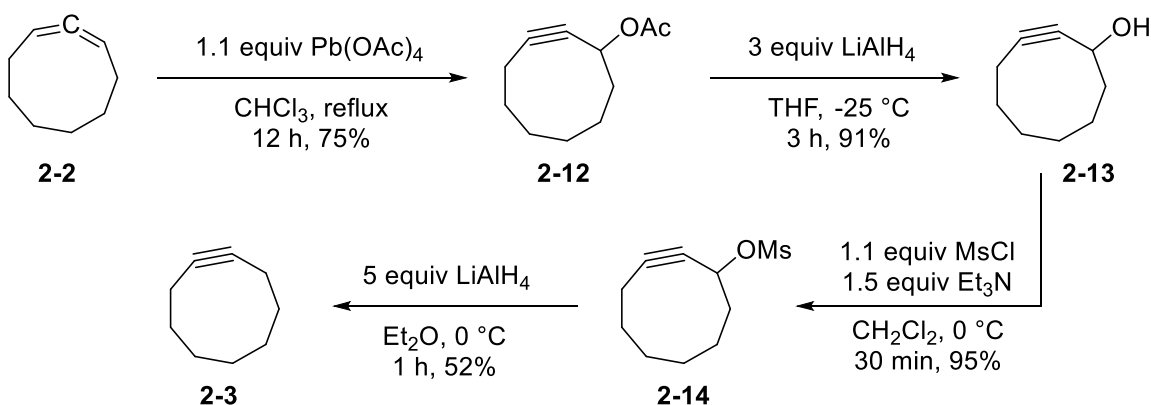
Results and Discussion

Scheme 2-5 shows the synthesis of cycloocta-1,2-diene (**2-2**), prepared as described in the literature.^{18,19} First, *cis*-cyclooctene **2-10** is reacted with dibromocarbene generated *in situ* from bromoform and base to give cyclopropane **2-11**. Second, a Skattebøl rearrangement provides the cyclic allene **2-2** in a 94% yield from the dibromocyclopropane.



Scheme 2-5 – Synthesis of cyclonona-1,2-diene via Skattebøl rearrangement.

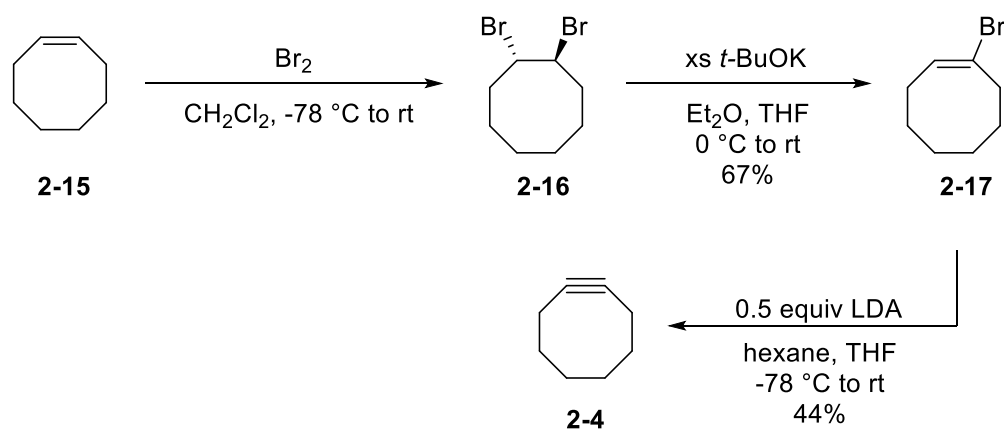
The preparation of cyclononyne (**2-3**) was considerably more laborious than the isomeric allene **2-2**. Base- and acid-catalyzed isomerizations of **2-2** into **2-3** were not attempted due to the thermodynamic equilibrium favoring the allene, as well as the difficulties in separating such isomers.²⁰ Thus, an alternative synthetic route was devised as shown in Scheme 2-6. Starting from **2-2**, Pb(OAc)₄-promoted oxidation²¹ to the propargylic acetate **2-12** was achieved in 75% yield. Reductive cleavage and derivatization of the resultant alcohol **2-13** to the methanesulfonate ester **2-14** proceeded in 86% yield over two steps. Finally, reduction of mesylate **2-14** with lithium aluminum hydride gave alkyne **2-3** in 52% yield (34% overall yield starting from **2-2**).²²



Scheme 2-6 – Synthesis of cyclononyne from cyclonona-1,2-diene via lead(IV) acetate-promoted oxidation and LiAlH₄-reduction sequence.

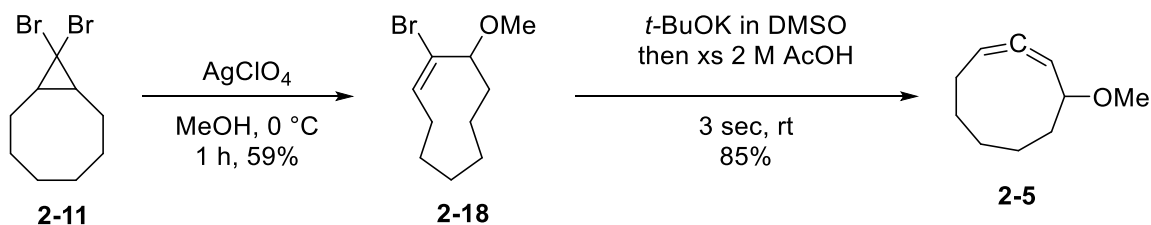
Cyclooctyne (**2-4**) was prepared using a previously reported synthetic strategy, which is shown in Scheme 2-7.²³ Bromination of *cis*-cyclooctene **2-15** with Br₂ gave **2-16**, which

underwent elimination with potassium *tert*-butoxide to the vinyl bromide **2-17** in 67% isolated yield. Vinyl bromide **2-17** was then added to a solution containing 0.5 equiv of LDA to promote elimination forming alkyne **2-4**. Using more base resulted in isomerization of **2-17** to unstable cycloocta-1,2-diene, which rapidly dimerized to give a high-boiling residue. Despite this unavoidable loss of material, **2-4** was obtained in a workable 29% overall yield from *cis*-cyclooctene.



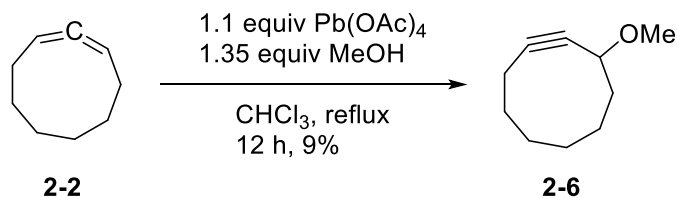
Scheme 2-7 – Synthesis of cyclooctyne via bromination-elimination.

4-Methoxycyclonona-1,2-diene (**2-5**) was obtained using a known protocol²² shown in Scheme 2-8. The synthesis begins with **2-11**, prepared from *cis*-cyclooctene as previously shown in Scheme 2-5. AgClO₄-promoted solvolysis and ring-expansion in methanol gave α -methoxy vinyl bromide **2-18**, which eliminated HBr to form the allene via the action of potassium *tert*-butoxide and subsequent quenching with excess aqueous acetic acid. The elimination step was only allowed to continue for 3 *seconds* before quenching, with longer times resulting in mixtures of alkyne/allene isomers. Using this method, **2-5** was obtained in 34% overall yield from *cis*-cyclooctene.



Scheme 2-8 – Synthesis of 4-methoxycyclonona-1,2-diene via silver-promoted solvolysis and elimination.

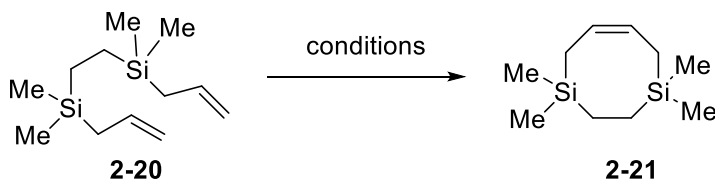
3-methoxycyclonon-1-yne (**2-6**) was obtained by exploiting a serendipitous observation made during the synthesis of **2-3**. When cyclonona-1,2-diene (**2-2**) was treated with $\text{Pb}(\text{OAc})_4$ in chloroform that had not been distilled, a side product identified as 3-ethoxycyclonon-1-yne was obtained. This product was proposed to have been formed via the trapping of a putative carbocation by ethanol that is added to commercial chloroform as a stabilizer. Since **2-6** was identified as a ligand worth testing, the lead(IV) oxidation reaction was conducted with 1.35 equivalents added methanol, providing **2-6** in 9% yield (Scheme 2-9).



Scheme 2-9 – Lead-promoted transformation of allene **2-2** into 3-methoxycyclonon-1-yne.

To assess the effect of ring-strain on ligand performance, 1,1,4,4-tetramethyl-1,4-disilacyclonona-6,7-diene (**2-7**) was prepared as an analog of **2-2**. Because the silicon-carbon bond length (1.84 \AA) is longer than the carbon-carbon bond length (1.54 \AA), **2-7** exhibits reduced ring strain relative to **2-2**. As shown in Scheme 2-10, the synthesis began with a double Grignard addition of allyl magnesium bromide to commercially available 1,2-bis(chlorodimethylsilyl)ethane **2-19**. The resulting ring closing metathesis-precursor **2-20** was subjected to metathesis conditions, furnishing the bis(dimethylsilyl) analog of *cis*-cyclooctene, **2-**

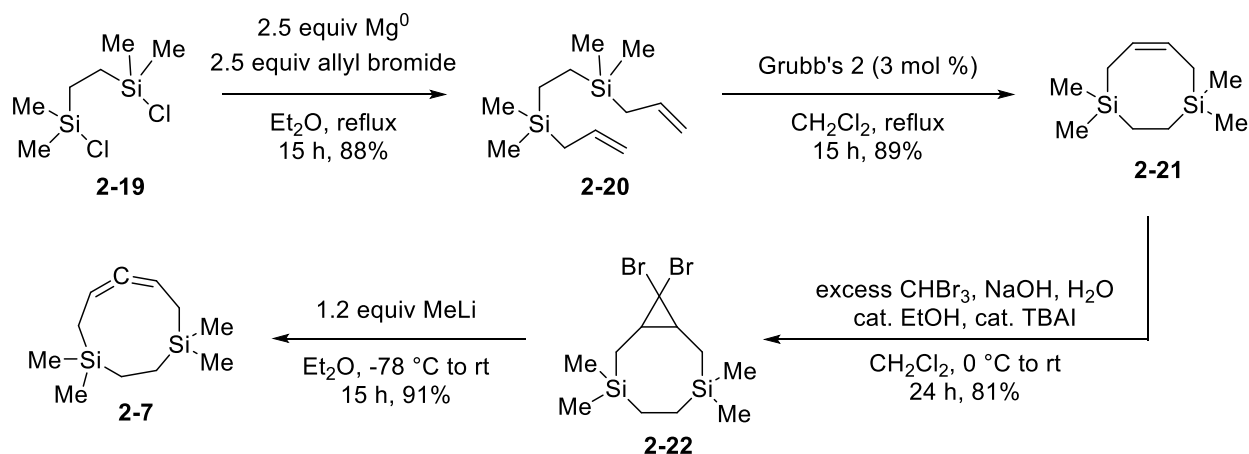
21. During optimization of the Grubb's metathesis conditions (Table 2-3) we found that dichloromethane gave greater conversions than toluene. In addition, we found Grubb's 2nd generation catalyst to be superior to Grubb's 1st generation or the Hoyveda-Grubb's catalyst. We were ultimately able to achieve complete conversion to **2-21** in 89% yield after performing the reaction in refluxing CH₂Cl₂ for 15 h (Table 2-3, entry 6).



Entry	Catalyst	Solvent	Temp. (°C)	Concentration (M)	Yield (%)
1	Grubb's 1	CH ₂ Cl ₂	23	0.05	82
2	Grubb's 1	PhMe	23	0.2	66
3	Grubb's 1	PhMe	65	0.2	50
4	Grubb's 2	CH ₂ Cl ₂	23	0.1	83
5	Hoyveda-Grubb's	CH ₂ Cl ₂	23	0.1	50
6	Grubb's 2	CH ₂ Cl ₂	40	0.1	89

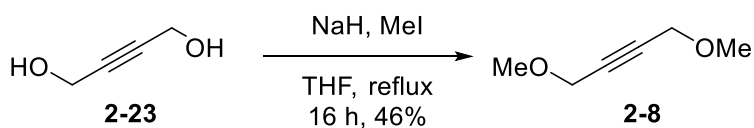
Table 2-3 – Optimization of Grubb's metathesis conditions for the synthesis of **2-21**.

With **2-21** in hand, we converted it to the dibromocyclopropane **2-22** using a modified aqueous dibromocarbene protocol.²⁴ Finally, treatment of the dibromocyclopropane with methyl lithium triggered the Skattebøl rearrangement to give **2-7** in a 91% reaction yield and a 58% overall yield.



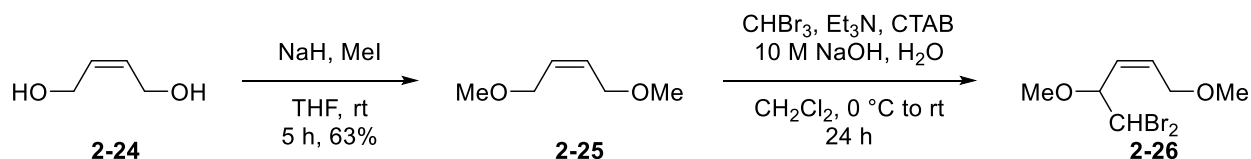
Scheme 2-10 – Synthesis of **2-7** from 1,2-bis(chlorodimethylsilyl)ethane

The synthesis of 1,4-dimethoxybut-2-yne (**2-8**) was straightforward; it was prepared via reaction of but-2-yne-1,4-diol (**2-23**) and methyl iodide in the presence of sodium hydride, as shown in Scheme 2-11.²⁵



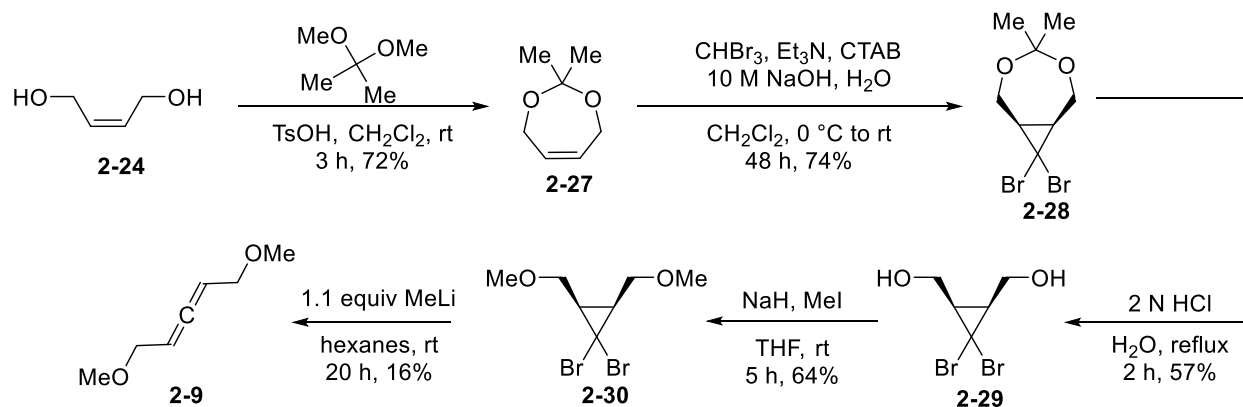
Scheme 2-11 – Alkylation of 1,4-butyne diol with methyl iodide.

1,5-Dimethoxypenta-2,3-diene (**2-9**) had not been previously reported in the literature and proved to be relatively difficult to prepare. After dimethylation of (*Z*)-2-butene-1,4-diol (**2-24**), the resulting 1,4-dimethoxybut-2-ene (**2-25**) would not undergo dibromocyclopropanation. This is perhaps due to deprotonation of the relatively acidic allylic positions under the reaction conditions, which explains the preferential formation of brominated compound **2-26** (Scheme 2-12).



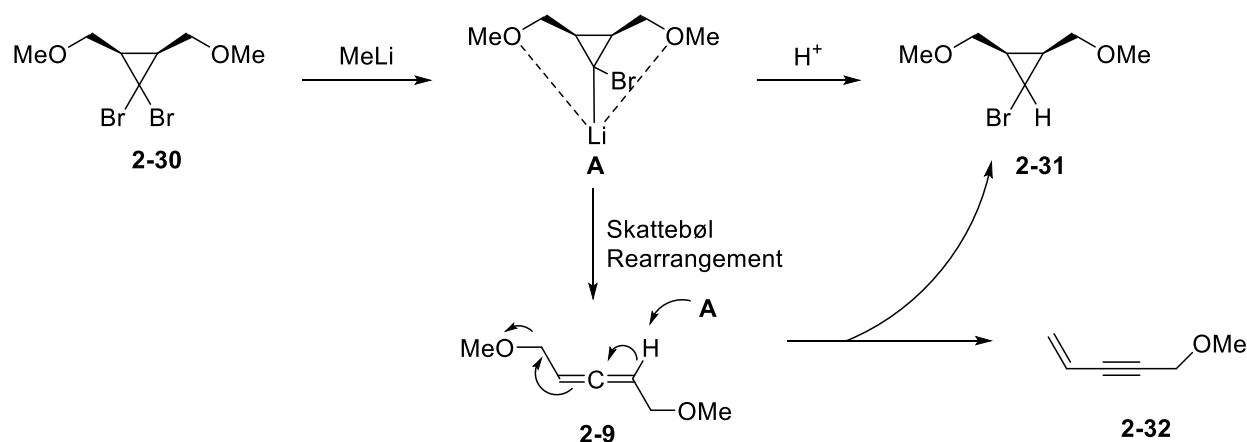
CTAB = cetyltrimethylammonium bromide

Scheme 2-12 – Failed dibromocyclopropanation of **2-25**.



Scheme 2-13 – Reworked synthesis of **2-9**, using a cyclic acetonide to facilitate dibromocyclopropane formation.

A related literature report on the synthesis of **2-29**²⁶ aided in the development of a workable protocol, which is shown in Scheme 2-13. First, diol **2-24** was protected as the cyclic acetonide **2-27** in 72% yield. The acetonide could be successfully dibromocyclopropanated in 74% yield, presumably because the cyclic alkene was nucleophilic enough to undergo the [2+1] reaction with dibromocarbene, while the linear alkene was not. The bromoacetonide **2-28** was cleaved to the diol **2-29** using aqueous HCl and the diol methylated using methyl iodide in the presence of sodium hydride to give **2-30** in 37% yield over two steps. With **2-30** in hand, all that remained was to perform the Skattebøl rearrangement to give **2-9**. Interestingly, the success of this final step was found to have a strong temperature and solvent dependence.



Scheme 2-14 – Generation of side products during the synthesis of **2-9** in ethereal solvents.

As shown in Scheme 2-14, when THF or Et₂O solvents were used, only protonated side product **2-31** and elimination side product **2-32** arose from treatment of **2-30** with MeLi. We proposed that intramolecular chelation of the lithium anion **A** by the flanking methoxy groups stabilized the intermediate and impeded the rearrangement from proceeding at low temperature in ethereal solvents. Upon warming to room temperature, **A** could undergo the Skattebøl Rearrangement, but a competing elimination reaction gave rise to **2-32** and **2-31**. These side reactions could only be suppressed by performing the Skattebøl rearrangement in nonpolar hexane solvent at room temperature, which finally gave access to the surprisingly elusive **2-9** in 16% yield.

2.3 – Effects of Alkyne and Allene Ligands on Coupling Yield

After the ligands were prepared as described above, they were tested for their effect on yield in an oxidative Cu-coupling reaction. We found the variations in yield among the different ligands to be quite dramatic, indicating the ligands certainly have a significant effect on the reaction. Among the alkynes, linear 3-hexyne (**2-33**) performed the best, while 1,4-dimethoxybut-2-yne (**2-8**) and the cyclic alkynes (**2-3**, **2-4**, **2-6**, **2-12**) decreased reaction yields

relative to the reaction conducted without added ligand (Table 2-4). Appearance of additional spots on the TLC plates suggested that the alkynes were undergoing side reactions.

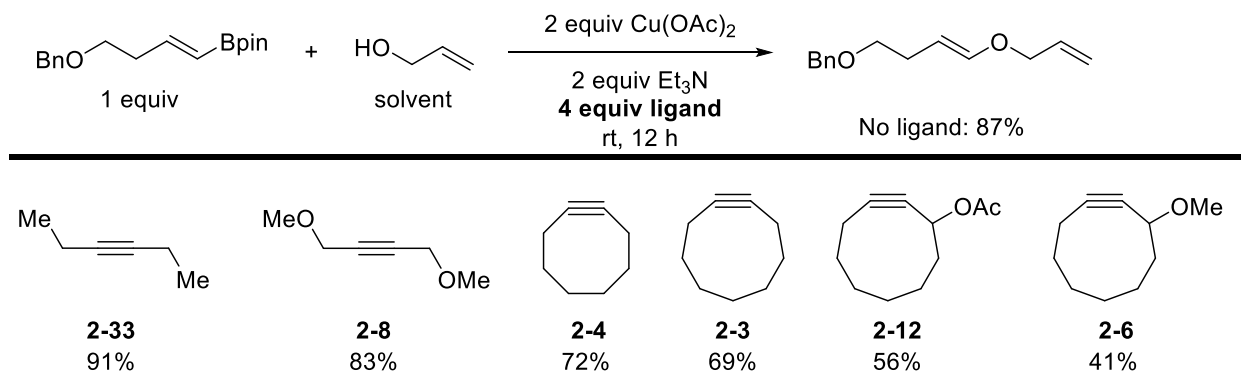


Table 2-4 – Alkyne ligand performance in a Cu-promoted vinyl ether synthesis.

We found that varying the allene ligands had a significant effect on coupling yield as well. In addition to the allene ligands synthesized as described above, several other linear allenes prepared by Tioga Martin and Brett Cory were also tested, as shown in Table 2-5. The results indicated that, contrary to what was observed with the alkynes, cyclic allenes (**2-2**, **2-5**, **2-7**) are better than linear allenes (**2-9**, **2-34**, **2-35**, **2-36**, **2-37**, **2-38**, **2-39**). Silicon-containing allene **2-7** performed poorly compared to its all-carbon counterpart **2-2**, perhaps because **2-7** is less strained (due to the longer C-Si bond length) and hence benefits less from the ring-strain relieving effects of metal binding described by the Dewar, Chatt, and Duncanson model. The data indicate that the effects of these π -bond additives are complex. If yield improvement was simply correlated with increased ligand binding affinity, one would expect cyclic, electron-deficient allenes and alkynes to perform best. However, we see that trend is not consistently observed. Although we can ascribe the great performance of cyclic allenes to ring-strain relief upon binding, the same is apparently untrue of the alkyne ligands. Similarly, we'd expect electron-poor π -ligands (**2-6**, **2-39**) to bind strongest, but they are among the worst performing ligands tested. Thus, we tend to believe that there exists an optimal zone of ligand structure. Ligands with poor binding affinity

have little-to-no effect on reaction yield, while ligands with electron-withdrawing groups that are predicted to have the highest binding affinity may encourage undesired pathways and/or decomposition of catalyst or substrate. The best ligands appear to be those with substitution patterns that favor an intermediate binding affinity, with cyclonona-1,2-diene (**2-2**) identified as the top performer.

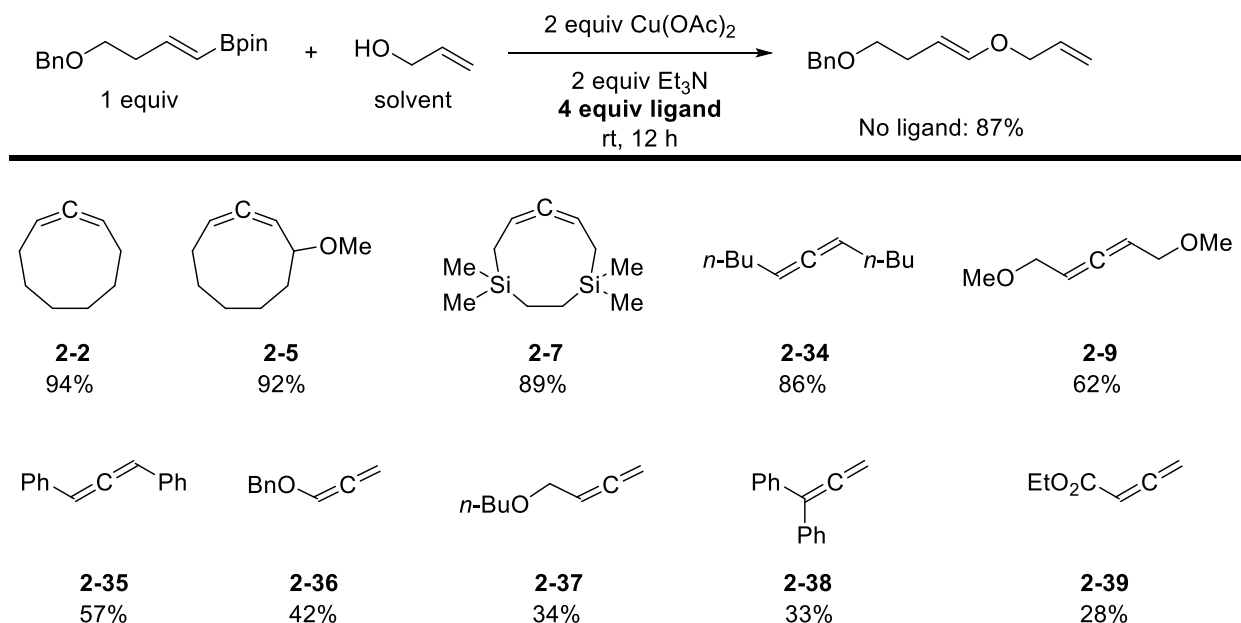
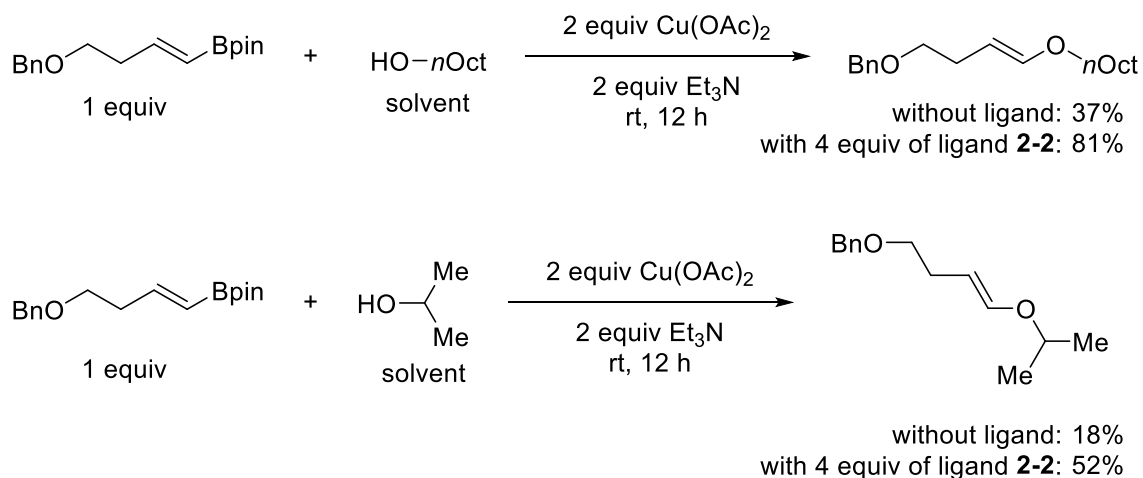


Table 2-5 – Allene ligand performance in a Cu-promoted vinyl ether synthesis.

To verify that the effect of cyclonona-1,2-diene **2-2** was truly impactful, we revisited the reactions of some of the poorest performing alcohol couplings, the vinyl ethers derived from *n*-octanol and *i*-propanol. As shown in Scheme 2-16, cyclonona-1,2-diene increased the yields for these reactions considerably. *n*-Octanol coupling yield more than doubled to 81%, while the coupling yield for *i*-propanol nearly tripled to 52%.



Scheme 2-16 – Significant yield improvements observed for *n*-octanol and 2-propanol with **2-2** ligand.

Having identified the benefits of allene **2-2** and elucidating some trends about the properties of π -bond ligands in this reaction, we also hoped to provide a rationale for the role of these ligands in the reaction. Based on a proposed mechanism of the Chan–Evans–Lam coupling, we formulated the following putative mechanism shown in Figure 2-3.

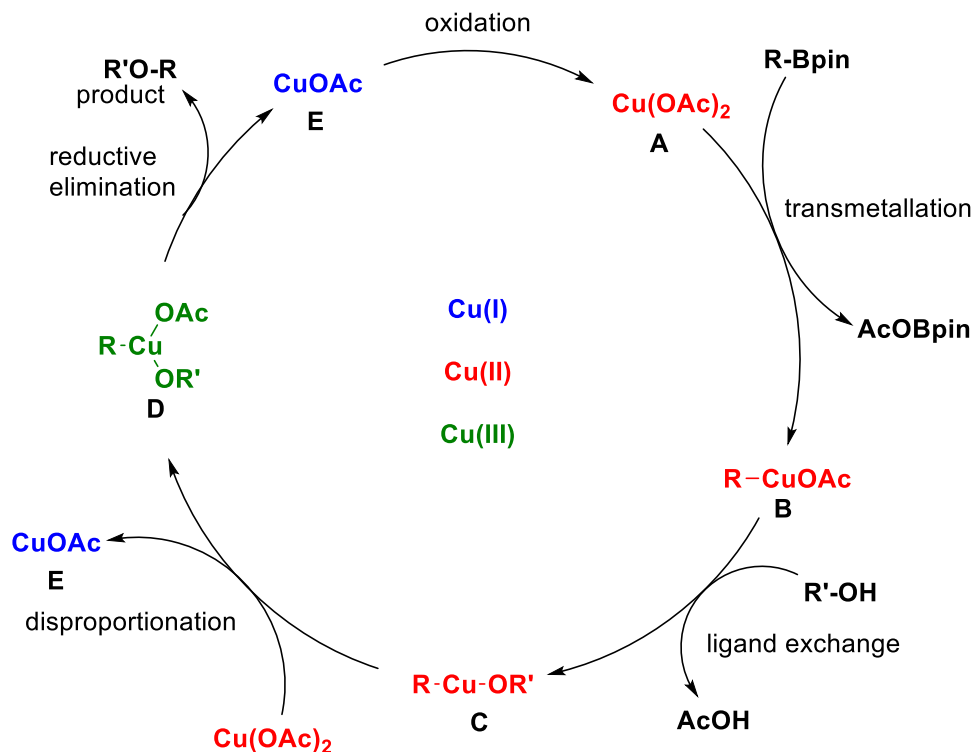


Figure 2-3 – Proposed mechanism of Cu-promoted vinyl ether synthesis.

Our proposal begins with transmetallation of Cu(OAc)_2 (**A**) with the vinyl boronate to produce vinyl Cu(II) species **B**. Next, ligand exchange of acetate with the alcohol solvent gives alkoxycuprate **C**. Disproportionation of **C** with another equivalent of Cu(OAc)_2 produces Cu(I) acetate (**E**) and a highly oxidized Cu(III) species **D**. Reductive elimination gives vinyl-ether product and **E** which can be reoxidized by atmospheric oxygen to regenerate **A**. Because it is known that Cu(I) has a higher affinity for alkenes and alkynes than other oxidation states of copper, we propose the π -bond ligand effects observed are a result of interaction with Cu(I) species.²⁷ Upon inspection of the proposed mechanism, Cu(I) intermediates are implicated in two steps (indicated in blue). Thus, we propose the added π -ligands stabilize the incipient Cu(I) species produced during the disproportionation and/or reductive elimination steps, facilitating productive turnover and increased yields. Indeed, calculations by another group member, Eric

Chen, find that coordination of a π -bond to the incipient Cu(I) dramatically lowers the activation energy for the key disproportionation step. Further studies are in progress to explore this and other aspects of π -bond ligands in other copper-promoted reactions.

2.4 – Conclusion

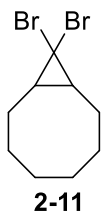
In summary, we synthesized a family of cyclic and acyclic alkynes and allenes, developing new methods for the syntheses of allenes **2-7** and **2-9** and alkyne **2-9** along the way. The alkyne and allene ligands were tested in copper-promoted coupling reactions and the results indicate that the reaction is very sensitive to the identity of ligand used, with the strained cyclic allenes **2-2** and **2-5** offering the highest improvement in yield compared to the reaction performed in the absence of ligand. When extremely strained alkyne ligands cyclononyne (**2-3**) and cyclooctyne (**2-4**) were used, diminished yields were observed. This suggests there is a balance at play; unstrained π -bonds may not bind strongly enough to exert an effect on yield, whereas highly strained π -bonds may bind too tightly and/or participate in side reactions that reduce yields. Further work is underway to definitively ascertain the mechanistic role of these π -bond ligands, both computationally and experimentally. Importantly, this work represents an important investigation into a long-neglected class of additives for transition metal catalyzed reactions, allenes. We are investigating if allenes can also impart benefits to other Cu-promoted reactions to assess whether our observations described herein represent a general strategy for improving yields in cross-couplings.

2.5 – Experimental Methods

General Information

Unless otherwise specified, all reactions were performed under a nitrogen atmosphere using dry solvents and anhydrous conditions. CHCl_3 was distilled from CaCl_2 and stored over 4Å molecular sieves in the dark. DCM, DMSO, and triethylamine were distilled from CaH_2 . Diisopropylamine was distilled from KOH. Et_2O and THF were distilled from sodium/benzophenone. Methanol was distilled from magnesium turnings. All other reagents were used as received from commercial sources, unless otherwise specified. NMR data obtained with Bruker ARX-400 or AV-500 instrument and calibrated to the solvent signal (CDCl_3 δ : = 7.26 ppm for ^1H NMR, δ : = 77.0 ppm for ^{13}C NMR. Multiplicities are reported by s (singlet), d (doublet), t (triplet), q (quartet), and m (multiplet). Reactions were monitored using thin layer chromatography performed on UV254 silica gel TLC plates and visualized with UV light, ceric ammonium molybdate (CAM) stain, or potassium permanganate (KMnO_4) stain. Flash column chromatography was performed using silica gel (40-63 microns) and compressed air. IR spectra were recorded with an ATR attachment and selected peaks are reported in cm^{-1} . High resolution mass spectral data was recorded with Thermo Fisher Scientific Exactive Plus with IonSense ID-CUBE Direct Analysis in Real Time (DART) ion source experiments.

9,9-dibromobicyclo[6.1.0]nonane



To a dry 250 mL round bottom flask equipped with a stir bar was added 6.3 g (56 mmol, 1.1 equiv) potassium tert-butoxide, 30 mL dry hexanes, and 6.5 mL (50 mmol, 1 equiv) *cis*-cyclooctene. The slurry was chilled to 0 °C, and 4.4 mL (50 mmol, 1 equiv) bromoform was

added dropwise with stirring. The solution was allowed to warm to room temperature and stirred overnight. The reaction mixture was then partitioned between Et₂O and water and extracted 2x with Et₂O. The combined organic extracts were washed with brine, dried with MgSO₄ and concentrated to give a brown oil. The crude product was placed under high vacuum for several hours until no bromoform or cyclooctene remained. The brown residuum was dissolved in hexane and filtered through a silica plug, which was subsequently washed with several portions of hexane. The filtrate was concentrated to give 9.62 g (68%) of 9,9-dibromobicyclo[6.1.0]nonane as a colorless oil. Spectral data matched reported values.²⁸

¹H NMR (400 MHz, CDCl₃) δ: 2.08-2.02 (m, 2H), 1.67-1.36 (m, 10H), 1.18-1.14 (m, 2H);

¹³C NMR (100 MHz, CDCl₃) δ: 37.0, 33.2, 27.9, 26.3, 25.3.

cyclonona-1,2-diene



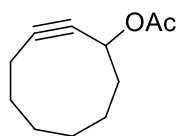
A 250 mL flask equipped with a stir bar was flame dried under vacuum and backfilled with N₂ gas. The flask was allowed to cool and charged with 6.967 g (24.7 mmol, 1 equiv) 9,9-32 dibromobicyclo[6.1.0]nonane. 35 mL of Et₂O was added and the solution cooled to -78 °C with stirring. With the aid of a syringe pump, 18.5 mL (29.6 mmol, 1.2 equiv) of a 1.6 M solution of methyllithium in diethyl ether was added over 1 h. The reaction mixture was allowed to gradually warm to room temperature over a period of 12 h, after which the reaction was cautiously quenched with 0.7 mL of water and allowed to stir for 10 min. MgSO₄ was added and the product mixture allowed to stir for an additional 20 min. The bulk of the solvent was

removed *in vacuo* to give crude product. The crude residue was dissolved in 20 mL of pentane and passed through a silica plug, which was subsequently washed with several portions of pentane. The filtrate was dried with MgSO_4 and concentrated to give 2.83 g (94%) of cyclonona-1,2-diene as a colorless oil with a pungent odor. Spectral data matched reported values.²⁸

^1H NMR (400 MHz, CDCl_3) δ : 5.28-5.24 (m, 2H), 2.25-2.18 (m, 2H), 1.80-1.36 (m, 10H);

^{13}C NMR (125 MHz, CDCl_3) δ : 205.6, 92.3, 27.9, 27.3, 33.

3-acetoxycyclononyne



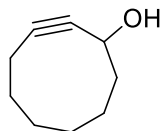
2-12

To a flame-dried 250 mL, 2-necked round bottom flask equipped with a reflux condenser, addition funnel, and stir bar was added 2.804 g (22.9 mmol, 1 equiv) of cyclonona-1,2-diene in 10 mL of chloroform. The flask was flushed with nitrogen and the solution brought to reflux. 10.781 g (24.3 mmol, 1.1 equiv) of lead tetraacetate dissolved in 50 mL of CHCl_3 was then added dropwise to the refluxing allene solution with the aid of the addition funnel. The solution was refluxed for 7 h, allowed to cool, then filtered through a silica plug and washed with 3x20mL portions of CH_2Cl_2 . The filtrate was concentrated under reduced pressure and partitioned between diethyl ether and a saturated solution of sodium carbonate. After washing 2x with sat. sodium carbonate, the combined organic extracts were washed with brine, then dried (MgSO_4) and concentrated. The crude residue was purified by flash column chromatography (14:1 hexanes:EtOAc) yielding 3.118 g (75%) of 3-acetoxycyclononyne as a colorless oil. Spectral data matched reported values.²¹

^1H NMR (400 MHz, CDCl_3) δ : 5.34-5.28 (m, 1H), 2.26- 2.18 (m, 2H), 2.06 (s, 3H), 2.00-1.45 (m, 10H);

^{13}C NMR (100 MHz, CDCl_3) δ : 205.6, 92.3, 27.9, 27.3, 25.2.

3-hydroxycyclononyne

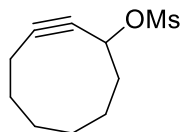


2-13

A two-necked round bottom flask equipped with an addition funnel, glass stopper, and stir bar was flame-dried under vacuum. 42 mL of THF was added and the flask was then cooled to $-30\text{ }^\circ\text{C}$ under a nitrogen atmosphere. The glass stopper was removed and 2.152 g (51.9 mmol, 3 equiv) of lithium aluminum hydride was added with stirring. The addition funnel was then charged with 3.118 g (17.3 mmol, 1 equiv) of 3-acetoxycyclononyne in 6 mL of THF. The 3-acetoxycyclononyne solution was then added dropwise and the temperature maintained between -30 to $-20\text{ }^\circ\text{C}$. The reaction was monitored for consumption of the starting material using TLC. Upon completion, the reaction was warmed to $0\text{ }^\circ\text{C}$ and quenched via the addition of 2 mL of H_2O , 4 mL of 2M NaOH, and finally 4 mL of additional water. After warming to room temperature and stirring for 15 minutes, MgSO_4 was added and the mixture was stirred for an additional 15 minutes. The white solids were removed by filtration through a celite pad and the filter cake was washed with several portions of ether. The filtrate was concentrated and the crude residue purified by flash column chromatography (4.5:1 hexanes:EtOAc) yielding 2.1792 g (91%) of 3-hydroxycyclononyne as a colorless oil. Spectral data matched reported values.²¹

^1H NMR (400 MHz, CDCl_3) δ : 4.46-4.39 (m, 1H), 2.28-2.13 (m, 2H), 1.96-1.88 (m, 1H), 1.80-1.40 (m, 10H).

cyclonon-2-yn-1-yl methanesulfonate



2-14

To a flame-dried, 250 mL round bottom flask equipped with a stir bar was added 2.0404 g (14.7 mmol) of 3-hydroxycyclononyne in 74 mL of CH_2Cl_2 . The solution was cooled to 0 °C in an ice bath, and 3.07 mL (22.05 mmol) of triethylamine was added. After dropwise addition of 1.25 mL (16.2 mmol) freshly distilled methanesulfonyl chloride, the reaction was stirred for an additional 30 minutes at 0 °C. The cold reaction mixture was transferred with the aid of several CH_2Cl_2 washes to a 500 mL separatory funnel and washed with cold water, cold aqueous 3M HCl, saturated aqueous sodium bicarbonate, and brine. The organic extract was dried with MgSO_4 and concentrated yielding 3.054 g (95%) of cyclonon-2-yn-1-yl methanesulfonate as a reddish oil which solidified upon freezing. The material decomposes rapidly on contact with silica gel. Spectral data matched reported values.²¹

^1H NMR (400 MHz, CDCl_3) δ : 5.22-5.16 (m, 1H), 3.10 (s, 3H), 2.29-2.23 (m, 2H), 2.10-1.96 (m, 2H), 1.80-1.43 (m, 8H);

^{13}C NMR (100 MHz, CDCl_3) δ : 98.0, 82.3, 72.7, 38.8, 35.3, 29.4, 26.3, 25.4, 21.5, 19.0.

cyclononyne



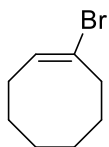
2-3

A two-necked round bottom flask equipped with an addition funnel, glass stopper, and stir bar was flame-dried under vacuum. 42 mL of THF was added and the flask was then cooled to 0 °C under a nitrogen atmosphere. The glass stopper was removed and 1.847 g (48.5 mmol, 5 equiv) of lithium aluminum hydride was added with stirring. 2.1077 g (9.7 mmol, 1 equiv) of cyclonon-2-yn-1-yl methanesulfonate in 8 mL of THF was then added to the LAH solution dropwise. After stirring for 1h at 0 °C, the reaction was quenched via the addition of 2 mL of H₂O, 3.75 mL of 2M NaOH, and finally 4 mL of additional water. After warming to room temperature and stirring for 15 minutes, MgSO₄ was added and the mixture was stirred for an additional 15 minutes. The white solids were removed by filtration through a celite pad and the filter cake was washed with several portions of ether. The filtrate was concentrated and the crude residue purified by flash column chromatography (pentane) yielding 0.612 g (52%) of cyclononyne as a colorless oil with a pungent odor. Spectral data matched reported values.²²

¹H NMR (400 MHz, CDCl₃) δ: 2.17-2.13 (m, 4H), 1.68-1.63 (m, 6H), 1.58-1.54 (m, 4H);

¹³C NMR (100 MHz, CDCl₃) δ: 88.1, 30.1, 27.1, 25.6, 19.2.

(*E*)-1-bromocyclooct-1-ene

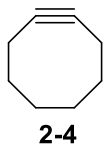


2-17

To a flame-dried 100 mL round bottom flask equipped with a stir bar was added 6.5 mL of *cis*-cyclooctene (50 mmol, 1 equiv) and 17.5 mL of CH₂Cl₂. Stirring was initiated and the solution cooled to -78 °C. Bromine (approx. 2.5 mL) was added to the cold solution dropwise via syringe until the brown color persisted. The cooling bath was removed and the solution allowed to warm to room temperature. The reaction mixture was stirred for 40 minutes, then concentrated under reduced pressure to give 1,2-dibromocyclooctane as a brown oil. The crude product was dissolved in 20 mL of Et₂O and cooled to 0 °C in an ice bath. To this solution of 1,2-dibromocyclooctane was added dropwise a solution of 8.42 g (75 mmol, 1.5 equiv) potassium tert-butoxide in 18.5 mL THF. The reaction mixture was allowed to warm to room temperature and stirred for 1 h. The mixture was poured into cold water and extracted 3x with Et₂O. The combined extracts were washed with brine, dried (MgSO₄), and concentrated. The crude product was distilled (90 °C, 20 mm Hg) to give 6.32 g (67%) of (E)-1-bromocyclooct-1-ene as a colorless oil. Spectral data matched reported values.²³

¹H NMR (400 MHz, CDCl₃) δ: 6.03 (t, *J* = 8.5 Hz, 1H), 2.72-2.56 (m, 2H), 2.15-2.02 (m, 2H), 1.69-1.52 (m, 8H).

cyclooctyne

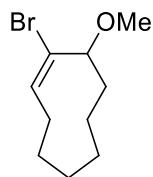


A flame-dried 250 mL flask equipped with a stir bar was charged with 2.47 mL (17.5 mmol, 1.05 equiv) diisopropylamine and 7.0 mL of THF. The solution was cooled to -78 °C and 10.43 mL (16.7 mmol, 1 equiv) of a 1.6 M solution of butyllithium in hexanes was added dropwise and stirred for 30 min. To this cold solution of LDA was added at once 6.319 g (33.4

mmol, 2 equiv) of (*E*)-1-bromocyclooct-1-ene. The reaction mixture was allowed to gradually warm to room temperature, then stirred for an additional 90 min. To quench the reaction, 35 mL of cold 1M HCl was added with stirring. The mixture was extracted 5x with pentane and the combined organic fractions washed with brine and dried (MgSO₄). The solvent was carefully removed using a rotary evaporator with a 0 °C bath temperature (as the product is volatile). The crude residue was then purified by flash column chromatography (pentane) giving 794 mg pure cyclooctyne (44%) as a colorless oil with a pungent odor. Spectral data matched reported values.²³

¹H NMR (400 MHz, CDCl₃) δ: 2.19-2.14 (m, 4H), 1.88-1.85 (m, 4H), 1.64-1.51 (m, 4H).

(*Z*)-1-bromo-9-methoxycyclonon-1-ene



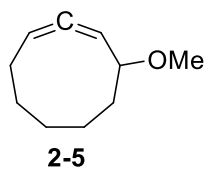
2-18

A flame dried 200 mL round bottom flask equipped with a stirbar was charged with 5.88 g (28.4 mmol, 2 equiv) of silver perchlorate and 14.2 mL of methanol. The flask was flushed with nitrogen, cooled to 0 °C, and protected from light. With strong stirring, 4.0 g (14.2 mmol, 1 equiv) of 9,9-dibromobicyclo[6.1.0]nonane was introduced to solution dropwise. After 20 minutes, the cloudy, light green solution was treated with 100 mL of a 0.25M solution of NaCO₃. The resulting solution was filtered, and the solids washed with several portions of acetone. The filtrate was concentrated to an approximate volume of 5 mL, then partitioned between Et₂O and water. The aqueous phase was extracted 2x with ether, and the combined organic extracts dried (MgSO₄) and concentrated. The crude residue was purified by flash column chromatography

(20:1, hexanes:EtOAc) yielding 1.96 g (59%) of (*Z*)-1-bromo-9-methoxycyclonon-1-ene as a pale yellow oil. Spectral data matched reported values.²²

¹H NMR (400 MHz, CDCl₃) δ: 6.09 (dd, *J* = 10.5, 5.4 Hz, 1H), 3.59 (dd, *J* = 10.5, 4.0 Hz, 1H), 3.30 (s, 3H), 2.55-2.45 (m, 1H), 2.21-2.13 (m, 1H), 1.95-1.69 (m, 3H), 1.62-1.23 (m, 8H).

4-methoxycyclonona-1,2-diene



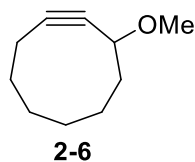
A flame-dried 50 mL flask equipped with a stir bar was purged with nitrogen and charged with 1.96 g (8.4 mmol, 1 equiv) of (*Z*)-1-bromo-9-methoxycyclonon-1-ene and 5 mL of dry DMSO. To this solution was added at once 16.8 mL of 1.5 M potassium *tert*-butoxide in dry DMSO. After 3 seconds of vigorous stirring, 17 mL of 2M acetic acid was added and the resulting yellow solution was allowed to cool to room temperature. The mixture was transferred to a separatory funnel and extracted 2x with Et₂O. The organic extracts were washed 2x with water and then 1x with brine. The combined ether extracts were dried (MgSO₄) and concentrated under reduced pressure. The crude residue was purified by flash column chromatography (20:1 hexanes:EtOAc) yielding 1.08 g (85%) of 4-methoxycyclonona-1,2-diene (4) as a yellow oil.

¹H NMR (400 MHz, CDCl₃) δ: 5.30-5.25 (m, 1H), 5.23-5.18 (m, 1H), 3.93-3.87 (m, 1H), 3.36 (s, 3H), 2.34-2.23 (m, 1H), 1.97-1.23 (m, 9H);

¹³C NMR (100 MHz, CDCl₃) δ: 202.5, 97.0, 92.8, 79.5, 56.6, 34.1, 28.1, 26.4, 26.3, 22.1.

Matches reported spectral data.²²

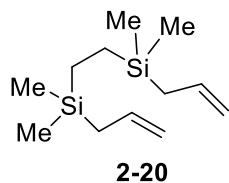
3-methoxycyclononyne



To a flame-dried 200 mL, 2-necked round bottom flask equipped with a reflux condenser, addition funnel, and stirbar was added 1.53 g (12.4 mmol, 1 equiv) of cyclonona-1,2-diene in 5.4 mL of chloroform. The flask was flushed with nitrogen and the solution brought to reflux. 6.04 g (13.6 mmol, 1.1 equiv) of lead tetraacetate dissolved in 27.3 mL of chloroform and 0.68 mL (16.2 mmol, 1.35 equiv) methanol was then added dropwise to the refluxing allene solution with the aid of the addition funnel. The solution was refluxed for 3 h, allowed to cool, then filtered through a silica plug and washed with 3x20mL portions of CH₂Cl₂. The filtrate was concentrated under reduced pressure and partitioned between diethyl ether and a saturated solution of sodium carbonate. After washing 2x with sat. sodium carbonate, the combined organic extracts were washed with brine, then dried (MgSO₄) and concentrated. The crude residue was purified by flash column chromatography (20:1 pentane:EtOAc) yielding 167 mg (9%) of 3-methoxycyclononyne as a colorless oil. Spectral data matched reported values.²²

¹H NMR (400 MHz, CDCl₃) δ: 4.04-4.01 (m, 1H), 3.35 (s, 3H), 2.22-2.19 (m, 2H), 1.91-1.89 (m, 2H), 1.79-1.55 (m, 8H).

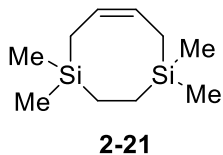
1,2-bis(allyldimethylsilyl)ethane



To a flame-dried 500 mL, three-necked round bottom flask fitted with a reflux condenser, addition funnel, septum, and stirbar was added 2.82 g (116 mmol, 5 equiv) of polished magnesium turnings and 6 mL of diethyl ether. To the addition funnel was transferred 5 mL (58 mmol, 2.5 equiv) of freshly distilled allyl bromide dissolved in 58 mL of diethyl ether. The allyl bromide solution was then added to the magnesium dropwise at a rate to maintain gentle reflux (about 1h). After refluxing for an additional hour, the solution was transferred via cannula to a 100 mL flask (fitted with reflux condenser) containing 5 g (23 mmol, 1 equiv) of 1,2-bis(chlorodimethylsilyl)ethane and a stir bar. The resulting mixture was refluxed overnight, then washed (2x with DI water, 1x brine), dried over MgSO₄, and concentrated, yielding 4.934 g of a yellow oil. This crude oil was dissolved in 20 mL of pentane and passed through a silica plug which was subsequently washed with 3x50 mL portions of pentane yielding 4.562 g (88%) of 1,2-bis(allyldimethylsilyl)ethane as a clear oil. Spectral data matched reported values.²⁹

¹H NMR (400 MHz, CDCl₃) δ: 5.82-5.72 (m, 2H), 4.86-4.80 (m, 4H), 1.55-1.52 (d, *J* = 8.5 Hz, 4H), 0.41 (s, 4H), -0.02 (s, 12H).

(Z)-1,1,4,4-tetramethyl-1,2,3,4,5,8-hexahydro-1,4-disilocene

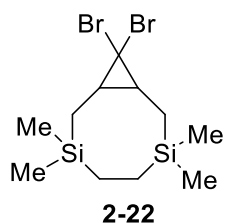


To a dry flask (equipped with a reflux condenser and stirbar) containing 463 mg of Grubb's 2nd generation catalyst (3 mol %) was transferred 4.138 g (18.3 mmol, 1 equiv) of 1,2-bis(allyldimethylsilyl)ethane dissolved in 165 mL of CH₂Cl₂. The resulting dark purple solution was refluxed overnight. After complete conversion was observed via ¹H NMR, the reaction mixture was passed through a silica plug, washed with 4x50 mL portions of pentane, and

concentrated to yield a brown oil. This crude residue was dissolved in 25 mL of pentane and passed through another silica plug, again washing with 4x50 mL portions of pentane. The filtrate was concentrated yielding 3.212 g (89%) of (Z)-1,1,4,4-tetramethyl-1,2,3,4,5,8-hexahydro-1,4-disilocine as a colorless oil. Spectral data matched reported values.³⁰

¹H NMR (400 MHz, CDCl₃) δ: 5.40-5.37 (m, 2H), 1.49 (d, *J* = 7.5 Hz, 4H), 0.62 (s, 4H), 0.00 (s, 12H).

9,9-dibromo-3,3,6,6-tetramethyl-3,6-disilabicyclo[6.1.0]nonane



To a dry, 25 mL flask containing (Z)-1,1,4,4-tetramethyl-1,2,3,4,5,8-hexahydro-1,4-disilocine (500 mg, 2.5 mmol, 1 equiv) was added tetrabutylammonium iodide (13 mg, 0.025 mmol). The flask was then sealed with a rubber septum and purged with N₂. After submerging the flask in a 0 °C ice bath, CH₂Cl₂ (2.5 mL), CHBr₃ (0.437 mL, 5 mmol, 2 equiv), and EtOH (3 drops) were added sequentially. A solution of sodium hydroxide prepared by dissolving 1 g of NaOH in 1 mL of water was then added dropwise. The reaction mixture was allowed to gradually warm to room temperature and stirred for 24 h, during which time the clear, colorless reaction mixture became dark brown. The reaction mixture was extracted 2x with Et₂O and the combined organic extracts were washed with brine. After drying (MgSO₄) and concentration, the crude residue was passed through a silica plug (pentane) yielding 0.7764 g (84%) of 9,9-dibromo-3,3,6,6-tetramethyl-3,6-disilabicyclo[6.1.0]nonane as a white solid.

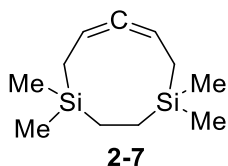
^1H NMR (400 MHz, CDCl_3) δ : 1.63-1.60 (m, 2H), 0.98 (dd, $J = 14.8, 2.0$ Hz, 2H), 0.70-0.55 (m, 4H), 0.44-0.40 (m, 2H), 0.08 (s, 6H), 0.00 (s, 6H);

^{13}C NMR (100 MHz, CDCl_3) δ : 44.4, 30.5, 13.4, 7.1, -2.7, -3.9;

FT-IR (ATR) $\tilde{\nu}$ [cm^{-1}] = 2949, 2882, 2799, 1427, 1413, 1372, 1249, 1194, 1185, 1175, 1163, 1135, 1090, 1052, 1004, 970, 832, 798, 757, 752, 735, 687, 677, 661;

HRMS (DART-TOF) m/z : calculated for $\text{C}_{11}\text{H}_{23}\text{Si}_2$ [$\text{M}-\text{Br}_2+\text{H}$] $^-$: 211.13328, found 211.13392.

1,1,4,4-tetramethyl-1,4-disilacyclonona-6,7-diene



3.0 g (8.1 mmol) of 9,9-dibromo-3,3,6,6-tetramethyl-3,6-disilabicyclo[6.1.0]nonane was added to a dry 250 mL flask and after flushing with N_2 , 100 mL of Et_2O was added. The solution was cooled to -78 $^\circ\text{C}$, and 6 mL of 1.6 M MeLi in Et_2O (9.6 mmol, 1.2 equiv) was added dropwise. The solution was allowed to warm to room temperature and stirred overnight. The solution was carefully quenched by addition of distilled H_2O , then extracted 2x with Et_2O , and washed with brine. The crude residue was passed through a silica plug and the filter cake washed with pentane to yield 1.560 g (91%) of 1,1,4,4-tetramethyl-1,4-disilacyclonona-6,7-diene as a colorless oil.

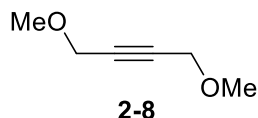
^1H NMR (400 MHz, CDCl_3) δ : 5.12-5.07 (m, 2H), 1.67-1.61 (m, 2H), 1.09-1.03 (m, 2H), 0.66-0.59 (m, 2H), 0.45-0.39 (m, 2H), 0.01 (s, 6H), -0.02 (s, 6H);

^{13}C NMR (100 MHz, CDCl_3) δ : 204.8, 86.6, 14.5, 4.3, -3.0, -4.0;

FT-IR (ATR) $\tilde{\nu}$ [cm^{-1}] = 2974, 2952, 2895, 1946, 1417, 1402, 1247, 1153, 1056, 984, 896, 834, 801, 751.

HRMS (DART-TOF) m/z : calculated for $\text{C}_{11}\text{H}_{22}\text{Si}_2\text{Na}$ $[\text{M}+\text{Na}]^+$: 233.11523, found 233.11510.

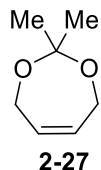
1,4-dimethoxybut-2-yne



In a nitrogen-flushed flame-dried 250 mL round bottom flask equipped with a stirbar and reflux condenser was added 80 mL of dry THF. The flask was cooled to 0 °C and 2.40 g (60 mmol, 2.4 equiv) of sodium hydride (60% dispersion in mineral oil) was added slowly. To this solution of sodium hydride was added slowly 2.15 g (25 mmol, 1 equiv) but-2-yne-1,4-diol in 20 mL in THF. The solution was stirred at 0 °C for 30 minutes, then 3.74 mL (60 mmol, 2.4 equiv) of methyl iodide was added via syringe. The white solution was brought to reflux for 4 h, then stirred at room temperature overnight. The reaction mixture was quenched via the addition of H_2O , after which the bulk of the solvent was removed in vacuo. The crude residue was partitioned between Et_2O and water and extracted 2x, the combined organic extracts were washed with brine, dried, and concentrated giving a yellow oil. This oil was distilled (50 °C, 20 mm Hg) giving 1.326 g of 1,4-dimethoxybut-2-yne as a clear, colorless distillate. Spectral data matched reported values.²⁵

^1H NMR (400 MHz, CDCl_3) δ : 4.15 (s, 4H), 3.39 (s, 6H).

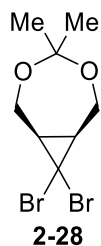
2,2-dimethyl-4,7-dihydro-1,3-dioxepine



To a 250 mL round bottom flask equipped with a stir bar was added 8.18 g (92.6 mmol, 1 equiv) but-2-ene-1,4-diol, 22.84 mL (185 mmol, 2 equiv) 2,2-dimethoxypropane, 872 mg (5 mmol, 0.05 equiv) TsOH, and 54.5 mL of CH₂Cl₂. The mixture was stirred under N₂ for 3 h. After complete reaction was observed by TLC, saturated NaHCO₃ solution was added to the mixture and the product extracted 2x with 50 mL portions of CH₂Cl₂. The combined organic extracts were dried and concentrated to give 8.60 g (72%) of 2,2-dimethyl-4,7-dihydro-1,3-dioxepine as a colorless oil which was used without further purification. Spectral data matched reported values.²⁶

¹H NMR (400 MHz, CDCl₃) δ: 5.66 (t, *J* = 1.6 Hz, 2H), 4.25 (d, *J* = 1.6 Hz, 4H), 1.44 (s, 6H).

8,8-dibromo-4,4-dimethyl-3,5-dioxabicyclo[5.1.0]octane

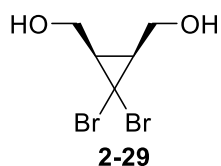


In a 250 mL flask equipped with a stir bar was combined 12.2 mL (140 mmol, 1.5 equiv) bromoform, 1.5 g cetyltrimethylammonium bromide (4.1 mmol, 0.05 equiv), 1 drop of triethylamine, and 25 mL of CH₂Cl₂. To this stirred solution was added 12.135 g (94.7 mmol, 1 equiv) 2,2-dimethyl-4,7-dihydro-1,3-dioxepine. The flask was cooled to 0 °C, and a solution of

NaOH prepared by dissolving 37.5 g NaOH in 38 mL of H₂O was added slowly with strong stirring. The green solution was allowed to slowly warm to room temperature and stirred for an additional 48 h. The mixture was poured into 100 mL of water and extracted 3x with CH₂Cl₂. The combined extracts were concentrated, then 75 mL of pentane was added. The solution was stirred for 15 min, while cetyltrimethylammonium bromide precipitated. The mixture was then filtered through celite and the filter cake washed with 350 mL of pentane. The orange filtrate was dried (MgSO₄) and concentrated to give an orange slurry, which was stripped of excess bromoform under high vacuum. The remaining material was triturated several times with pentane, after which 21.138 g (74%) of 8,8-dibromo-4,4-dimethyl-3,5-dioxabicyclo[5.1.0]octane was obtained as a colorless solid. Spectral data matched reported values.²⁶

¹H NMR (400 MHz, CDCl₃) δ: 4.26-4.21 (m, 2H), 3.96-3.91 (m, 2H), 2.08-2.06 (m, 2H), 1.38 (s, 3H), 1.28 (s, 3H).

(3,3-dibromocyclopropane-1,2-diyl)dimethanol

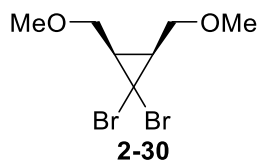


9.715 g (32.4 mmol, 1 equiv) of 8,8-dibromo-4,4-dimethyl-3,5-dioxabicyclo[5.1.0]octane was added to 50 mL of 2 M HCl in a 250 mL round bottom flask equipped with a stir bar and reflux condenser. The solution was refluxed for 2 h, then allowed to cool to room temperature. The product mixture was extracted 8x with 50 mL portions of CH₂Cl₂. The combined organic extracts were washed with 10 mL of saturated sodium bicarbonate solution, then decolorized by stirring with 1 g charcoal for 30 min. The charcoal was removed by filtration; the filtrate was

dried (MgSO₄) and concentrated to give 4.827 g (57%) of (3,3-dibromocyclopropane-1,2-diyl)dimethanol as a colorless solid. Spectral data matched reported values.²⁶

¹H NMR (400 MHz, CDCl₃) δ: 4.14-4.07 (m, 2H), 3.70-3.63 (m, 2H), 2.17-2.06 (m, 4H).

1,1-dibromo-2,3-bis(methoxymethyl)cyclopropane



To a 250 mL round bottom flask equipped with a stir bar was added 3.6 g (13.85 mmol, 1 equiv) (3,3-dibromocyclopropane-1,2-diyl)dimethanol, 3.16 mL (50.7 mmol, 3.7 equiv) methyl iodide, and 70 mL of THF. Then, 1.39 g (34.6 mmol, 2.5 equiv) sodium hydride (60% dispersion in mineral oil) was added slowly at room temperature with stirring. The reaction was stirred for 5 h at room temperature, then 10 mL of a saturated solution of NH₄Cl was added slowly to quench the reaction. The product mixture was poured into 50 mL of H₂O, then extracted 3x with 75 mL portions of CH₂Cl₂. The combined organic extracts were dried (MgSO₄) and concentrated in vacuo. The crude residue was purified by flash column chromatography (6:1, hexanes:EtOAc) to give 2.53 g (64%) 1,1-dibromo-2,3-bis(methoxymethyl)cyclopropane as a pale yellow oil.

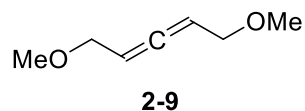
¹H NMR (400 MHz, CDCl₃) δ: 3.50-3.48 (m, 4H), 3.40 (s, 6H), 2.03-2.00 (m, 2H);

¹³C NMR (100 MHz, CDCl₃) δ: 70.0, 58.7, 32.3, 31.3;

FT-IR (ATR) $\tilde{\nu}$ [cm⁻¹] = 2984, 2927, 2894, 2816, 1454, 1413, 1392, 1317, 1283, 1251, 1233, 1195, 1125, 1103, 1073, 1025, 995, 961, 915, 875, 769, 736;

HRMS (DART-TOF) *m/z*: calculated for C₇H₁₁BrO₂ [M-HBr]⁻: 205.99369, found 205.99295.

1,5-dimethoxypenta-2,3-diene



A flame-dried 250 mL round bottom flask equipped with a stir bar was flushed with nitrogen. To this flask was added 3.069 g (10.7 mmol, 1 equiv) 1,1-dibromo-2,3-bis(methoxymethyl)cyclopropane and 70 mL of freshly distilled hexanes. Then, 7.32 mL (11.7 mmol, 1.1 equiv) of 1.6 M methyllithium in Et₂O was added at room temperature over a period of 30 min. The reaction was stirred for 20 h, then cautiously quenched with H₂O. The mixture was transferred to a separatory funnel and extracted 3x with 50 mL portions of Et₂O. The combined organic fractions were dried (MgSO₄) and concentrated. The crude residue was distilled (20 mm Hg, 50 °C) to give 223 mg (16%) of 1,5-dimethoxypenta-2,3-diene as a colorless oil.

¹H NMR (400 MHz, CDCl₃) δ: 5.34-5.29 (m, 2H), 3.99-3.96 (m, 4H), 3.35 (s, 6H);

¹³C NMR (100 MHz, CDCl₃) δ: 205.6, 89.2, 70.2, 57.7;

FT-IR (ATR) $\tilde{\nu}$ [cm⁻¹] = 2983, 2926, 2887, 2849, 2841, 2819, 1966, 1453, 1365, 1289, 1187, 1094, 1045, 1012, 957, 910, 867, 858, 725, 708;

HRMS (DART-TOF) *m/z*: calculated for C₇H₁₁O₂ [M-H]⁺ : 127.07535, found 127.07583.

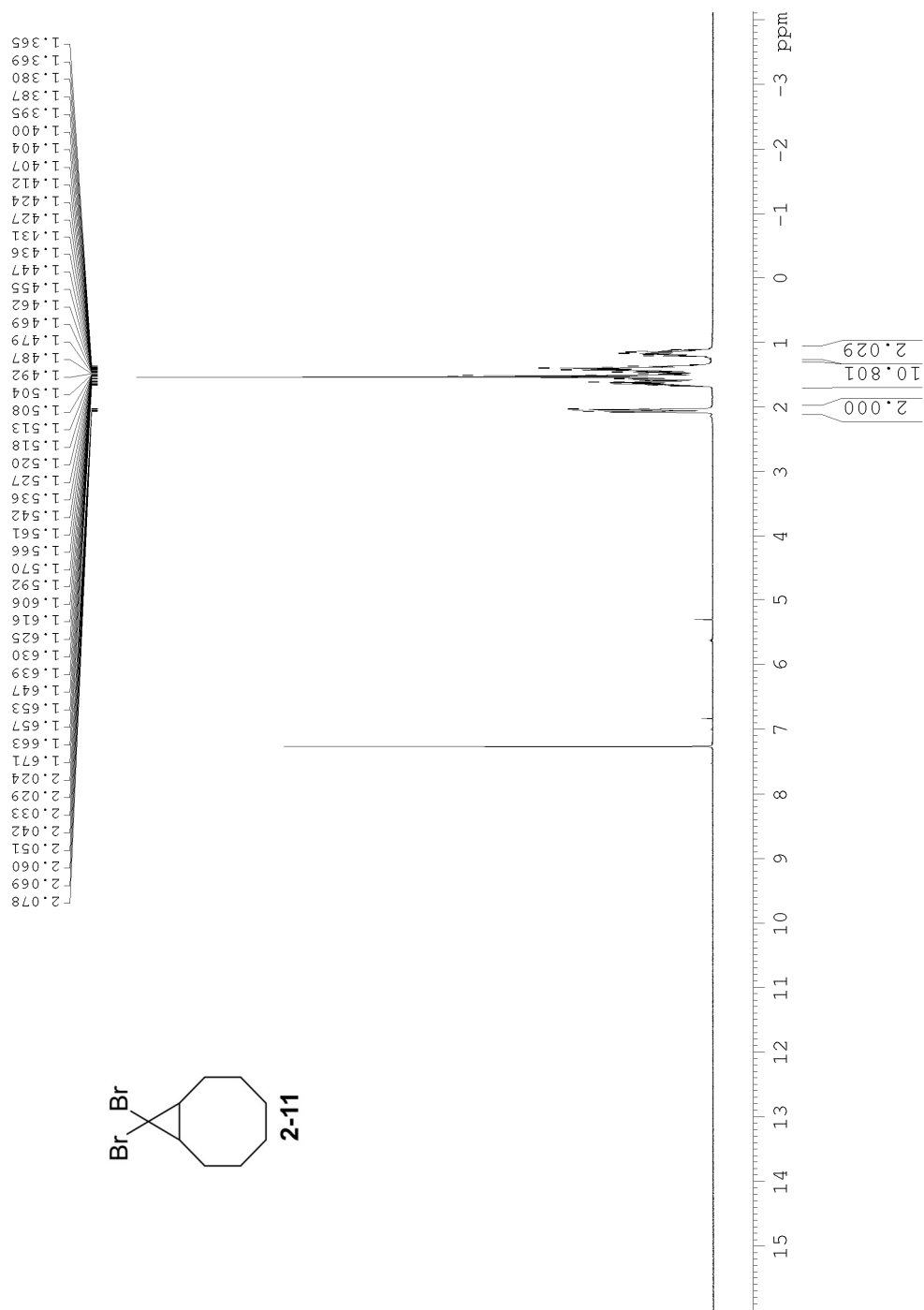
2.6 – References

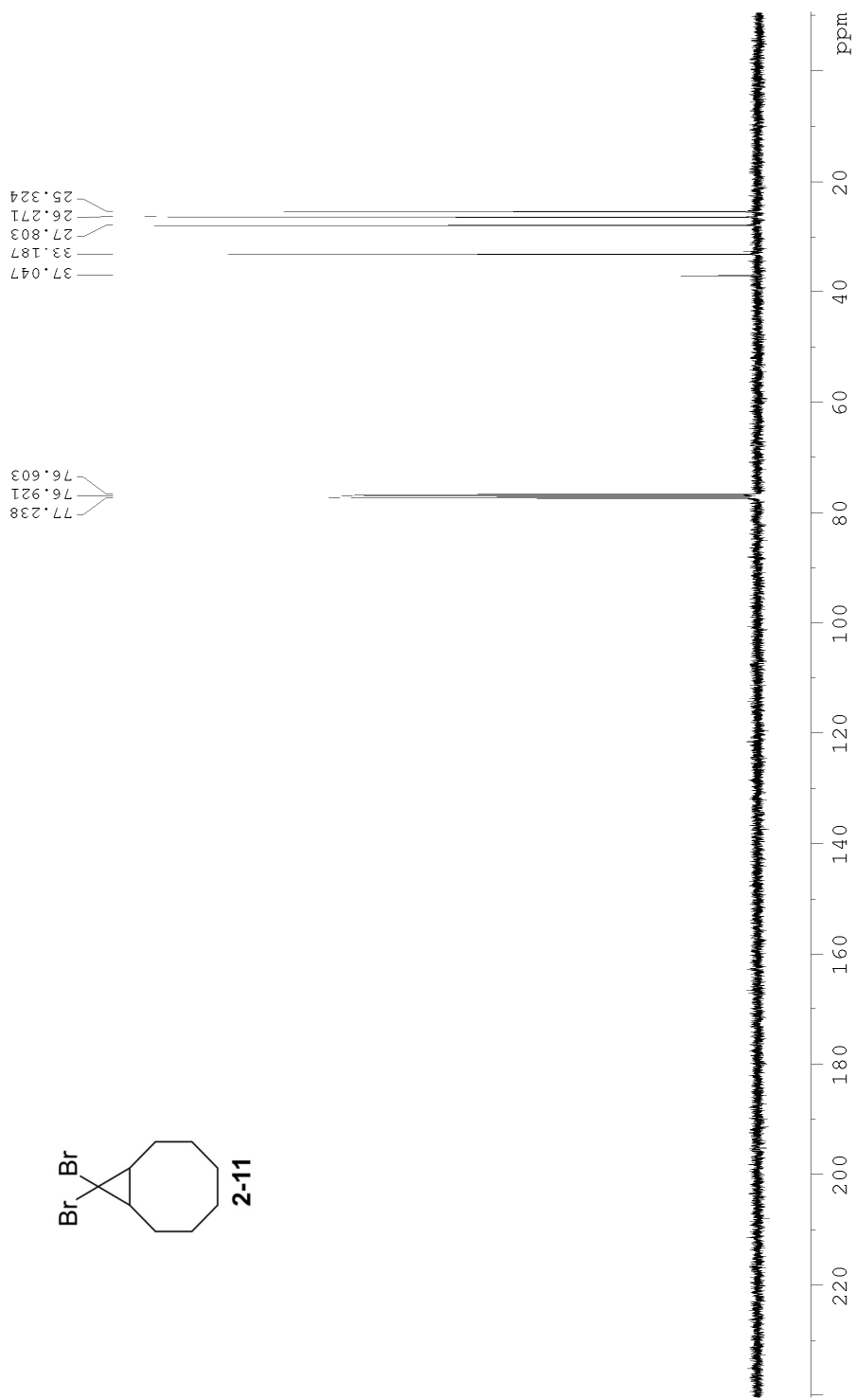
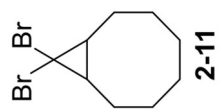
- (1) Zeise, W. C. *Ann. der Phys. und Chemie* **1831**, 97, 497.
- (2) Dewar, M. *Bull. Soc. Chim. Fr.* **1951**, 1, C79.
- (3) Chatt, J.; Duncanson, L. A. *J. Chem. Soc.* **1953**, 2939.
- (4) Chatt, J.; Duncanson, L. A.; Venanzi, L. M. *J. Chem. Soc.* **1955**, 4456.
- (5) Tolman, C. A. *J. Am. Chem. Soc.* **1974**, 96, 2780.
- (6) Johnson, J. B.; Rovis, T. *Angew. Chem. Int. Ed.* **2008**, 47, 840.
- (7) Takahashi, G.; Shirakawa, E.; Tsuchimoto, T.; Kawakami, Y. *Chem. Commun.* **2005**, 1459.
- (8) Terao, J.; Todo, H.; Begum, S. A.; Kuniyasu, H.; Kambe, N. *Angew. Chem. Int. Ed.* **2007**, 46, 2086.
- (9) Shirakawa, E.; Yasuhara, Y.; Hayashi, T. *Chem. Lett.* **2006**, 35, 768.
- (10) Cai, F.; Pu, X.; Qi, X.; Lynch, V.; Radha, A.; Ready, J. M. *J. Am. Chem. Soc.* **2011**, 133, 18066.
- (11) Iafe, R. G.; Chan, D. G.; Kuo, J. L.; Boon, B. A.; Faizi, D. J.; Saga, T.; Turner, J. W.; Merlic, C. A. *Org. Lett.* **2012**, 14, 4282.
- (12) Chan, D. M. T.; Monaco, K. L.; Wang, R.-P.; Winters, M. P. *Tetrahedron Lett.* **1998**, 39, 2933.
- (13) Evans, D. A.; Katz, J. L.; West, T. R. *Tetrahedron Lett.* **1998**, 39, 2937.

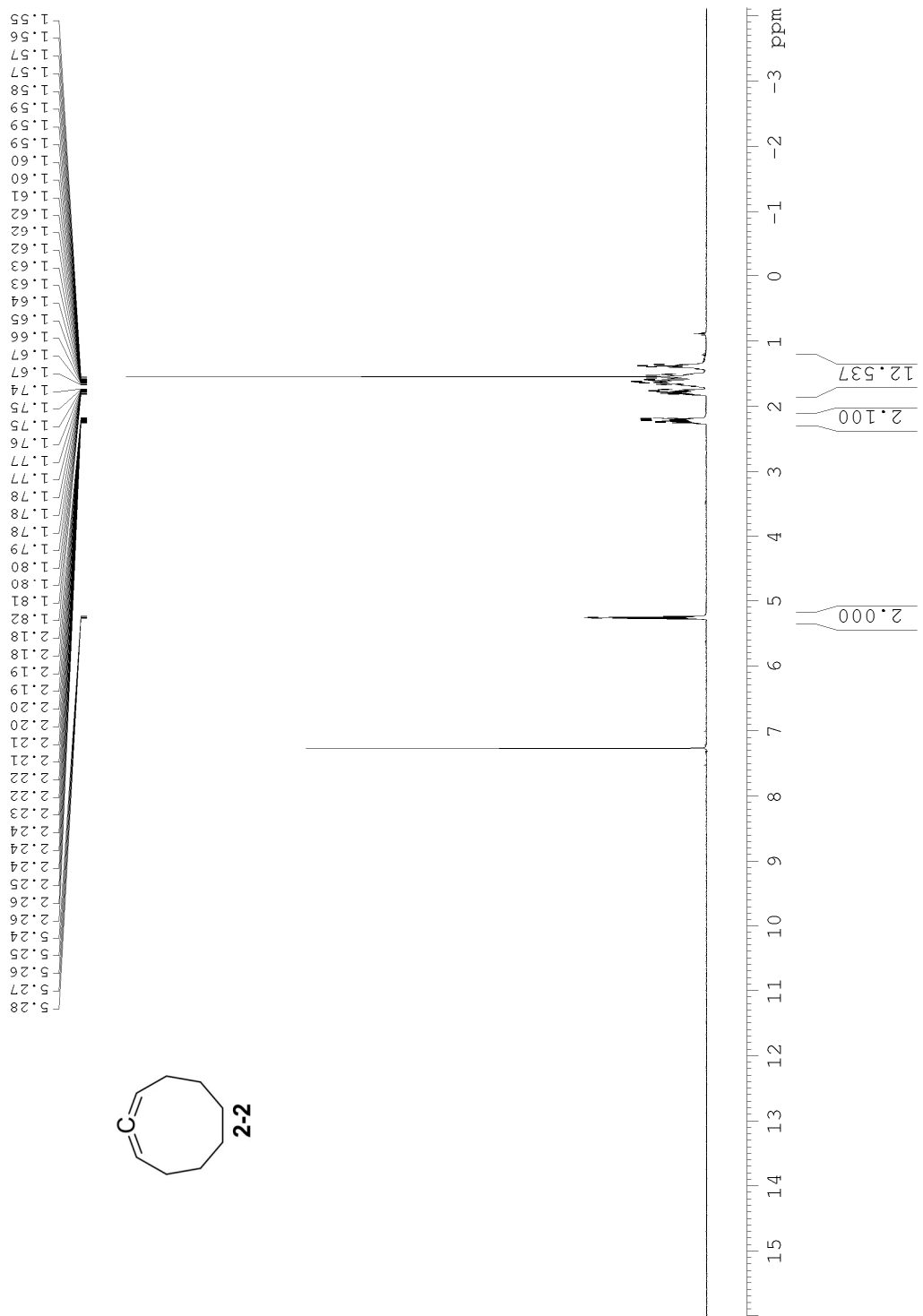
- (14) Lam, P.; Clark, C.; Saubern, S.; Adams, J.; Winters, M.; Chan, D.; Combs, A. *Tetrahedron Lett.* **1998**, *39*, 2941.
- (15) Shade, R. E.; Hyde, A. M.; Olsen, J.-C.; Merlic, C. A. *J. Am. Chem. Soc.* **2010**, *132*, 1202.
- (16) Chan, D. G.; Winternheimer, D. J.; Merlic, C. A. *Org. Lett.* **2011**, *13*, 2778.
- (17) Winternheimer, D. J.; Merlic, C. A. *Org. Lett.* **2010**, *12*, 2508.
- (18) Skattebøl, L.; Solomon, S. *Org. Synth.* **1969**, *49*, 35.
- (19) Baird, M. S.; Reese, C. B. *Tetrahedron* **1976**, *32*, 2153.
- (20) Moore, W. R.; Ward, H. R. *J. Am. Chem. Soc.* **1963**, *85*, 86.
- (21) Hanack, M.; Wächtler, A. E. F. *Chem. Ber.* **1987**, *120*, 727.
- (22) Reese, C. B.; Shaw, A. *J. Chem. Soc. Perkin Trans. 1* **1976**, 890.
- (23) Brandsma, L.; Verkruijsse, H. D. *Synthesis* **1978**, 290.
- (24) Shea, K. J.; Kim, J. S. *J. Am. Chem. Soc.* **1992**, *114*, 3044.
- (25) Tenaglia, A.; Marc, S. *J. Org. Chem.* **2008**, *73*, 1397.
- (26) Al-Dulayymi, A.; Li, X.; Neuenschwander, M. *Helv. Chim. Acta* **2000**, *83*, 1633.
- (27) Yamamoto, Y. *J. Org. Chem.* **2007**, *72*, 7817.
- (28) Campbell, K. A.; House, H. O.; Surber, B. W.; Trahanovsky, W. S. *J. Org. Chem.* **1987**, *52*, 2474.
- (29) Shibato, A.; Itagaki, Y.; Tayama, E.; Hokke, Y.; Asao, N.; Maruoka, K. *Tetrahedron* **2000**, *56*, 5373.

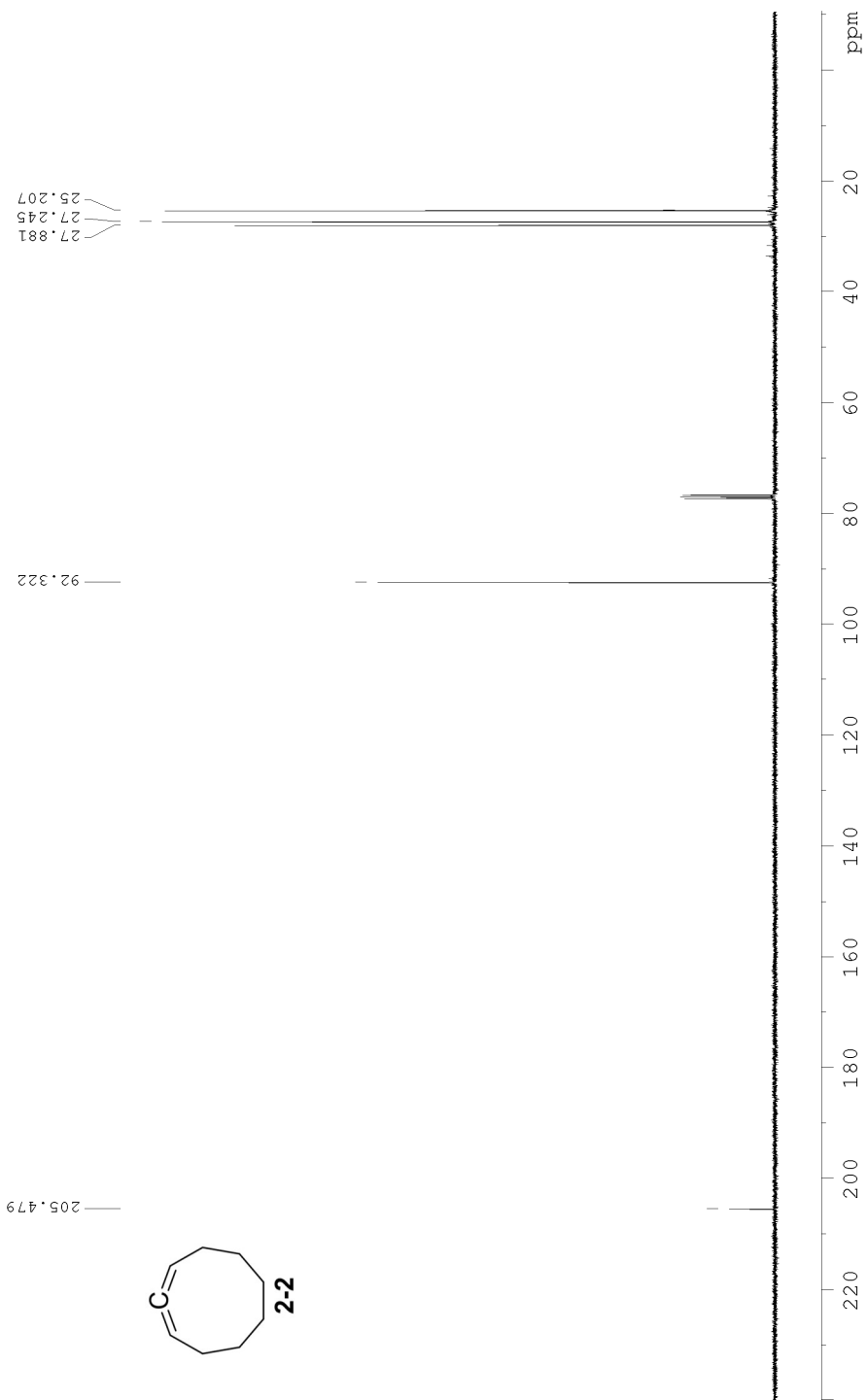
(30) Hoshi, T.; Yasuda, H.; Sanji, T.; Sakurai, H. *Bull. Chem. Soc. Jpn.* **1999**, 72, 821.

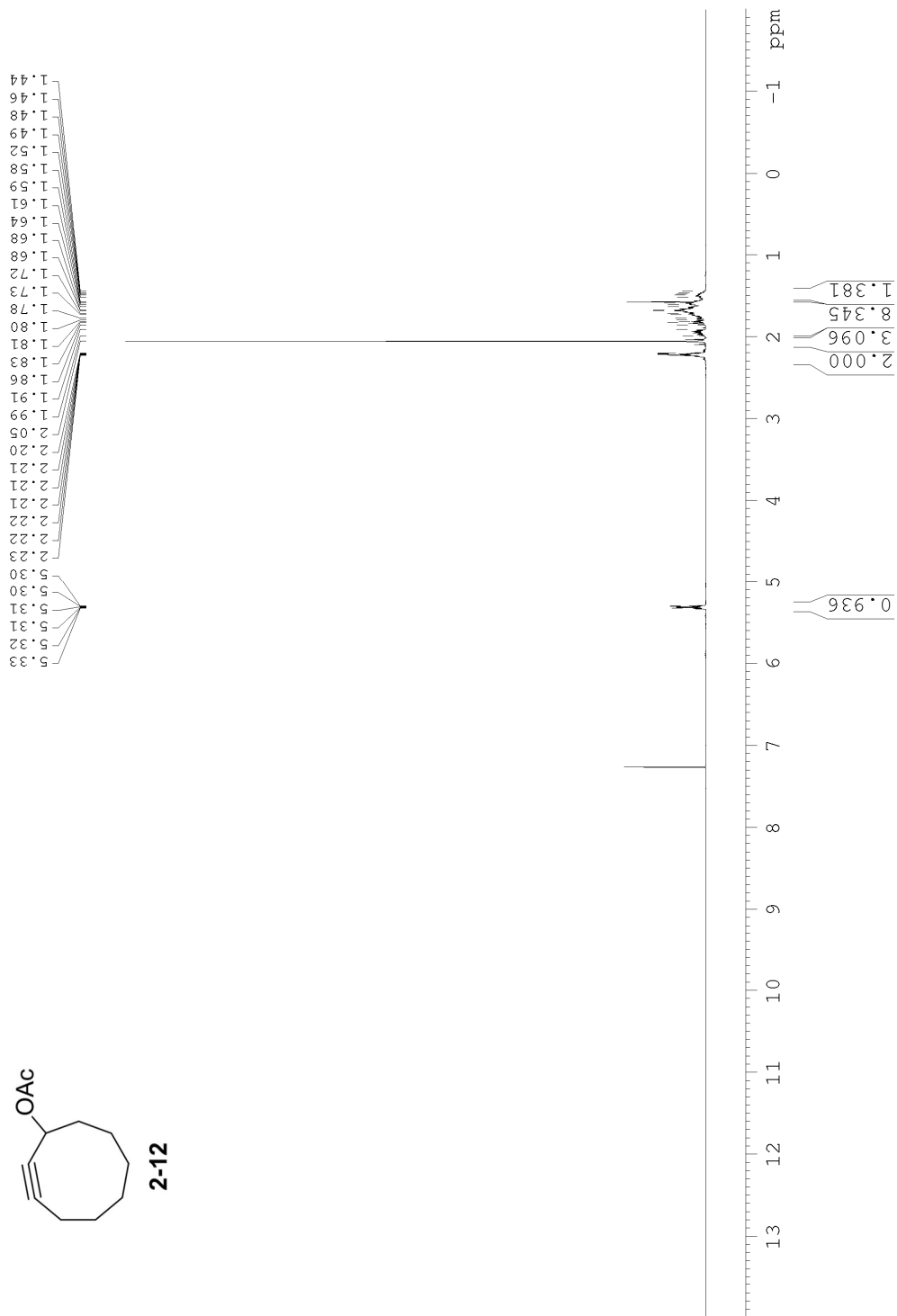
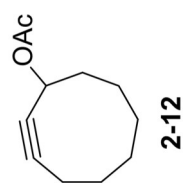
2.7 – NMR Spectra

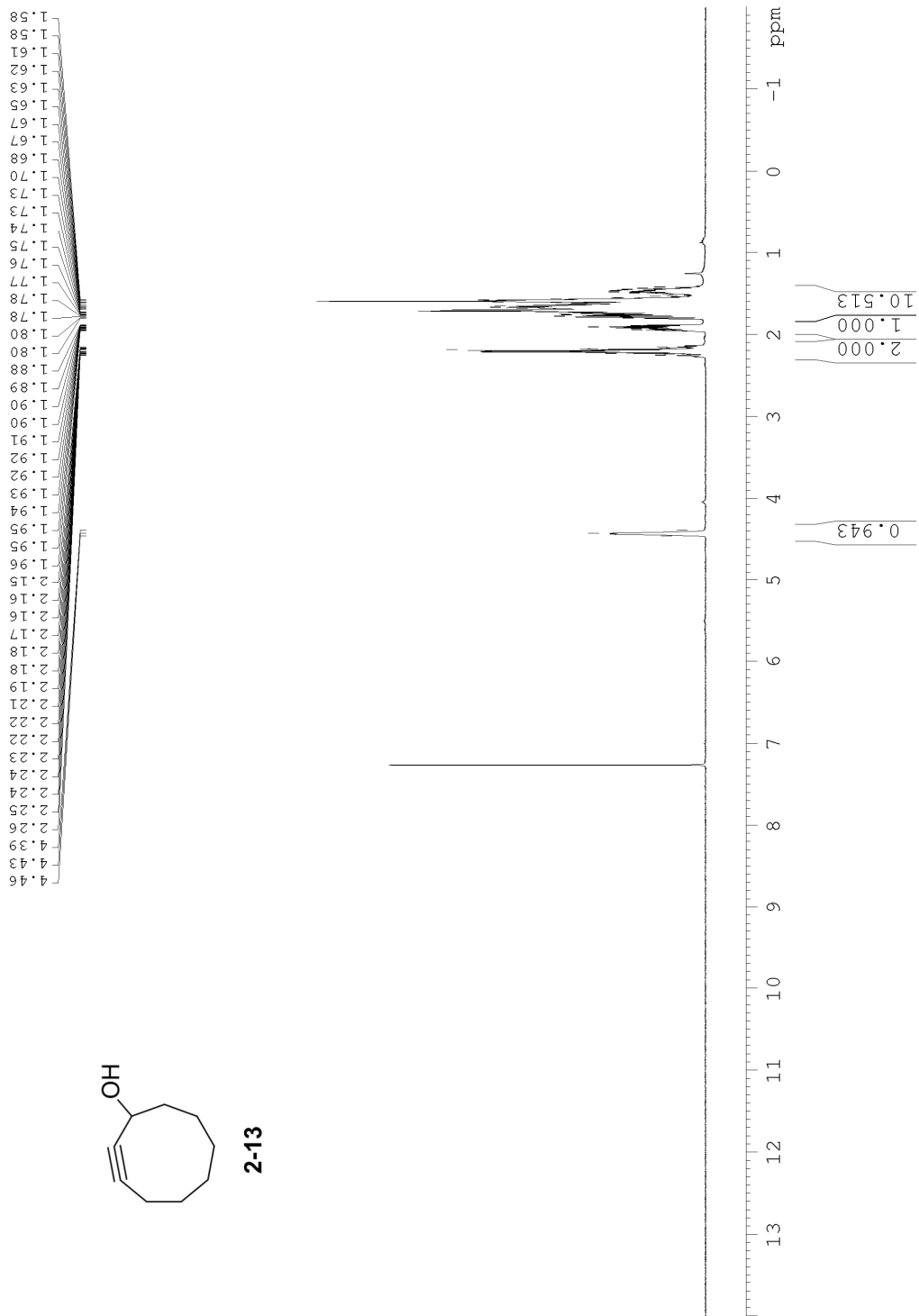


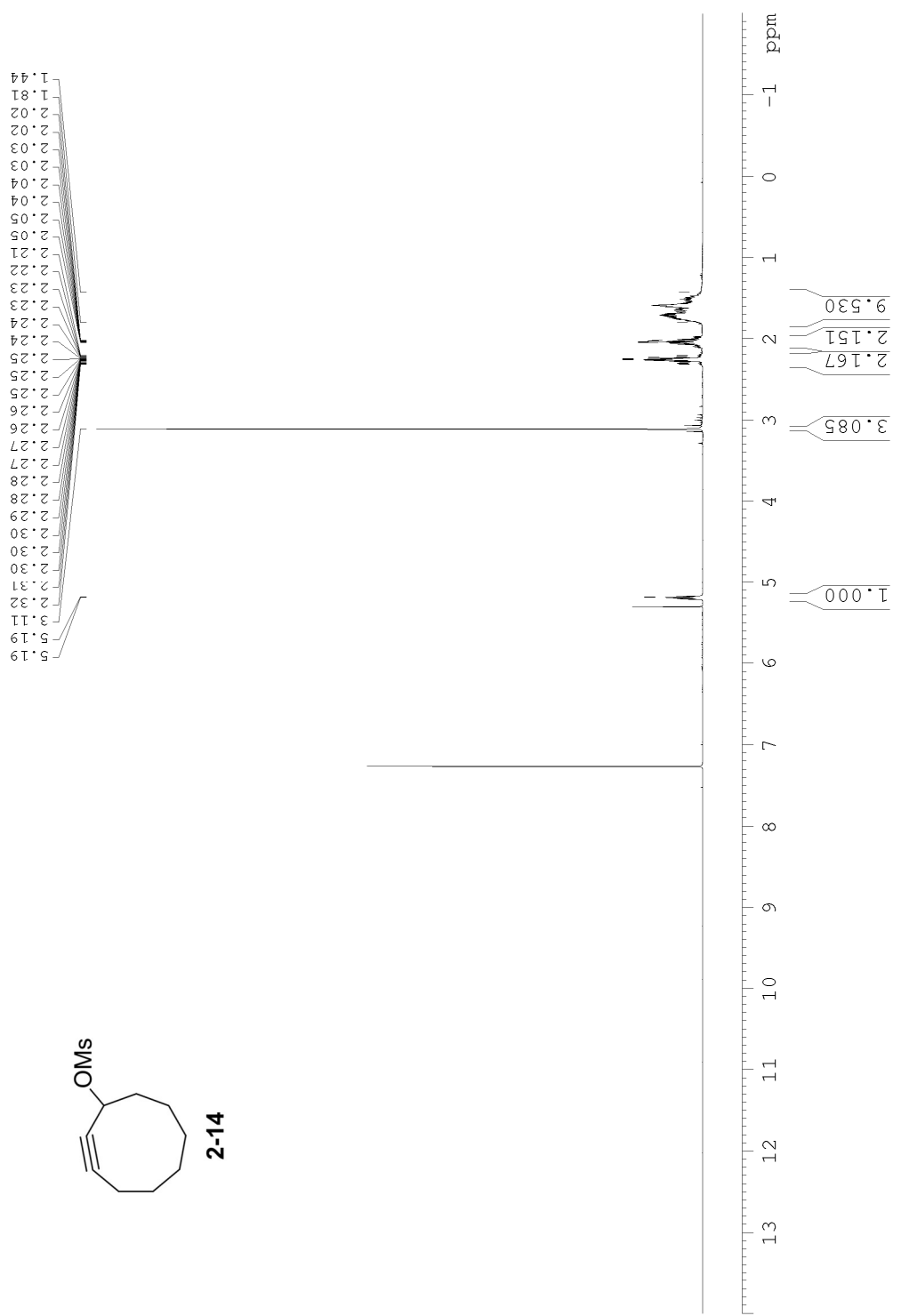


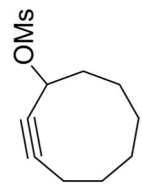










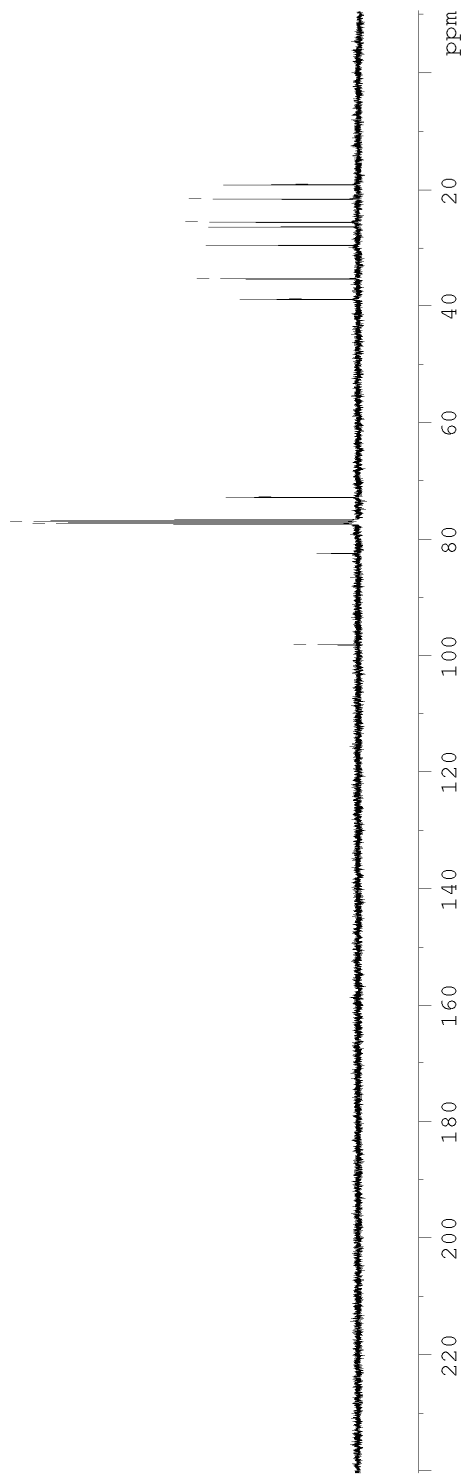


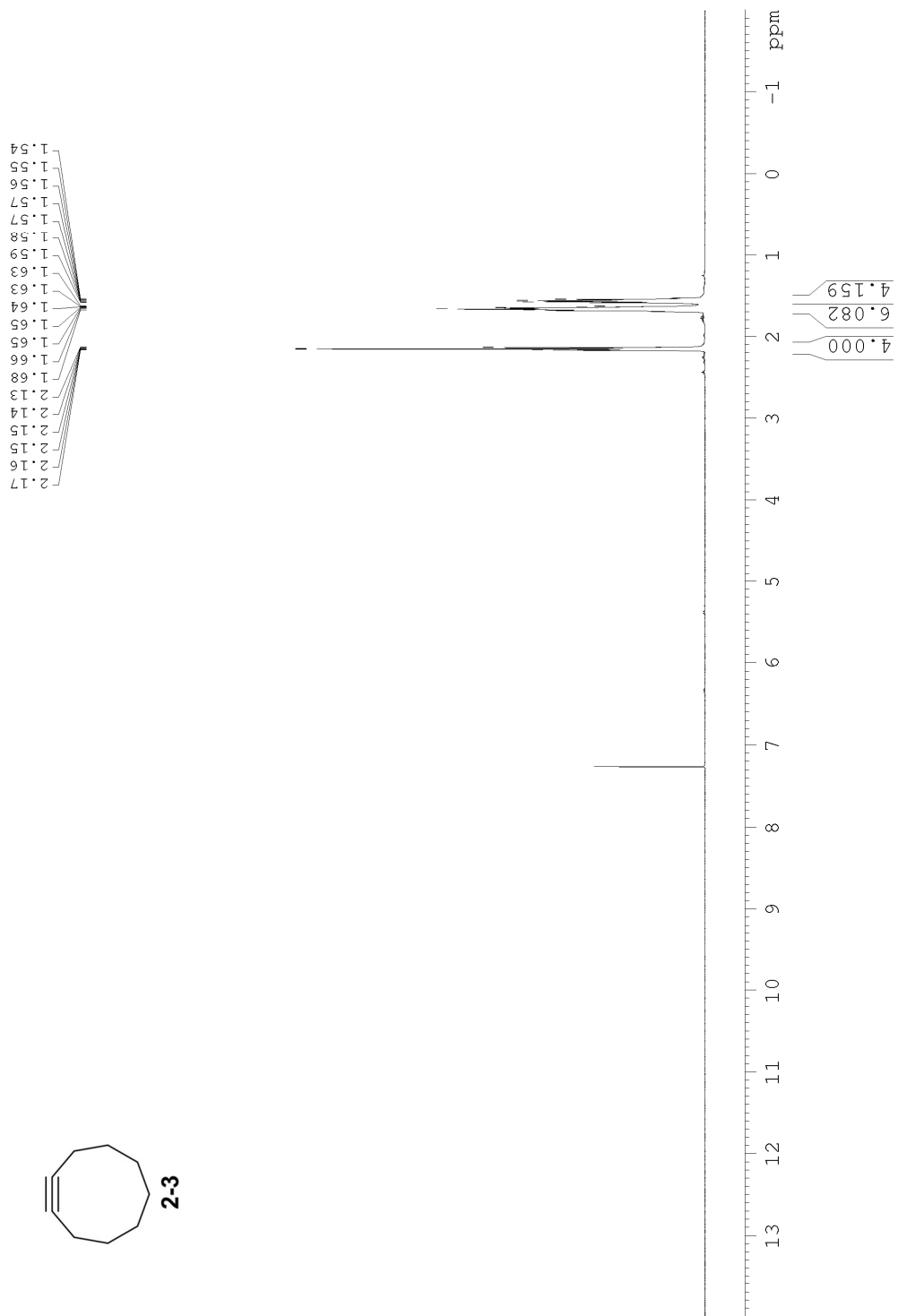
2-14

38.820
35.295
29.420
26.264
25.444
21.492
19.039

82.345
77.250
76.932
76.615
72.741

97.960

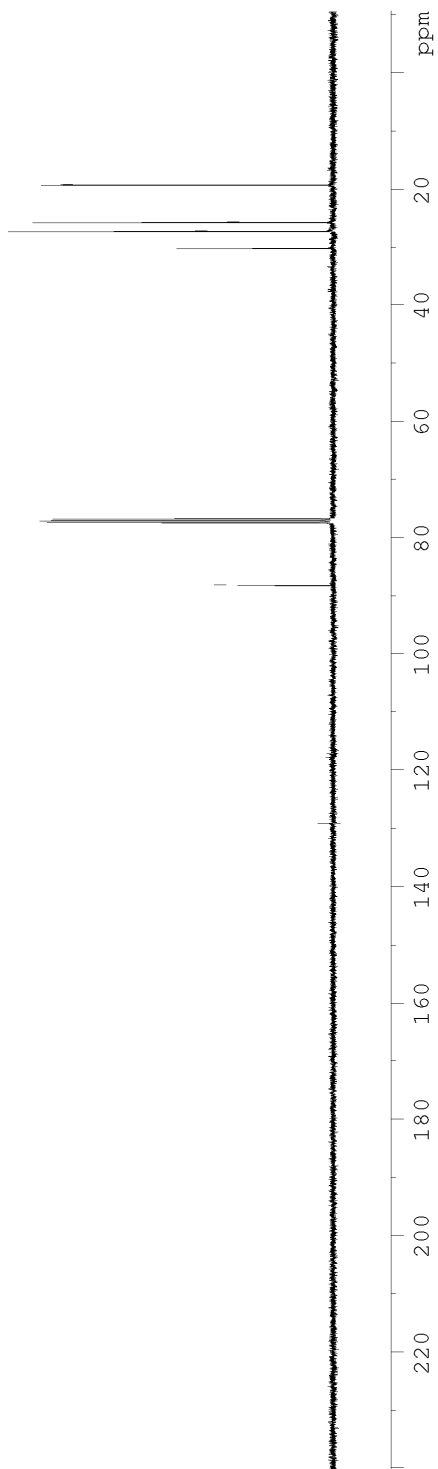


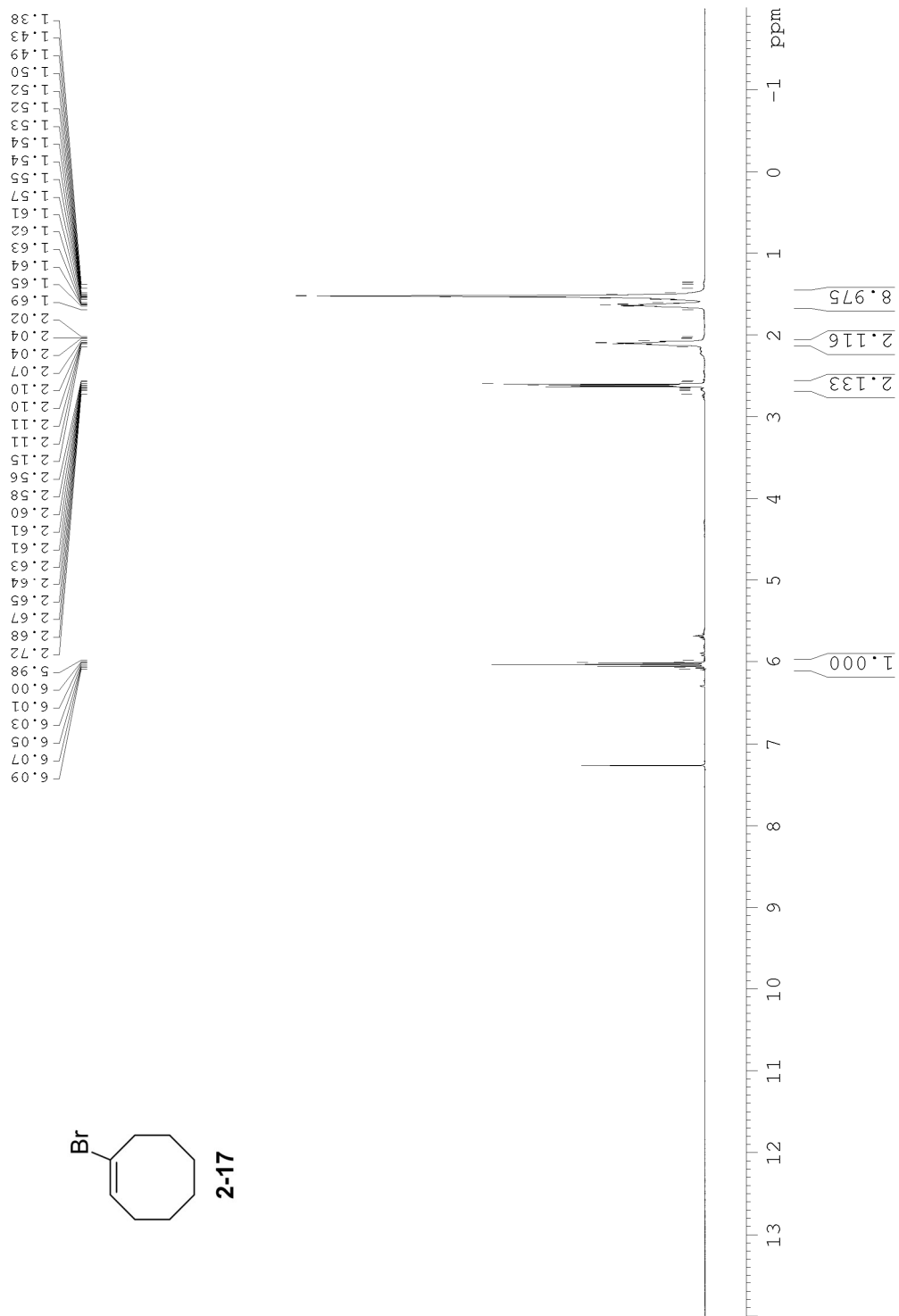


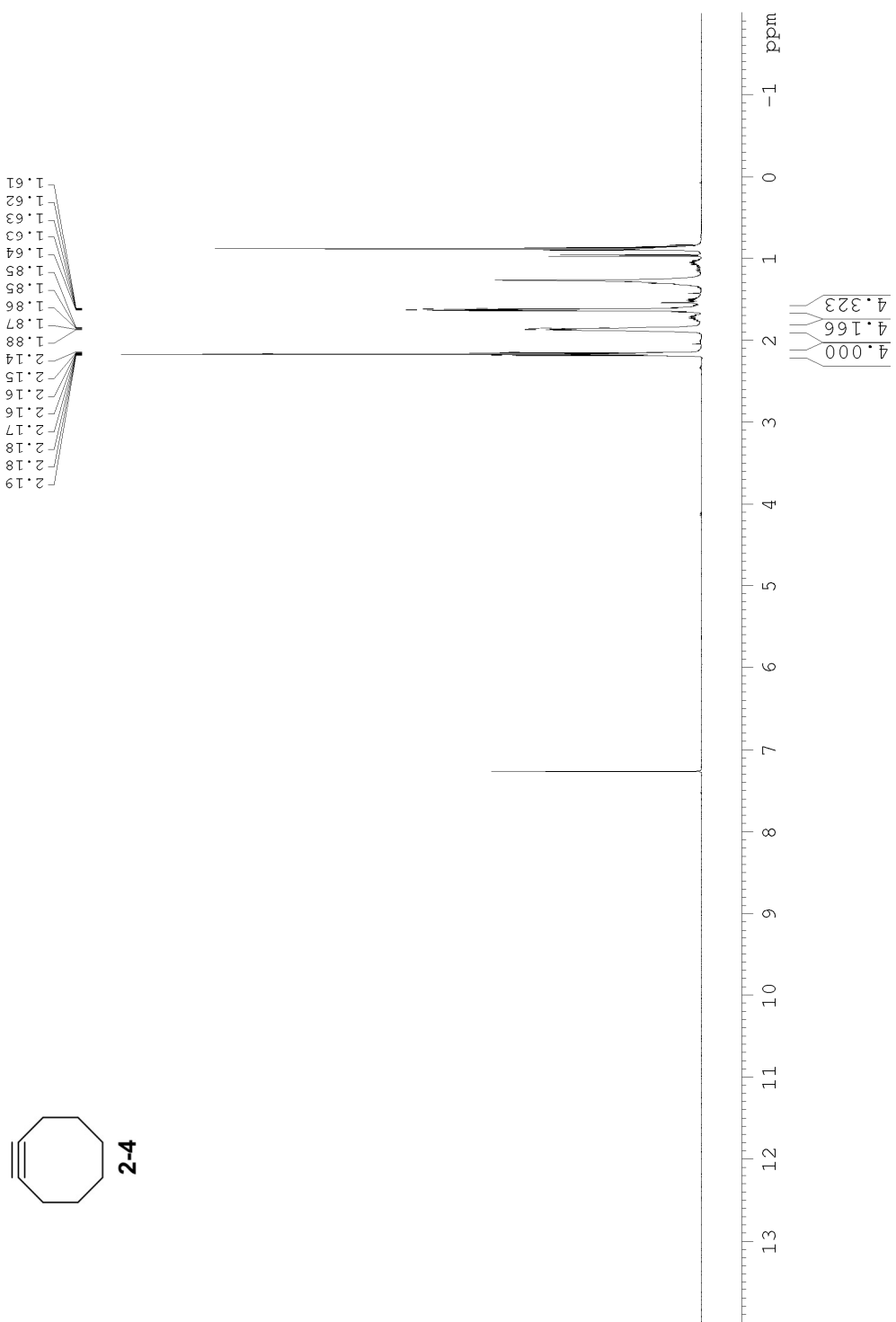


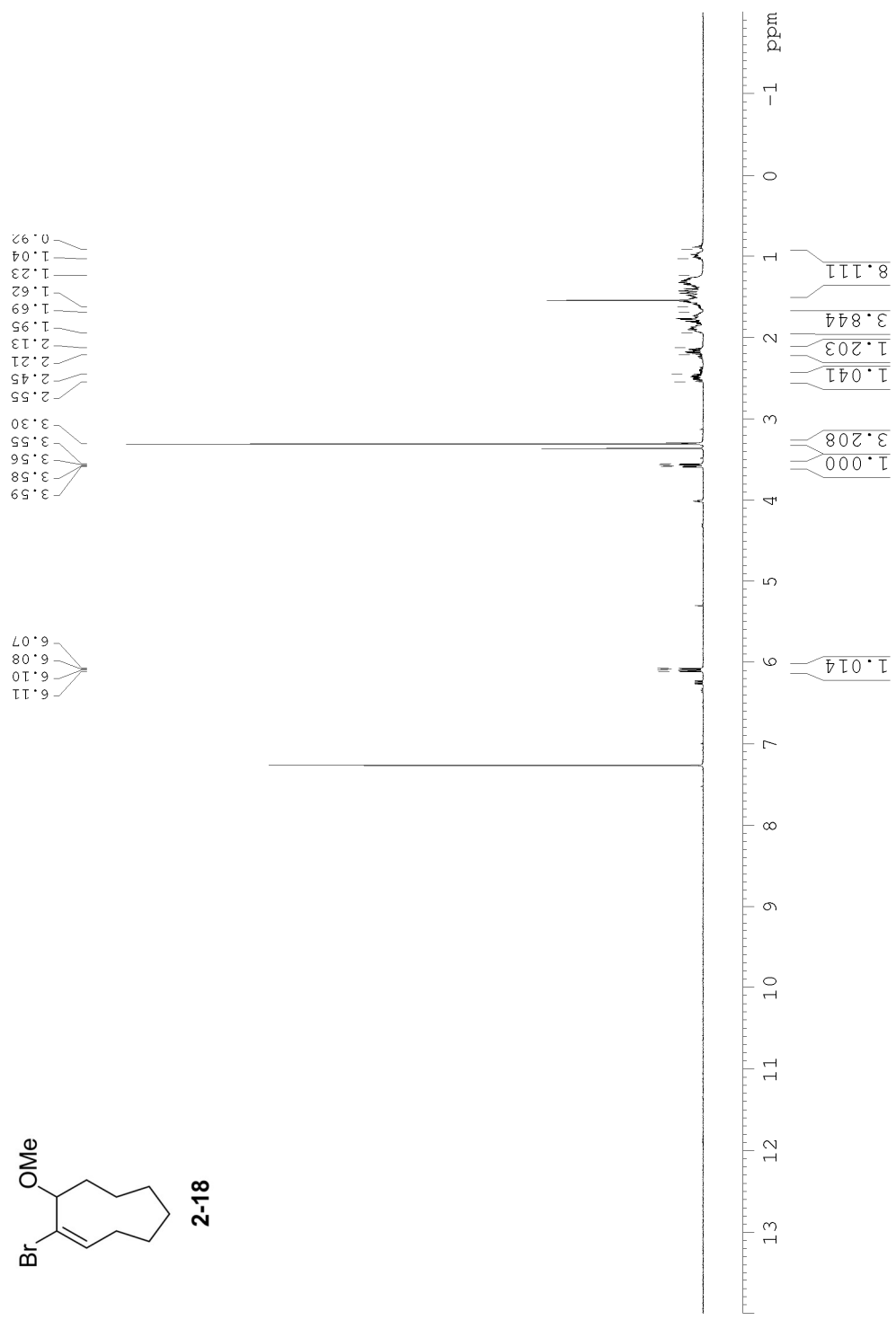
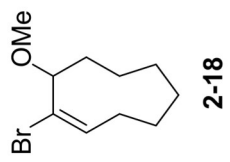
30.132
27.168
25.629
19.197

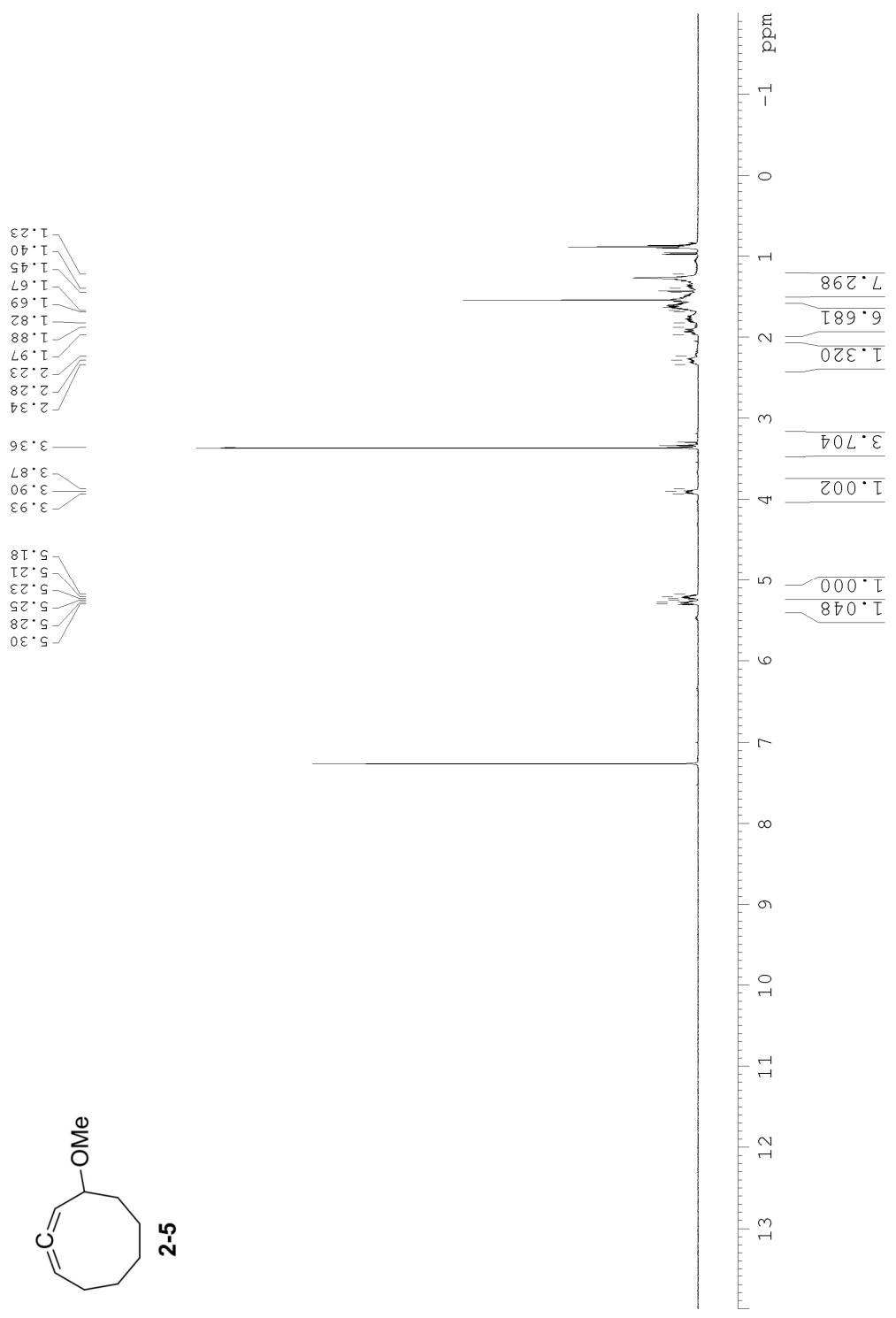
88.143

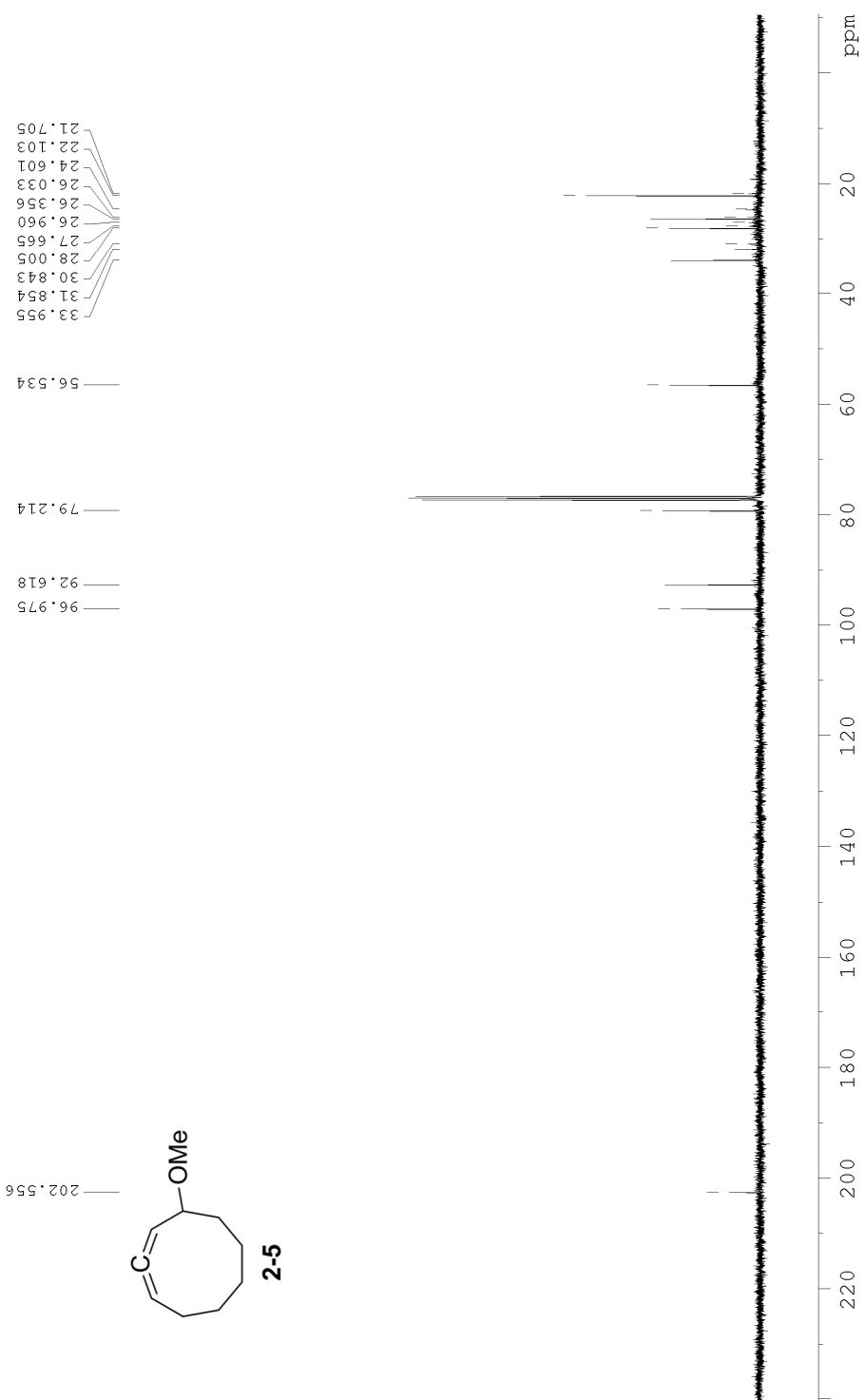


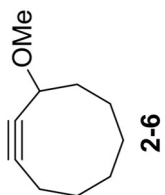
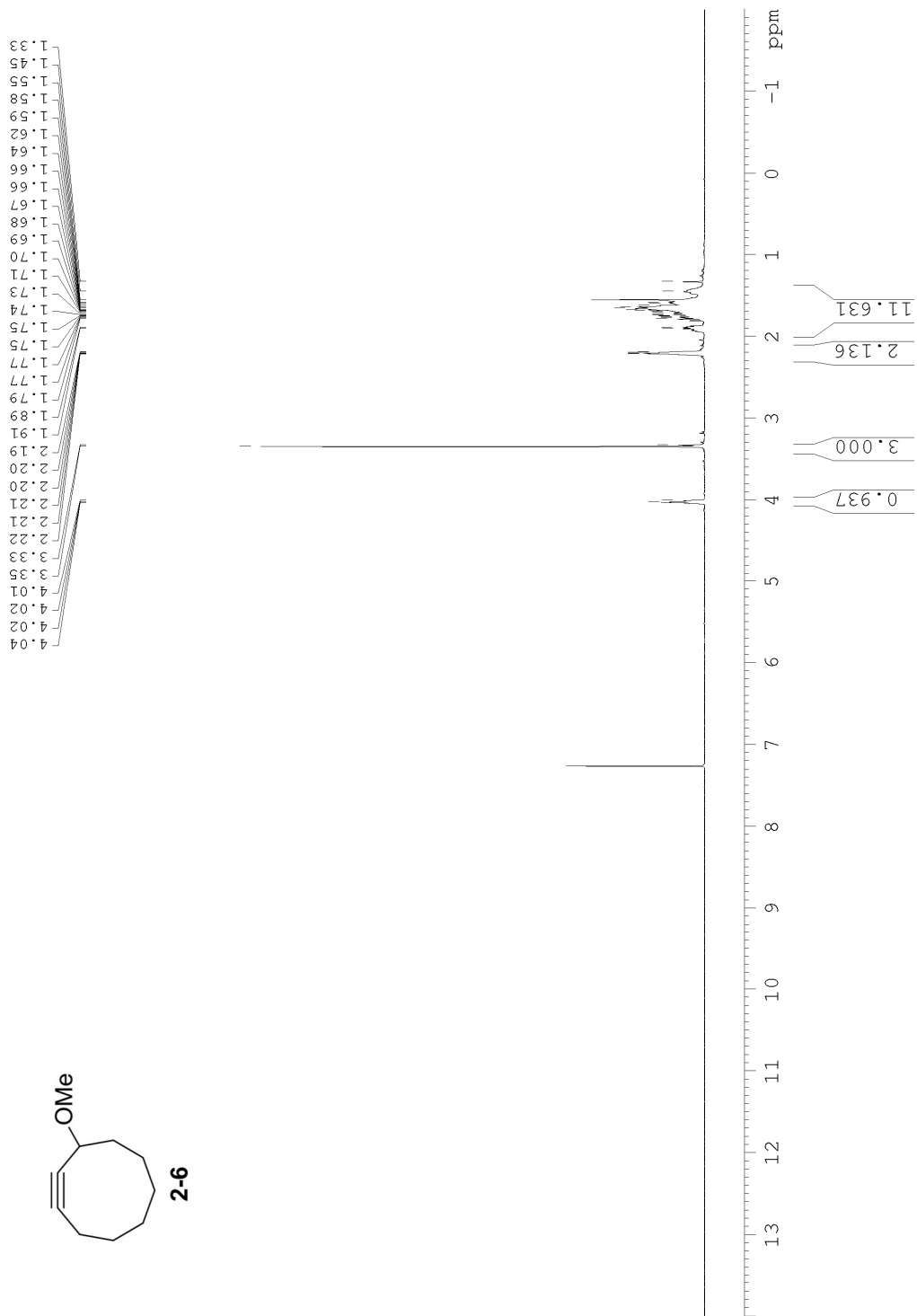


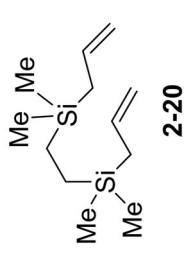
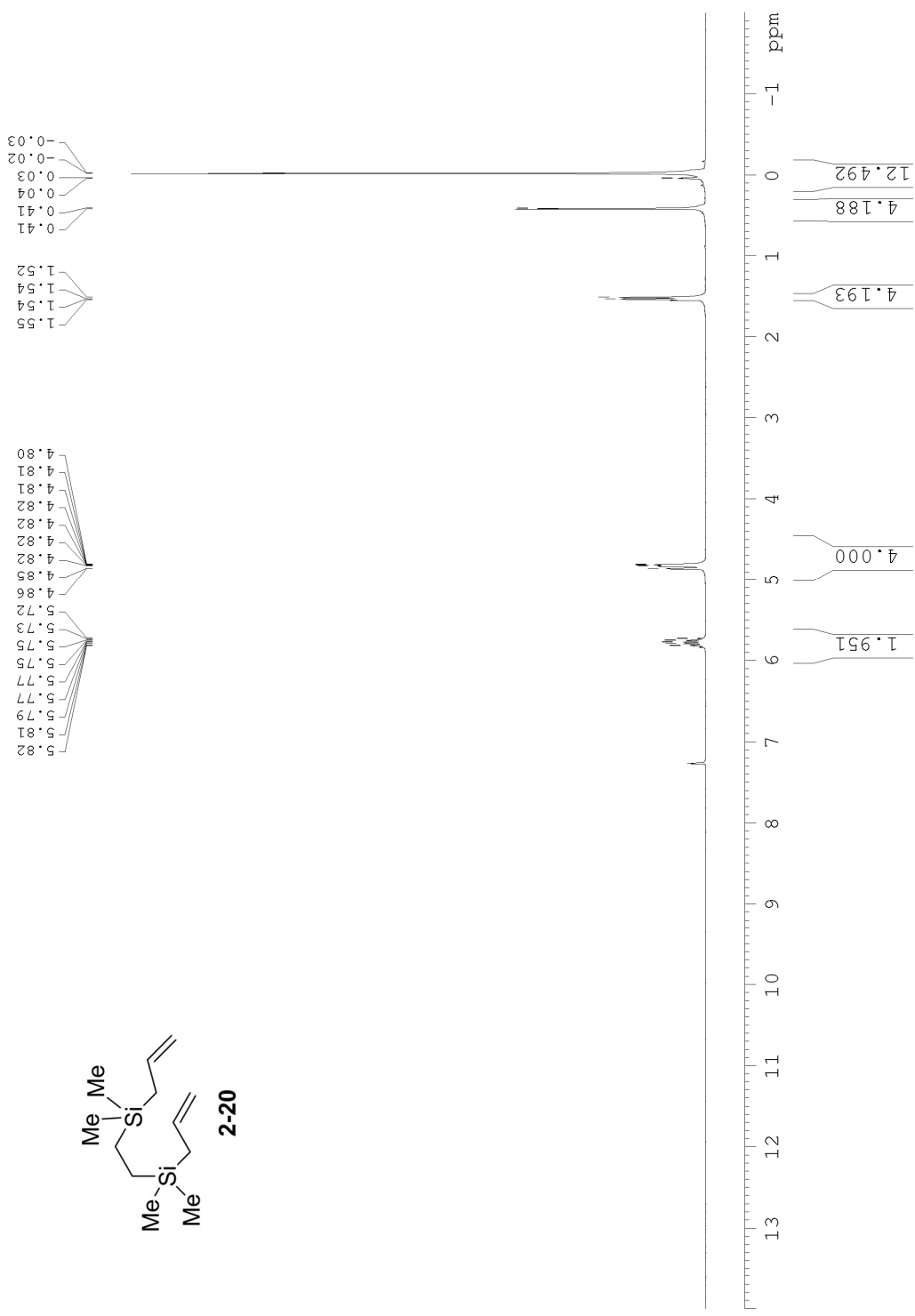


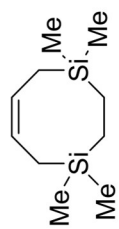




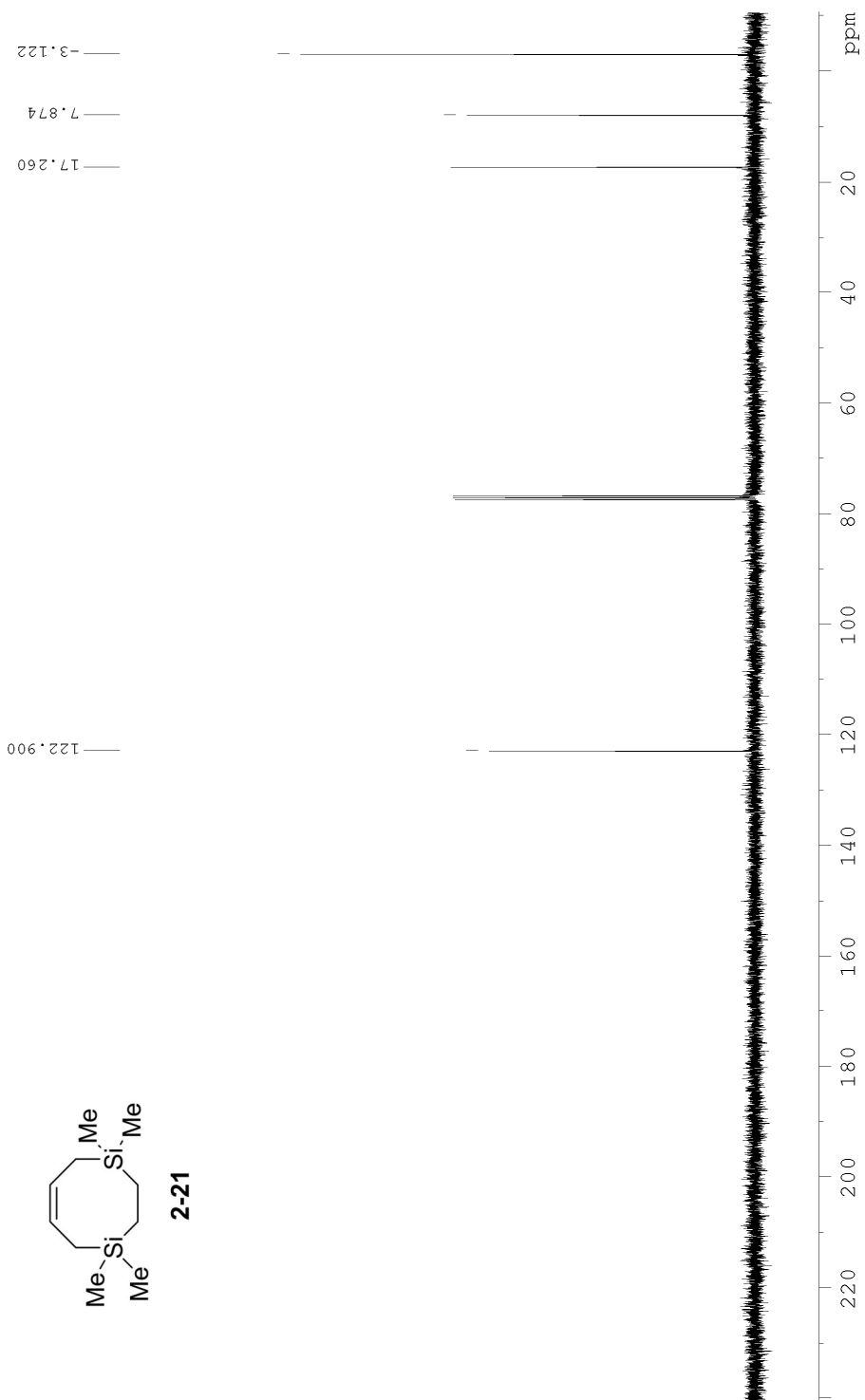


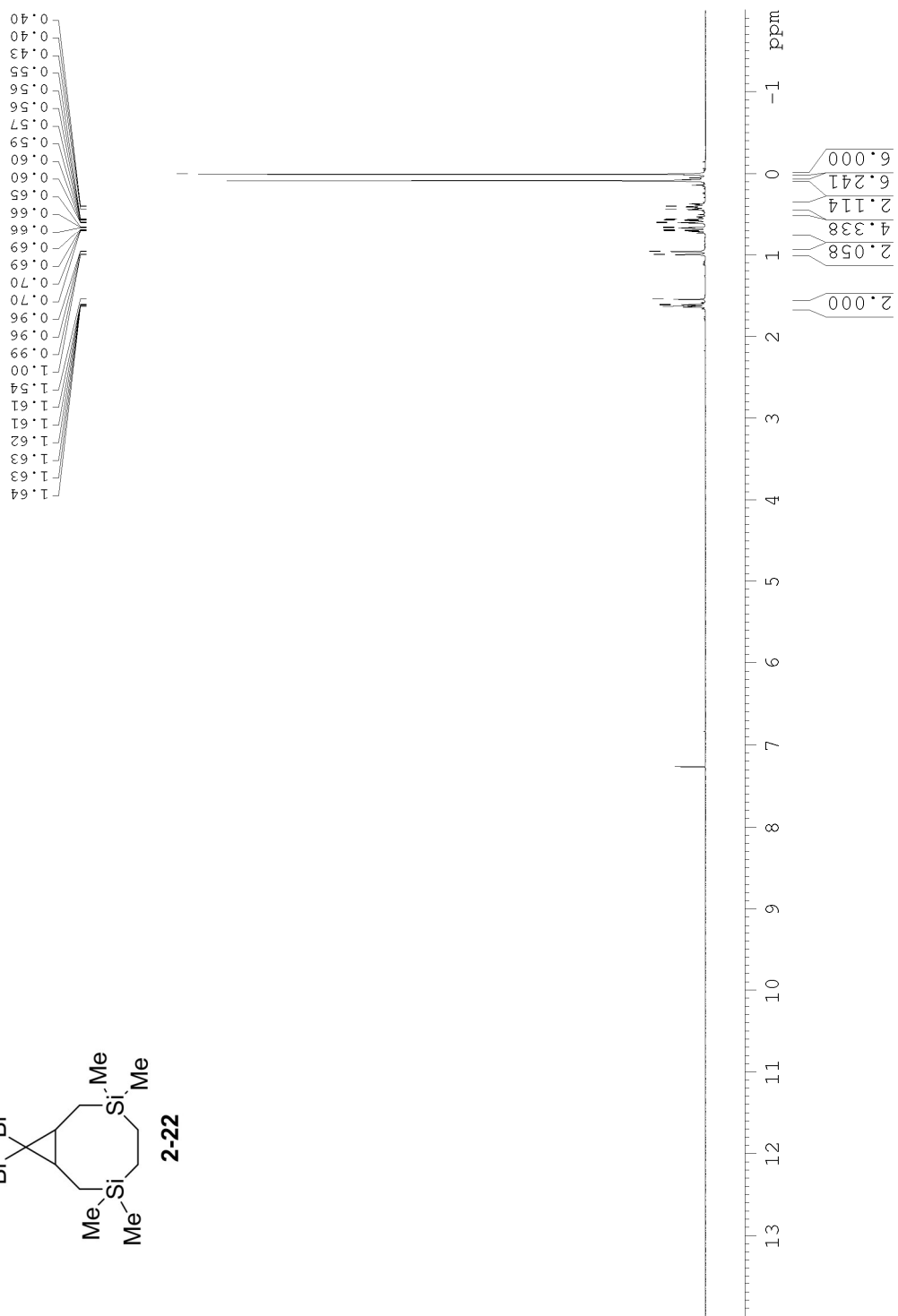
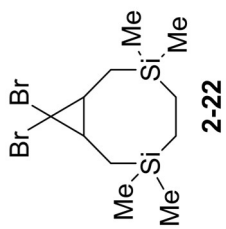


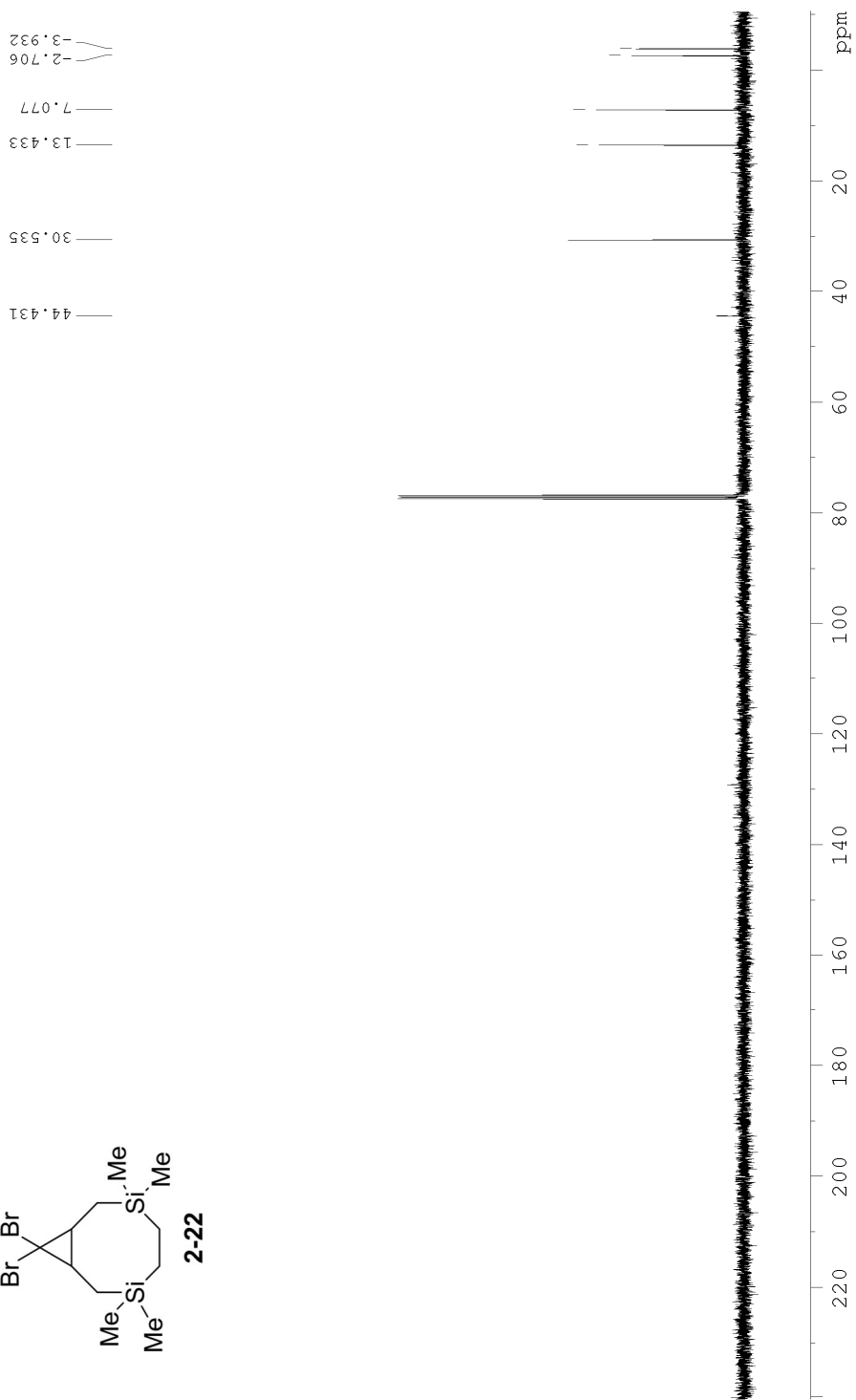
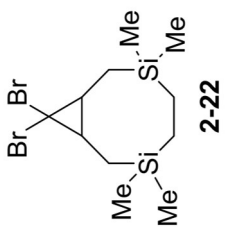


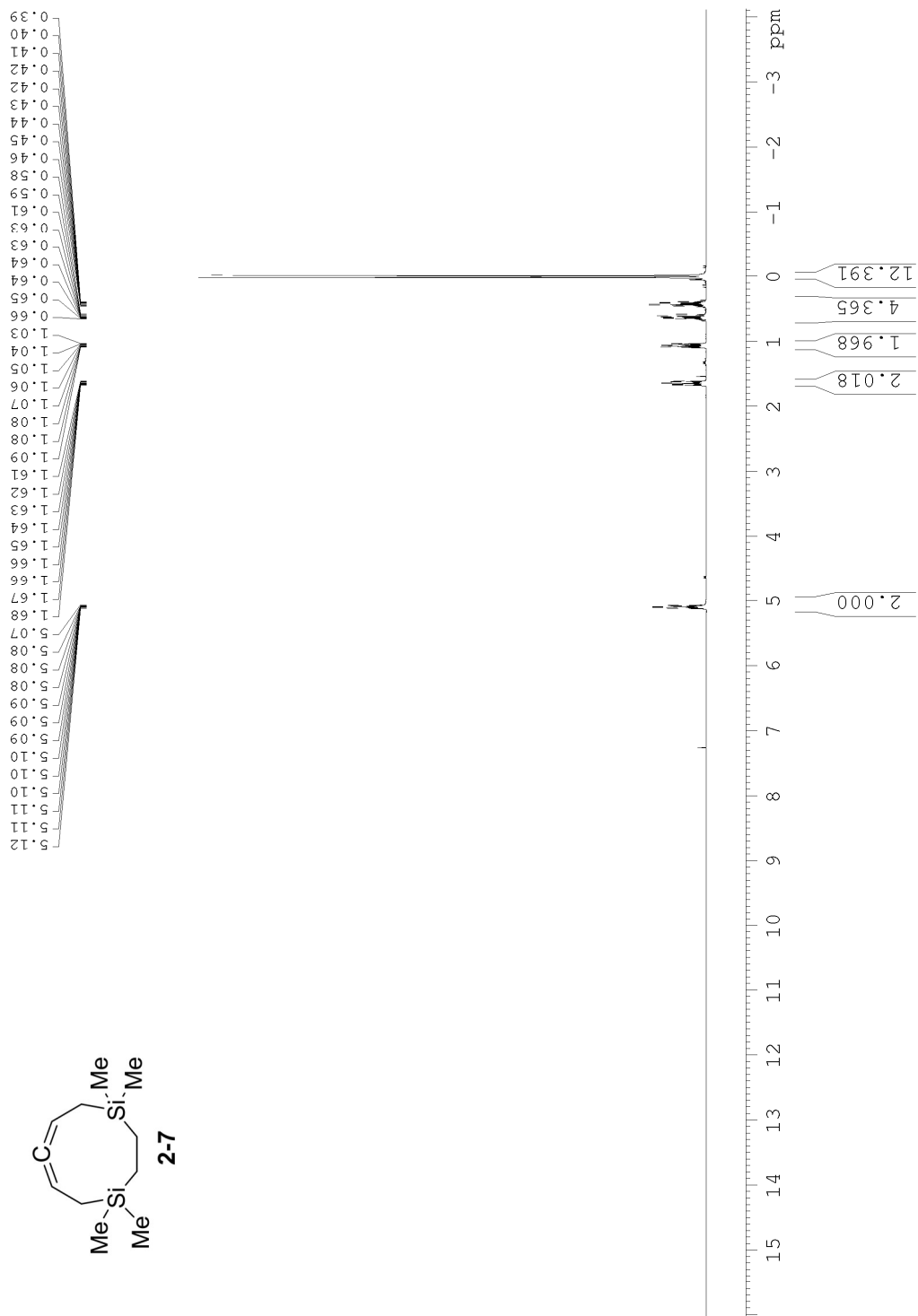


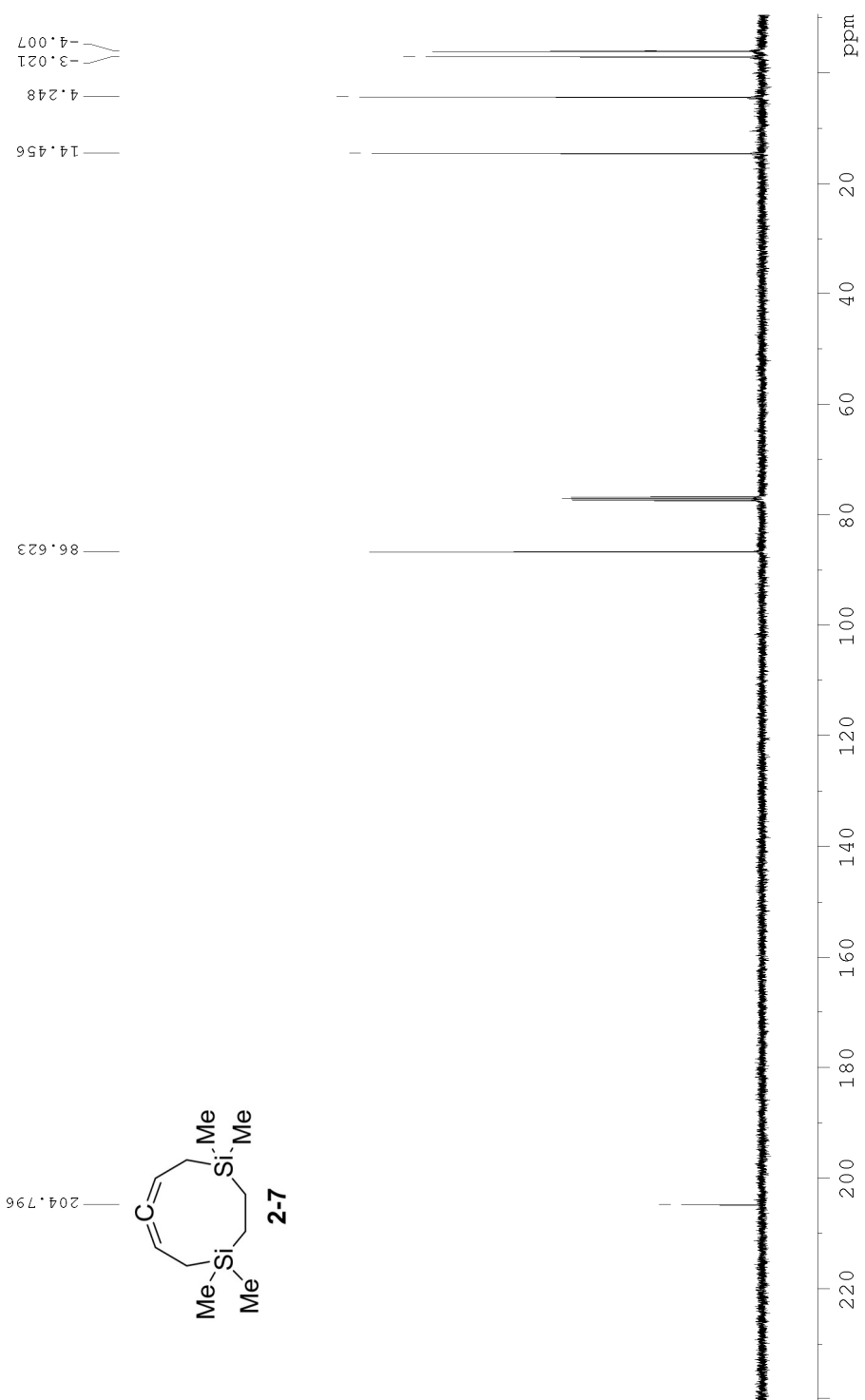
2-21

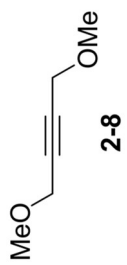




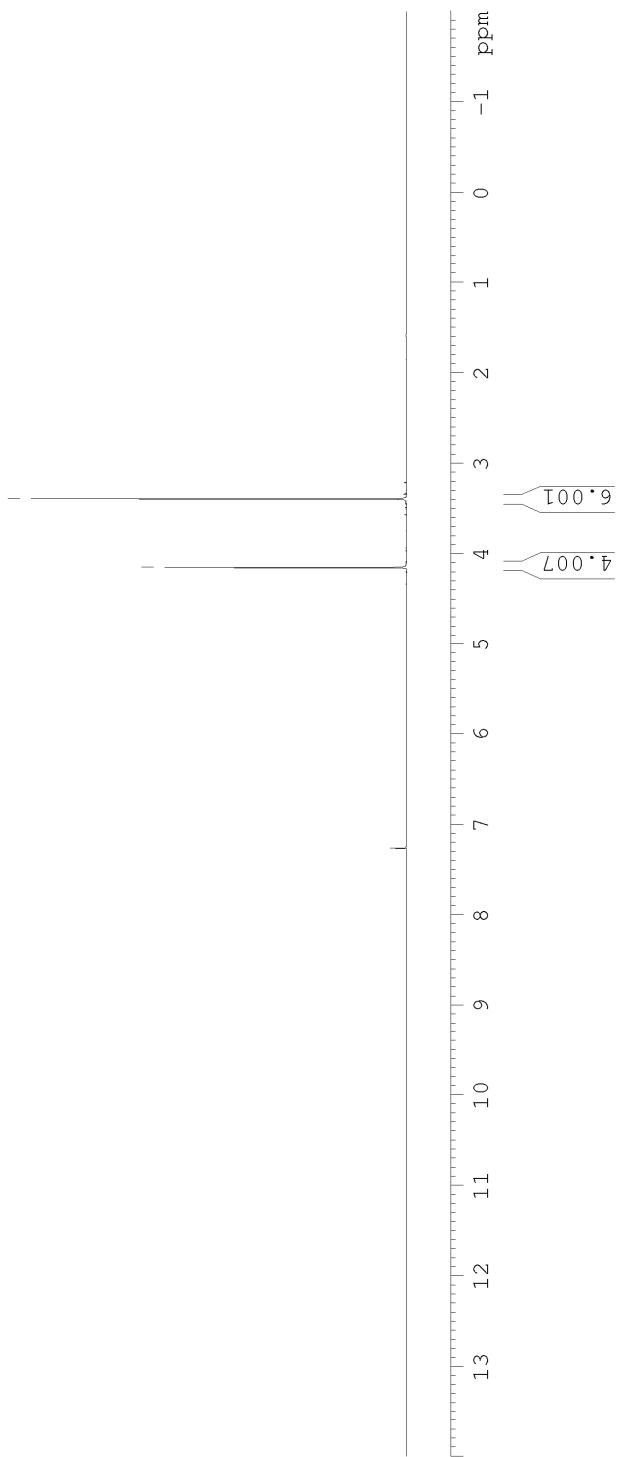


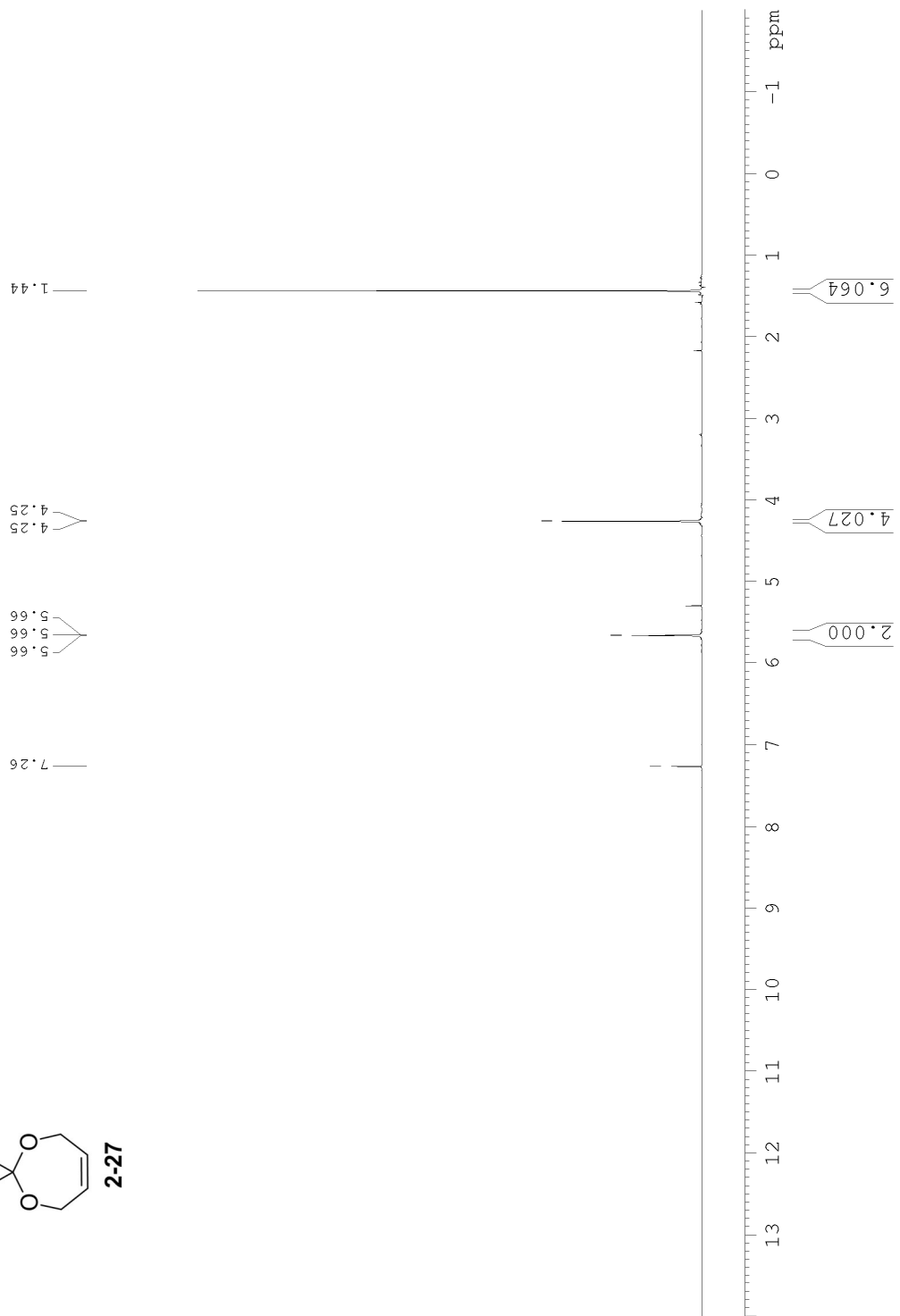
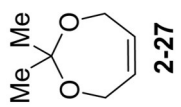


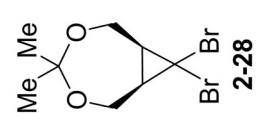
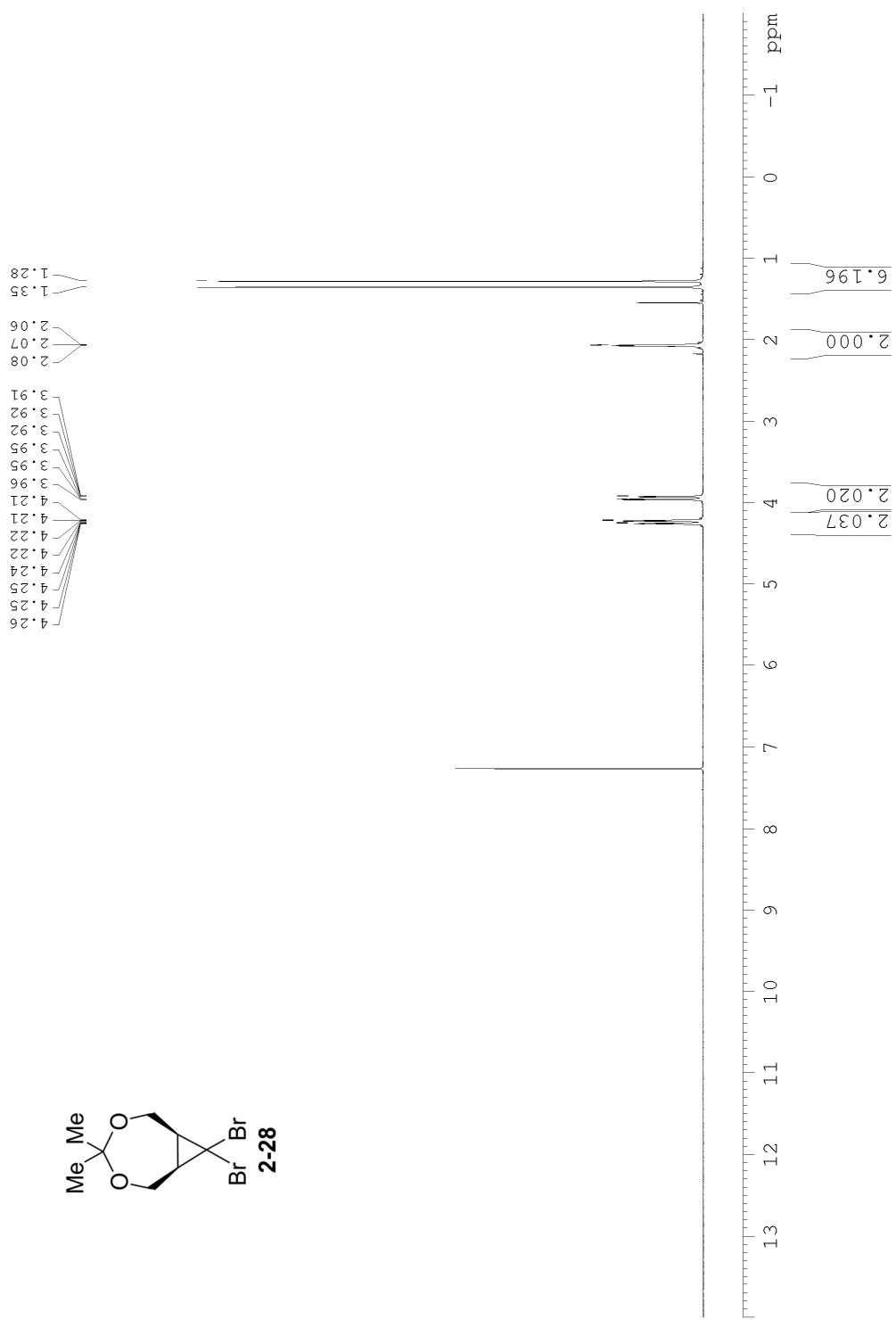


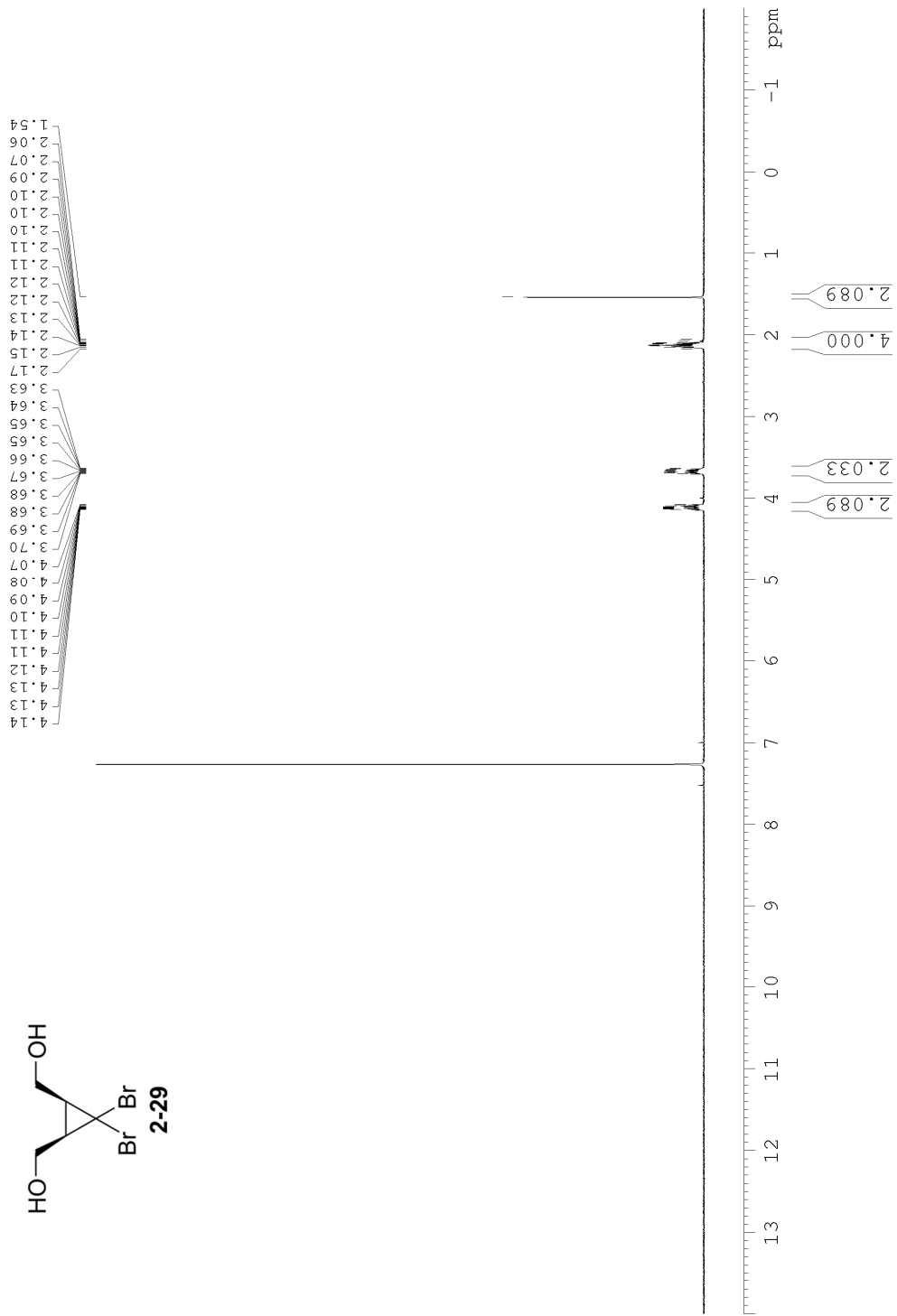
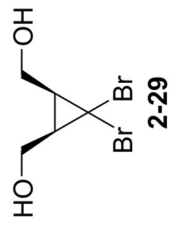


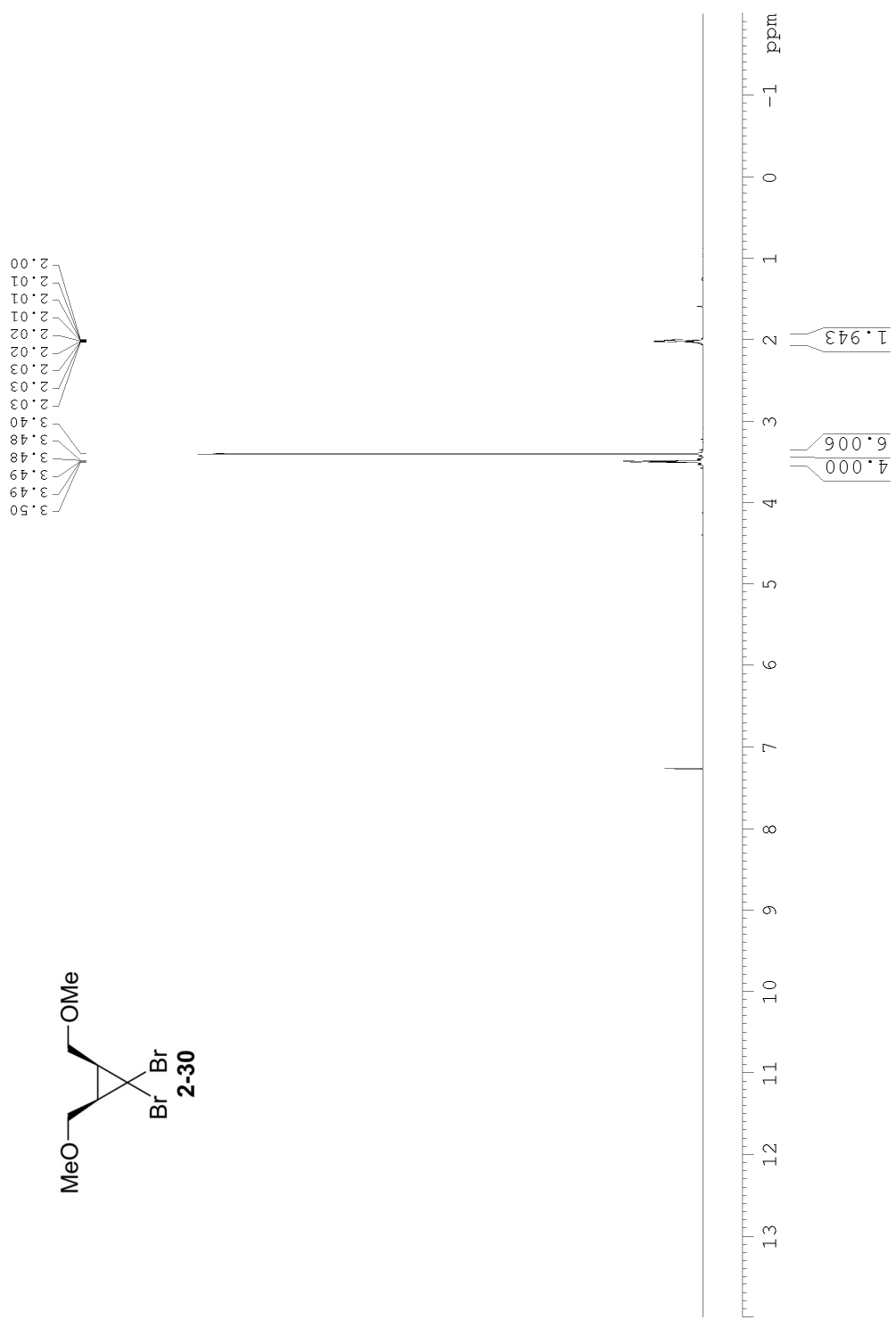
3.39
4.15

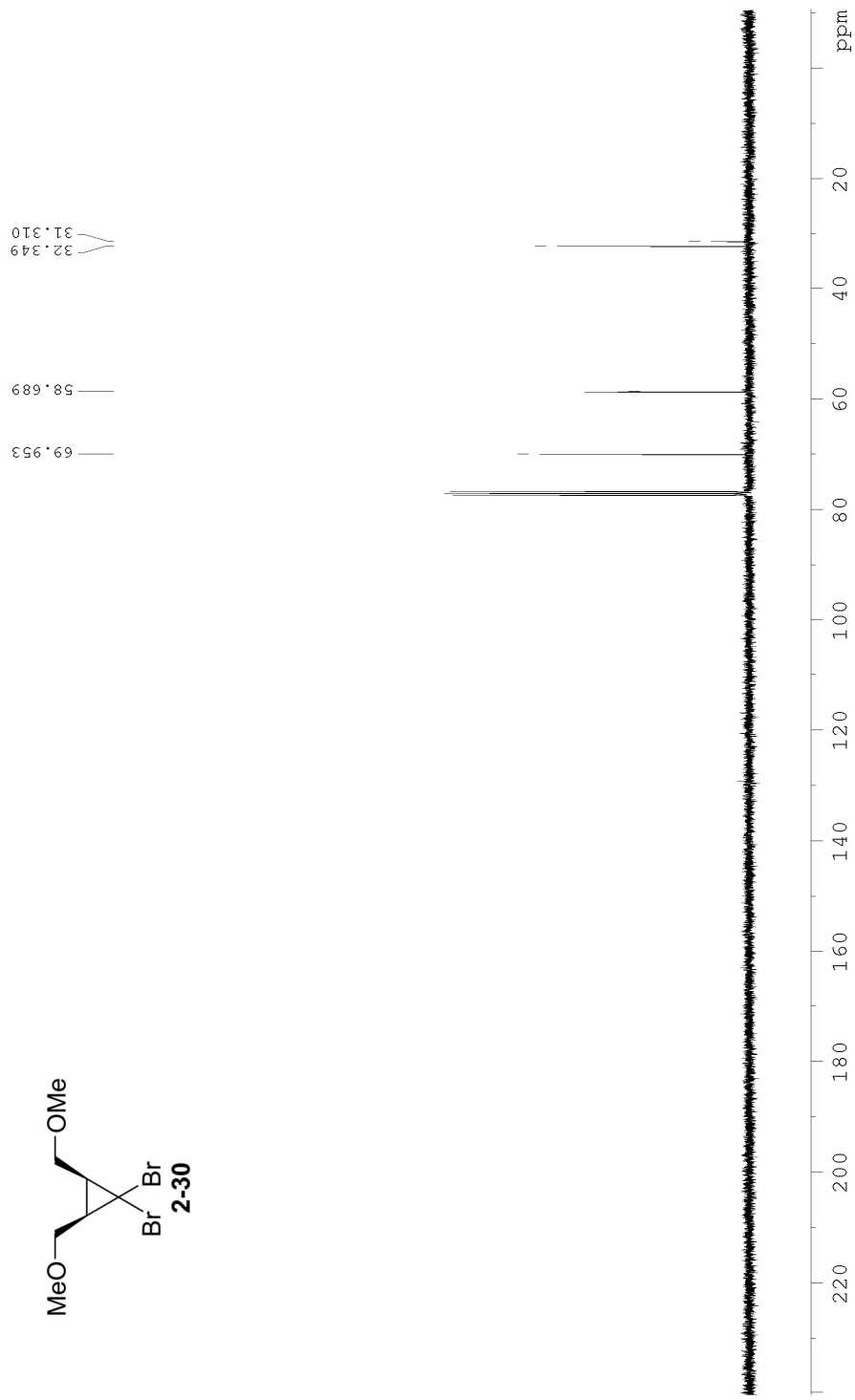
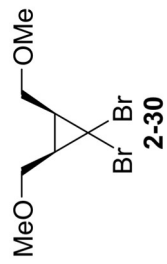


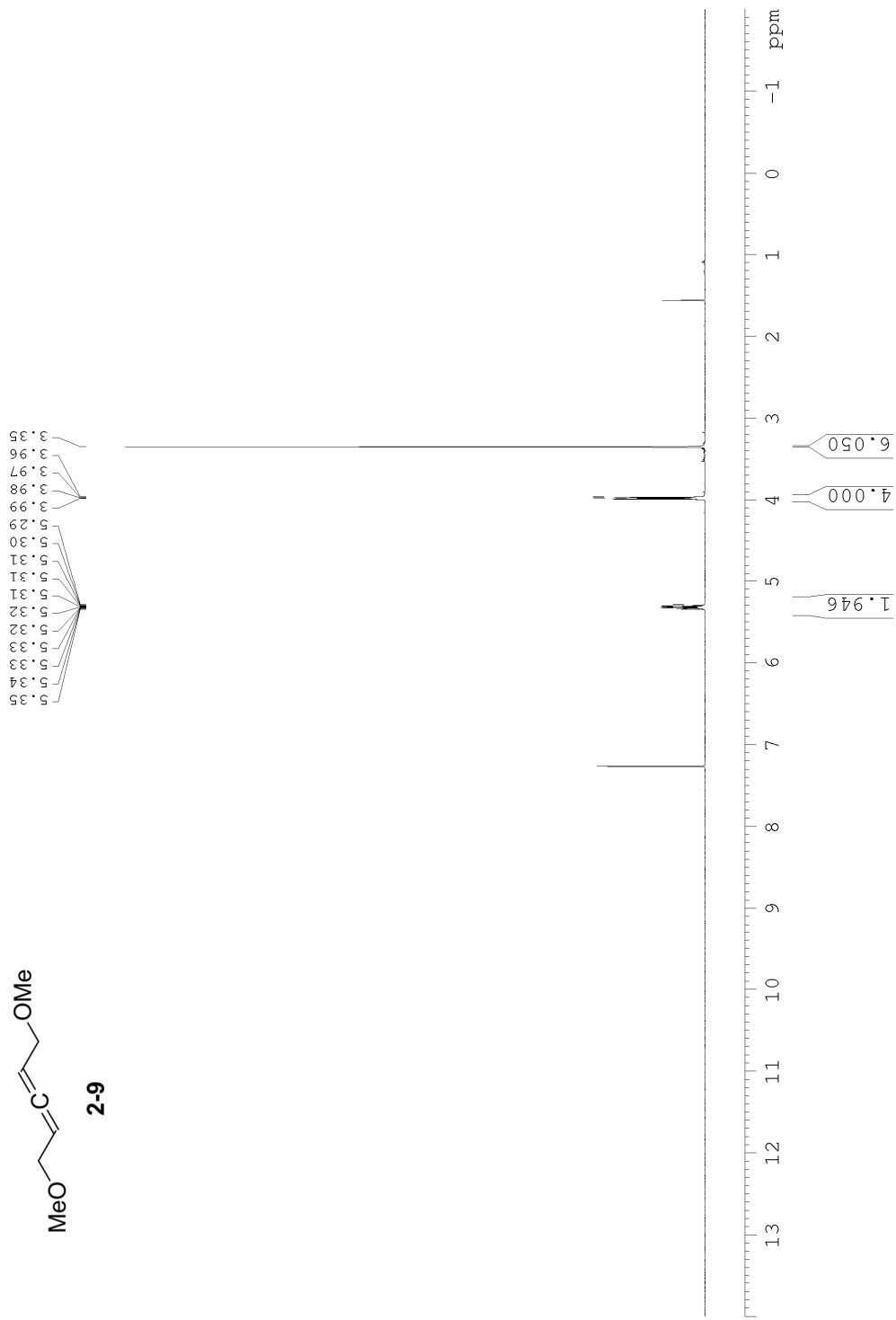
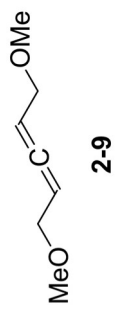


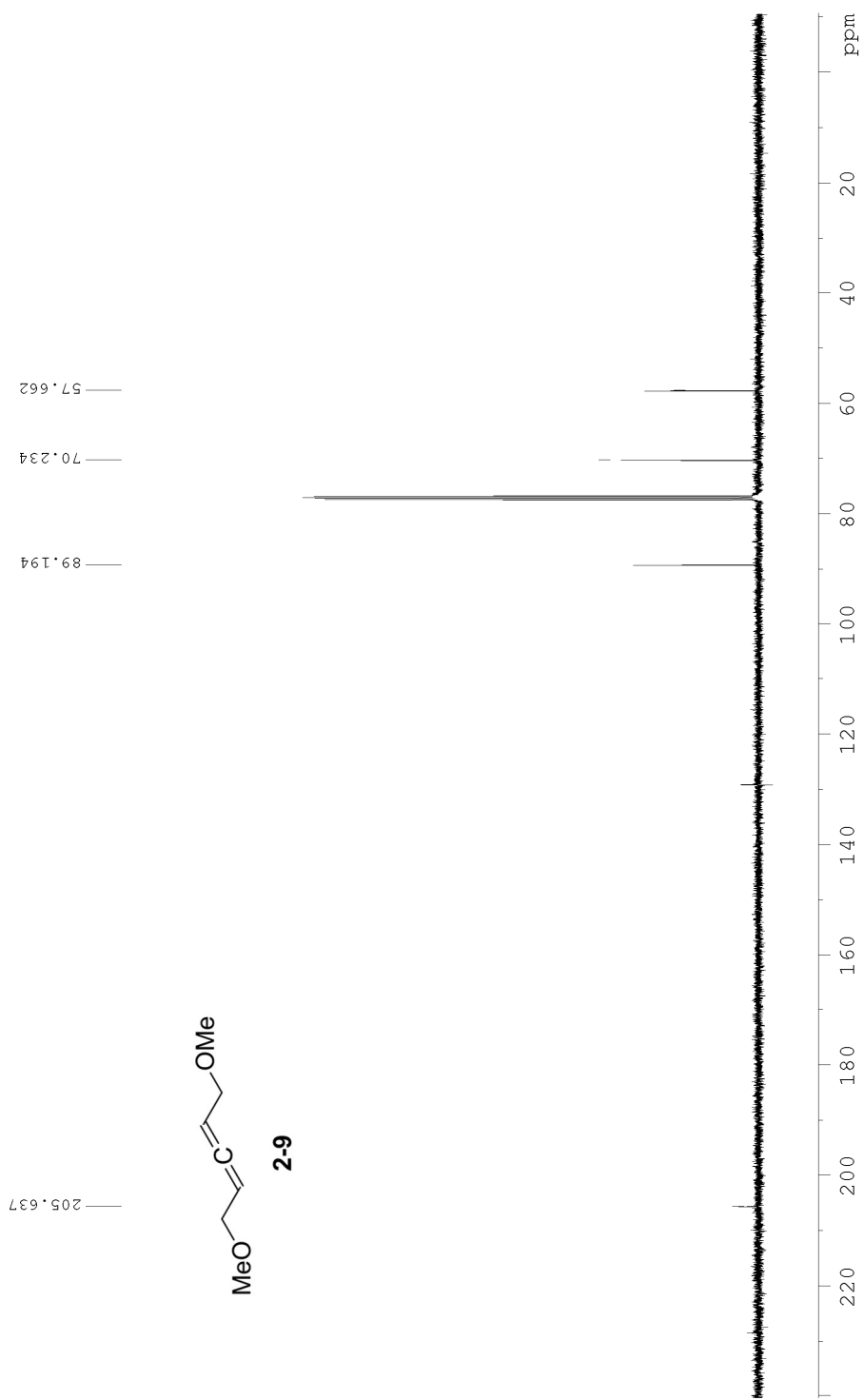








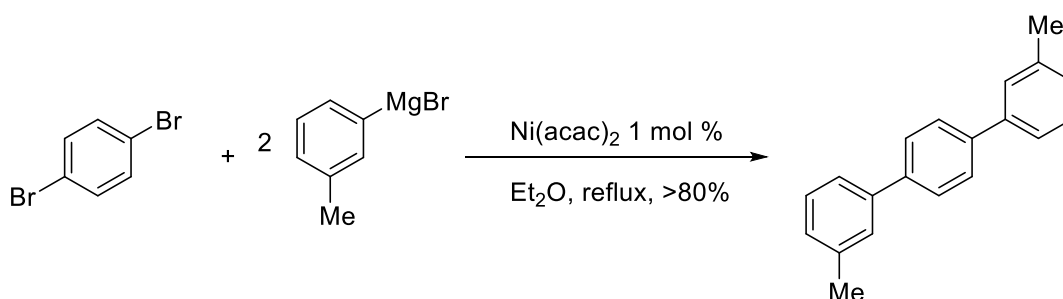




Chapter III – Nickel-Catalyzed Oxidative Coupling of Aryl- and Vinyl Boronates

3.1 Introduction

Metal-catalyzed cross couplings are incredibly powerful tools in the arsenal of a synthetic organic chemist. From small-scale academic research, to bulk production of fine chemicals and pharmaceuticals, cross coupling reactions have achieved mainstream glory beyond their niche beginnings in 1972 with seminal reports from Kumada¹ and Corriu² (Scheme 3-1).

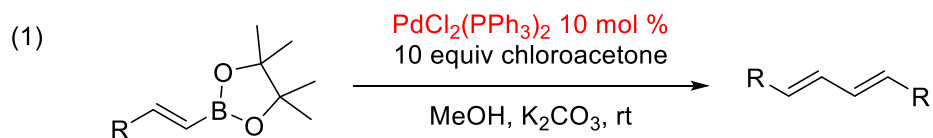


Scheme 3-1 – One of the first examples of a transition-metal catalyzed cross-coupling reaction, reported by Corriu in 1972.

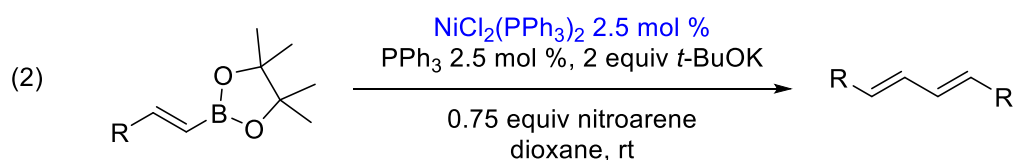
The utility and popularity of cross coupling reactions arises from their high-yielding carbon-carbon bond forming abilities, low catalyst loadings, and broad scope. Perhaps most importantly, they can enable couplings of sp- and sp²-hybridized carbons not amenable to S_N2-type reactions. However, traditional metal-catalyzed cross couplings suffer from various drawbacks: (1) these reactions often require heating to achieve the oxidative addition step, (2) they require expensive, precious metal catalysts, and (3) genotoxic vinyl halides³ are often employed as coupling partners. Wishing to do away with many of these shortcomings of cross couplings, our group developed palladium-catalyzed oxidative-couplings of boronate esters (Scheme 3-2, line 1).⁴ However, this method still required an expensive palladium catalyst. In

this chapter, I describe my discovery of conditions to enable this transformation using a cheap and abundant nickel catalyst (Scheme 3-2, line 2).

Previous work:



This work:



Scheme 3-2 – Our group has developed both palladium (line 1) and nickel (line 2) catalyzed oxidative coupling reactions of vinyl boronates.

As shown along the left side of Figure 3-1, the mechanism for a traditional cross coupling (e.g. the Suzuki reaction⁵) is as follows: Oxidative addition to an active metal (0) species to form a haloalkylated metal (II) intermediate, followed by transmetallation to form a bis-alkylated metal (II) species; reductive elimination forms the product and regenerates the active metal (0) catalyst. On the other hand, the oxidative coupling reaction mechanism, shown on the right side of Figure 3-1 begins with a metal (II) salt, which undergoes sequential transmetallation with two equivalents of a boronate ester. This is followed by reductive elimination to form product and a metal (0) species. Reoxidation of the metal (0) regenerates the metal (II) species.

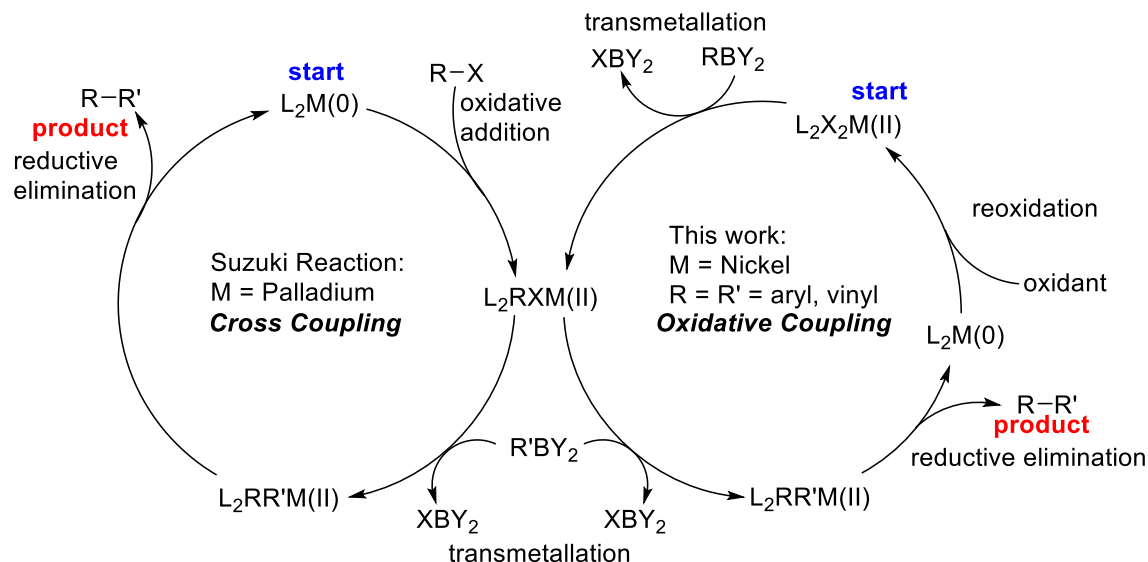
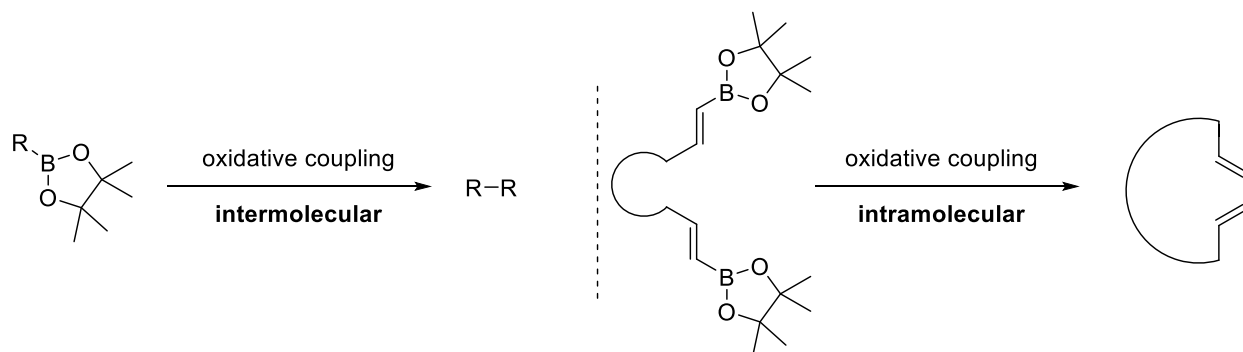


Figure 3-1 – Comparison of cross coupling (left) and oxidative coupling (right) mechanisms.

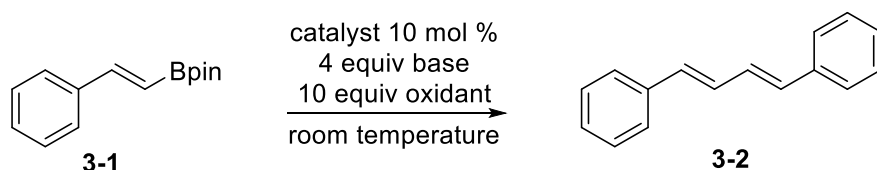
The oxidative coupling strategy avoids the high energy oxidative addition step and thus the reaction proceeds at room temperature. The reaction does suffer from the limitation that, in the intermolecular case, only symmetric, homocoupled products can be obtained. However, intramolecular oxidative coupling of (bis)boronate esters can enable ring closure of linear molecules into macrocycles (Scheme 3-3). Our group has demonstrated this to be a synthetically useful strategy towards accessing complex natural products and initiating cascade reactions, such as transannular Diels-Alder reactions (TADA)^{6,7} or 4π electrocyclizations.⁸



Scheme 3-3 – Depiction of the outcomes of intermolecular (homocoupling) vs. intramolecular (ring closure) oxidative coupling reactions.

3.2 – Initial Screening Results

As a starting point, we investigated whether our previously-reported oxidative coupling conditions for palladium were amenable for nickel catalysis. Styryl boronate **3-1** was chosen as the test substrate because the product **3-2** is fluorescent and easy to detect and isolate. Although palladium provided an 87% yield of product (Table 3-1, entry 1), only a trace amount of product was formed with various nickel(II) salts (Table 3-1, entries 2-9).

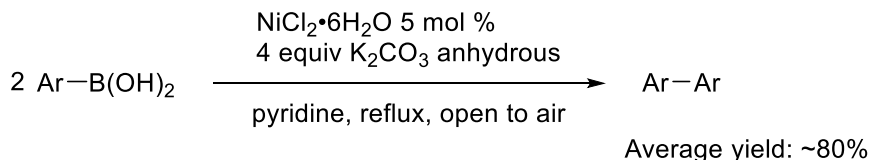


Entry	Catalyst	Base	Oxidant	Solvent	Yield (%) ^a
1	PdCl ₂ (PPh ₃) ₂	2M aq. K ₂ CO ₃	chloroacetone	MeOH	87
2	NiCl ₂ (PPh ₃) ₂	2M aq. K ₂ CO ₃	chloroacetone	MeOH	4
3	NiCl ₂ (dppe)	2M aq. K ₂ CO ₃	chloroacetone	MeOH	trace
4	NiCl ₂ (dppe)	K ₂ CO ₃ (anhydrous)	chloroacetone	MeOH	trace
5	NiCl ₂ (dppe)	2M aq. K ₂ CO ₃	open to air	MeOH	trace
6	NiCl ₂ (dppe)	1M TBAF in THF	chloroacetone	MeOH	trace
7	NiCl ₂ (bpy)	2M aq. K ₂ CO ₃	open to air	THF	trace
8	NiCl ₂ (dppm)	2M aq. K ₂ CO ₃	chloroacetone	MeOH	trace
9 ^b	NiCl ₂ (dppe)	2M aq. K ₂ CO ₃	chloroacetone	MeOH	trace

^aIsolated yields. ^bHeated to 60 °C.

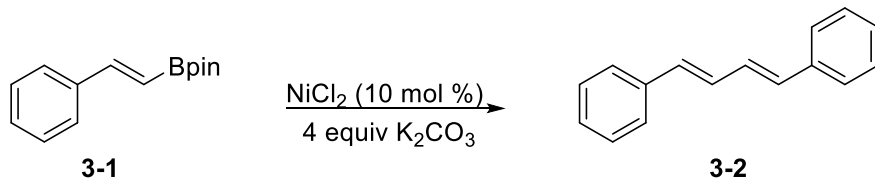
Table 3-1 – Initial screening results.

Because small amounts of **3-2** were formed in nearly all the nickel-catalyzed conditions tested, we suspected that reoxidation was the problematic step. However, after screening other oxidants (benzoquinone, chloranil, iodine, sodium persulfate, O₂, Ag₂O, pyridine N-oxide) with no success, we decided to take a step back and examine conditions developed specifically around nickel. A related nickel-catalyzed homocoupling report by Liu et al. appeared to be an attractive starting point, although its reliance on pyridine was problematic (Scheme 3-4).⁹



Scheme 3-4 – Liu’s reported⁹ conditions for Ni-catalyzed homocoupling of aryl boronic acids in refluxing pyridine.

If we were to adapt Liu’s conditions, large quantities of expensive, hazardous, and malodorous pyridine solvent would be required, especially in the case of the intramolecular oxidative coupling which employs high dilution to avoid oligomerization. We hoped that by modifying Liu’s conditions, we could identify a more convenient solvent. The results of this endeavor were not encouraging, as it suggested that pyridine solvent was required (Table 3-2).



Entry	Temp (°C)	Added Pyridine	Solvent	Yield (%) ^a
1	115	solvent	pyridine	64
2	63	50 equiv	THF	trace
3	100	50 equiv	dioxane	46
4	100	none	dioxane	85 ^b
5	110	100 equiv	toluene	31
6	80	-	benzene	trace
7	80	50 equiv	DME	0
8	80	-	DCE	0
9	110	100 equiv	DMF	0
10	115	150 equiv	DMSO	14
11	100	100 equiv	<i>o</i> -dichlorobenzene	trace
12	23	50 equiv	MeOH	trace
13	115	-	quinoline	trace

^aIsolated yields. ^bContaminated with an unidentified, inseparable byproduct.

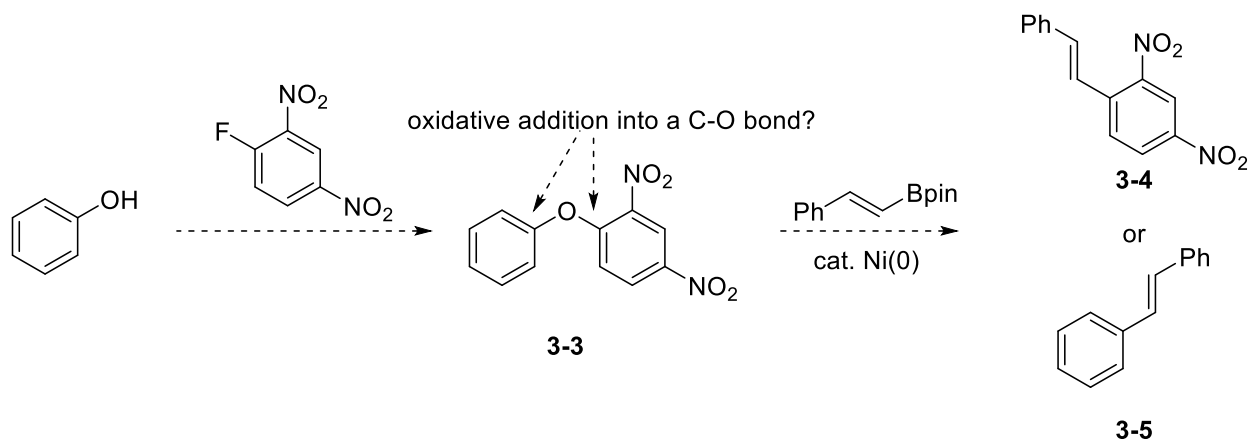
Table 3-2 – Selected variations on Liu’s conditions to minimize pyridine solvent requirements.

Dioxane (entries 3-4) proved to be an interesting candidate as an alternative solvent, however, under the reaction conditions in the absence of pyridine, it gave rise to an unidentified,

inseparable byproduct in unacceptable amounts. Otherwise, THF, toluene, benzene, DCE, DMF, DMSO, *o*-dichlorobenzene, and MeOH all proved ineffective, even with added pyridine cosolvent (entries 2, 5-12). We were also surprised to discover that quinoline, despite its similarities to pyridine, was not able to promote the reaction whatsoever (entry 13). Even with pyridine solvent, we were never able to observe product formation below 100 °C. This was very disappointing because a room temperature reaction was one of the main goals of the oxidative coupling strategy.

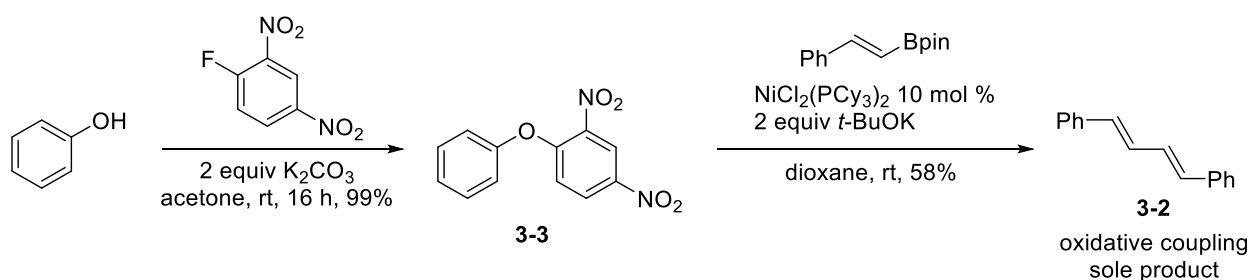
3.3 – A Serendipitous Discovery

Pessimistic about the prospects of getting this reaction to work, we began to explore other research ideas based around nickel-catalysis. We were intrigued by nickel's ability to oxidatively insert into nontraditional electrophiles, such as sulfonates, carbonates, esters, and ethers,¹⁰ so we decided to investigate a nitroaromatic-ether electrophile (**3-3**) we hoped would be amenable to cross couplings (Scheme 3-4).



Scheme 3-4 – Proposed synthesis and reaction of a non-traditional electrophile **3-3** in a Ni(0)-catalyzed cross coupling reaction.

We felt that the design of **3-3** as a coupling electrophile was quite clever: not only would the nitro groups allow its simple preparation by S_NAr , but they would also be predicted to lower the LUMO of the C-O bond by inductive effects, facilitating oxidative addition. We recognized that nickel could potentially insert into either one of the C-O bonds present in ether **3-3**, and by analyzing the ratio of products **3-4** and **3-5** we could quantify this preference. Formation of the biarylether **3-3** via S_NAr proceeded in 99% yield. For the nickel-catalyzed cross coupling, we opted to use the $NiCl_2(PCy_3)_3/t-BuOK$ /dioxane system after noting that it been effective in other reported Ni-catalyzed cross couplings.¹¹ However, the result of the cross-coupling reaction was surprising (Scheme 3-5).



Scheme 3-5 – Serendipitous discovery of conditions for oxidative coupling of vinyl boronates with Ni-catalysis.

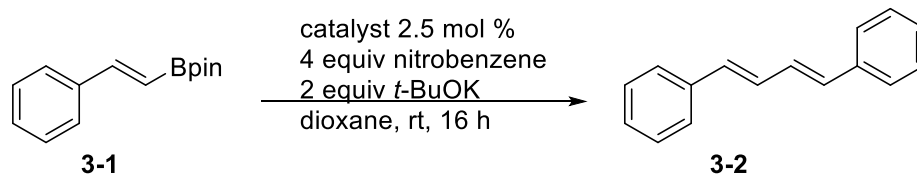
Expected cross coupling products **3-4** or **3-5** were not detected, instead *oxidative* coupling product **3-2** was isolated in 58% yield! This unexpected result encouraged reinvestigation of the all-but-abandoned nickel-catalyzed oxidative coupling protocol. Central to our renewed effort was the hypothesis that nitroarene **3-3** was acting as a stoichiometric oxidant for nickel.

Nitroarenes have long been reported to be incompatible coupling substrates under nickel catalysis.^{12–15} However, employing a nitroarene as an oxidant in organic synthesis is not unheard of. For example, the Skroup quinoline synthesis reported in 1880 uses a nitroarene as oxidant.¹⁶ A more modern example uses nitroarenes as both a substrate and an oxidant in a transition-metal free synthesis of anilines.¹⁷ Raney nickel has been used for the reduction of nitroarenes to amines

with concomitant oxidation of the nickel.¹⁸ However, reports of nitroaromatics used as oxidants in transition-metal catalyzed coupling reactions are extremely rare.^{19,20} To the best of our knowledge, our finding is the first example of a nitroarene being used intentionally as an oxidant to promote a Ni-catalyzed coupling reaction.

3.4 – Optimization of the Nitroarene-Mediated Nickel-Catalyzed Oxidative Coupling of Boronate Esters

Turning our serendipitous discovery into a useful method began by confirming that simple nitroarenes could replace the more complex **3-3** as the oxidant. We screened a few nitroarenes and found that nitrobenzene, nitroanisole, and *p*-chloronitrobenzene could all be used interchangeably in place of **3-3**. In our early screenings, we sometimes we opted to use nitroanisole over nitrobenzene since its increased polarity facilitated chromatographic purification of nonpolar products. We next turned to the catalyst and screened various ligands. As shown in Table 3-3, PPh₃ and PCy₃ were identified as the top performers. Although PCy₃ gave superior results, NiCl₂(PPh₃)₂ is considerably more air stable, so moving forward we optimized the conditions for that catalyst.

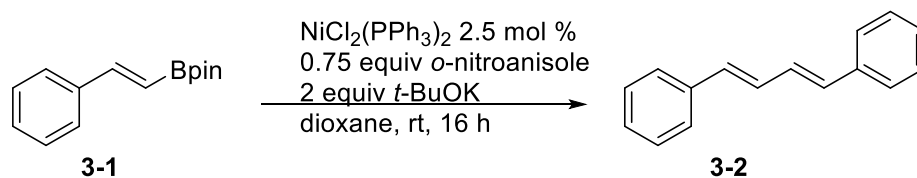


Entry	Catalyst	Yield (%) ^a
1	NiCl ₂ (PPh ₃) ₂	55
2	NiCl ₂ (PCy ₃) ₂	67
3	NiCl ₂ (dppe)	16
4	NiCl ₂ (glyme)	0
5	NiCl ₂	0
6	none	0

^aIsolated yield.

Table 3-3 – Ligand screening results.

We also discovered that we could use as little as 0.75 molar equivalents of the nitroarene without reducing the reaction yield. A concentration study was performed to ascertain the ideal concentration of the reaction, which was determined to be roughly 0.08 M (Table 3-4). As the reaction became increasingly concentrated or dilute, diminished yields were observed.



Entry	Concentration of Boronate	Yield (%) ^a
1	0.0416 M	47
2	0.083 M	52
3	0.166 M	24

^aIsolated yield.

Table 3-4 – Concentration study results.

Up to now, these results were very promising, but the yields were not yet synthetically attractive. TLC analysis of the reaction mixture over time indicated an initial burst of reactivity followed by gradual cessation of product formation, suggesting that the active catalyst was

stalling out after several turnovers. We hypothesized that reduction products of nitrobenzene could be interfering with the reaction over time. To validate this hypothesis, GCMS was used to analyze the products of a 1:1:2 mixture of Ni(COD)₂ : nitrobenzene : PPh₃. Ni(COD)₂ was chosen as a convenient nickel(0) source to mimic a nickel(0) intermediate that would be susceptible to oxidation by nitrobenzene in the oxidative coupling catalytic cycle. The study showed formation of azoxybenzene alongside significant quantities of triphenylphosphine oxide. These findings could be explained by the sequence shown in Figure 3-2. In this putative pathway, a nitrene is generated via reaction of a nitroso intermediate and PPh₃ in a known process, followed by reaction of the nitrene with nitrosobenzene to form azoxybenzene.²¹

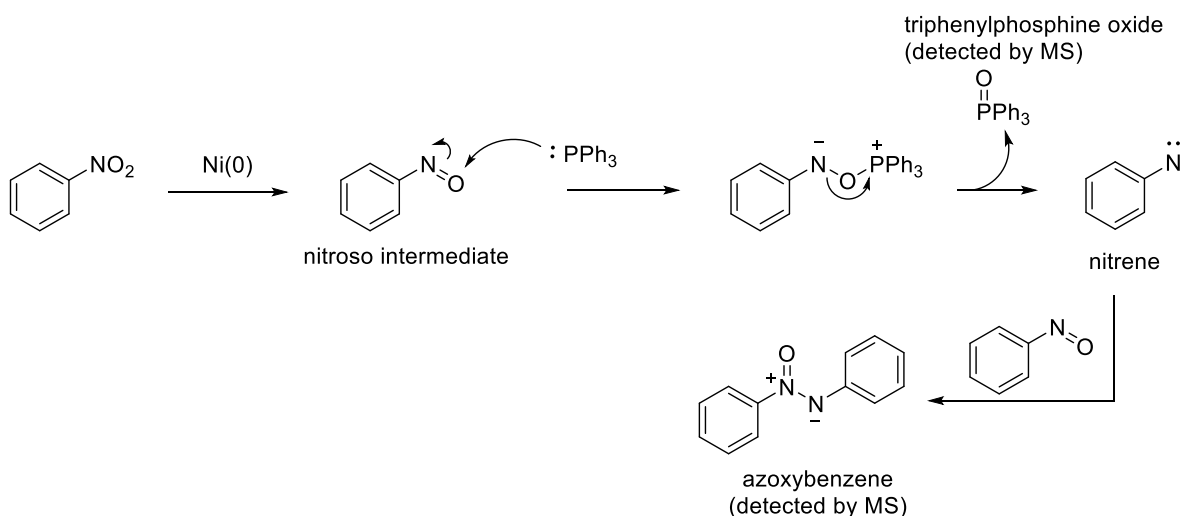
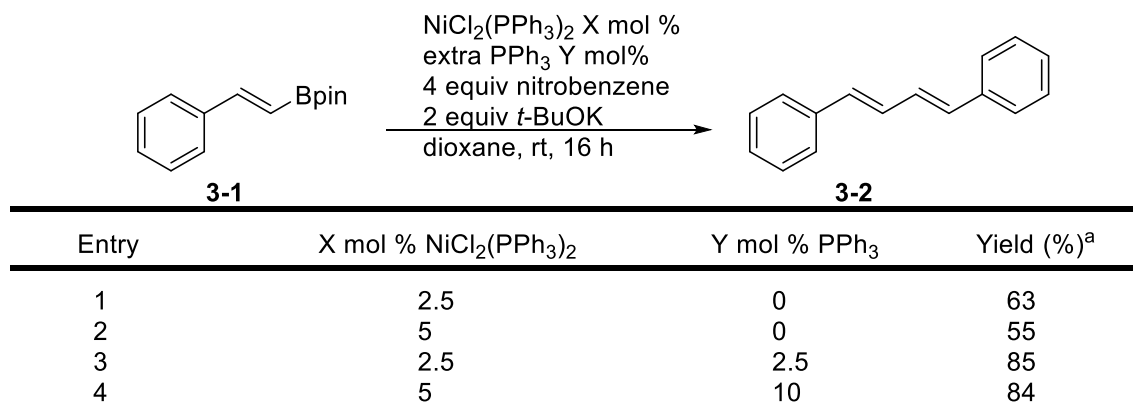


Figure 3-2 – Mechanism accounting for formation of triphenylphosphine oxide and azoxybenzene when a nickel(0) source reacts with nitrobenzene.

The GCMS results revealed that the triphenylphosphine ligand was being oxidized. This suggested the diminished yields in the coupling reaction were due to consumption of ligand in a side reaction, which in turn would result in loss of catalyst. Armed with this knowledge, we were gratified to find that adding just 2.5 mol % extra PPh₃ to the coupling reaction gave a significant

improvement in yield, up to 85% (Table 3-5, entry 3). Interestingly, addition of 10% extra PPh₃ did not improve the yields further (Table 3-5, entry 4).



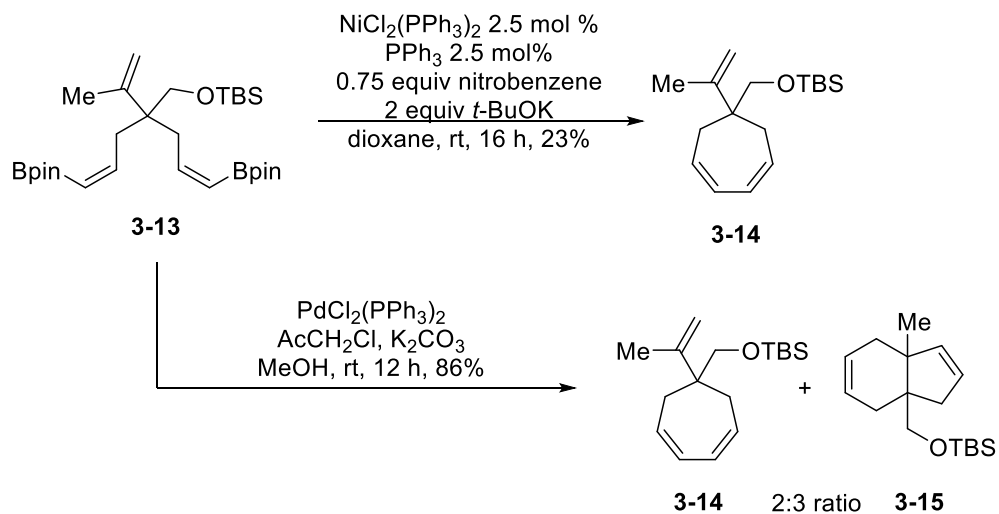
^aIsolated yield.

Table 3-5 – Effect of added PPh₃ on coupling yield.

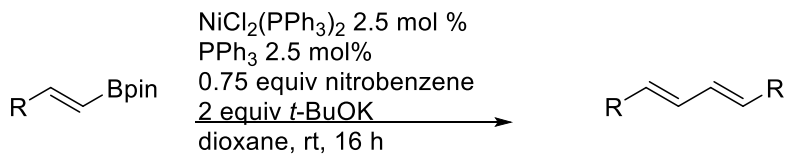
3.5 – Reaction Scope

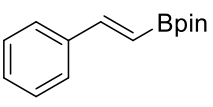
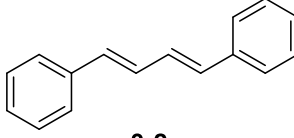
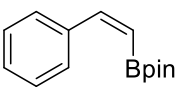
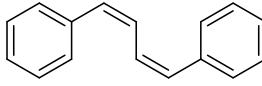
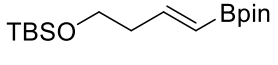
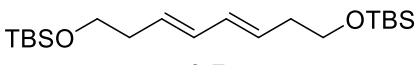
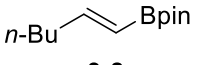
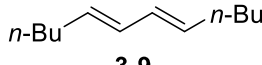
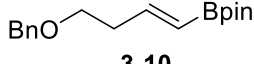
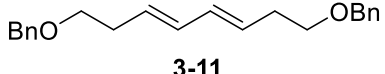
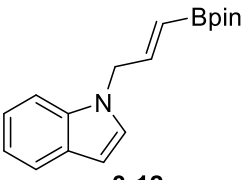
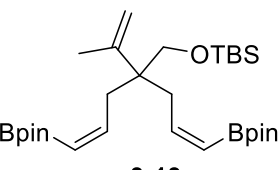
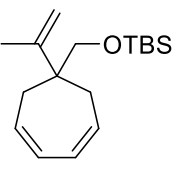
The next stage of this project was to explore the scope of the reaction. A family of vinyl boronates were synthesized by hydroboration²² of the corresponding alkynes using Schwartz's reagent.²³ We also synthesized a *cis*-vinyl boronates **3-4** and **3-13** using a method we developed previously.²⁴ With a collection of vinyl boronates in hand, we subjected them to the oxidative coupling reaction and determined the coupling yield (Table 3-6). The reaction was determined to be stereospecific, with *cis*-vinyl boronate **3-4** giving the *Z,Z* butadiene **3-5** in 81% yield (entry 2). The TBS-protected and 1-hexyne derived vinyl boronates **3-6** and **3-8** gave butadiene coupling products **3-7** and **3-9** in good yield (entries 3 and 4). However, benzyl-protected **3-10** performed quite poorly, giving only a 30% yield of **3-11** (entry 5). Indole boronate **3-12** failed completely and decomposed under the reaction conditions (entry 6). Finally, bis(boronate) **3-13** did couple under high-dilution conditions to give intramolecular coupling product **3-14**, albeit in a low 24% yield (entry 7). Interestingly, the reaction of **3-13** under nickel catalysis gave 7-membered ring **3-**

14 as the sole product, while the related reaction using palladium²⁴ gave both **3-14** and alkene insertion product **3-15** (Scheme 3-6).



Scheme 3-6 – Reaction of **3-13** under nickel (top) and palladium (bottom) conditions.



Entry	substrate	product	Yield (%) ^a
1	 3-1	 3-2	85
2	 3-4	 3-5	81
3	 3-6	 3-7	76
4	 3-8	 3-9	64
5	 3-10	 3-11	30
6	 3-12	decomposition	na
7 ^b	 3-13	 3-14	23

^aIsolated yields. ^bReaction conducted at high dilution (0.005 M)

Table 3-6 – Vinyl boronate substrate scope.

We also assessed whether aryl boronates participate in the oxidative coupling reaction to give biaryl products. Starting from phenyl boronic acid **3-16**, we prepared the neopentylglycolate phenylboronate (**3-17**) and pinacolate phenylboronates (**3-18**) and subjected them to the coupling reaction to produce biphenyl (**3-19**). As shown in Table 3-7, **3-18** performed best (89%) while lower yields were observed for **3-17** (70%) and **3-16** (24%).

3-19

Entry	substrate	Yield (%) ^a
1	 3-16	24
2	 3-17	70
3	 3-18	89

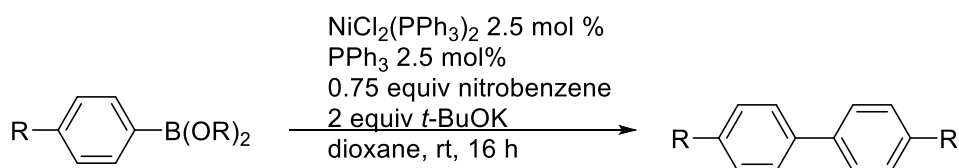
^aIsolated yield.

Table 3-7 – Aryl boronic acid and ester screening results.

Next, various *para*-substituted aryl pinacol boronates were subjected to the coupling reaction. As shown in Table 3-8, the yields were dependent on the electronic nature of the substituent.

Electron-rich boronates (entries 1-3) gave the highest yields of coupling product, while electron-deficient boronates (entries 4-6) performed poorly. This trend is consistent with the role of the

boronate as a nucleophile in the coupling reaction. Reduced nucleophilicity would result in reduced transmetallation efficiency to a nickel catalytic intermediate. Although the yields are low, the fact that halogens are tolerated in this reaction is testament to one of the unique advantages of oxidative couplings. Under the conditions of a typical cross coupling, aryl halides would be susceptible to oxidative addition, making products like **2-22** and **2-23** difficult or impossible to access.



Entry	R	Yield (%) ^a [Product]
1	H	89 (3-19)
2	N(Me) ₂	79 (3-20)
3	Me	77 (3-21)
4	Cl	34 (3-22)
5	Br	23 (3-23)
6	CF ₃	15 (3-24)

^aIsolated yield.

Table 3-8 – Aryl boronate substrate scope.

3.6 –Summary and Outlook

In conclusion, we developed a protocol to conjoin two boronate esters via an oxidative coupling reaction catalyzed by nickel. This methodology is important within the context of our research group since we can now add a nickel-catalyzed alternative to our repertoire of palladium-based oxidative coupling strategies. The reaction also represents a rare example of a nitroarene transition-metal oxidant, serendipitously discovered to be effective for nickel during the pursuit of another research project. We performed GCMS studies to uncover some details about the mechanism of oxidation and identified a problematic side reaction, the oxidation of the ligand. To rectify this problem, we added extra ligand and were able to increase the coupling

yield significantly. We determined the reaction is stereoselective and amenable to both inter- and intramolecular oxidative coupling, although further optimization is required for the intramolecular case. We also demonstrated that the reaction works with aryl boronate coupling partners as well, providing access to symmetric biaryls. Unfortunately, the reaction does suffer from some drawbacks. Potassium *tert*-butoxide is essential for the reaction, which raises concerns about functional group compatibility. Furthermore, although nitrobenzene is a cheap oxidant, it is nonvolatile and can be difficult to remove. It's also quite toxic. Moving forward, we would like to study the intramolecular reaction of bis(vinylboronates) more closely. We can now compare the nickel-catalyzed oxidative reaction alongside the palladium-catalyzed version; there may be interesting differences between them. Also, we'd like to attempt the oxidative coupling of internal vinyl boronates using nickel catalysis, if successful, this could represent a convenient synthesis of dendralenes. Finally, although we only attempted to perform symmetric oxidative couplings, we hope to explore the viability of selective asymmetric couplings using two different boronates.

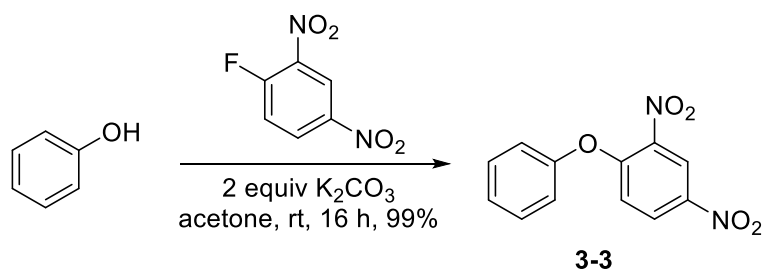
3.7 – Experimental Methods

Unless otherwise specified, all reactions were performed under a nitrogen atmosphere using dry solvents and anhydrous conditions. DCM, DMSO, DME, toluene, benzene, and triethylamine were distilled fresh from CaH₂. Methanol was distilled fresh from magnesium turnings.

Nitroarenes were purified by distillation from MgSO₄. Dioxane and THF were distilled fresh from sodium/benzophenone. Phenylboronic acid, phenylboronic acid pinacol ester, phenylboronic acid neopentylglycol ester, 4-(trifluoromethyl)phenylboronic acid, 4-bromophenylboronic acid pinacol ester, 4-chlorophenylboronic acid, and p-tolylboronic acid were purchased from Sigma-Aldrich. All other reagents were used as received from commercial

sources. ^1H NMR and ^{13}C NMR data obtained with Bruker ARX-400. Multiplicities are indicated by s (singlet), d (doublet), t (triplet), q (quartet), p (pentet), m (multiplet), or b (broadened). IR spectra were recorded with an ATR attachment and selected peaks are reported in cm^{-1} . High resolution mass spectral data was recorded with Thermo Fisher Scientific Exactive Plus with IonSense ID-CUBE Direct Analysis in Real Time (DART) ion source experiments. GCMS was performed on an Agilent 6890-5975 GC-MS with EI. Reactions were monitored using thin layer chromatography performed on MachereyNagel POLYGRAM® SIL G/UV254 silica gel TLC plates and visualized under UV light or with ceric ammonium molybdate (CAM) stain. Flash column chromatography was performed using DAVISIL® silica gel (40-63 microns) and compressed air.

2,4-dinitro-1-phenoxybenzene (3-3)

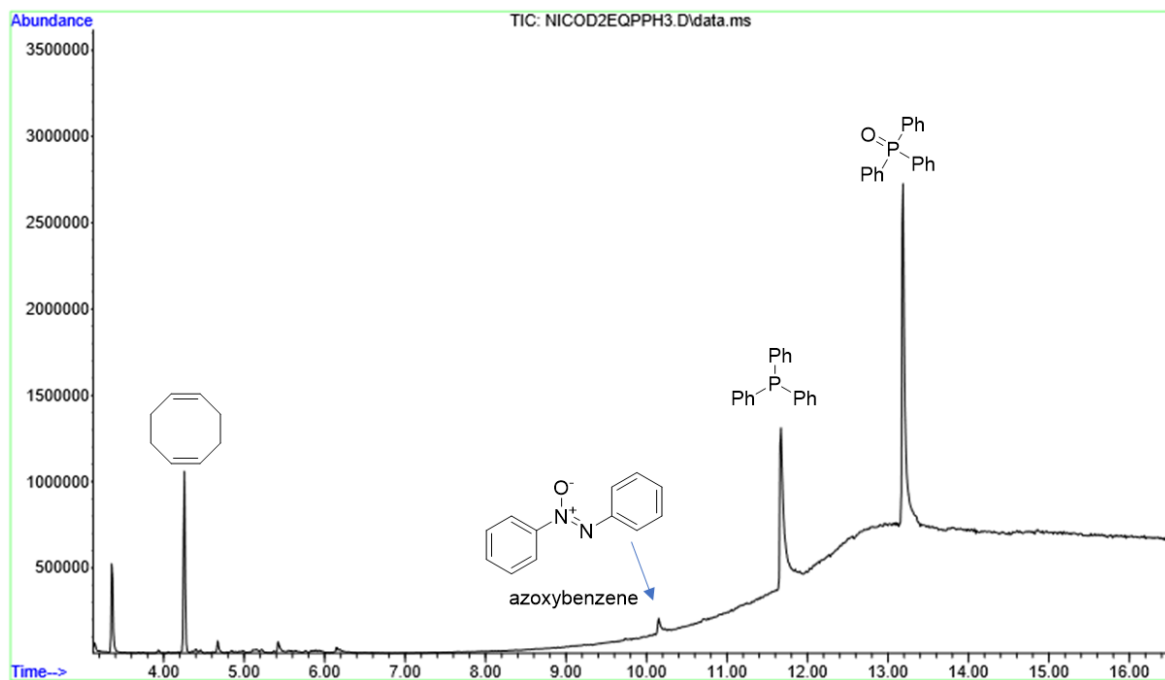


Prepared by $\text{S}_{\text{N}}\text{Ar}$ according to the procedure reported by Du et. al.²⁵

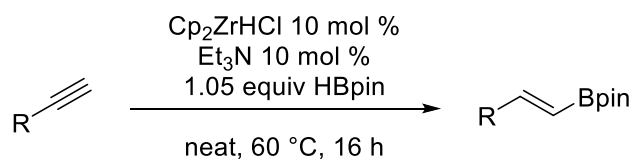
GCMS Study

$\text{Ni}(\text{COD})_2$ (20 mg, 0.073 mmol) was dissolved in 14.2 mL of dioxane (freshly distilled and then degassed by freeze-pump-thaw method) and stirred at room temperature. To this yellow solution was added 38 mg of PPh_3 (0.146 mmol), followed by addition of 7.48 μL (0.073 mmol) of nitrobenzene. The reaction was allowed to continue overnight, then the black solution was

analyzed by GCMS. The results show formation of azoxybenzene and triphenylphosphine oxide; cycloocta-1,5-diene and residual PPh₃ were also detected.



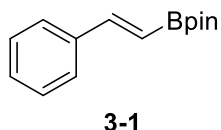
Preparation of *E*-vinyl boronates 3-3, 3-6, 3-8, 3-10, and 3-12:



Prepared according to protocol developed by Wang et al.²² To a 50 mL round bottom flask equipped with a stirbar was added Cp₂ZrHCl (0.1 equiv), triethylamine (0.1 equiv), and pertinent alkyne (1 equiv). After stirring under N₂ for 2 min, the resulting cloudy solution was treated with dropwise addition of 4,4,5,5-tetramethyl-1,3,2-dioxaborolane (1.05 equiv). The reaction mixture was subsequently heated to 60°C and monitored by TLC for consumption of alkyne. Upon completion, the reaction mixture was diluted with 20 mL of ethyl acetate, filtered through a silica

plug, washed with ethyl acetate, and concentrated. The resulting residue was purified by silica gel flash column chromatography (hexanes: ethyl acetate).

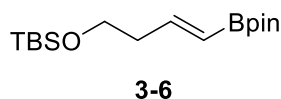
(E)-4,4,5,5-tetramethyl-2-styryl-1,3,2-dioxaborolane (3-3)



Colorless solid isolated in 78% yield. Spectral data matched reported values.²⁶

¹H NMR (400 MHz, CDCl₃) δ: 7.50-7.28 (m, 6H), 6.16 (d, 1H, *J* = 18.4 Hz), 1.26 (s, 12H).

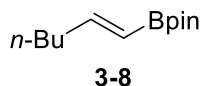
(E)-tert-butyldimethyl((4-(4,4,5,5-tetramethyl-1,3,2-dioxaborolan-2-yl)but-3-en-1-yl)oxy)silane (3-6)



Colorless oil isolated in 45% yield. Spectral data matched reported values.²⁷

¹H NMR (400 MHz, CDCl₃) δ: 6.59 (dt, *J* = 17.9, 6.6 Hz, 1H), 5.48 (dt, *J* = 18.0, 1.5 Hz, 1H), 3.68 (t, *J* = 6.7 Hz, 2H), 2.38 (qd, *J* = 6.9, 1.5 Hz, 2H), 1.26 (s, 12H), 0.81 (s, 9H), 0.04 (s, 6H).

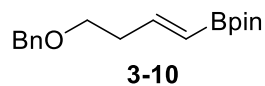
(E)-2-(hex-1-en-1-yl)-4,4,5,5-tetramethyl-1,3,2-dioxaborolane (3-8)



Colorless oil isolated in 65% yield. Spectral data matched reported values.²⁸

¹H NMR (400 MHz, CDCl₃) δ: 6.63 (dt, 1H, *J* = 17.9, 6.4 Hz), 5.42 (dt, 1H, *J* = 17.9, 1.56 Hz), 2.16 (m, 2H), 1.42-1.30 (m, 4H), 1.28 (s, 12H), 0.88 (t, 3H, *J* = 7.2 Hz).

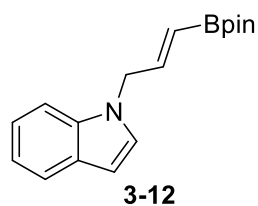
(E)-2-(4-(benzyloxy)but-1-en-1-yl)-4,4,5,5-tetramethyl-1,3,2-dioxaborolane (3-10)



Colorless solid isolated in 79% yield. Spectral data matched reported values.²⁹

¹H NMR (400 MHz, CDCl₃) δ: 7.52-7.25 (m, 5H), 6.63 (dt, 1H, *J* = 18.0, 6.8 Hz), 5.53 (d, 1H, *J* = 18.0 Hz), 4.49 (s, 2H), 3.56 (t, 1H, *J* = 6.8 Hz), 2.51-2.45 (m, 2H), 1.26 (s, 12H).

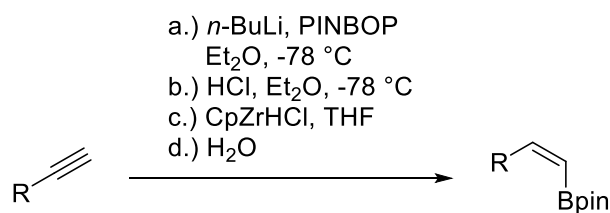
(E)-1-(3-(4,4,5,5-tetramethyl-1,3,2-dioxaborolan-2-yl)allyl)-1H-indole (3-12)



Orange solid isolated in 56% yield. Spectral data matched reported values.²⁹

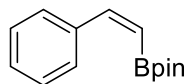
¹H NMR (400 MHz, CDCl₃) δ: 7.66 (ddd, 1H, *J* = 7.9, 0.8, 0.8 Hz), 7.30 (d, 1H, *J* = 8.2 Hz), 7.22 (td, 1H, *J* = 7.2, 0.8 Hz), 7.13 (td, 1H, *J* = 7.2, 0.8 Hz), 7.08 (d, 1H, *J* = 3.2 Hz), 6.74 (dt, 1H, *J* = 18.0, 4.7 Hz), 6.55 (dd, 1H, *J* = 3.2, 0.8 Hz), 5.38 (dt, 1H, *J* = 18.0, 1.8 Hz), 4.82 (dd, 2H, *J* = 4.7, 1.8 Hz), 1.26 (s, 12 H).

Preparation of (Z)-vinyl boronates 2-3 and 2-14:



3-4 and **2-14** were made according to the protocol developed by Iafe.^{4,24}

(E)-4,4,5,5-tetramethyl-2-styryl-1,3,2-dioxaborolane (3-4)

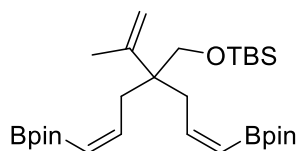


3-4

Yellow oil isolated in 47% yield. Spectral data matched reported values.³⁰

¹H NMR (400 MHz, CDCl₃) δ: 7.62-7.58 (m, 2H), 7.39-7.24 (m, 4H), 5.65 (d, *J* = 14.8 Hz, 1H), 1.34 (s, 12H).

tert-butyl dimethyl((1-(prop-1-en-2-yl)cyclohepta-3,5-dien-1-yl)methoxy)silane (3-13)

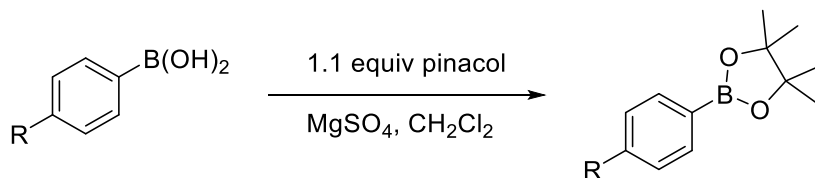


3-13

White solid isolated in 41% yield. Spectral data matched reported values.²⁴

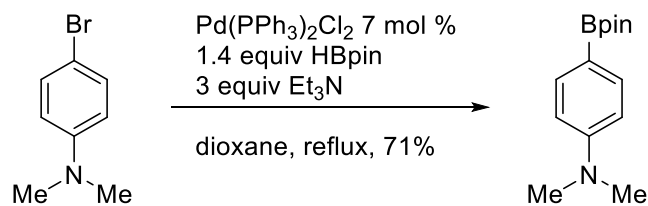
¹H NMR (400 MHz, CDCl₃) δ: 6.43 (ddd, *J* = 13.9, 7.0, 7.0 Hz, 2H), 5.37 (ddd, *J* = 13.6, 1.4, 1.4 Hz, 2H), 4.87-4.85 (m, 1H), 4.69 (d, *J* = 0.5 Hz, 1H), 3.58 (s, 2H), 2.65 (ddd, *J* = 15.2, 7.1, 1.6 Hz), 2.57 (ddd, *J* = 15.2, 7.1, 1.6 Hz, 2H), 1.71 (d, *J* = 0.8 Hz, 3H), 1.25 (s, 24H), 0.88 (s, 9H), 0.02 (s, 6H).

General boronic acid esterification method:



Procedure adapted from protocol reported by Matsuda.³¹ The pertinent boronic acid (2 mmol) and pinacol (2.2 mmol) were combined in 4 mL of CH₂Cl₂. To this solution was added 250 mg of MgSO₄ and the reaction was stirred overnight at room temperature. The pinacol ester products were isolated using flash column chromatography. *p*-Tolylboronic acid pinacol ester (97%), 4-chlorophenylboronic acid pinacol ester (90%), and 4-(trifluoromethyl)phenylboronic acid pinacol ester (88%) were made using this method.

Preparation of 4-(4,4,5,5-Tetramethyl-1,3-dioxaborolan-2-yl)-*N,N*-dimethylaniline:

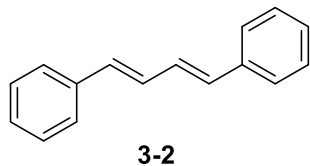


Prepared according to the procedure reported by Okamoto et. al.³²

General oxidative coupling procedure:

To an oven-dried, 15 mL round bottom flask was added potassium *t*-butoxide (112 mg, 1 mmol, 2 equiv), vinyl or aryl boronate (0.5 mmol, 1 equiv), NiCl₂(PPh₃)₂ (8.2 mg, 0.0125 mmol, 0.025 equiv), and PPh₃ (3.2 mg, 0.0125 mmol, 0.025 equiv). The flask was briefly flushed with nitrogen, followed by addition of dioxane (6 mL) via syringe. The resulting brown solution was then treated with nitroarene (0.375 mmol, 0.75 equiv) and allowed to stir for 18 h under a nitrogen atmosphere. The crude mixture was then filtered through a silica plug, washed with ethyl acetate, and concentrated to yield an oil. The crude residue was then purified by silica gel flash column chromatography (hexanes: ethyl acetate).

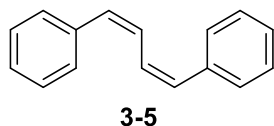
(1E,3E)-1,4-diphenylbuta-1,3-diene



White solid isolated in 85% yield. Spectral data matched reported values.³³

¹H NMR (400 MHz, CDCl₃) δ: 7.45 (d, *J* = 7.4 Hz, 4H), 7.34 (t, *J* = 7.2 Hz, 4H), 7.26-7.22 (m, 2H), 7.00-6.92 (m, 2H), 6.76-6.63 (m, 2H)

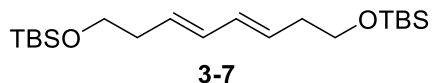
(1Z,3Z)-1,4-diphenylbuta-1,3-diene



Tan solid isolated in 81% yield. Spectral data matched reported values.³⁴

¹H NMR (400 MHz, CDCl₃) δ: 7.48-7.32 (m, 8H), 7.30 (t, *J* = 7.2 Hz, 1H), 6.76-6.71 (m, 2H), 6.64-6.56 (m, 2H);

(7E,9E)-2,2,3,3,14,14,15,15-octamethyl-4,13-dioxa-3,14-disilahexadeca-7,9-diene



White solid isolated in 76% yield.

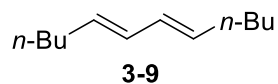
¹H NMR (400 MHz, CDCl₃) δ: 6.09-5.99 (m, 2H), 5.62-5.51 (m, 2H), 3.63 (t, *J* = 6.8 Hz, 4H), 2.77 (q, *J* = 6.8 Hz, 4H), 0.89 (s, 18H), 0.04 (s, 12H).

¹³C NMR (100 MHz, CDCl₃) δ: 132.0, 128.7, 62.9, 36.2, 25.9, 18.3, -5.1, -5.4;

IR (neat, ATR): 2954, 2928, 2888, 2858, 1469, 1258, 1063, 837 cm^{-1} ;

HRMS (DART-TOF) m/z : $[\text{M}-t\text{-Bu}+\text{H}_2]^+$ Calcd for $\text{C}_{14}\text{H}_{29}\text{O}_2\text{Si}$ 257.1931; Found 257.1932.

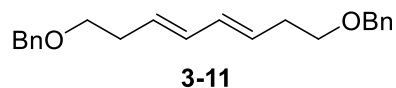
(5*E*,7*E*)-dodeca-5,7-diene



Colorless oil isolated in 74% yield. Spectral data matched reported values.³⁵

^1H NMR (400 MHz, CDCl_3) δ : 6.03-5.94 (m, 2H), 5.61-5.49 (m, 2H), 2.05 (q, $J = 7$ Hz, 4H), 1.40-1.27 (m, 8H), 0.88 (t, $J = 7$ Hz, 6H).

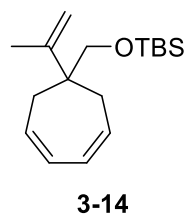
(3*E*,5*E*)-1,8-bis(benzyloxy)octa-3,5-diene



White solid isolated in 30% yield. Spectral data matched reported values.³⁶

^1H NMR (400 MHz, CDCl_3) δ : 7.38-7.35 (m, 8H), 7.33-7.27 (m, 2H), 6.14-6.06 (m, 2H), 5.68-5.57 (m, 2H), 4.53 (s, 4H), 3.52 (t, $J = 6.8$ Hz, 4H), 2.41 (q, $J = 6.7$ Hz, 4H).

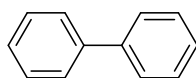
tert-butyl dimethyl((1-(prop-1-en-2-yl)cyclohepta-3,5-dien-1-yl)methoxy)silane



White solid isolated in 23% yield. Spectral data matched reported values.²⁴ Reaction performed at high dilution to prevent oligomerization: 133 mg (0.25 mmol, 0.5 equiv) of **3-13** used with 51 mL of dioxane (0.0049 M).

¹H NMR (400 MHz, CDCl₃) δ: 5.81 (s, 4H), 4.86 (t, *J* = 1.4 Hz, 1H), 4.72 (s, 1 H), 3.62 (s, 2H), 2.42-2.33 (m, 4H), 1.75 (t, *J* = 0.6 Hz, 3H), 0.88 (s, 9H), 0.01 (s, 6H).

1,1'-biphenyl

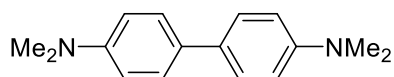


3-19

White solid isolated in 89% yield starting from pinacol boronate, 70% yield from neopentylglycol boronate, and 24% yield from boronic acid. Spectral data matched reported values.³³

¹H NMR (400 MHz, CDCl₃) δ: 7.62 (d, *J* = 7.8, 4H), 7.46 (t, *J* = 7.8, 4H), 7.38-7.33 (m, 2H).

N,N,N,N-tetramethyl-[1,1'-biphenyl]-4,4'-diamine

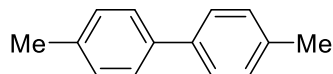


3-20

Tan solid isolated in 79% yield. Spectral data matched reported values.³⁷

¹H NMR (400 MHz, CDCl₃) δ: 7.45 (d, *J* = 8.4 Hz, 4H), 6.80 (d, *J* = 8.4 Hz, 4H), 2.97 (s, 12H).

4,4'-dimethyl-1,1'-biphenyl

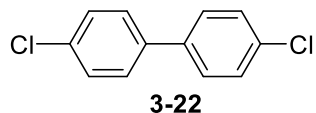


3-21

White solid isolated in 77% yield. Spectral data matched reported values.³³

¹H NMR (400 MHz, CDCl₃) δ: 7.49 (d, *J* = 8.0 Hz, 4H), 7.24 (d, *J* = 8.0 Hz, 4H), 2.40 (s, 6H).

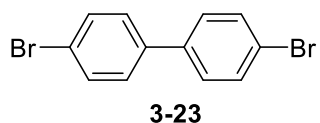
4,4'-dichloro-1,1'-biphenyl



White solid isolated in 34% yield. Spectral data matched reported values.³³

¹H NMR (400 MHz, CDCl₃) δ 7.48 (d, *J* = 8.4 Hz, 4H), 7.41 (d, *J* = 8.4 Hz, 4H).

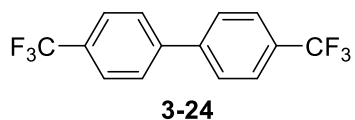
4,4'-dibromo-1,1'-biphenyl



White solid isolated in 23% yield. Spectral data matched reported values.³⁸

¹H NMR (400 MHz, CDCl₃) δ: 7.56 (d, *J* = 8.4 Hz, 4H), 7.41 (d, *J* = 8.4 Hz, 4H).

4,4'-bis(trifluoromethyl)-1,1'-biphenyl



White solid isolated in 15% yield. Spectral data matched reported values.³⁹

¹H NMR (400 MHz, CDCl₃) δ: 7.75-7.69 (m, 8H).

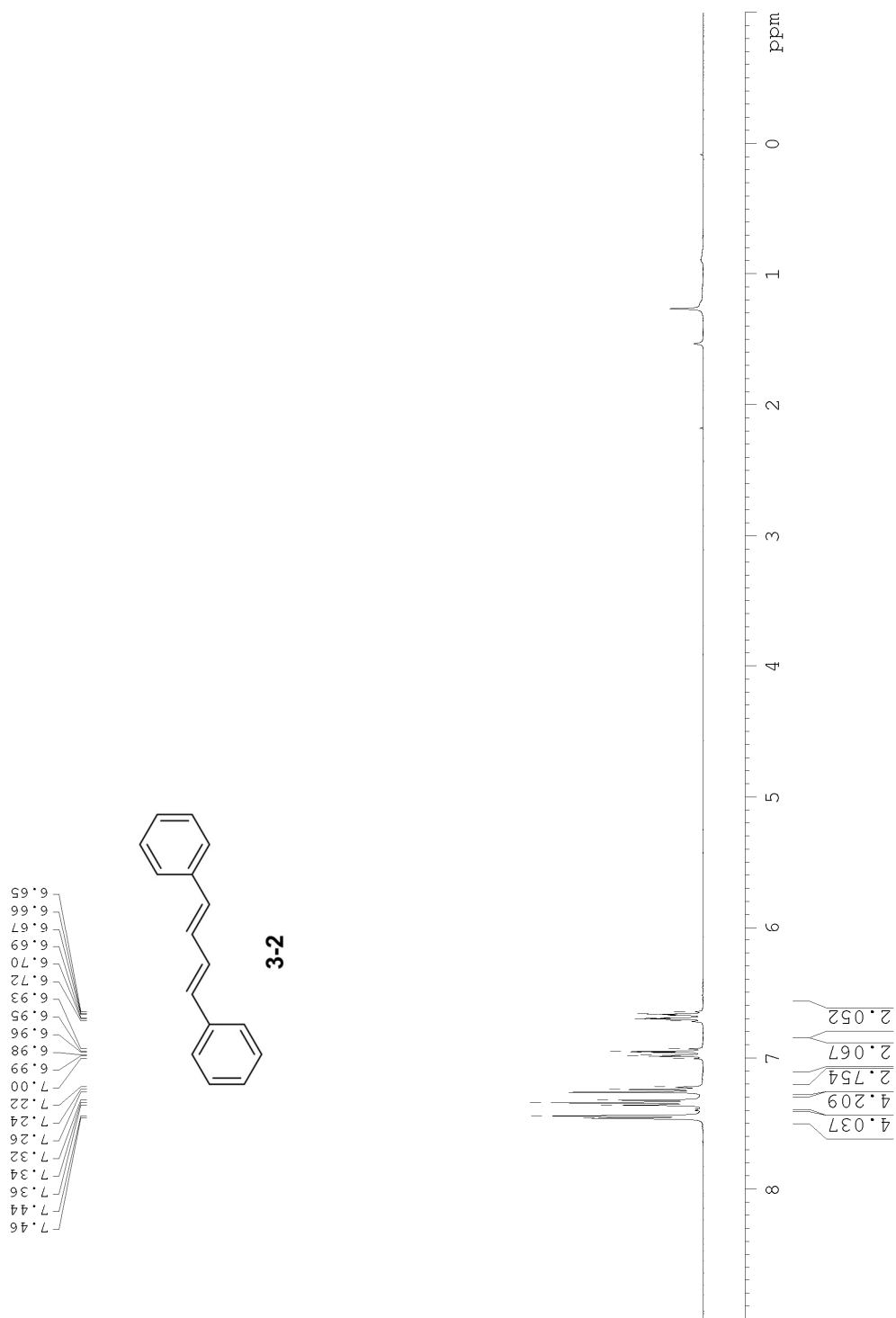
3.8 – References

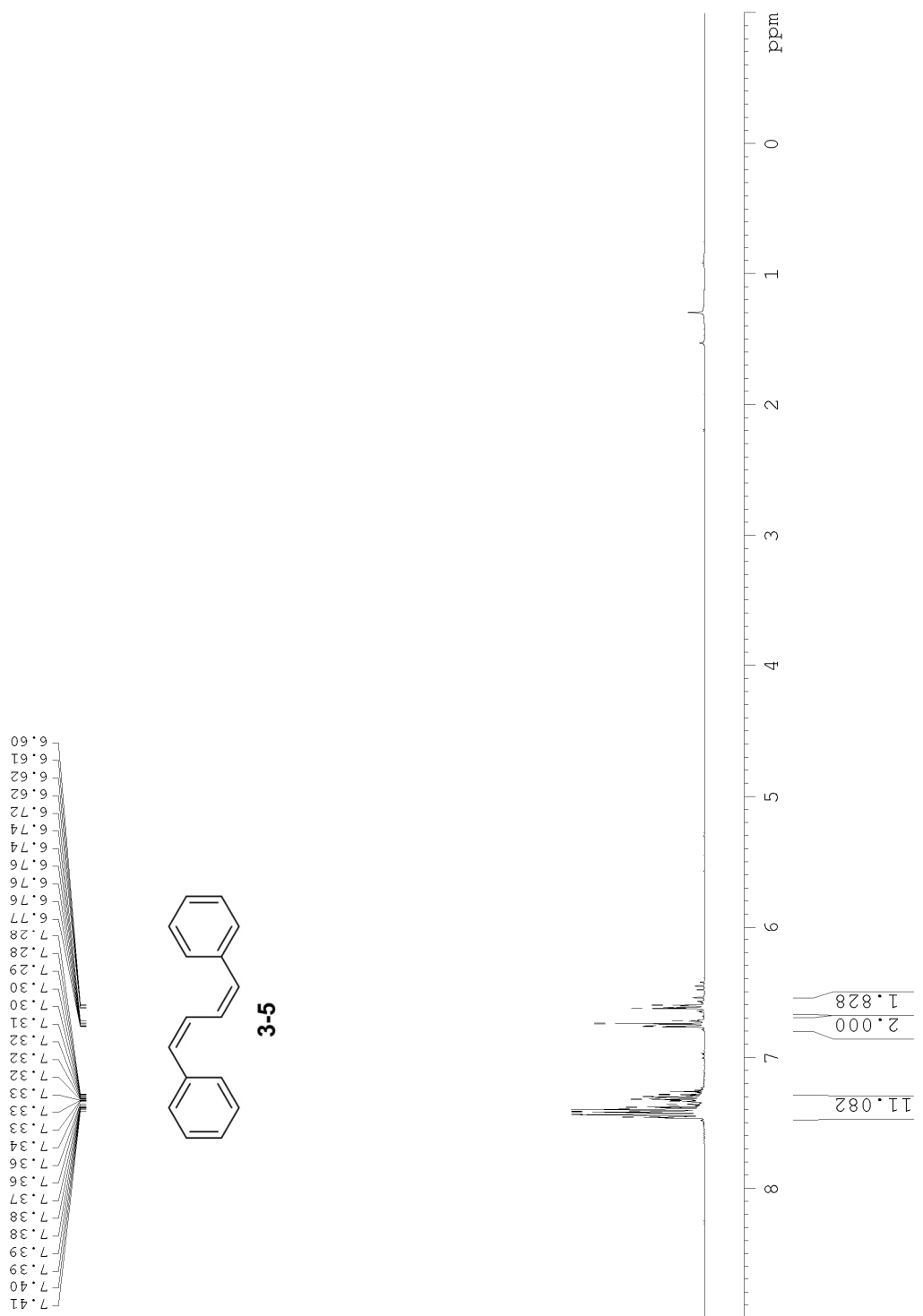
- (1) Tamao, K.; Sumitani, K.; Kumada, M. *J. Am. Chem. Soc.* **1972**, *94*, 4374.
- (2) Corriu, R. J. P.; Masse, J. P. *J. Chem. Soc. Chem. Commun.* **1972**, 144a.
- (3) Snodin, D. *J. Org. Process Res. Dev.* **2010**, *14*, 960.
- (4) Iafe, R. G.; Chan, D. G.; Kuo, J. L.; Boon, B. A.; Faizi, D. J.; Saga, T.; Turner, J. W.; Merlic, C. A. *Org. Lett.* **2012**, *14*, 4282.
- (5) Miyaura, N.; Yamada, K.; Suzuki, A. *Tetrahedron Lett.* **1979**, 3437.
- (6) Iafe, R. G.; Kuo, J. L.; Hochstatter, D. G.; Saga, T.; Turner, J. W.; Merlic, C. A. *Org. Lett.* **2013**, *15*, 582.
- (7) He, C. Q.; Chen, T. Q.; Patel, A.; Karabiyikoglu, S.; Merlic, C. A.; Houk, K. N. *J. Org. Chem.* **2015**, *80*, 11039.
- (8) Boon, B. A.; Green, A. G.; Liu, P.; Houk, K. N.; Merlic, C. A. *J. Org. Chem.* **2017**, *82*, 4613.
- (9) Liu, G.; Du, Q.; Xie, J.; Zhang, K.; Tao, X. *Chinese J. Catal.* **2006**, *27*, 1051.
- (10) Rosen, B. M.; Quasdorf, K. W.; Wilson, D. A.; Zhang, N.; Resmerita, A.-M.; Garg, N. K.; Percec, V. *Chem. Rev.* **2011**, *111*, 1346.
- (11) Yu, D.-G.; Yu, M.; Guan, B.-T.; Li, B.-J.; Zheng, Y.; Wu, Z.-H.; Shi, Z.-J. *Org. Lett.* **2009**, *11*, 3374.
- (12) Matsumoto, H.; Inaba, S.; Rieke, R. D. *J. Org. Chem.* **1983**, *48*, 840.
- (13) Percec, V.; Bae, J.-Y.; Zhao, M.; Hill, D. H. *J. Org. Chem.* **1995**, *60*, 176.

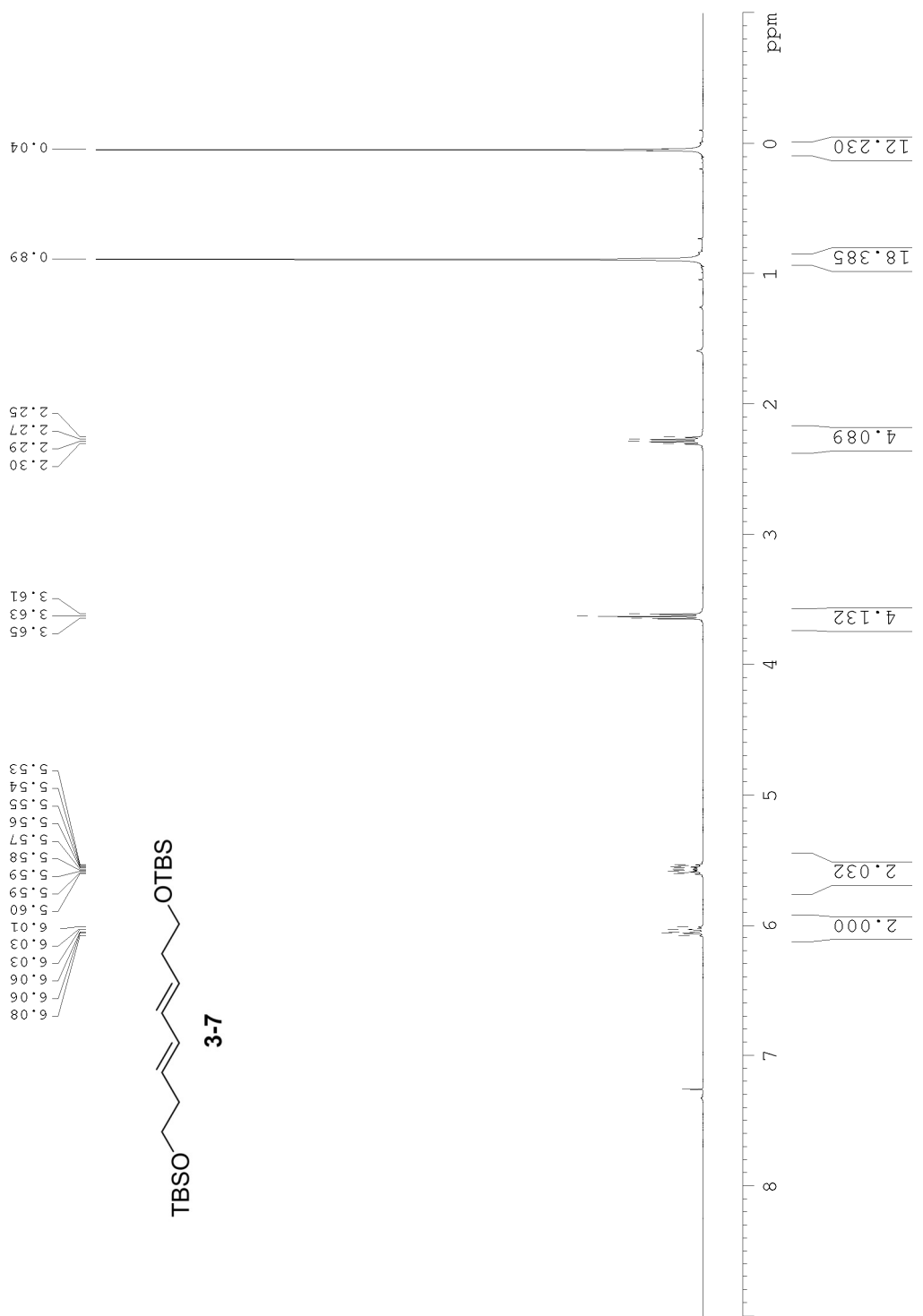
- (14) Vilas B., P.; Manuel, G.; Elena, B.; Diego J., C. *Chem. – A Eur. J.* **2009**, *15*, 12681.
- (15) Fan, X.-H.; Yang, L.-M. *European J. Org. Chem.* **2010**, *2010*, 2457.
- (16) Skraup, Z. H. *Chem. Ber.* **1880**, *13*, 2086.
- (17) Gulevskaya, A. V.; Tyaglivaya, I. N.; Verbeeck, S.; Maes, B. U. W.; Tkachuk, A. V. *Arkivoc* **2011**, *2011*, 238.
- (18) Pogorelić, I.; Filipan-Litvić, M.; Merkaš, S.; Ljubić, G.; Capanec, I.; Litvić, M. *J. Mol. Catal. A Chem.* **2007**, *274*, 202.
- (19) Zhong, J.-J.; Wu, C.-J.; Meng, Q.-Y.; Gao, X.-W.; Lei, T.; Tung, C.-H.; Wu, L.-Z. *Adv. Synth. Catal.* **2014**, *356*, 2846.
- (20) Li, D. Y.; Chen, H. J.; Liu, P. N. *Org. Lett.* **2014**, *16*, 6176.
- (21) Cadogan, J. I. G.; Kulik, S. *J. Chem. Soc. C Org.* **1971**, 2621.
- (22) Wang, Y. D.; Kimball, G.; Prashad, A. S.; Wang, Y. *Tetrahedron Lett.* **2005**, *46*, 8777.
- (23) Hart, D. W.; Schwartz, J. *J. Am. Chem. Soc.* **1974**, *96*, 8115.
- (24) Iafe, R. G. Palladium(II)-Catalyzed Reactions of Pinacol Vinylboronates: New Cyclization Strategies to Prepare Polyene Macrocycles and Transannular Diels-Alder Cycloaddition Substrates, Ph.D. Dissertation, University of California, Los Angeles, CA, 2011.
- (25) Du, Z.-T.; Xu, Y.; Yu, H.-R.; Li, Y. *Acta Crystallogr. Sect. E Struct. Reports Online* **2010**, *66*, o415.
- (26) Tai, C.-C.; Yu, M.-S.; Chen, Y.-L.; Chuang, W.-H.; Lin, T.-H.; Yap, G. P. A.; Ong, T.-G.

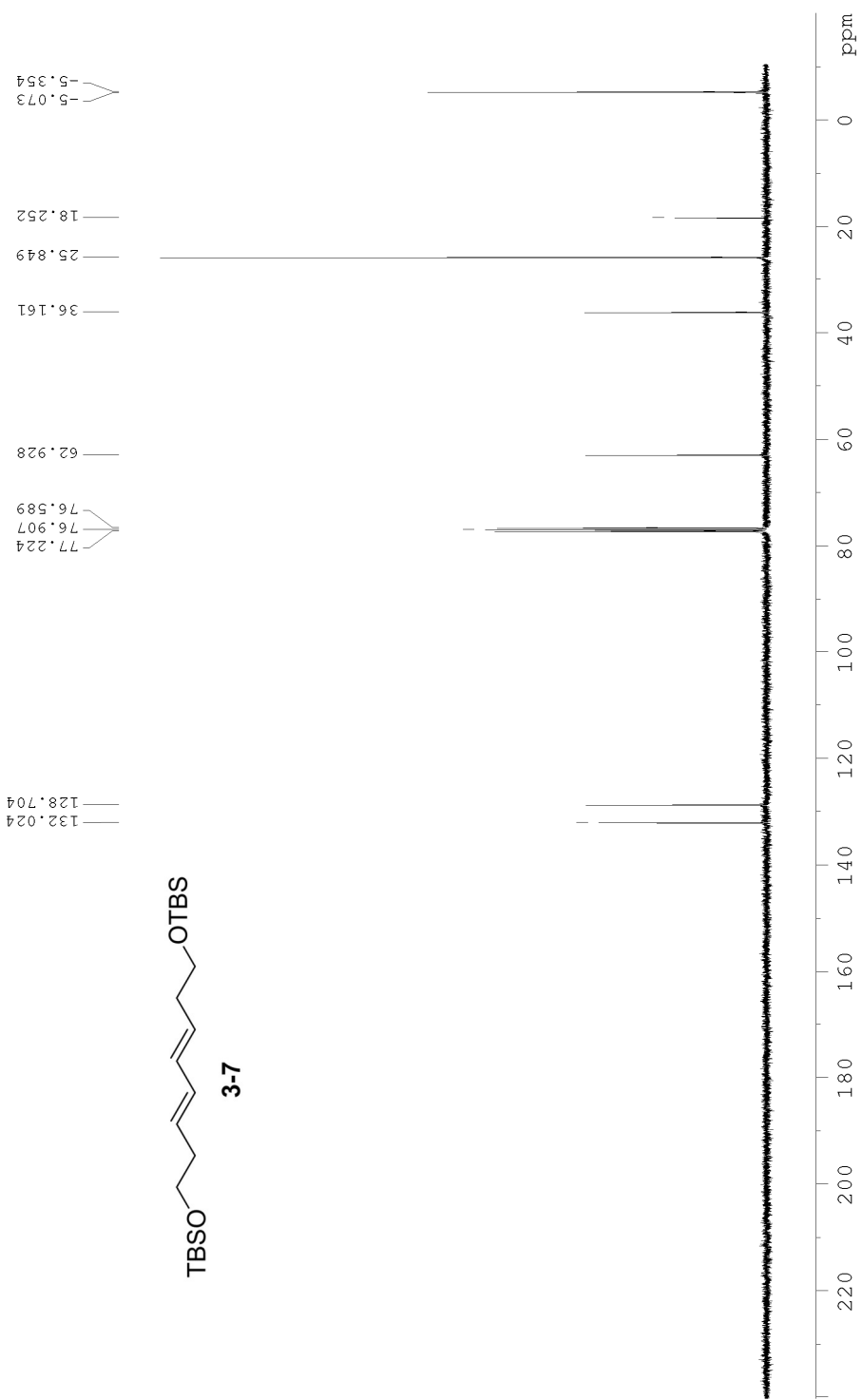
- Chem. Commun.* **2014**, 50, 4344.
- (27) Yoshida, H.; Kageyuki, I.; Takaki, K. *Org. Lett.* **2014**, 16, 3512.
- (28) Ojha, D. P.; Prabhu, K. R. *Org. Lett.* **2016**, 18, 432.
- (29) Shade, R. E.; Hyde, A. M.; Olsen, J.-C.; Merlic, C. A. *J. Am. Chem. Soc.* **2010**, 132, 1202.
- (30) Huang, H.; Yu, C.; Li, X.; Zhang, Y.; Zhang, Y.; Chen, X.; Mariano, P. S.; Xie, H.; Wang, W. *Angew. Chem. Int. Ed.* **2017**, 56, 8201.
- (31) Matsuda, T.; Makino, M.; Murakami, M. *Org. Lett.* **2004**, 6, 1257.
- (32) Okamoto, A.; Tainaka, K.; Nishiza, K. I.; Saito, I. *J. Am. Chem. Soc.* **2005**, 127, 13128.
- (33) Hua, S.-K.; Hu, Q.-P.; Ren, J.; Zeng, B.-B. *Synthesis* **2013**, 45, 518.
- (34) Solorio-Alvarado, C. R.; Wang, Y.; Echavarren, A. M. *J. Am. Chem. Soc.* **2011**, 133, 11952.
- (35) Conn, C.; Lloyd-Jones, D.; Kannangara, G. S. K.; Baker, A. T. *J. Organomet. Chem.* **1999**, 585, 134.
- (36) Boon, B. A. Palladium-Catalyzed Oxidative Couplings and Applications to the Synthesis of Macrocycles and Strained Cyclic Dienes, Ph.D. Dissertation, University of California, Los Angeles, CA, 2017.
- (37) Jiang, X.; Wang, C.; Wei, Y.; Xue, D.; Liu, Z.; Xiao, J. *Chem. - A Eur. J.* **2014**, 20, 58.
- (38) Dahl, B. J.; Mills, N. S. *Org. Lett.* **2008**, 10, 5605.
- (39) Luo, H.-Q.; Dong, W. *Synth. Commun.* **2013**, 43, 2733.

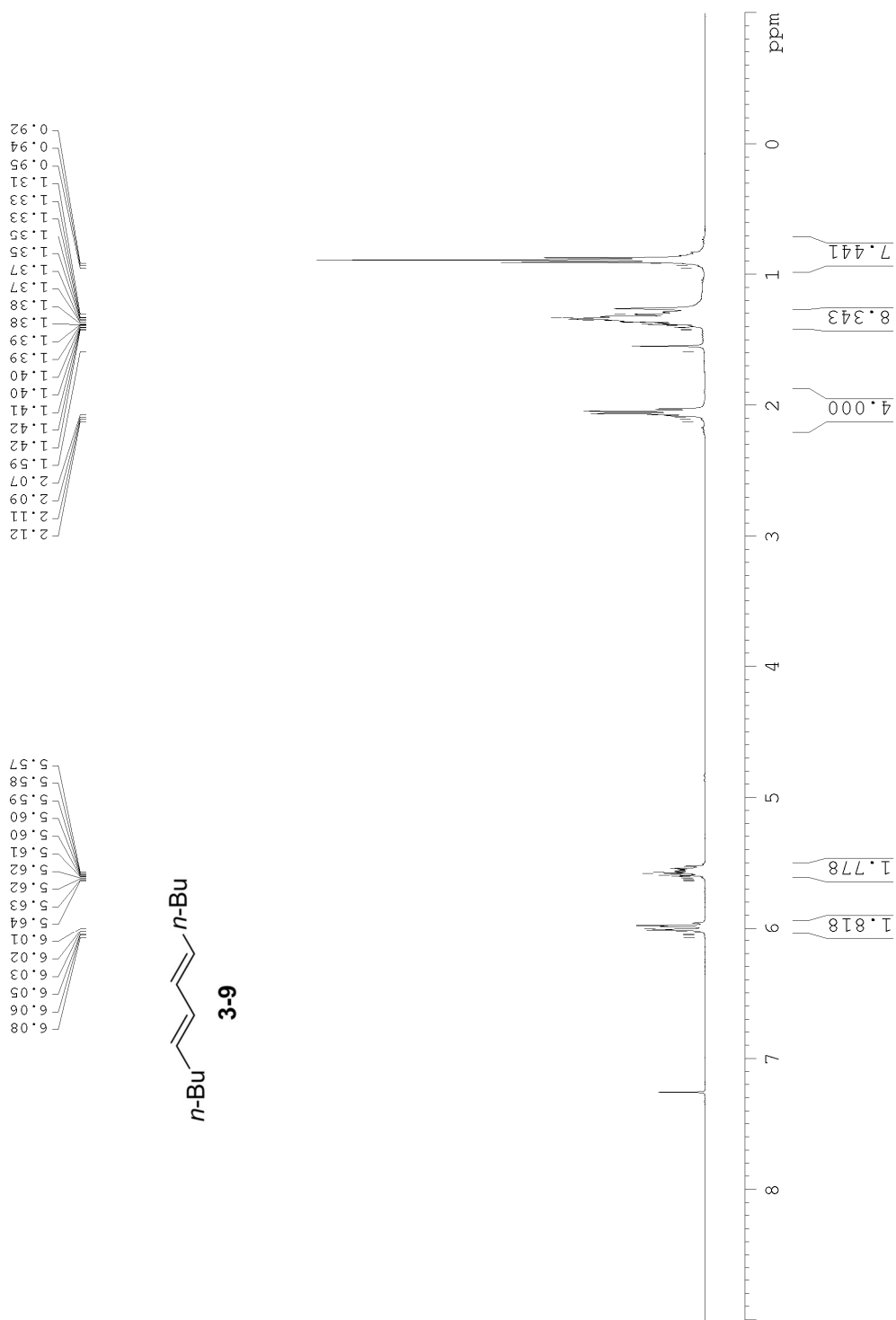
3.9 –NMR Spectra

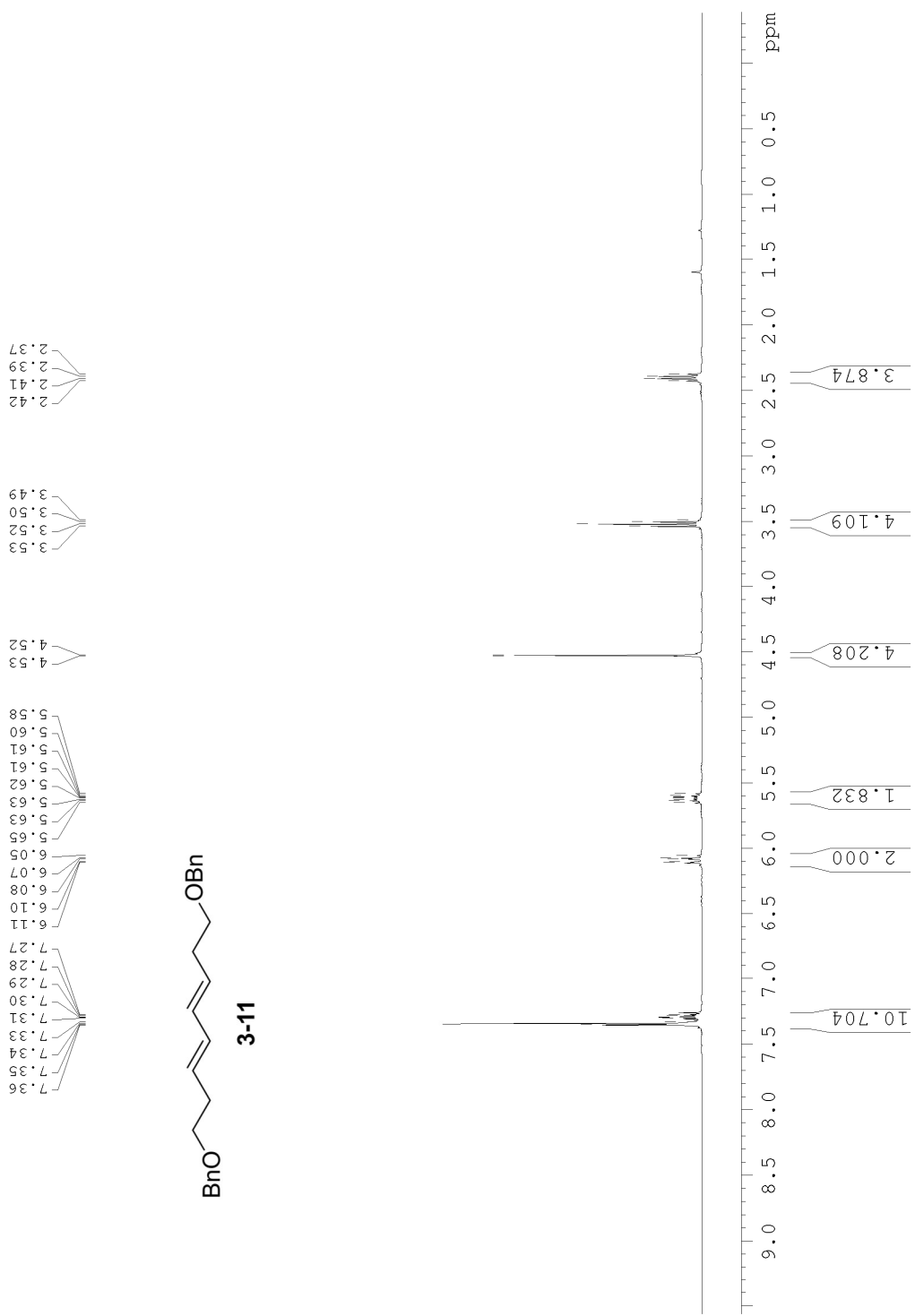


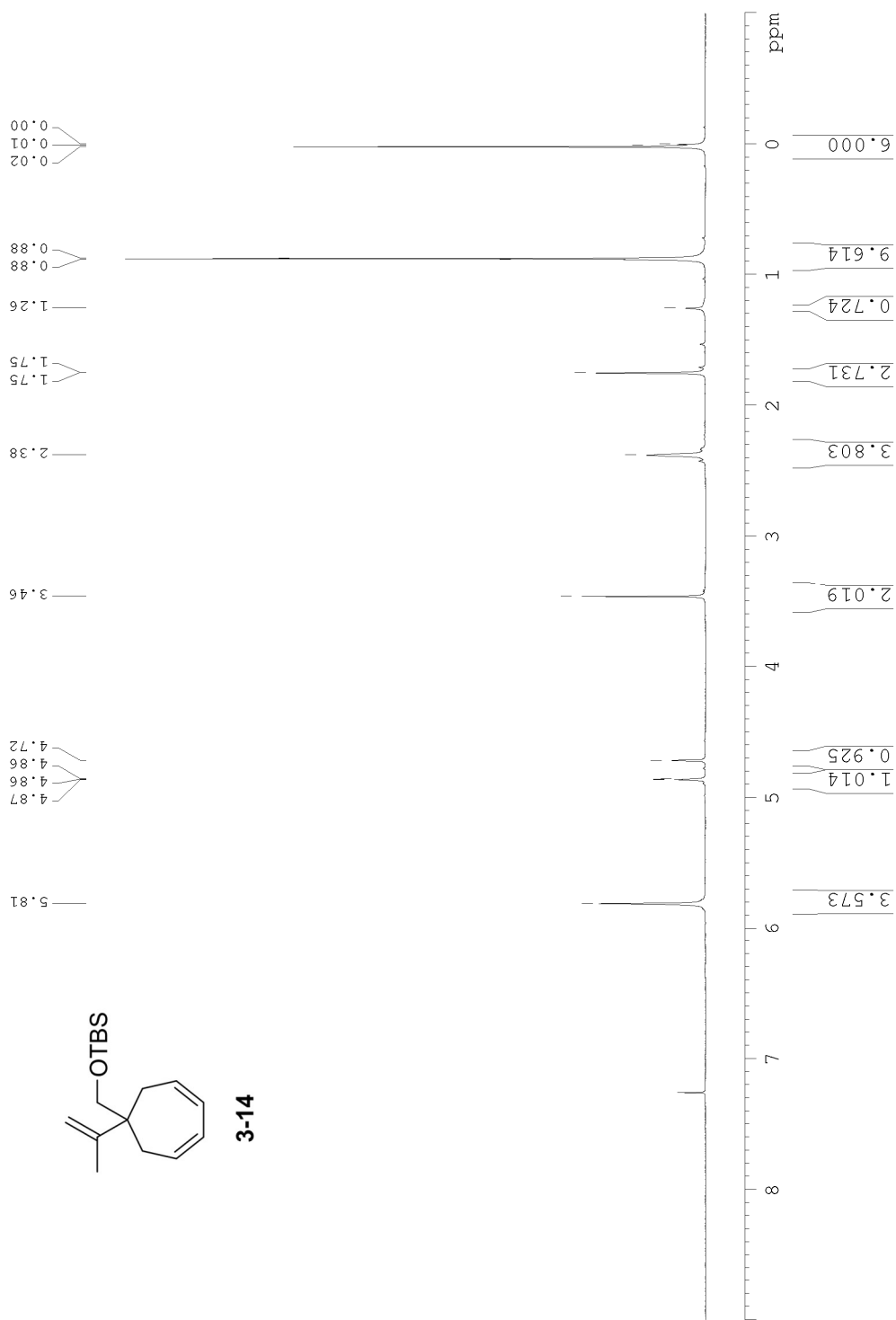


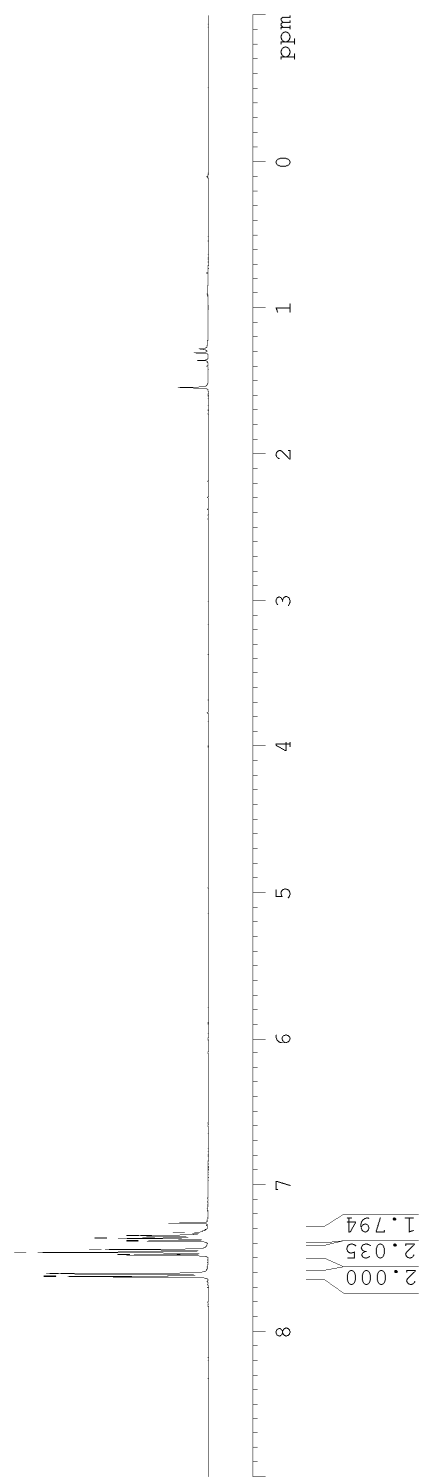
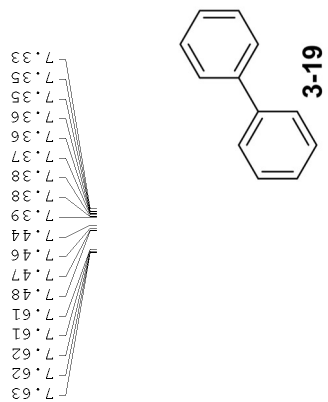


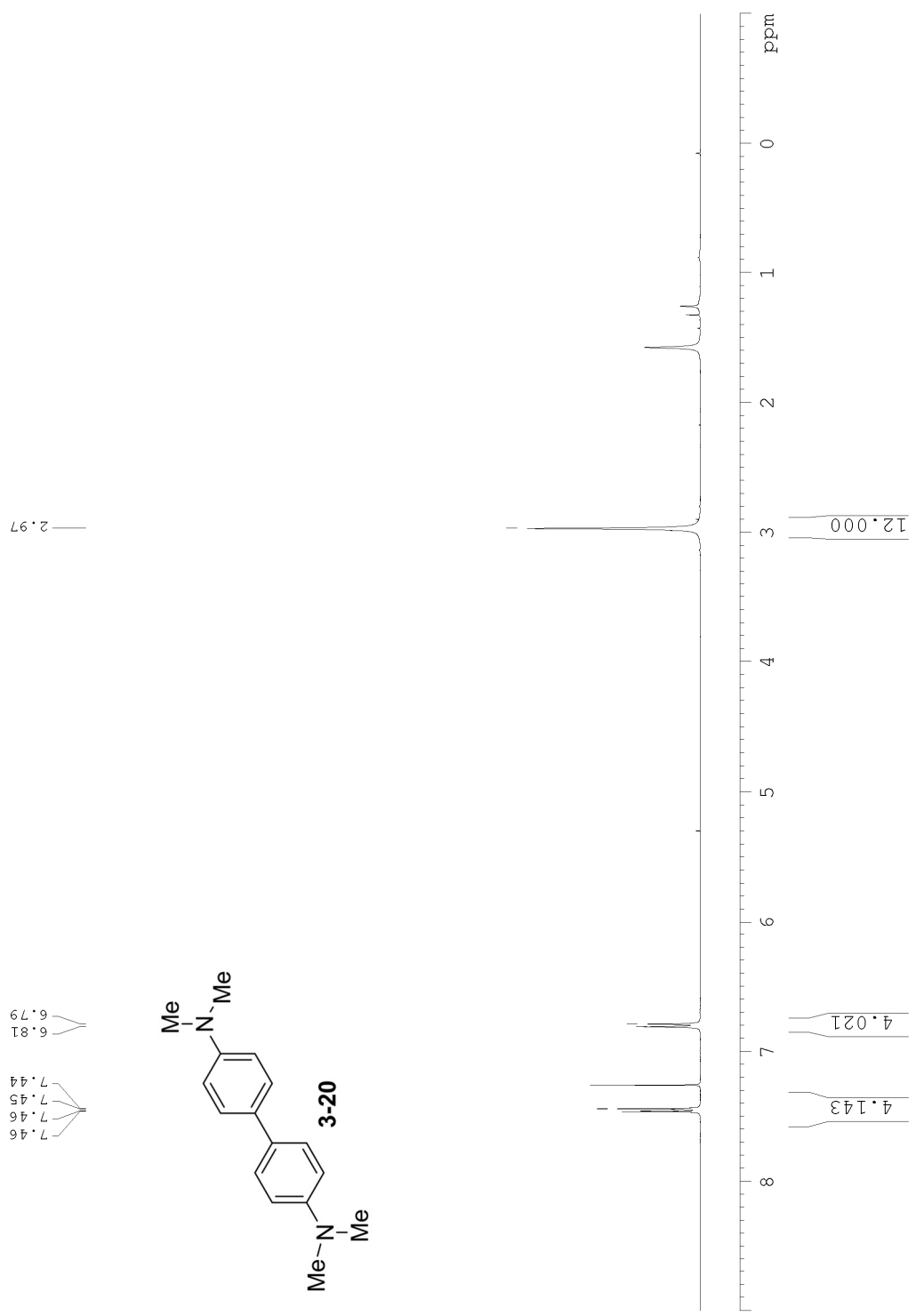


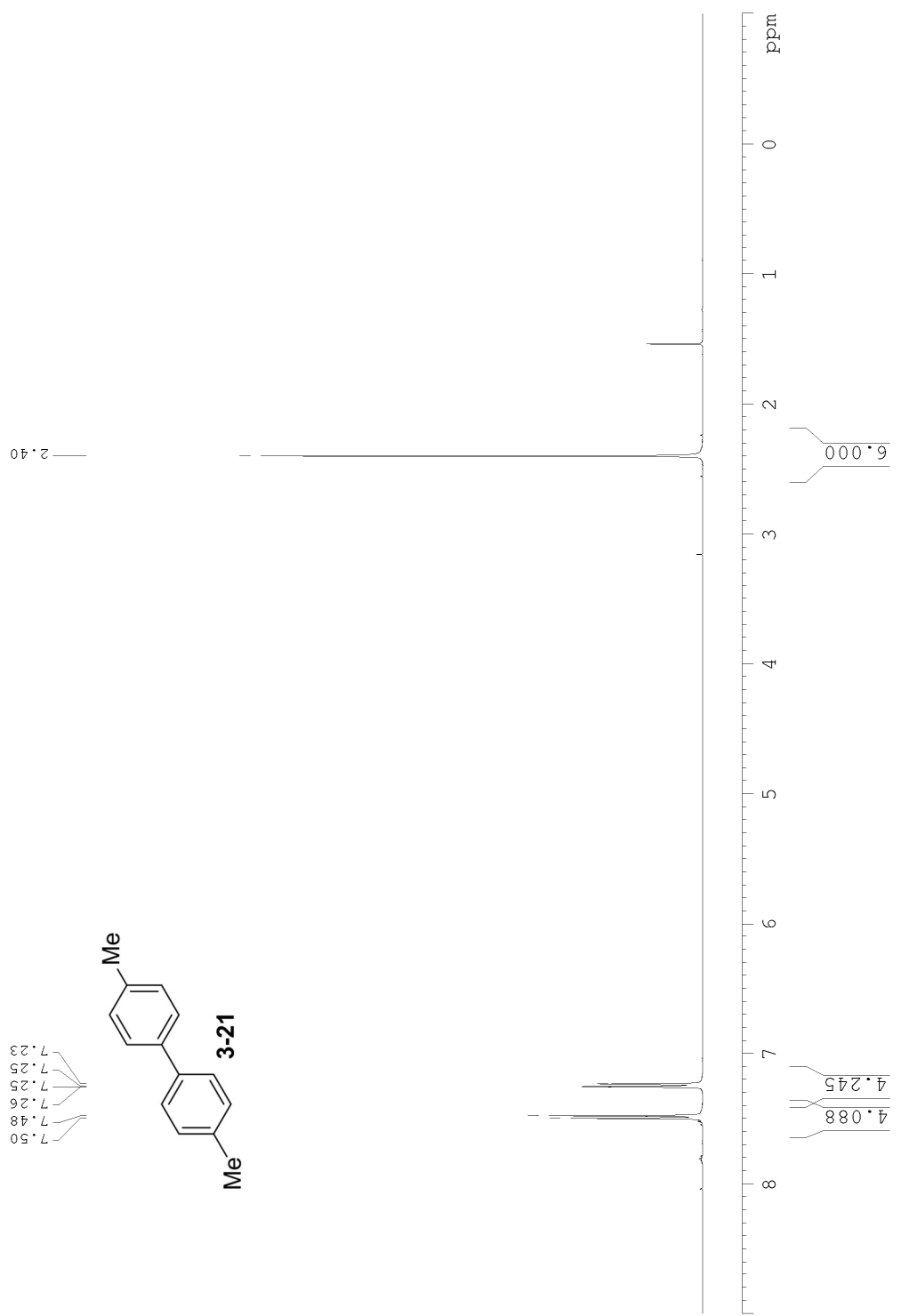


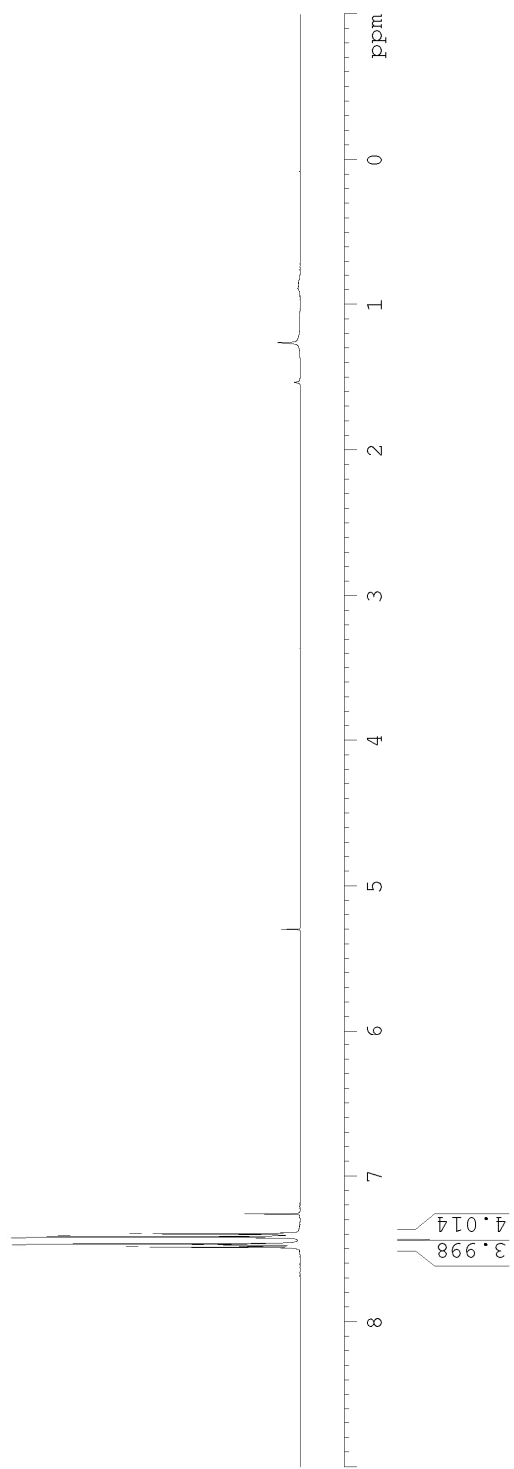
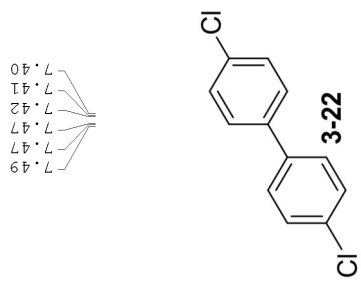




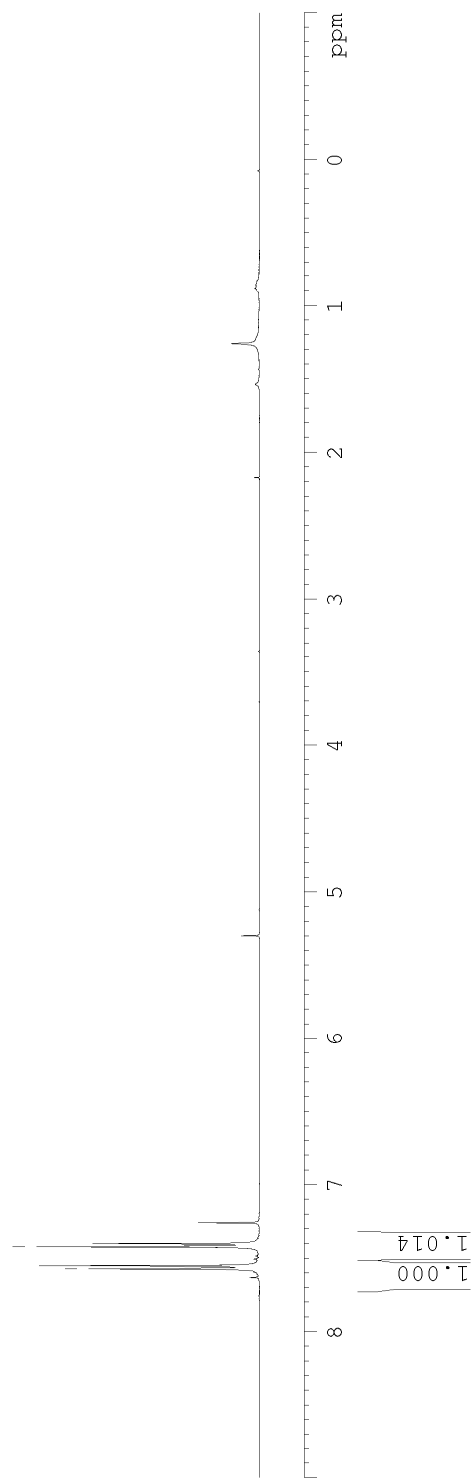
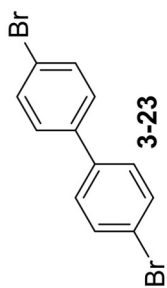




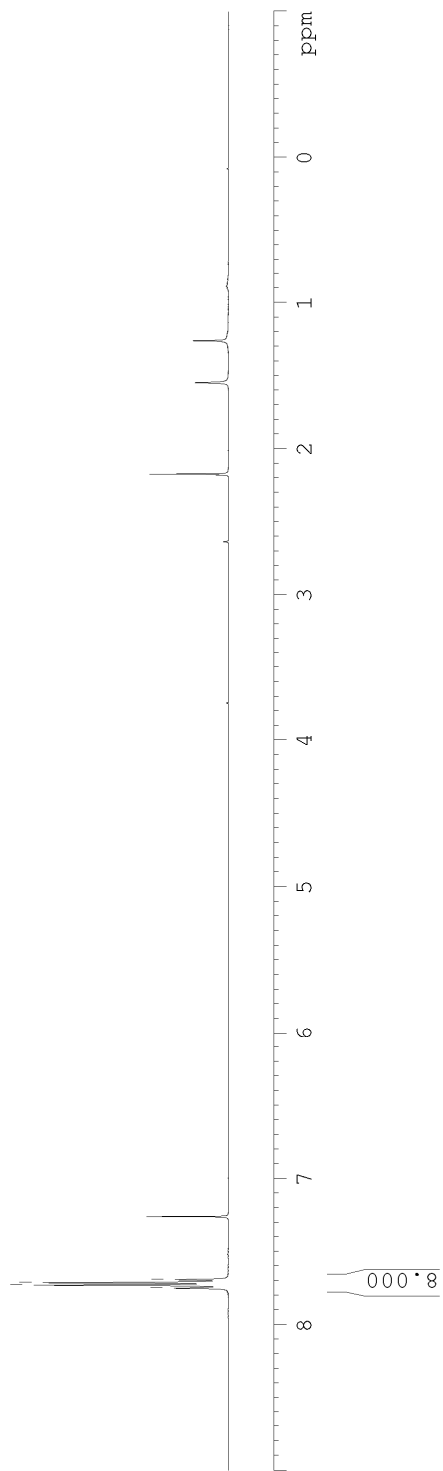
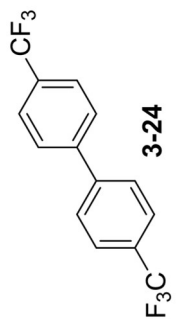




7.57
7.55
7.42
7.40



7.75
7.73
7.71
7.69



Chapter IV – Design and Synthesis of a Gene Expression-Dependent CO-Releasing Molecule

4.1 – Introduction

Intercellular and intracellular communication is as important to biology as it is complex. Chemical signaling molecules make up an incredibly diverse family of compounds, showcasing the ingenuity of Nature's solution to the problem of getting a message from point A to point B. From behemoth proteins to small molecule amines, there exists great diversity among signaling molecules. Perhaps the most well-studied class of chemical messengers are the neurotransmitters, without which the operation of the neuron and its propagating action potentials would not be possible. Most neurotransmitters are amino acid derivatives that are stored in synaptic vesicles and released with each neural impulse. These small molecule messengers travel across the synaptic cleft to neighboring cells and bind to specialized receptor sites, relaying their signal. This interaction between small molecules and receptors forms the basis of drug development and design, but there exists a different realm of cellular communication agents, gases.¹

Endogenously-produced gaseous signaling molecules, first identified in the 1980s with the discovery of biogenic NO, reinvented the traditional cellular communication paradigm.² Unlike neurotransmitters, which can be stored and released from vesicles, gaseous signaling molecules (gasotransmitters) must be enzymatically-produced and released on-demand. It's not believed that these gaseous molecules randomly diffuse through neighboring tissues; instead, these molecules are delivered to their targets via the help of specialized transport enzymes, usually the same enzymes responsible for their synthesis. Furthermore, gasotransmitters are unique in that they can chemically modify their protein targets, usually by binding to metallic

cofactors such as heme. The general differences between small-molecule signal transmission and that of gaseous transmitters are represented in the scheme shown in Figure 4-1.

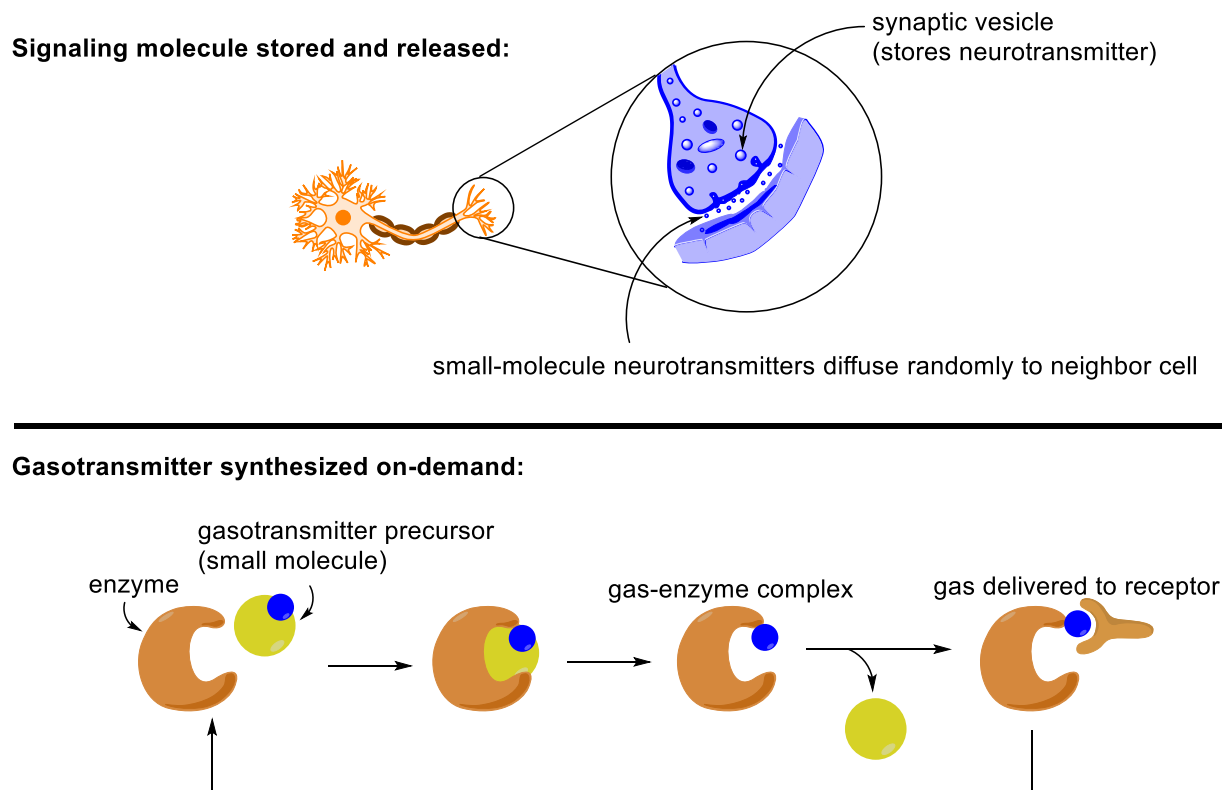
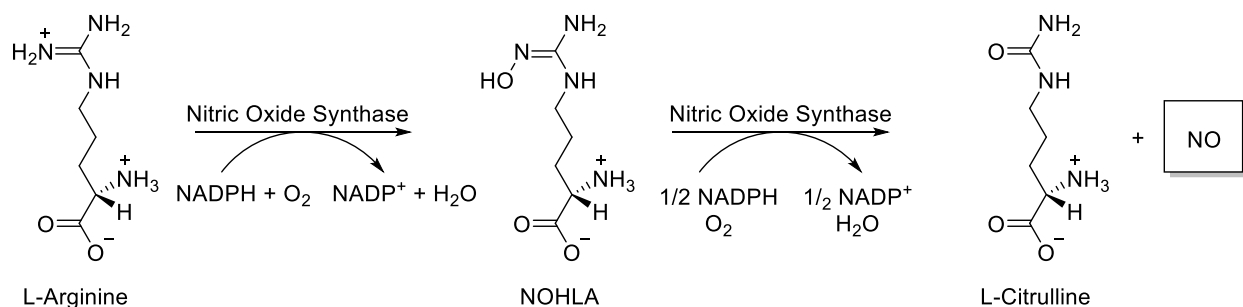


Figure 4-1 – Schematic representing the differences between traditional signal transmission involving small molecules (top) versus enzymatic gasotransmitter production and delivery (bottom).

In this chapter, I introduce the three most-studied gasotransmitters: nitric oxide (NO), hydrogen sulfide (H₂S), and carbon monoxide (CO) in a review on gasotransmitter-releasing compounds. Then, I describe my efforts towards the synthesis and design of a gene-expression dependent CO-releasing molecule based on a galactose-linked iron carbonyl complex.

4.2 – Nitric Oxide as a Gasotransmitter

Nitric oxide is an extremely reactive gaseous free radical, so its role as an essential signaling molecule in biology is quite surprising.³⁻⁶ The mechanism for the biosynthesis of NO by the enzyme nitric oxide synthase (NOS) is shown in Scheme 4-1.⁷

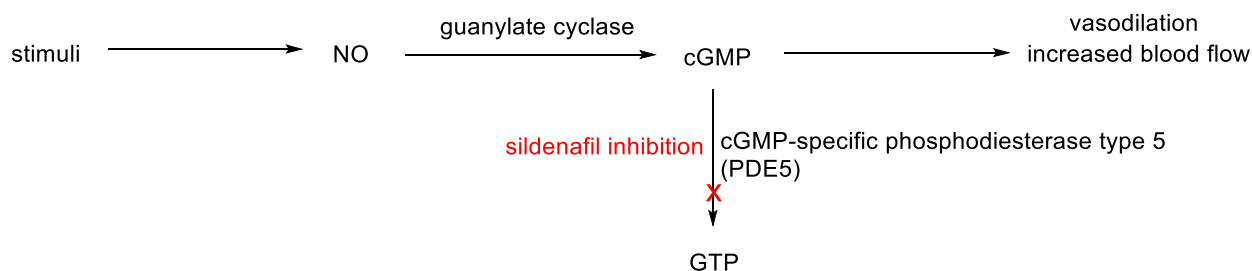


Scheme 4-1 – Oxidation of L-arginine to L-citrulline and NO by NOS.

The guanidinium moiety of L-arginine undergoes a net 5-electron oxidation, proceeding through the intermediacy of N-hydroxy-L-arginine (NOHLA), and then finally arriving at L-citrulline with extrusion of NO gas. The enzyme accomplishes the transformation with the help of five cofactors: flavin adenine dinucleotide (FAD), flavin mononucleotide (FMN), tetrahydrobiopterin (BH₄), calmodulin, and heme. The role of nitric oxide in biology has been extensively studied, culminating with the 1998 Nobel Prize in Medicine awarded to Robert F. Furchgott, Louis J. Ignarro and Ferid Murad for their work elucidating the effects of NO on the cardiovascular system. Studies have shown that nitric oxide release is implicated in immune response, vasodilation, and smooth muscle tone. Because of these important physiological and pharmacological responses triggered by NO release, several therapeutics have been developed to exploit these pathways. There exist two major categories of drugs that affect NO-related systems: (1) compounds which mimic NO binding or otherwise interfere with normal NO signaling, and (2) compounds which directly release NO gas as prodrugs.

Sildenafil (Viagra®), a treatment for erectile dysfunction, works by potentiating the downstream signals of NO release in men. As shown in Scheme 4-2, sexual arousal causes the production of NO in the corpus cavernosum, the erectile tissue of the penis. The endogenously produced NO binds to guanylate cyclase, upregulating production of cyclic guanosine monophosphate (cGMP). The cGMP causes smooth muscle relaxation, resulting in increased

blood flow. Sildenafil works by inhibiting the enzyme that degrades cGMP, PDE5, the net result of which is amplification of the NO-mediated signal.



Scheme 4-2 – NO-mediated signaling pathway depicting role of sildenafil for the treatment of sexual dysfunction in men.

Some drugs and research compounds affect the NO-mediated signaling pathways by releasing NO directly. The most salient example is nitroglycerin, used for over 100 years for the treatment of high blood pressure and angina. Nitroglycerin and related nitrates (Figure 4-2) work as NO prodrugs, releasing the gas upon reduction by thiols in vivo.

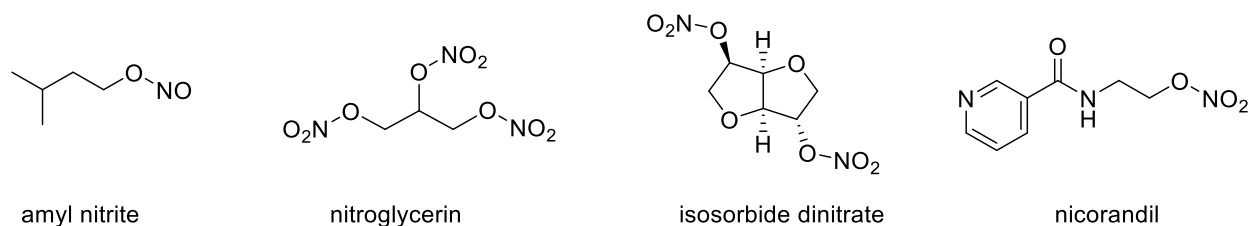


Figure 4-2 – Organic nitrites/nitrates with vasodilatory effects.

More recently, photoactivated NO-releasing molecules have been developed with the hope that a light-activated molecule could allow spatiotemporal control of NO-release, unlike traditional therapeutics that have an uncontrolled and difficult-to-predict mode of activation. For example, Flu-DNB (**4-1**) was shown to cause vasodilation via NO-release in mice brains, but only after exposure to 735 nm light (Figure 4-3).^{8,9}

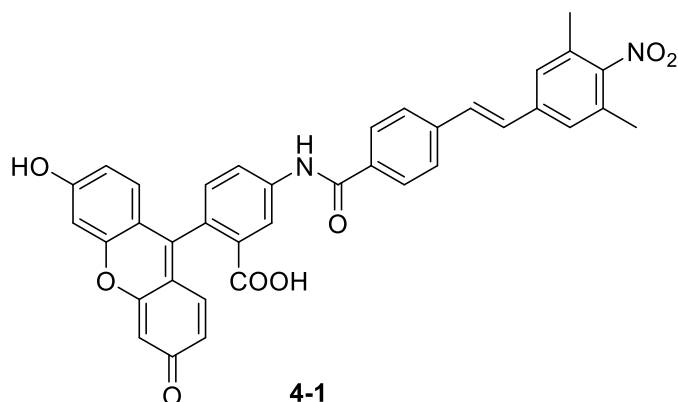
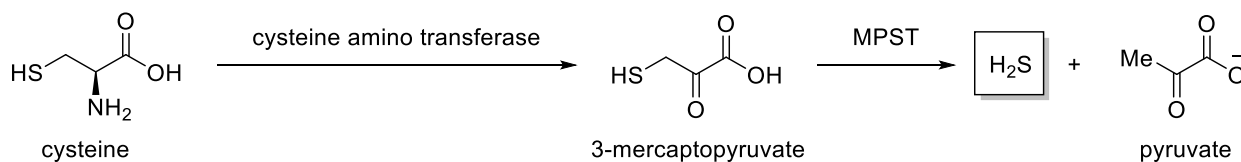


Figure 4-3 – Structure of Flu-DNB, a photoactivated NO-releasing compound.

4.3 – Hydrogen Sulfide as a Gasotransmitter

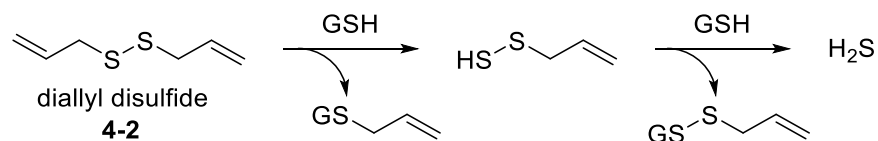
H₂S is a noxious, poisonous gas with the characteristic odor of rotten eggs. Like nitric oxide, hydrogen sulfide plays an essential role in mammals as an endogenously produced signaling molecule.^{10,11} H₂S has vasodilatory effects and has been detected in the brain, where it acts as an *N*-methyl-D-aspartate (NMDA) receptor potentiator. For these reasons, hydrogen sulfide signaling pathways have been investigated as possible targets for cardiovascular¹² and neurological¹³ therapeutics. As shown in Scheme 4-3, cysteine is the major biosynthetic precursor for H₂S.



Scheme 4-3 – Biosynthesis of H₂S by the action of CAT and MPST on cysteine.

In the predominant mechanism for the biosynthesis of H₂S, cysteine is first converted into 3-mercaptopyruvate by cysteine amino transferase (CAT). Next, 3-mercaptosulfurtransferase (MPST) catalyzes the extrusion of H₂S to give pyruvate. Additional natural products and manmade compounds which release H₂S upon metabolism are well known. Diallyl disulfide (4-

2), a flavor component in garlic, is known to be a naturally-occurring H₂S-releasing molecule.¹⁴ The mechanism of H₂S release from **4-2** is deallylation followed by reduction of the disulfide by glutathione (GSH) as shown in Scheme 4-4.



Scheme 4-4 – Release of H₂S via reduction of diallyl disulfide by glutathione.

Studies have shown that dietary garlic consumption has cardioprotective effects,¹⁵ which have been recently ascribed to the hydrogen sulfide release by metabolism of compounds present in the plant.¹⁶ Synthetic hydrogen sulfide releasing compounds have also been developed.¹⁷ The most common class of H₂S-releasing compounds, many of which have been shown to have anti-inflammatory and anti-cancer activity, are H₂S prodrugs with the 1,2-dithiole-3-thione (DTT) motif.^{17,18} The mechanism for H₂S release from the DTT functional group is believed to be hydrolysis.^{19,20} DTT derivatives of various drugs have been synthesized in order to release H₂S alongside a small-molecule to exert an improved pharmacological effect compared to drug alone. For example, DTT derivatives of various NSAIDs were prepared (ibuprofen derivative **4-3** shown in Figure 4-4) and tested for activity.²¹ The NSAIDs modified with the H₂S releasing moiety showed reduced toxicity and gastric damage compared to the non-modified NSAIDs.

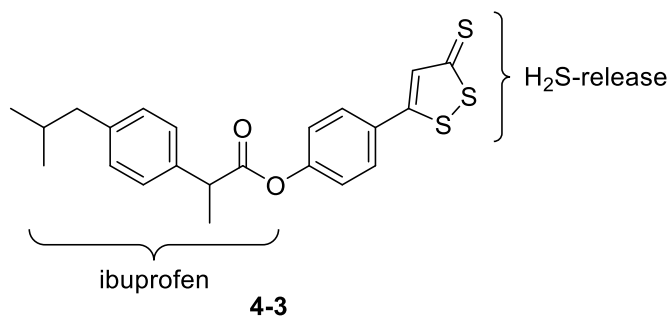
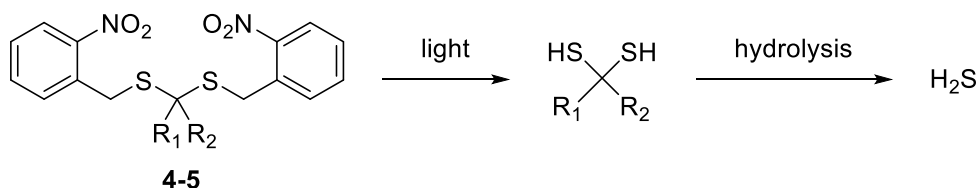


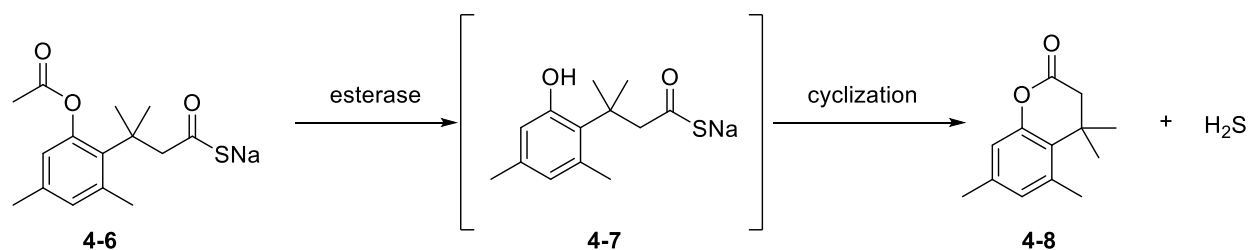
Figure 4-4 – DTT-modified ibuprofen, an example of an H₂S prodrug that exhibits improved pharmacological properties.

Attaining control over H₂S release is an ongoing challenge. One recent attempt at developing controlled release explored the use of photocaged H₂S donors (**4-5**) that decompose to H₂S upon exposure to light; such a compound is shown in Scheme 4-5.²²



Scheme 4-5 – Photocaged *gem*-sulfide (**4-5**) as H₂S-releasing compound.

Unfortunately, these *gem*-sulfide compounds appear to be less-than-ideal for use in living systems for several reasons. First, the rate of decomposition is dependent on the rate of hydrolysis of the *gem*-dithiol in aqueous solution, eroding the goal of tunable control over H₂S-release. Complicating the situation further, the byproduct of photolysis, 2-nitrosobenzaldehyde, is not innocuous and reacts with the *gem*-dithiol, reducing the yield of H₂S. Finally, the wavelength of light required for photolysis was in the UVA region (365nm) which may cause damage to DNA and have difficulties with penetration. A more attractive solution to controlled H₂S release was reported by Zheng et al in 2016.²³ In this report, an enzyme-triggered H₂S-releasing prodrug **4-6** was conceived by strategically placing an ester in proximity to a thiocarboxylate. Upon hydrolysis of the ester by an esterase enzyme to the phenol **4-7**, intramolecular cyclization followed by collapse of the tetrahedral intermediate gives **4-8** and H₂S gas as a leaving group (Scheme 4-6). Because esterase enzymes are plentiful inside mammalian cells,²⁴ this design enables selective release of the gas within the cell. In this way, **4-6**'s enzyme trigger provides a level of spatial control over the gas transmitter's release that is not possible using photo- or hydrolysis-activated H₂S-releasing molecules.



Scheme 4-6 – Mechanism of H₂S release from pronucleophilic ester/thiocarboxylate **4-6** upon hydrolysis by esterase enzyme.

4.4 – Carbon Monoxide as a Gasotransmitter

The toxic properties of carbon monoxide have been known since antiquity. Today, the colorless, odorless gas remains one of most pervasive toxins in the environment, causing an estimated 1,300 deaths in the US alone in 2014.²⁵ Despite its reputation as a silent killer, carbon monoxide is in fact an essential, endogenously-produced signaling molecule in mammals.^{26,27} One of the very first reports of CO acting as a signaling molecule was published in 1993 with the discovery that the gas caused relaxation of the internal anal sphincter of the opossum.²⁸ This discovery of CO-mediated smooth muscle vasodilation was soon followed by a report that CO was detected in brain tissue and determined to be a physiologic regulator of cGMP.²⁹ The biogenesis of endogenous CO is mostly from the metabolism of heme-containing proteins by heme oxygenase (HO-1). The mechanism for its formation is shown in Figure 4-5. Using oxygen and NADPH cofactors, HO-1 catalyzes the 2-electron oxidation of heme to alpha-*meso*-hydroxyheme. The enzyme then catalyzes this species' transformation into verdoheme, producing an equivalent of CO in the process. In a final step, the enzyme performs a 4-electron oxidation and ring opening of verdoheme to biliverdin.³⁰

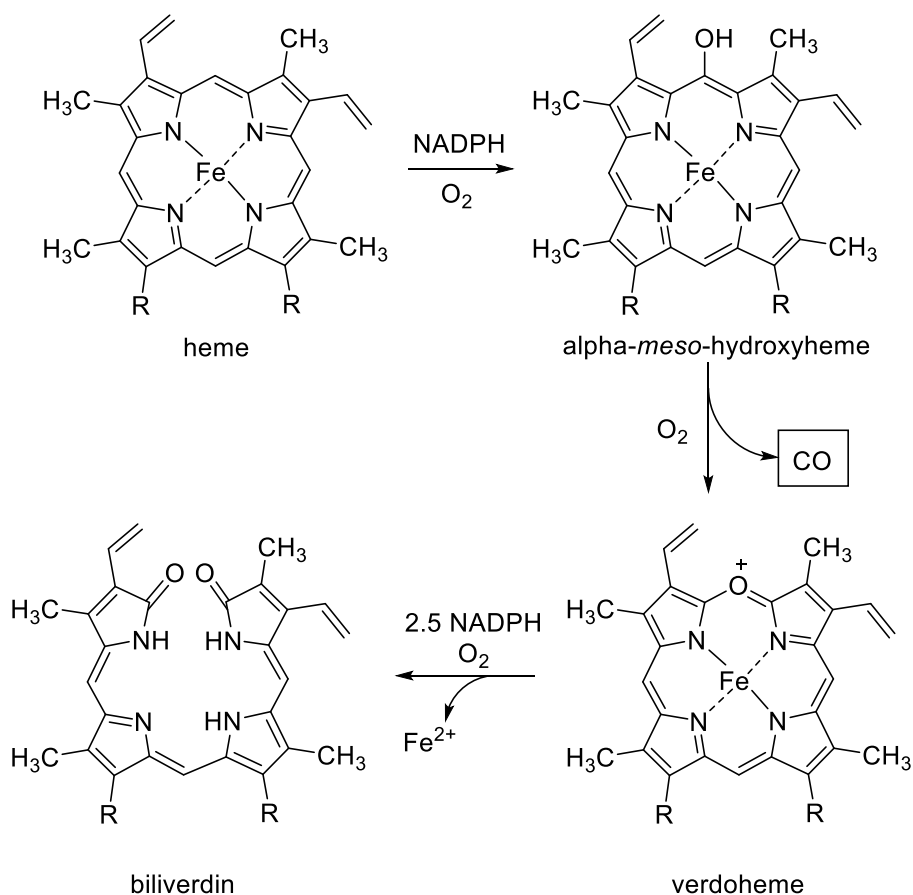
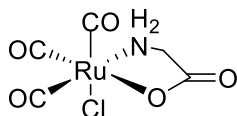


Figure 4-5 – Mechanism of endogenous CO production by oxidation of heme by heme oxygenase (HO-1).

The development of synthetic CO-releasing molecules (CORMs) is particularly exciting in the field of organometallic chemistry, since metal carbonyls provide a unique entry into the therapeutic space of delivering CO.^{31,32} The very first compounds investigated for CO-release under physiological conditions were the commercially available metal carbonyl complexes Mn₂(CO)₁₀, Fe(CO)₅, and Ru₂(CO)₆Cl₄. Studies in rats showed these compounds exhibited vasodilatory properties *ex vivo*, but their abysmal water solubility meant that further work was required before CORMs could be of value *in vivo*. The synthesis of the first water-soluble CORM, CORM-3 (**4-9**), was reported in 2003 by Clark et al. (Figure 4-6).³³



CORM-3 (4-9)

Figure 4-6 – Structure of CORM-3.

The authors determined that CORM-3 was stable in acidic pH, but in physiological buffers it rapidly released CO. The addition of CORM-3 to cardiac cells was shown to significantly increase resistance to damage caused by hypoxia and oxidative stress.³³ Although this finding demonstrated the potential of CORMs for therapeutic applications, the release of CO was very rapid under physiological conditions, highlighting the need for a more controllable compound.

4.5 – Triggered CO-Releasing Molecules

After discovery of first generation of CORMs such as CORM-3, reports soon emerged of synthetic CO-releasing molecules designed to activate in response to a diverse range of triggers (Figure 4-7).

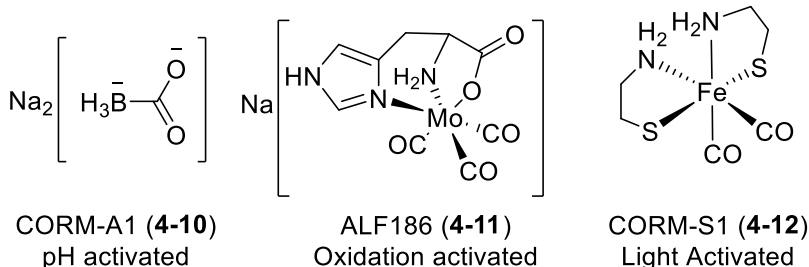


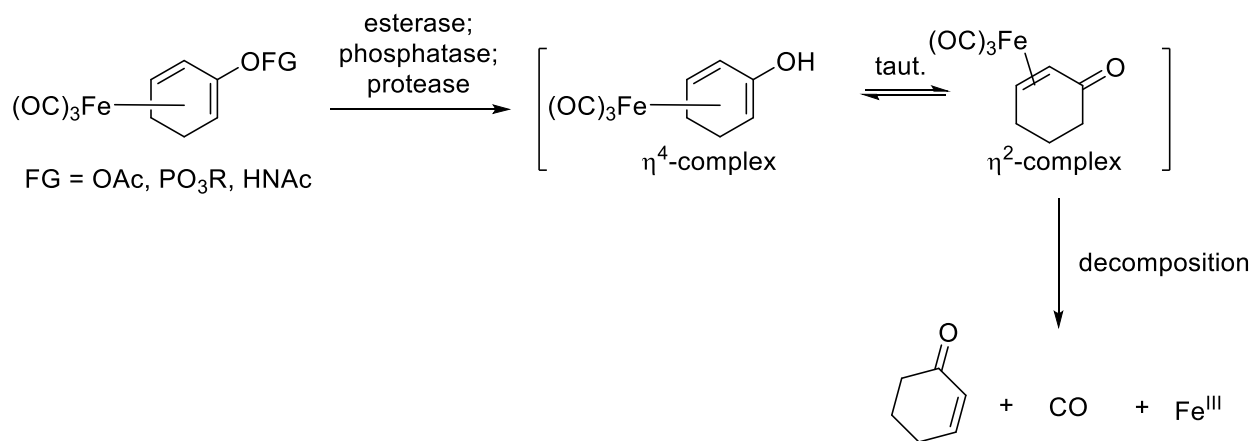
Figure 4-7 – Examples of pH, oxidation, and light triggered CORMs.

In 2004, Motterlini et al. reported the pH-dependent CORM-A1 (4-10), which was found to liberate CO within minutes in acidic media.³⁴ ALF186 (4-11) represents another class of triggered CORM: the molecule is stable under nitrogen atmosphere, but is prone to oxidation by O₂. The authors demonstrated that 4-11 rapidly released CO when exposed to the aerobic environment of the blood, mimicking the effects of inhaled CO.³⁵ Yet another entrant to this

category of compounds is the light-activated CORM-S1 (**4-12**).³⁶ The iron-carbonyl complex **4-12** was found to be susceptible to photolysis by 470 nm LED light, releasing its entire payload of CO within 10 minutes. Although conceptually fascinating, these triggered CORMs are not viable as therapeutic agents for the delivery of CO. One critical shortcoming shared by all the compounds is the rapid release of CO upon activation of their trigger conditions, mimicking more the effects of inhaled toxic CO gas, rather than endogenous CO production. To exhibit a “normal” pharmacokinetic profile, the ideal CORM would penetrate tissues in a targeted manner and deliver CO over a well-defined duration.

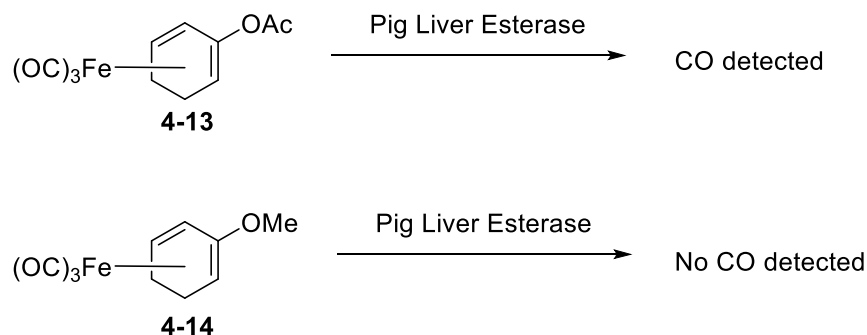
4.6 – Enzyme Triggered CO Releasing Molecules (ET-CORMs)

CO-prodrugs that rely on processing by certain enzymes before releasing CO provide a solution to some of the problems discussed above. The trigger condition of enzymatic degradation is more restrictive, therefore it can provide greater control over the rate and location of CO release than physical triggers like pH, oxidation, and light. As a pioneer in the field, the Schmalz group reported several enzyme-triggered CO-releasing molecules that rely on the action of esterases,³⁷ phosphatases,³⁸ and recently, proteases.³⁹



Scheme 4-7 – Mechanism of CO-release by ET-CORMs.

As shown in Scheme 4-7, Schmalz's ET-CORM designs are based on an iron-carbonyl-diene scaffold. Upon enzymatic cleavage of the ester, phosphate, or amide group, the resulting η^4 -iron complex undergoes a hapticity change to the η^2 -complex after tautomerization. This complex is unstable and decomposes to release CO. To demonstrate the enzyme-dependent quality of CO release, the authors subjected compounds **4-13** and **4-14** to an esterase enzyme (Scheme 4-8). CO release was only detected from compound **4-13**, since **4-14** contains no ester and thus cannot be enzymatically processed.³⁷



Scheme 4-8 – Control experiment demonstrating that CO release is enzyme-dependent.

4.7 – Designing a Gene Expression-Dependent CO-Releasing Molecule

Our group was inspired by the ET-CORMs developed by Schmalz, but we identified a key shortcoming that we hoped to overcome. Phosphatases and esterases are ubiquitous enzymes present in every mammalian cell, which makes hinging intracellular CO release on the activity of these enzymes an inherently nonselective process. We envisioned an enzyme-triggered CO-releasing molecule activated by a genetically-encodable enzyme would allow a greater level of control, since cells could be programmed to either react with the compound or not depending on their genotype. Figure 4-8 depicts a possible example of how such a compound could be used. In the upper scenario, the gene expression-dependent CO-releasing molecule is exposed to wild type cells that naturally produce the enzyme of choice, this results in enzymatic cleavage of the

linked trigger, thereby promoting CO release. In the lower scenario, genetically-modified knockout cells that don't produce the enzyme fail to cleave the linked trigger and thus CO release cannot occur. One could also envision conducting the reverse experiment, where the wild-type cells don't produce the target enzyme while mutant transgenic cells do.

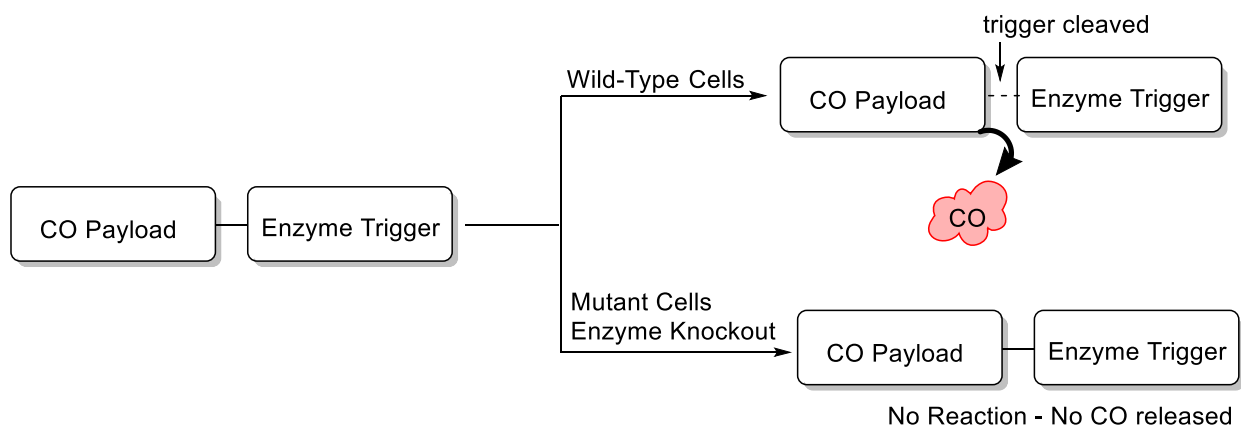


Figure 4-8 – Gene-expression dependent CO-releasing molecule can be used to target specific cells with CO.

We identified β -galactosidase (encoded by the LacZ gene) as an ideal enzyme, since it's one of the most well-studied enzymes for reporter assays and several transgenic strains of mice with varying level of LacZ activity are available.⁴⁰ It's also possible to knockout LacZ in specific cell types or tissues using Cre/Lox mice.⁴¹ Thus, a β -galactosidase-activated CO-releasing molecule would represent an important biochemical tool to study the effects of dosing specific cells with CO. In addition, biochemists use LacZ as a reporter gene to track whether another gene of interest has been successfully incorporated into the genome of an organism. Typically, the transfected cells are then separated from the wild type colonies using an enzyme-activated dye compound X-Gal. However, with a β -galactosidase-activated CO-releasing molecule, one could selectively release CO to cells transfected with a gene of interest without the need for separation, as shown in Figure 4-9. This could enable a study on the effects of CO release in a particular genotype.

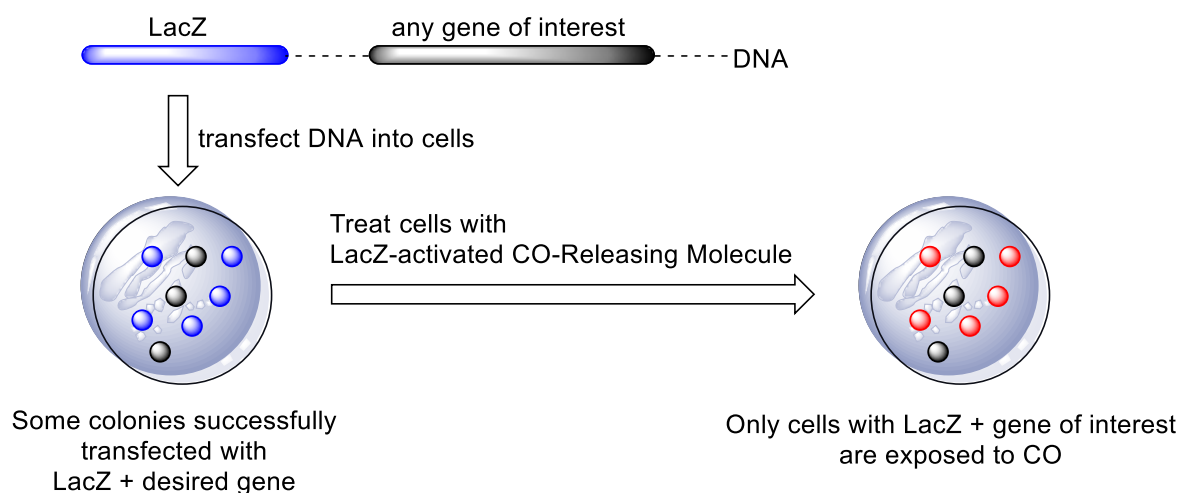
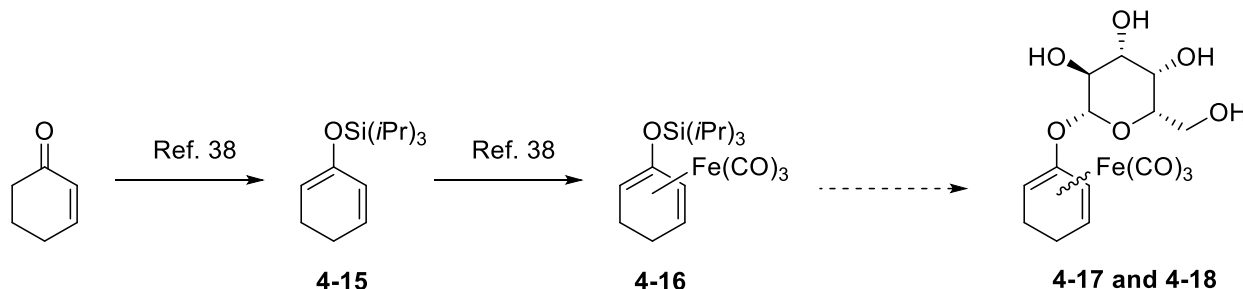


Figure 4-9 – LacZ reporter gene could be used alongside a galactosidase activated CORM to selectively dose transgenic colonies with CO.

Lastly, β -galactosidase has been identified as a biomarker for cell senescence⁴² and ovarian cancer.⁴³ Thus, a β -galactosidase-triggered CO-releasing molecule could have therapeutic applications by enabling preferential dosing of CO to aging or cancerous cells. One potential complication is that any CO-releasing molecule we synthesize will possess structural differences from the enzyme's native substrate. Despite this, we will require the molecule to undergo the enzymatic reaction because this is the basis for our trigger condition. Thankfully, although β -galactosidase is highly specific for galactose, it is promiscuous for the aglycone rest of the molecule, so providing an unnatural substrate for this enzyme is possible and well-precedented.⁴⁴

To realize our goal of obtaining a gene-expression dependent CO-releasing molecule, we planned the synthesis of a galactose-linked iron-carbonyl-diene complex as shown in Scheme 4-9. Our synthesis predicted that we would obtain a mixture of diastereomers **4-17** and **4-18** due to the planar chirality of iron associating with either diastereotopic face of the diene. We recognized the two diastereomers produced could be separated and tested independently, since

the different stereoisomers may have different properties. For example, one of the diastereomers may react faster with the enzyme.



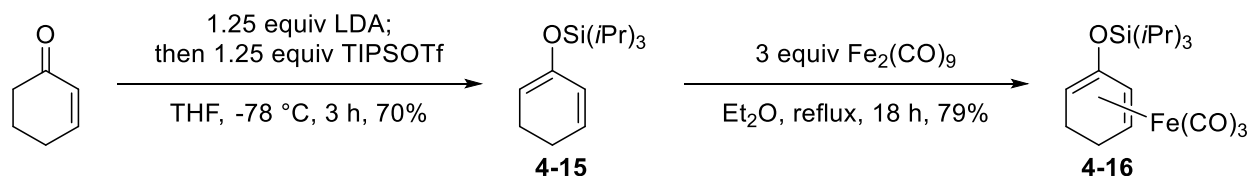
Scheme 4-9 – Planned synthesis of gene expression dependent CO-releasing molecules **4-17** and **4-18**.

Fortunately, the first two steps of our synthesis were already optimized by Schmalz during the synthesis of esterase-triggered CORM **4-13**.³⁸ Thus, our synthetic plan was as follows:

cyclohexenone would be converted to the silyl-enol ether using LDA and silyl triflate, which would be complexed to iron using diiron nonacarbonyl. Next, we would develop conditions to achieve a one-pot deprotection/glycosylation reaction to remove the silyl group and install galactose in a single chemical step.

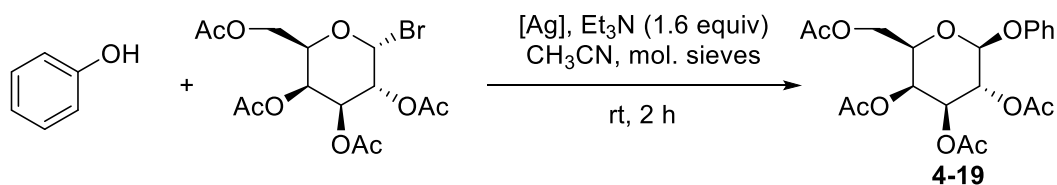
4.8 – Synthesis of Galactose-Linked Iron-Diene Complexes

To begin the synthesis, we prepared the triisopropylsilyl enol ether **4-15** using the protocol developed by Schmalz.³⁸ Complexation by iron to provide **4-16** proved extremely facile and proceeded in 80% yield after refluxing **4-15** with excess $\text{Fe}_2(\text{CO})_9$ overnight in ether (Scheme 4-10).



Scheme 4-10 – Synthesis of **4-16** starting from cyclohexenone.

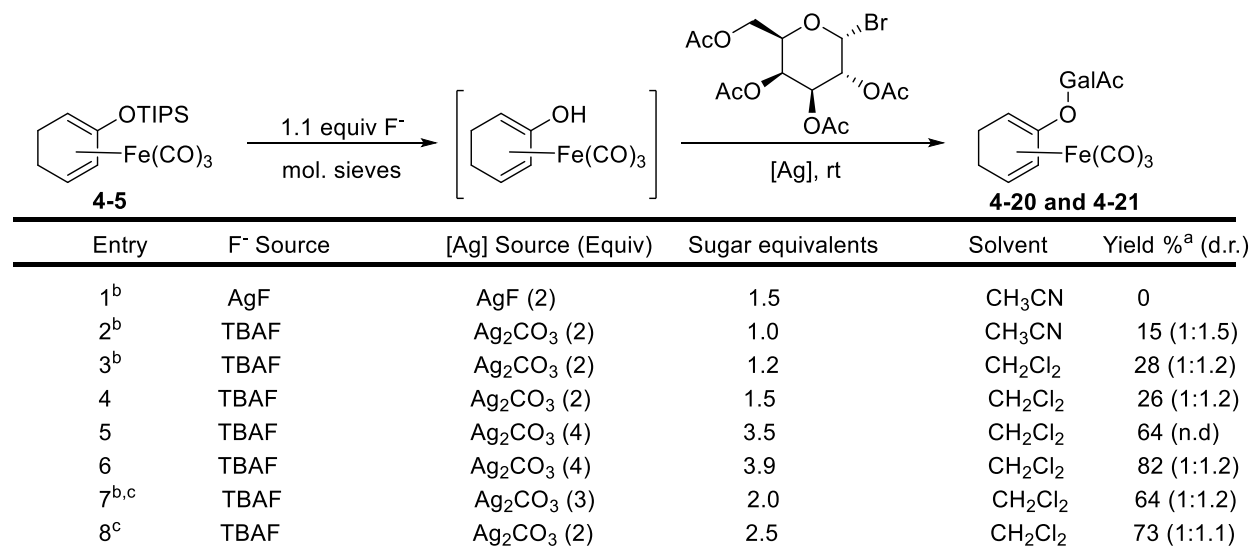
Next, we developed conditions to achieve the one-pot deprotection/glycosylation reaction. To enable selective linkage of our CO-payload to the anomeric carbon, we opted to use commercially-available peracetylated bromo-galactose as our glycosyl donor. Before attempting the real reaction, we first performed a study using phenol as a model glycosyl acceptor to give glycoside **4-17**. We were able to obtain acceptable results after four test reactions, as shown in Table 4-1. Halophilic silver salts activated the sugar towards nucleophilic attack by the alcohol, while molecular sieves were used to remove advantageous water that could compete for the sugar. Our initial attempts also included triethylamine to enhance the nucleophilicity of the alcohol. With respect to the source of silver, silver fluoride proved ineffective, but silver carbonate gave a 22% yield of coupled product. We then altered the stoichiometry of the Ag_2CO_3 and the bromo-galactose and found that we could obtain glycosylated phenol **4-19** in 46% yield. The product was obtained solely as the β anomer, which was determined by analyzing the *J*-coupling of the anomeric proton at 5.05 ppm ($J = 8.0$ Hz). This anomer is expected: during the glycosylation, the adjacent acetyl group undergoes neighboring group participation, forming a cyclic acetoxonium ion that encourages preferential formation of the β -glycoside.⁴⁵



Entry	[Ag] Source	[Ag] equivalents	Sugar equivalents	Yield %
1	AgF	1.6	1.6	n.r
2	Ag_2CO_3	3.6	1.6	22
3	Ag_2CO_3	7.2	1.6	46
4	Ag_2CO_3	7.2	3.2	44

Table 4-1 – Glycosylation of phenol as a test reaction.

With these results in hand, we then turned to the actual substrate using the silyl enol ether. This reaction was considerably more complex, because now we had to consider the efficiency of the deprotection reaction as well as the stability of the intermediate η^4 -dienol iron tricarbonyl complex (See Scheme 4-7). Despite its ineffectiveness in the test reaction, we again attempted to use silver fluoride as the halophile with the idea that the fluoride counterion would also promote desilylation, in effect killing two birds with one stone. Unfortunately, this idea never worked, and we reverted to silver carbonate as the halophile and TBAF as the desilylation reagent.



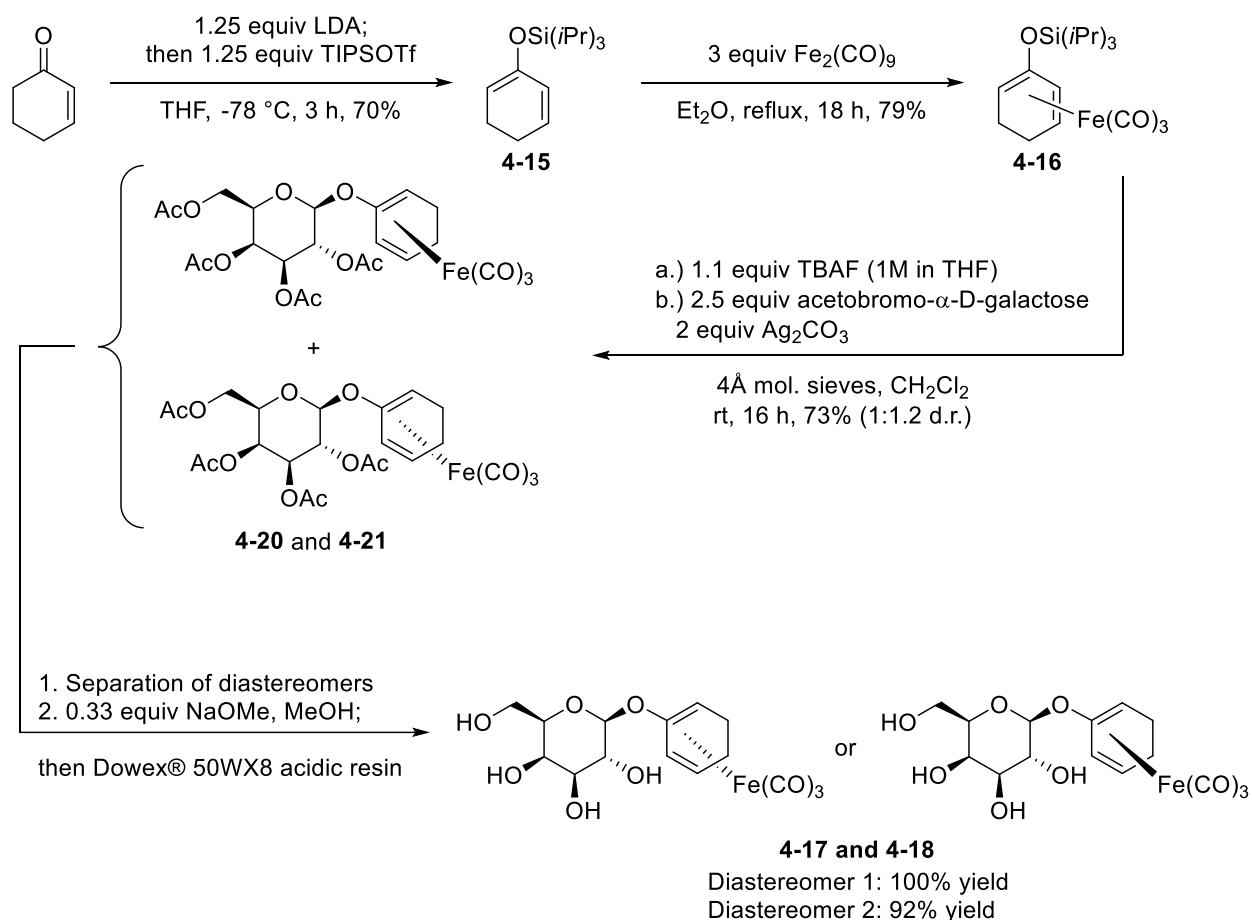
^aIsolated yields. ^b1.2 equiv Et₃N added. ^cMolecular sieves premixed for 2 h with TBAF.

Table 4-2 – Optimization of deprotection/glycosylation sequence.

As shown in Table 4-2, changing the solvent from acetonitrile to dichloromethane was associated with an increase in yield from 15% to 28% (entries 2 vs. 3). We also determined that excess sugar was beneficial to the reaction and triethylamine was not required. Finally, as a precaution we began premixing the molecular sieves with the TBAF for several hours to ensure complete removal of water from the reaction. We allowed **4-5** to react with TBAF for just five

minutes before adding the sugar, fearing a longer deprotection reaction time would lead to decomposition of the unstable dienol. We were able to obtain yields up to 82% when a large excess of silver and bromo-galactose were used. However, we found that it was more economical to use less of these expensive reagents and settle for an acceptable 73% yield. As we predicted, due to the planar chirality imparted by the iron-diene complex, the reaction produced a mixture of diastereomers that could be separated. As observed with our model glycosyl donor phenol, we obtained only the β anomers, confirmed by the J couplings of the anomeric protons in the ^1H NMRs of the products. While we were able to separate the diastereomers **4-20** and **4-21**, we were not able to assign their absolute configuration. In the future, we plan to use X-ray crystallography to elucidate their exact structures. For the purposes of this chapter, I will label them based on their elution time on silica gel chromatography, with the first eluting compound referred to “diastereomer 1” and the later eluting stereoisomer as “diastereomer 2.”

With acetylated compounds **4-20** and **4-21** in hand, we turned to the deprotection protocol. Global deprotection of peracylated sugars is a well-known process and is typically performed using catalytic NaOMe.⁴⁶ Although the original 1924 report of the so-called “Zemplèn deprotection” uses acetic acid to quench the reaction, we opted for a modern twist employing acidic Dowex® resin beads. The resin could be easily filtered out of the reaction, simplifying the workup. The deprotection reaction worked extremely well, providing excellent yields of the deprotected compounds **4-17** and **4-18**. The complete synthesis is shown in Scheme 4-11 and represents an overall combined yield of 39% of **4-17** and **4-18** from cyclohexenone.

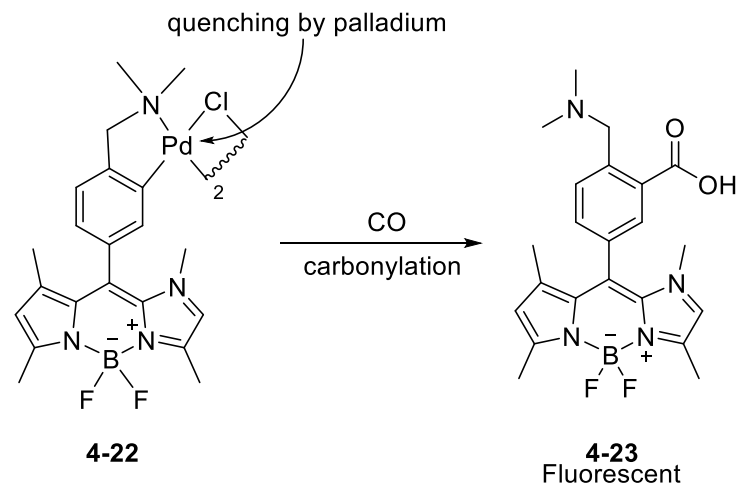


Scheme 4-11 – Full synthesis of gene expression-dependent CO-releasing molecules.

4.9 – Progress towards Detection of CO Release

With our synthesis fully completed, we next sought to enzymatically promote deglycosylation. To accomplish this, we opted to use commercially available β -galactosidase from *E. coli*. We believed this enzyme would be able to cleave the glycosidic linkage in **4-17** and **4-18** to give an unstable dienol iron tricarbonyl complex. At the same time, we also explored methods to detect and quantify CO release from the products of this enzymatic reaction. Work in detecting CO-release from these compounds is still ongoing, and a summary of our efforts are described below. There exist four major methods used to detect carbon monoxide: (1) myoglobin assay,⁴⁷ (2) iNOS inhibition assay,^{37,48} (3) gas chromatography,³⁸ and (4) organometallic

fluorescence probe.⁴⁹ The myoglobin assay is a simple spectroscopic method for detecting CO. In this method, a spectrophotometer is used to observe a change in the UV-VIS absorbance of myoglobin upon binding CO. While operationally simple, the myoglobin assay is generally used for qualitative rather than quantitative detection of CO. This is because turbidity and protein impurities in the myoglobin can cause significant errors in the data.⁵⁰ The iNOS inhibition assay is quantitative, but considerably more complex. This experiment takes advantage of CO's inhibitory activity on the nitric oxide synthase enzyme. In a CO-rich environment, the purified iNOS enzyme used in the assay will be inhibited, and thus produce less NO. The NO produced is quantified by its reaction with a fluorescent probe, providing a quantitative measure of inhibition. Headspace gas chromatography analysis is a useful method for detecting CO release, although a laborious calibration procedure is required for accurate results.³⁸ Unlike the myoglobin or iNOS assays, the detection of CO by GC can provide real time information about the rate of CO release from CORMs directly without relying on the interaction between CO and an enzyme. Finally, a recently reported method of detecting CO uses a palladium-BODIPY complex dimer **4-22** as a fluorogenic probe.⁴⁹ The complex reacts with CO and then performs a Pd-mediated carbonylation reaction to produce a fluorescent compound **4-23** (Scheme 4-12).



Scheme 4-12 – Chang and Coworker’s Pd-Based Probe for CO.

Among these detection methods, the myoglobin assay is the simplest and fastest. With help from Ralph Cacho and his advisor Professor Yi Tang, we prepared solutions of β -galactosidase, equine heart myoglobin, and purified diastereomer 1 from the **4-17/4-18** mixture. As shown in Figure 4-10, we were able to obtain some encouraging preliminary results. The background spectra of deoxymyoglobin shows a single peak with a maximum at about 560 nm (blue line). After adding a solution of β -galactosidase and **4-17/4-18** we observed a dramatic change in the spectrum (yellow line). Then, after the sealed cuvette was incubated for 16 h at 37 °C, the double peak pattern suggestive of CO-myoglobin was detected (orange line).

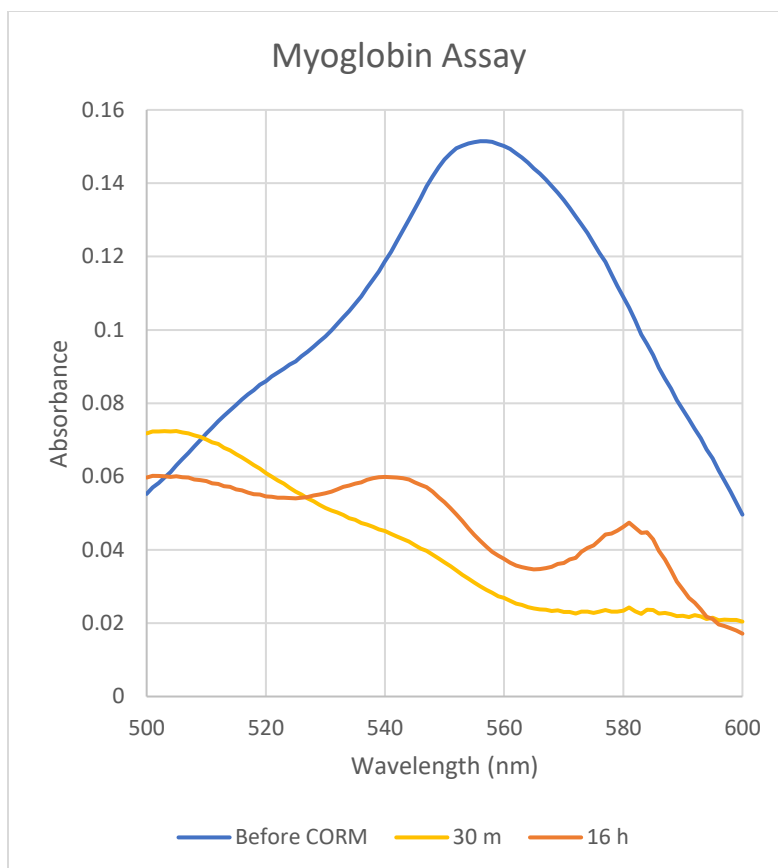


Figure 4-10 – UV-VIS spectra of myoglobin before and after addition of β -galactosidase and diastereomer 1 of **4-17/4-18**.

Although these results are promising, more work is necessary to determine the CO-releasing qualities of our newly developed CORMs. A key issue with the myoglobin assay results obtained is the dramatic decrease in net absorbance after addition of the β -galactosidase and **4-17/4-18** solution. Similar myoglobin assays in the literature maintain roughly the same absorbance after the addition of CORM, suggesting our myoglobin CO-detection experiment may be flawed or incompatibilities between the two proteins (myoglobin and β -galactosidase) may exist. For example, some of the reagents used to reconstitute the β -galactosidase enzyme, such as $MgCl_2$ and thioethanol may react with the myoglobin.

Moving forward, we believe GC headspace analysis will be far more amendable to detecting CO release from our compounds. The experiment will be performed as follows: β -

galactosidase will be combined with **4-17** or **4-18** in a sealed vial. Periodic measurements of the headspace fed into a GC will allow for not only qualitative detection of CO release, but also quantitative information about the rate of CO release. Most importantly, the experiment will not require additional proteins other than β -galactosidase, thus the CO detection will not be perturbed by the factors that we believe caused problems in the myoglobin assay. Group member Andrew Teuthorn is synthesizing more **4-17** and **4-18**, along with other structural analogs to perform this experiment.

4.10 – Conclusion

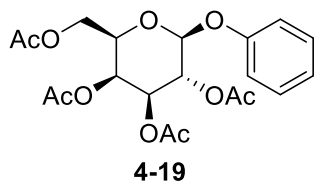
In summary, we have contributed to the exciting field of gasotransmitter research by synthesizing a galactose-tethered iron-diene complex designed to release CO in the presence of β -galactosidase. Key to the success of our synthesis of CORMs **4-17** and **4-18** was the development of conditions that allowed a one-pot deprotection/glycosylation reaction to occur in good yield. Because β -galactosidase is a genetically-programmable enzyme, compounds **4-17** and **4-18** represent a new class of CO-releasing molecule. If enzymatic release of CO is proven successful from **4-17** and **4-18**, our designed gene-expression dependent CORMs will be useful biochemical tools to study the effects of CO in vivo. Furthermore, because β -galactosidase activity has been shown to be a biomarker for various diseases, including ovarian cancer, it's possible **4-17** and **4-18** could even have therapeutic applications. Future work is ongoing to (1) quantitatively measure CO release from the β -galactosidase-triggered CORMs using GC and (2) synthesize structural analogs of **4-17** and **4-18** to assess the effects of structural changes on the rate of CO-release.

4.11 – Experimental Methods

General Methods

Unless otherwise specified, all reactions were performed under a nitrogen atmosphere using dry solvents and anhydrous conditions. DCM, DMSO, and triethylamine were distilled from CaH₂. Et₂O and THF were distilled from sodium/benzophenone. Methanol was distilled from magnesium turnings. β -galactosidase from *E. coli* and myoglobin from equine heart was purchased from Sigma-Aldrich. All other reagents were used as received from commercial sources, unless otherwise specified. NMR data obtained with Bruker ARX-400 or AV-500 instrument and calibrated to the solvent signal (CDCl₃ δ : = 7.26 ppm for ¹H NMR, δ : = 77.0 ppm for ¹³C NMR). Multiplicities are reported by s (singlet), d (doublet), t (triplet), q (quartet), and m (multiplet). Reactions were monitored using thin layer chromatography performed on UV254 silica gel TLC plates and visualized with UV light, ceric ammonium molybdate (CAM) stain, or potassium permanganate (KMnO₄) stain. Flash column chromatography was performed using silica gel (40-63 microns) and compressed air. IR spectra were recorded with an ATR attachment and selected peaks are reported in cm⁻¹. High resolution mass spectral data was recorded with Thermo Fisher Scientific Exactive Plus with IonSense ID-CUBE Direct Analysis in Real Time (DART) ion source experiments and ESI LC-TOF Micromass LCT. UV-VIS spectra were obtained using an Agilent/HP 8453 spectrophotometer.

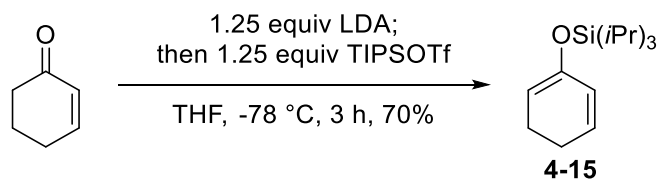
Phenyl 2,3,4,6-tetra-O-acetyl- β -D-galactopyranoside (4-19)



A flame-dried round bottom flask was charged with 94 mg (1 mmol) of phenol, 8.3 mL of CH₃CN, 124 mg 4 Å molecular sieves, 0.233 mL (1.6 mmol) of triethylamine, and 882 mg (3.2 mmol) of Ag₂CO₃. The mixture was protected from light and stirred for 30 min. Then, 616 mg (1.5 mmol) of acetobromo- α -D-galactose was added at once. The reaction was stirred overnight, then filtered through a silica gel plug (EtOAc) and concentrated to a brown oil. The crude product was then purified by flash column chromatography (4:1 hexane:EtOAc to 2:1 hexane:EtOAc) to give 196 mg (46%) of **4-19** as a white solid. Spectral data matches literature values.⁵¹

¹H NMR (400 MHz, CDCl₃, ppm) δ : 7.33-7.27 (m, 2H), 7.10-7.05 (m, 1H), 7.02-6.98 (m, 2H), 5.49 (dd, $J = 10.5, 8.0$ Hz, 1H), 5.45 (dd, $J = 3.4, 0.9$ Hz, 1H), 5.11 (dd, $J = 10.5, 3.4$ Hz, 1H), 5.05 (d, $J = 8.0$ Hz, 1H), 4.26-4.13 (m, 2H), 4.08-4.04 (m, 1H), 2.19 (s, 3H), 2.07 (s, 3H), 2.06 (s, 3H), 2.01 (s, 3H).

(cyclohexa-1,5-dien-1-yloxy)triisopropylsilane (4-15)

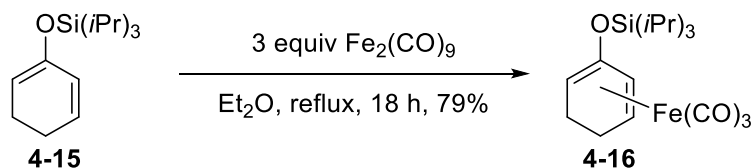


A flame-dried, nitrogen-purged, 3-necked round bottom flask was charged with 30 mL of THF and *N,N*-diisopropylamine (3.2 mL, 22.9 mmol). The solution was chilled to -78 °C, then *n*BuLi (1.6 M in hexane, 12.5 mL, 20.1 mmol) was added dropwise with stirring via an addition funnel. After 20 min of stirring, a cyclohexenone (1.45 g, 15.7 mmol) solution in 10 mL of THF was added over 1.5 h. The temperature was maintained at -78 °C and stirred for an additional 30 min after the ketone solution was added. TIPSOTf (4.6 mL, 18.8 mmol) in 20 mL of THF was added over 30 min, then stirred an additional 30 min. The reaction mixture was warmed to room

temperature, after which NH_4Cl was added. After 10 m of stirring, the products were extracted with Et_2O and washed 3x with H_2O and 1x with brine. The organic phase was dried with MgSO_4 and concentrated to yield 4.220g of a yellow oil. The crude product was chromatographed on silica gel (40:1 petroleum ether:EtOAc with 1% triethylamine) to give 2.7662 g (70%) of (cyclohexa-1,5-dien-1-yloxy)triisopropylsilane as a colorless oil. Spectral data matches literature values.³⁸

^1H NMR (400 MHz, CDCl_3 , ppm) δ : 5.87 (dtd, $J = 10.0, 4.2, 0.7$ Hz, 1H), 5.77 (dq, $J = 9.6, 1.9$ Hz, 1H), 4.90 (tdd, $J = 4.2, 2.0, 0.7$ Hz, 1H), 2.19-2.04 (m, 4H), 1.09 (d, $J = 1$ Hz, 18H), 1.05-1.03 (m, 3H).

(RS)-[η^4 -(cyclohexa-1,5-dien-1-yloxy)triisopropyl-tricarbonyliron(0)] silane

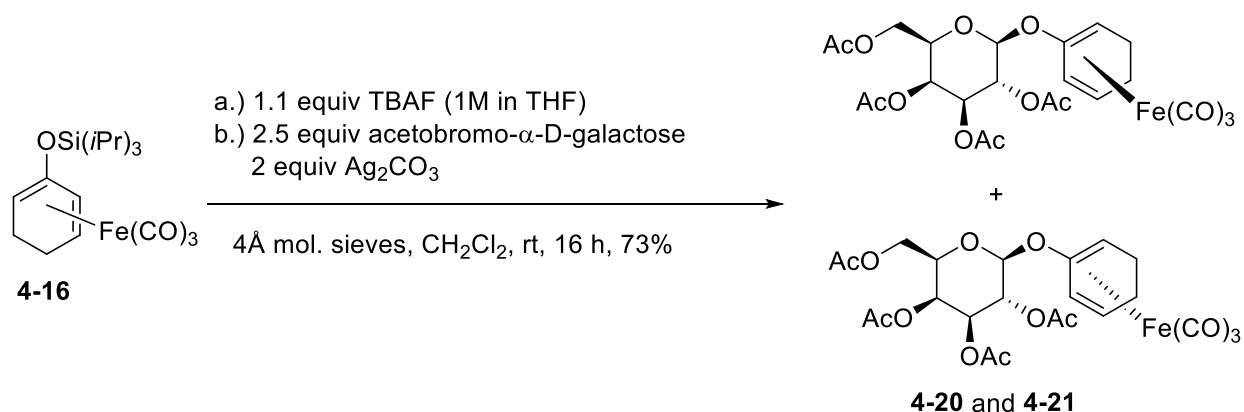


In a round bottom flask, (cyclohexa-1,5-dien-1-yloxy)triisopropylsilane **4-15** (1.4861g, 5.88 mmol) was dissolved in 52 mL of Et_2O and degassed with N_2 bubbling. In a flame-dried Schlenk tube equipped with a stirbar, $\text{Fe}_2(\text{CO})_9$ (6.423g, 17.66 mmol) was added and the flask purged 3x with N_2 . The ethereal solution of the silyl enol ether was added to the iron complex, and the orange solution was refluxed under N_2 overnight, during which time the reaction darkens considerably. The next day, Et_2O was removed by vacuum, and the crude reaction mixture purified by column chromatography on silica gel (hexane) to give 1.071g (79%) of **4-16** as a yellow oil. Spectral data matches literature values.³⁸

^1H NMR (400 MHz, CDCl_3 , ppm) δ : 5.28 (dd, $J = 6.5, 1.2$ Hz, 1H), 3.43-3.37 (m, 1H), 2.73-2.67 (m, 1H), 1.82-1.64 (m, 2H), 1.58-1.45 (m, 2H), 1.29-1.18 (m, 3H), 1.12 (d, $J = 7.2$ Hz, 9H), 1.11 (d, $J = 7.2$ Hz, 9H);

^{13}C NMR (100 MHz, CDCl_3 , ppm) δ : 211.6, 136.5, 58.6, 50.5, 25.4, 23.1, 17.8, 17.7, 12.4;

(R)-[η^4 -cyclohexa-1,5-dienyl-tricarbonyliron (0)]-2,3,4,6-tetraacetyl- β -galactoside and (S)-[η^4 -cyclohexa-1,5-dienyl-tricarbonyliron (0)]-2,3,4,6-tetraacetyl- β -galactoside



In a 50 mL round bottom flask equipped with a stirbar was combined: powderized 4Å molecular sieves (400mg), TBAF (1M in THF, 0.84 mL, 0.84 mmol), and CH_2Cl_2 (10 mL). This mixture was stirred for 5 h at room temperature, then **4-16** (300 mg, 0.76 mmol) was added as a solution in 5 mL of CH_2Cl_2 . After 5 min of stirring and covering the flask with foil to protect from light, Ag_2CO_3 (314 mg, 1.14 mmol) was added. The mixture was stirred for another 5 m, then acetobromo- α -D-galactose (781 mg, 1.9 mmol) was added at once. The reaction was stirred overnight in the dark, then passed through a silica plug (EtOAc) rinse. The crude product was purified by chromatography on silica gel (2.5:1 hexanes/EtOAc) to give a separable mixture of diastereomers **4-20** and **4-21** as a white solid. First eluting, “Diastereomer 1:” 161 mg (37%)

Second eluting, "Diastereomer 2:" 153 mg (36%). The absolute configuration of each diastereomer was not determined.

First eluting, Diastereomer 1

^1H NMR (400 MHz, CDCl_3 , ppm) δ : 5.49 (dd, $J = 3.4, 0.8$ Hz, 1H), 5.41 (dd, $J = 10.5, 8.0$ Hz, 1H), 5.29 (dd, $J = 6.8, 1.5$ Hz, 1H), 5.14 (dd, $J = 10.5, 3.4$ Hz, 1H), 4.84 (d, $J = 8.0$ Hz, 1H), 4.34-4.20 (m, 2H), 4.15-4.08 (m, 1H), 3.50-3.46 (m, 1H), 2.79-2.94 (m, 1H), 2.21 (s, 3H), 2.13 (s, 3H), 2.03 (s, 3H), 2.01 (s, 3H), 1.74-1.71 (m, 2H), 1.64-1.49 (m, 2H);

^{13}C NMR (125 MHz, CDCl_3 , ppm) δ : 210.9, 170.3, 170.2, 170.0, 169.6, 135.8, 98.1, 72.2, 71.4, 70.7, 67.8, 66.8, 61.5, 56.4, 50.1, 24.6, 23.3, 20.7, 20.6, 20.5;

IR (neat, ATR): 2040, 1955, 1747, 1467, 1447, 1367, 1214, 1199, 1164, 1127, 1069, 1041, 1016 cm^{-1} .

HRMS (ESI) m/z : calculated for $\text{C}_{23}\text{H}_{26}\text{FeO}_{13}\text{Na}$ $[\text{M}+\text{Na}]^+$: 587.0667, found 587.0690.

Second eluting, Diastereomer 2

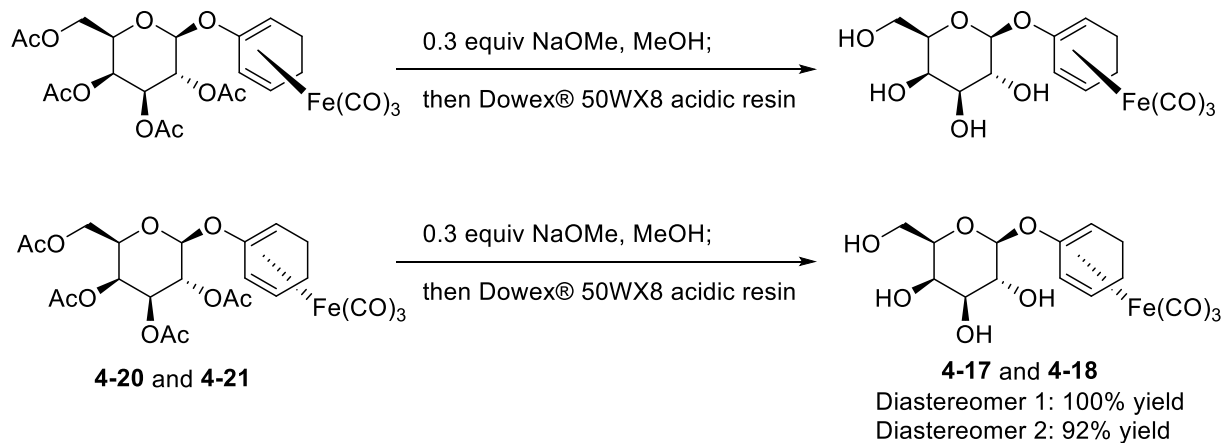
^1H NMR (400 MHz, CDCl_3 , ppm) δ : 5.41 (dd, $J = 3.4, 0.9$ Hz, 1H), 5.35-5.33 (m, 1H), 5.32-5.29 (m, 1H), 5.05 (dd, $J = 10.4, 3.4$ Hz, 1H), 4.95 (d, $J = 7.8$ Hz, 1H), 4.19-4.11 (m, 2H), 3.99-3.95 (m, 1H), 3.45-3.43 (m, 1H), 2.82-2.79 (m, 1H), 2.16 (s, 3H), 2.04 (s, 3H), 2.03 (s, 3H), 1.99 (s, 3H), 1.78-1.63 (m, 2H), 1.57-1.39 (m, 2H);

^{13}C NMR (125 MHz, CDCl_3 , ppm) δ : 210.7, 170.2, 170.0, 169.9, 169.2, 135.1, 98.5, 74.5, 71.3, 70.7, 68.1, 66.8, 61.3, 54.6, 51.2, 24.7, 23.3, 20.5, 20.5, 20.4;

IR (neat, ATR): 2945, 2857, 2040, 1955, 1746, 1464, 1447, 1433, 1368, 1213, 1164, 1123, 1072, 1058, 1042, 952, 914 cm^{-1} .

HRMS (DART-TOF) m/z : calculated for $C_{23}H_{26}FeO_{13}$ $[M]^+$: 564.0764, found 564.0739.

(R)-[η^4 -cyclohexa-1,5-dienyl-tricarbonyliron (0)]- β -galactoside and (S)-[η^4 -cyclohexa-1,5-dienyl-tricarbonyliron (0)]- β -galactoside



Diastereomer 1 Hydrolysis

To a solution of Diastereomer 1 of **4-20/4-21** (118.9 mg, 0.2 mmol) in 1 mL of MeOH was added 0.3 mL (0.066 mmol) of a 0.22 M solution of NaOMe in MeOH (prepared fresh by the addition of 100 mg of sodium to 20 mL of MeOH). The reaction was stirred for 1 h, then Dowex® 50WX8 acidic resin was added until pH was neutral. The reaction was filtered through a coarse glass fritted funnel and washed with MeOH. After evaporation, 86 mg (100%) of Diastereomer 1 of **4-17/4-18** was isolated as a white solid.

1H NMR (400 MHz, DMSO, ppm) δ : 5.54 (dd, $J = 6.7, 1.8$ Hz, 1H), 5.13-4.54 (m, 4H), 4.45 (d, $J = 7.2$ Hz, 1H), 3.65-3.62 (m, 1H), 3.57-3.49 (m, 4H), 3.39-3.32 (m, 2H), 2.81-2.75 (m, 1H), 1.65-1.58 (m, 2H), 1.50-1.36 (m, 2H);

^{13}C NMR (125 MHz, DMSO, ppm) δ : 212.0, 137.9, 101.2, 79.6, 76.3, 73.5, 72.8, 70.2, 68.4, 60.9, 55.7, 24.8, 23.7;

IR (neat, ATR): 3365, 3010, 2931, 2901, 2856, 2041, 1951, 1464, 1392, 1200, 1061, 1034 cm^{-1} .

HRMS (DART-TOF) m/z : calculated for $\text{C}_{15}\text{H}_{18}\text{FeO}_9\text{K}$ $[\text{M}+\text{K}]^-$: 434.9979, found 434.9959.

Diastereomer 2 hydrolysis

To a solution of Diastereomer 2 of **4-20/4-21** (119.2 mg, 0.2 mmol) in 1 mL of MeOH was added 0.3 mL (0.066 mmol) of a 0.22 M solution of NaOMe in MeOH (prepared fresh by the addition of 100 mg of sodium to 20 mL of MeOH). The reaction was stirred for 1 h, then Dowex® 50WX8 acidic resin was added until pH was neutral. The reaction was filtered through a coarse glass fritted funnel and washed with MeOH. After evaporation, 77 mg (92%) of Diastereomer 2 of **4-17/4-18** was isolated as a white solid.

^1H NMR (400 MHz, DMSO, ppm) δ : 5.50 (dd, $J = 6.5, 1.7$ Hz, 1H), 5.13 (d, $J = 4.8$ Hz, 1H), 4.81-4.77 (m, 2H), 4.48 (t, $J = 5.1$ Hz, 1H), 4.41 (d, $J = 4.3$ Hz, 1H), 3.67-3.64 (m, 1H), 3.55-3.32 (m, 6H), 2.86-2.84 (m, 1H), 1.66-1.59 (m, 2H), 1.48-1.32 (m, 2H);

^{13}C NMR (125 MHz, DMSO, ppm) δ : 212.2, 137.0, 100.7, 79.7, 75.7, 73.7, 72.4, 70.4, 67.9, 59.9, 54.9, 25.1, 23.5;

IR (neat, ATR): 3356, 2931, 2899, 2854, 2037, 1945, 1465, 1446, 1390, 1321, 1200, 1321, 912 cm^{-1} .

HRMS (DART-TOF) m/z : calculated for $\text{C}_{15}\text{H}_{18}\text{FeO}_9\text{K}$ $[\text{M}+\text{K}]^-$: 434.9979, found 434.9960.

Myoglobin Assay

A 0.5 $\mu\text{mol/mL}$ solution of β -galactosidase was prepared in 0.1 M phosphate buffer (pH = 7.3). Next, to 2.6 mL of 0.1 M phosphate buffer (pH = 7.3) was added 0.1 mL of a 3.36 M solution of 2-thioethanol and 0.1 mL of a 0.1 M solution of $\text{MgCl}_2 \cdot 6\text{H}_2\text{O}$. After shaking, 0.1 mL of the β -galactosidase solution was added, then the mixture was incubated at 37 °C for 3 minutes.

1 mL of a 20 μM solution of equine heart myoglobin was prepared in 0.1 M phosphate buffer (pH = 6.8) and degassed with nitrogen for 10 minutes. Then 0.2 mL of 0.1% aqueous sodium dithionite solution was added, and the mixture was degassed again for 10 minutes. The deoxymyoglobin solution was transferred to a quartz cuvette and its UV-VIS spectrum recorded.

To the β -galactosidase solution was added 0.1 mL of a 0.068 M solution of Diastereomer 1 of **4-17** and **4-18** in 0.1 M phosphate buffer (pH = 7.3). 0.1 mL of the CORM/galactosidase solution was added to the myoglobin solution and the sealed quartz cuvette was incubated at 37 °C for 30 min, then its UV-VIS spectrum was recorded. The quartz cuvette was then incubated at 37 °C for 16 h and its UV-VIS spectrum recorded again.

4.12 –References

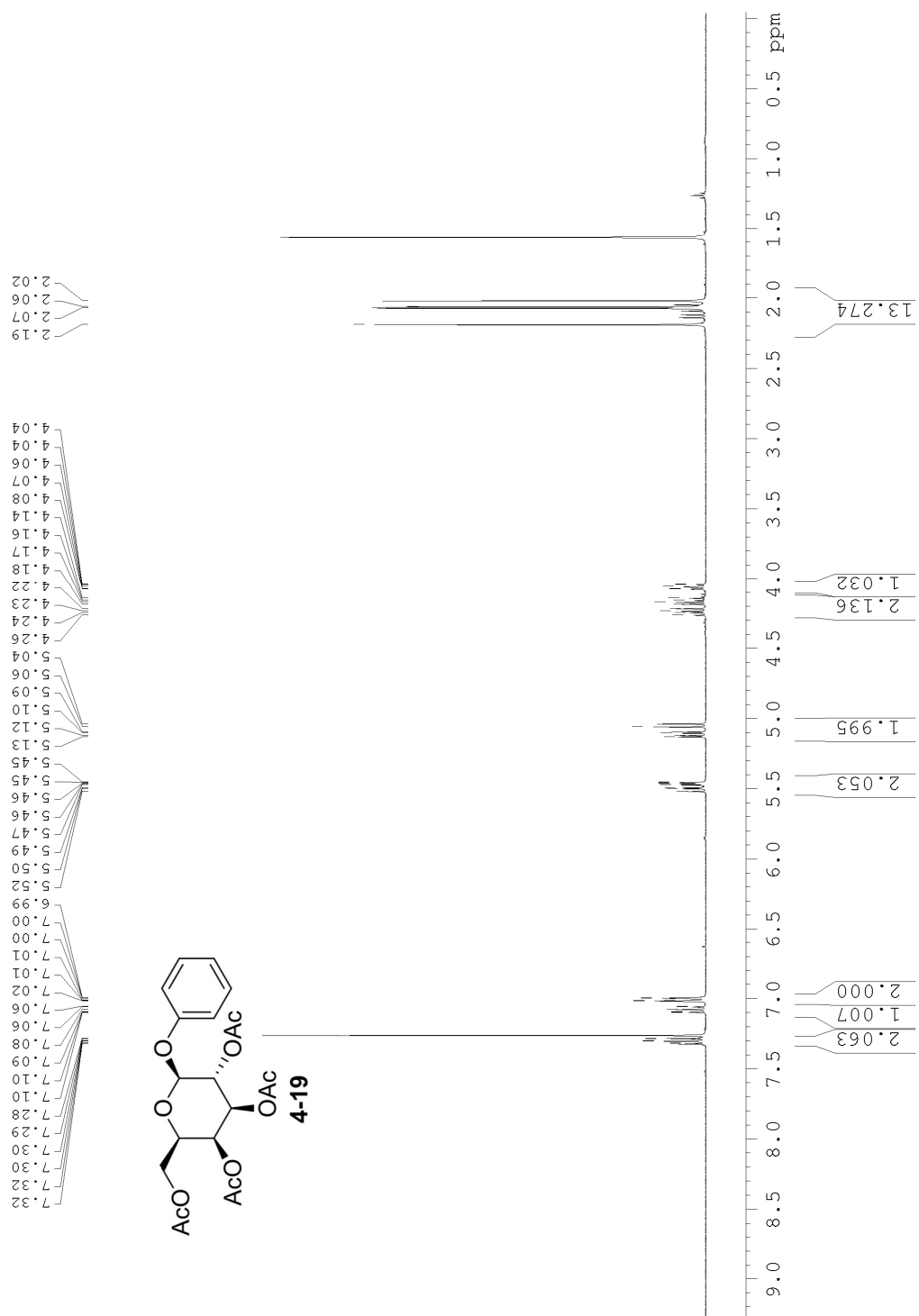
- (1) Mustafa, A. K.; Gadalla, M. M.; Snyder, S. H. *Sci. Signal.* **2009**, 2, re2.
- (2) Ignarro, L. J. *Hypertension* **1990**, 16, 477.
- (3) Lamattina, L.; García-Mata, C.; Graziano, M.; Pagnussat, G. *Annu. Rev. Plant Biol.* **2003**, 54, 109.
- (4) Korde Choudhari, S.; Chaudhary, M.; Bagde, S.; Gadbail, A. R.; Joshi, V. *World Journal of Surgical Oncology*. BioMed Central May 30, 2013, p 118.
- (5) Bryan, N. S. *Free Radic. Biol. Med.* **2006**, 41, 691.
- (6) McCleverty, J. A. Chemistry of Nitric Oxide Relevant to Biology. *Chemical Reviews*, 2004, 104, 403–418.
- (7) Boucher, J. L.; Moali, C.; Tenu, J. P. *Cell. Mol. Life Sci. C.* **1999**, 55, 1015.
- (8) Nakagawa, H.; Hishikawa, K.; Eto, K.; Ieda, N.; Namikawa, T.; Kamada, K.; Suzuki, T.; Miyata, N.; Nabekura, J. *ACS Chem. Biol.* **2013**, 8, 2493.
- (9) Nakagawa, H. *J. Clin. Biochem. Nutr.* **2016**, 58, 2.
- (10) Li, L.; Rose, P.; Moore, P. K. *Annu. Rev. Pharmacol. Toxicol.* **2011**, 51, 169.
- (11) Vandiver, M. S.; Snyder, S. H. *J. Mol. Med.* **2012**, 90, 255.
- (12) Predmore, B. L.; Lefer, D. J.; Gojon, G. *Antioxid. Redox Signal.* **2012**, 17, 119.
- (13) Eto, K.; Asada, T.; Arima, K.; Makifuchi, T.; Kimura, H. *Biochem. Biophys. Res. Commun.* **2002**, 293, 1485.

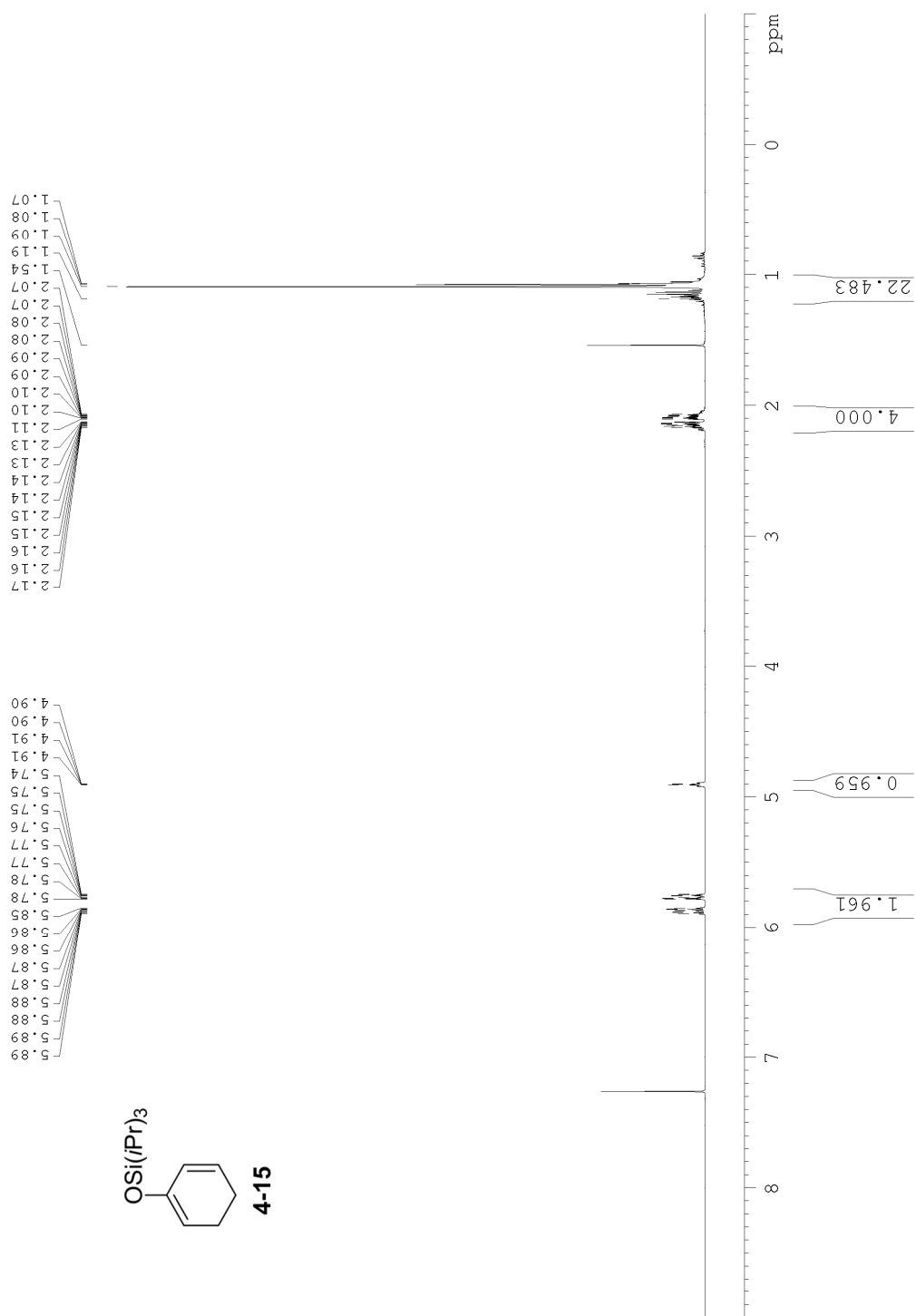
- (14) Amagase, H. *J. Nutr.* **2006**, *136*, 716S.
- (15) Varshney, R.; Budoff, M. J. *J. Nutr.* **2016**, *146*, 416S.
- (16) Benavides, G. A.; Squadrito, G. L.; Mills, R. W.; Patel, H. D.; Isbell, T. S.; Patel, R. P.; Darley-USmar, V. M.; Doeller, J. E.; Kraus, D. W. *Proc. Natl. Acad. Sci. U. S. A.* **2007**, *104*, 17977.
- (17) Zhao, Y.; Biggs, T. D.; Xian, M. *Chem. Commun.* **2014**, *50*, 11788.
- (18) Zheng, Y.; Ji, X.; Ji, K.; Wang, B. *Acta Pharmaceutica Sinica B*. Elsevier September 2015, pp 367–377.
- (19) Qandil, A.; M., A. *Int. J. Mol. Sci.* **2012**, *13*, 17244.
- (20) Zanatta, S. D.; Jarrott, B.; Williams, S. J. *Aust. J. Chem.* **2010**, *63*, 946.
- (21) Fiorucci, S.; Antonelli, E.; Distrutti, E.; Rizzo, G.; Mencarelli, A.; Orlandi, S.; Zanardo, R.; Renga, B.; Di Sante, M.; Morelli, A.; Cirino, G.; Wallace, J. L. *Gastroenterology* **2005**, *129*, 1210.
- (22) Devarie-Baez, N. O.; Bagdon, P. E.; Peng, B.; Zhao, Y.; Park, C.-M.; Xian, M. *Org. Lett.* **2013**, *15*, 2786.
- (23) Zheng, Y.; Yu, B.; Ji, K.; Pan, Z.; Chittavong, V.; Wang, B. *Angew. Chem. Int. Ed.* **2016**, *55*, 4514.
- (24) Wang, R. *Physiol. Rev.* **2012**, *92*, 791.
- (25) Hampson, N. B. *Ann. Am. Thorac. Soc.* **2016**, *13*, 1768.
- (26) Ryter, S. W.; Otterbein, L. E. *BioEssays* **2004**, *26*, 270.

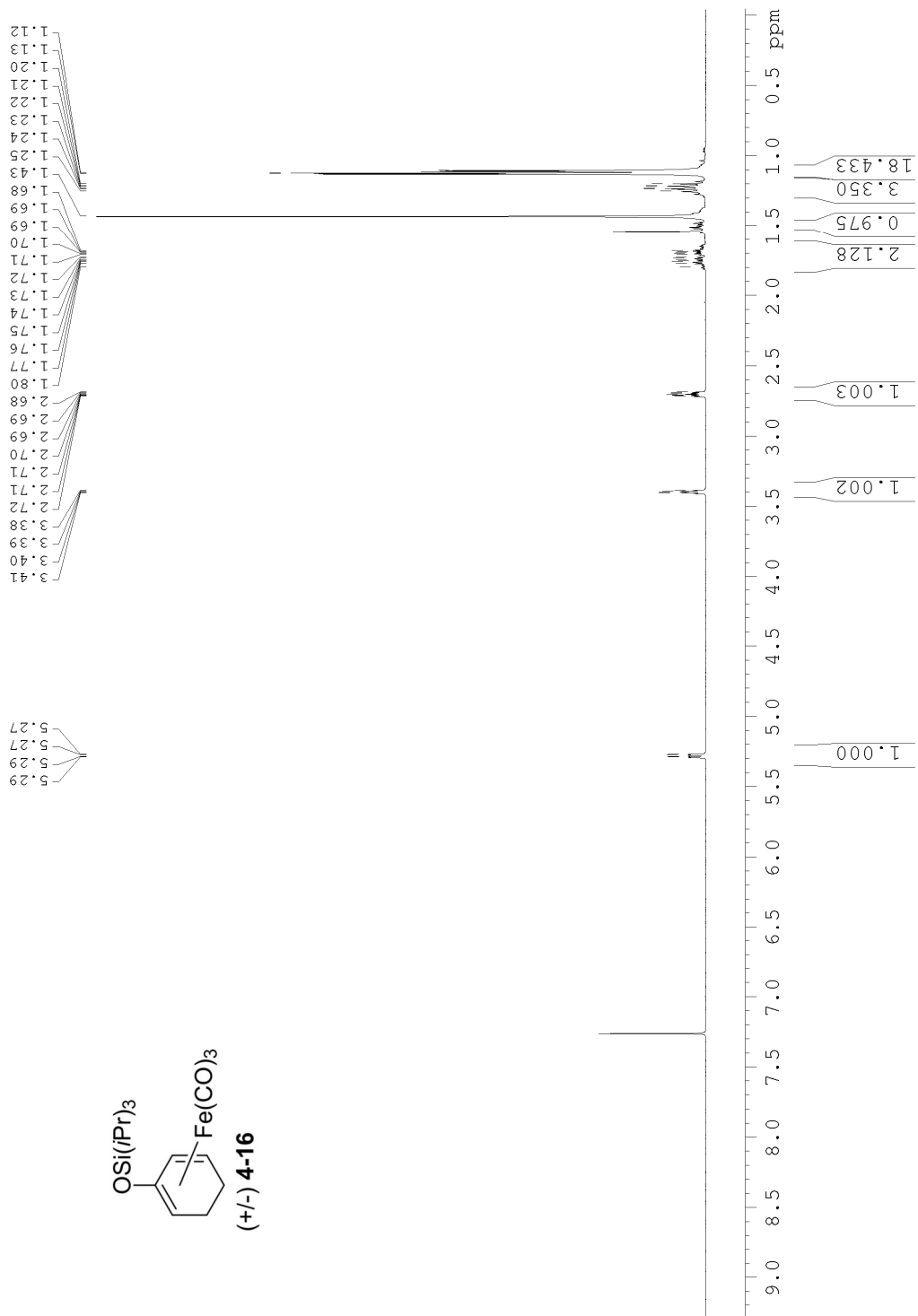
- (27) Hong, P. K.; Ryter, S.; Choi, A. *Annu. Rev. Pharmacol. Toxicol.* **2006**, *46*, 411.
- (28) Rattan, S.; Chakder, S. *Am. J. Physiol. Liver Physiol.* **1993**, *265*, G799.
- (29) Verma, A.; Hirsch, D. J.; Glatt, C. E.; Ronnett, G. V.; Snyder, S. H. *Science* **1993**, *259*, 381.
- (30) Lai, W.; Chen, H.; Matsui, T.; Omori, K.; Unno, M.; Ikeda-Saito, M.; Shaik, S. *J. Am. Chem. Soc.* **2010**, *132*, 12960.
- (31) Schatzschneider, U. *Br. J. Pharmacol.* **2015**, *172*, 1638.
- (32) Kautz, A. C.; Kunz, P. C.; Janiak, C. *Dalt. Trans.* **2016**, *45*, 18045.
- (33) Clark, J. E.; Naughton, P.; Shurey, S.; Green, C. J.; Johnson, T. R.; Mann, B. E.; Foresti, R.; Motterlini, R. *Circ. Res.* **2003**, *93*, E2.
- (34) Motterlini, R.; Sawle, P.; Hammad, J.; Bains, S.; Alberto, R.; Foresti, R.; Green, C. J. *FASEB J.* **2005**, *19*, 284.
- (35) Seixas, J. D.; Mukhopadhyay, A.; Santos-Silva, T.; Otterbein, L. E.; Gallo, D. J.; Rodrigues, S. S.; Guerreiro, B. H.; Gonçalves, A. M. L.; Penacho, N.; Marques, A. R.; Coelho, A. C.; Reis, P. M.; Romão, M. J.; Romão, C. C. *Dalt. Trans.* **2013**, *42*, 5985.
- (36) Kretschmer, R.; Gessner, G.; Görls, H.; Heinemann, S. H.; Westerhausen, M. *J. Inorg. Biochem.* **2011**, *105*, 6.
- (37) Romanski, S.; Kraus, B.; Schatzschneider, U.; Neudörfl, J.-M.; Amslinger, S.; Schmalz, H.-G. *Angew. Chem. Int. Ed.* **2011**, *50*, 2392.
- (38) Romanski, S.; Rucker, H.; Stamellou, E.; Guttentag, M.; Neudörfl, J.-M.; Alberto, R.;

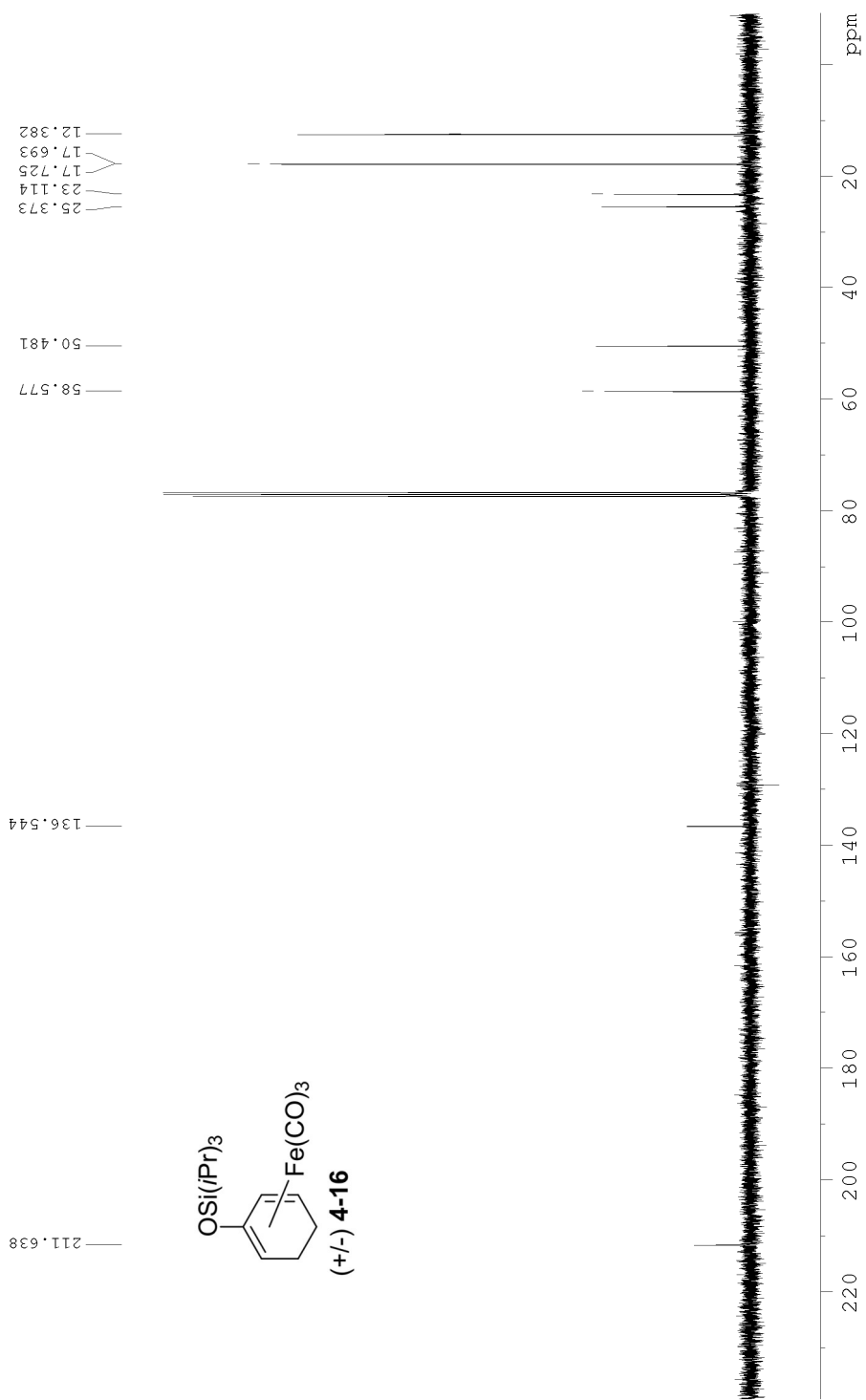
- Amslinger, S.; Yard, B.; Schmalz, H.-G. *Organometallics* **2012**, *31*, 5800.
- (39) Sitnikov, N. S.; Li, Y.; Zhang, D.; Yard, B.; Schmalz, H.-G. *Angew. Chem. Int. Ed.* **2015**, *54*, 12314.
- (40) Spergel, D. J.; Krüth, U.; Shimshek, D. R.; Sprengel, R.; Seeburg, P. H. *Prog. Neurobiol.* **2001**, *63*, 673.
- (41) Metzger, D.; Chambon, P. *Methods* **2001**, *24*, 71.
- (42) Dimri, G. P.; Lee, X.; Basile, G.; Acosta, M.; Scott, G.; Roskelley, C.; Medrano, E. E.; Linskens, M.; Rubelj, I.; Pereira-Smith, O. *Proc. Natl. Acad. Sci. U. S. A.* **1995**, *92*, 9363.
- (43) Chatterjee, S. K.; Bhattacharya, M.; Barlow, J. J. *Cancer Res.* **1979**, *39*, 1943.
- (44) Juers, D. H.; Matthews, B. W.; Huber, R. E. *Protein Sci.* **2012**, *21*, 1792.
- (45) Miljković, M.; Jokić, A.; Davidson, E. A. *Carbohydr. Res.* **1971**, *17*, 155.
- (46) Zemplén, G.; Kunz, A. *Chem. Ber.* **1924**, *57*, 1357.
- (47) Motterlini, R.; Clark, J. E.; Foresti, R.; Sarathchandra, P.; Mann, B. E.; Green, C. J.; Foresti, R.; Motterlini, R. *Circ. Res.* **2002**, *90*, 17e.
- (48) Watts, R. N.; Ponka, P.; Richardson, D. R. *Biochem. J.* **2003**, *369*, 429.
- (49) Michel, B. W.; Lippert, A. R.; Chang, C. J. *J. Am. Chem. Soc.* **2012**, *134*, 15668.
- (50) Atkin, A. J.; Lynam, J. M.; Moulton, B. E.; Sawle, P.; Motterlini, R.; Boyle, N. M.; Pryce, M. T.; Fairlamb, I. J. S. *Dalt. Trans.* **2011**, *40*, 5755.
- (51) Talisman, I. J.; Kumar, V.; Deschamps, J. R.; Frisch, M.; Malhotra, S. V. *Carbohydr. Res.* **2011**, *346*, 2337.

4.13 – NMR Spectra

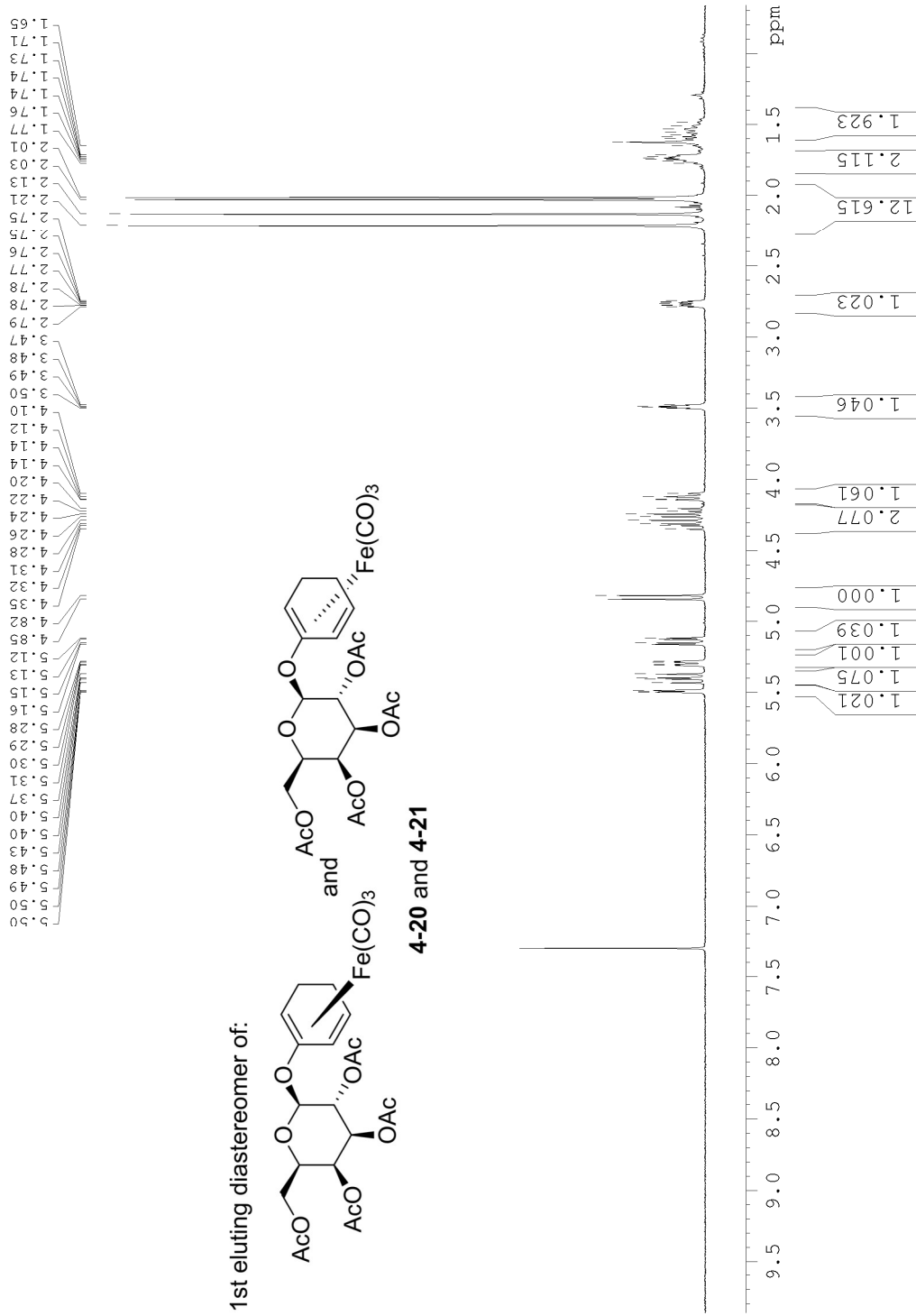




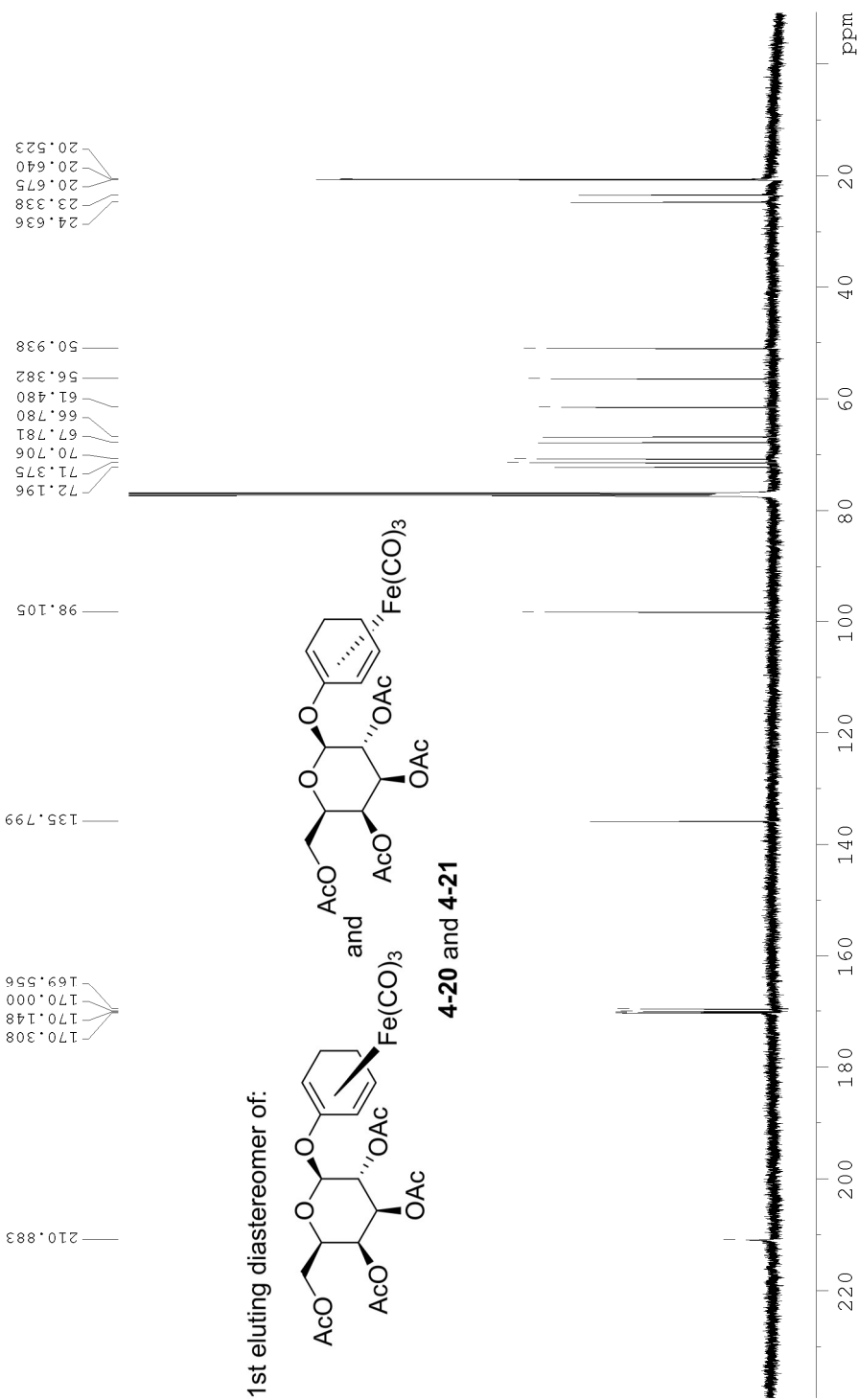


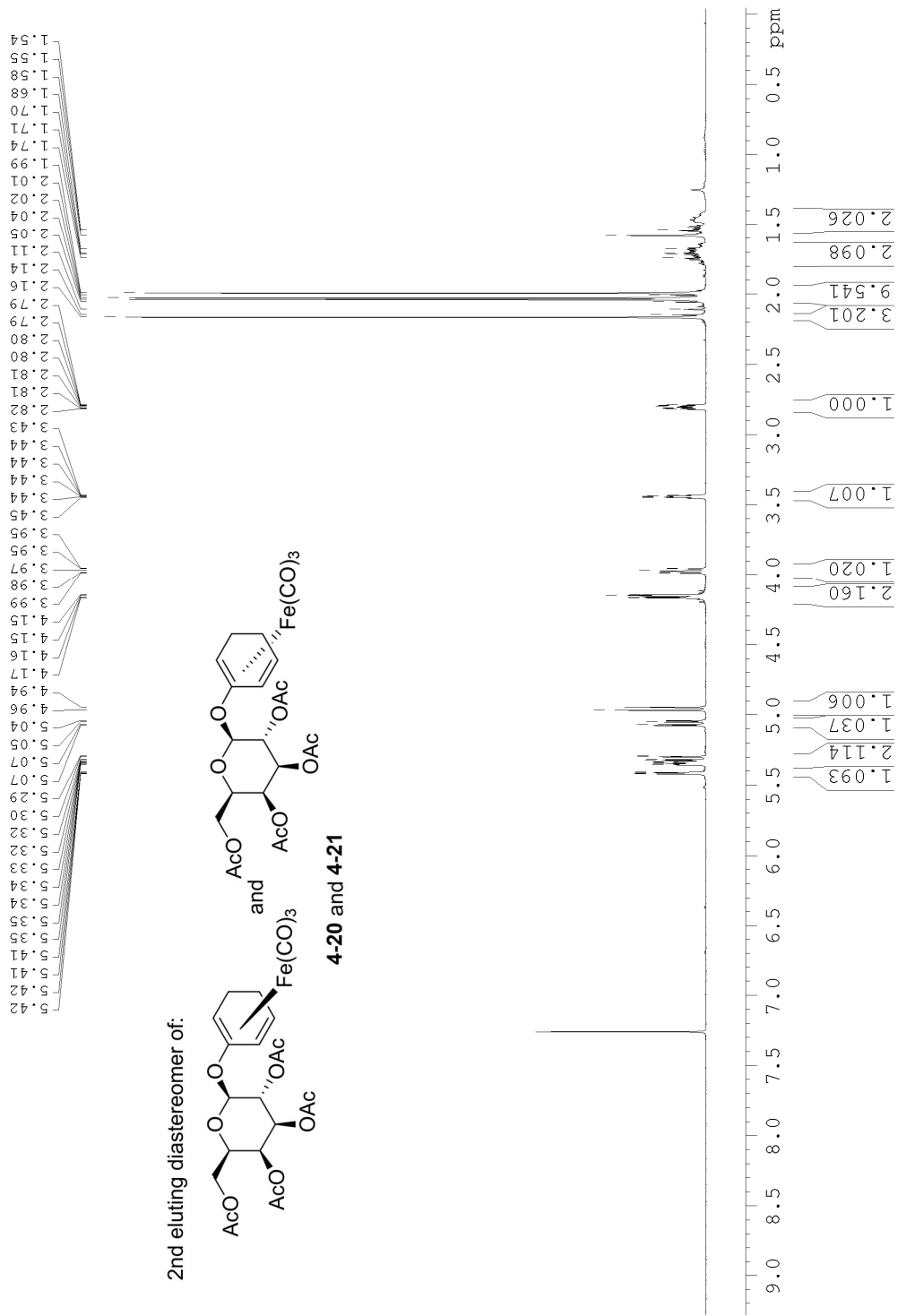


1st eluting diastereomer of:

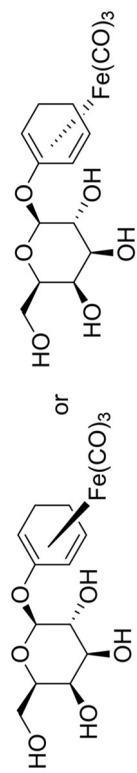


1st eluting diastereomer of:

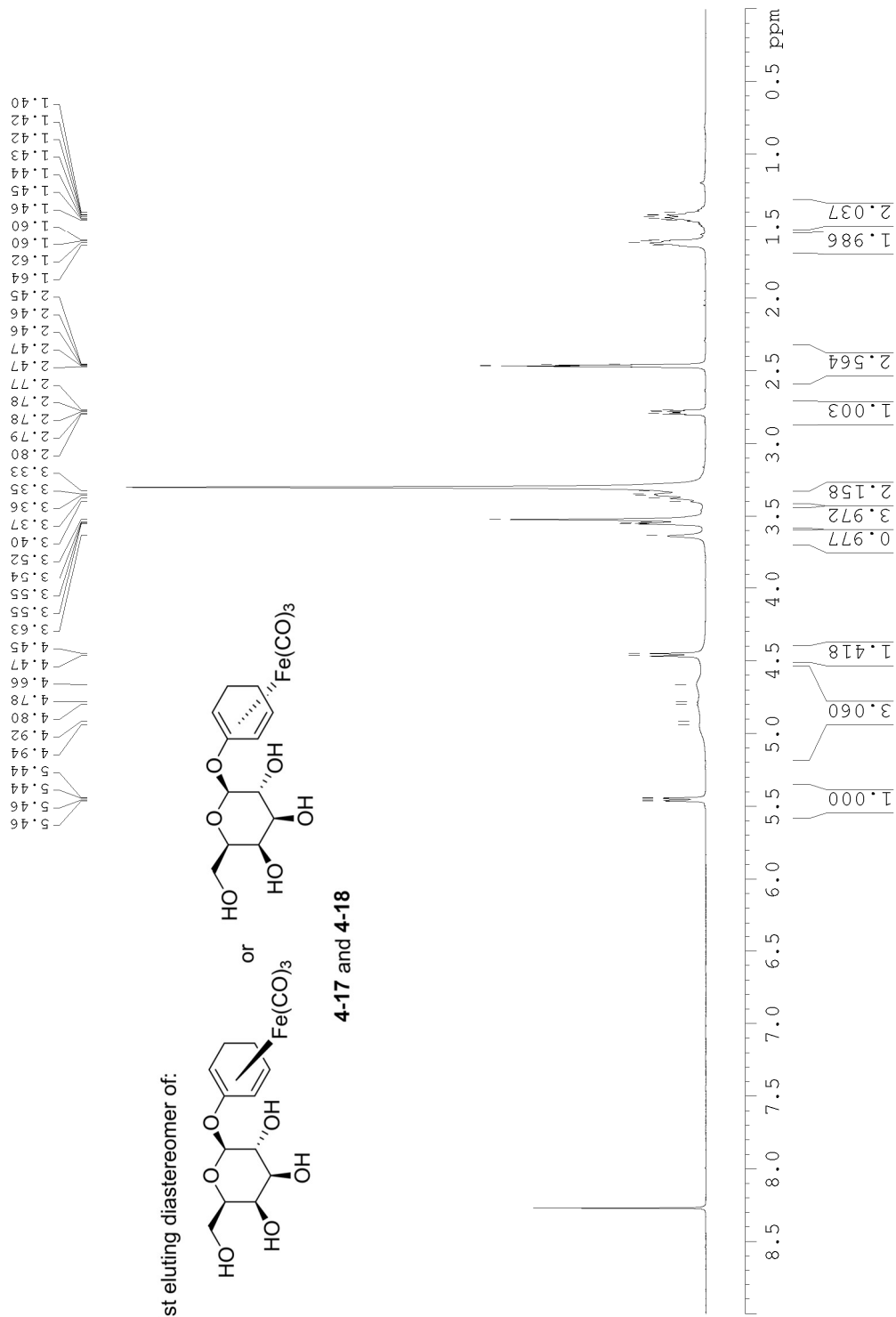


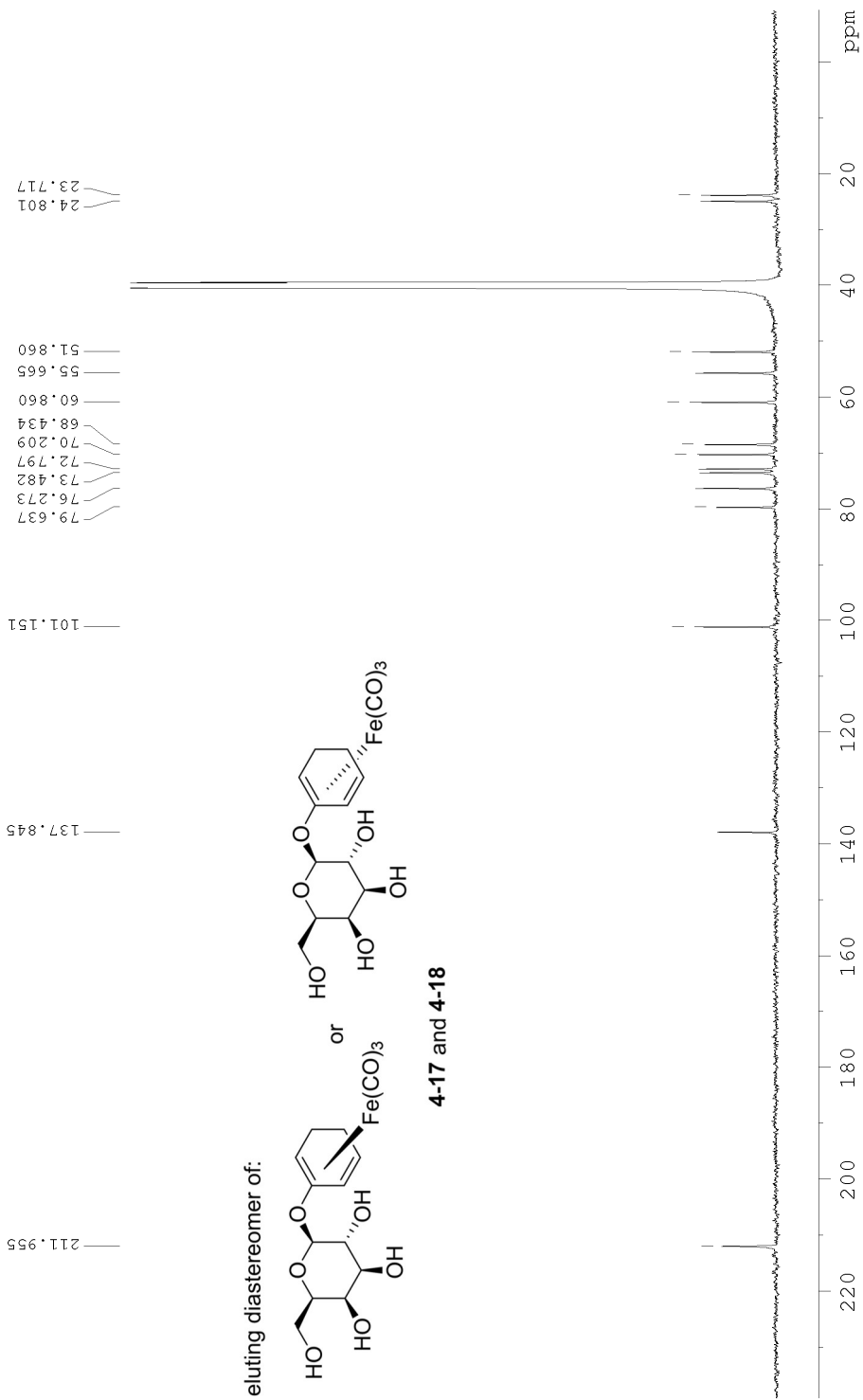


1st eluting diastereomer of:

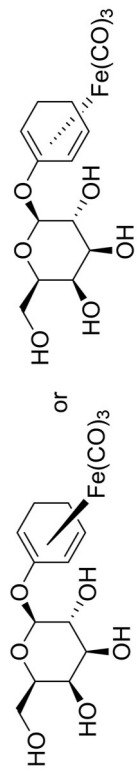


4-17 and 4-18

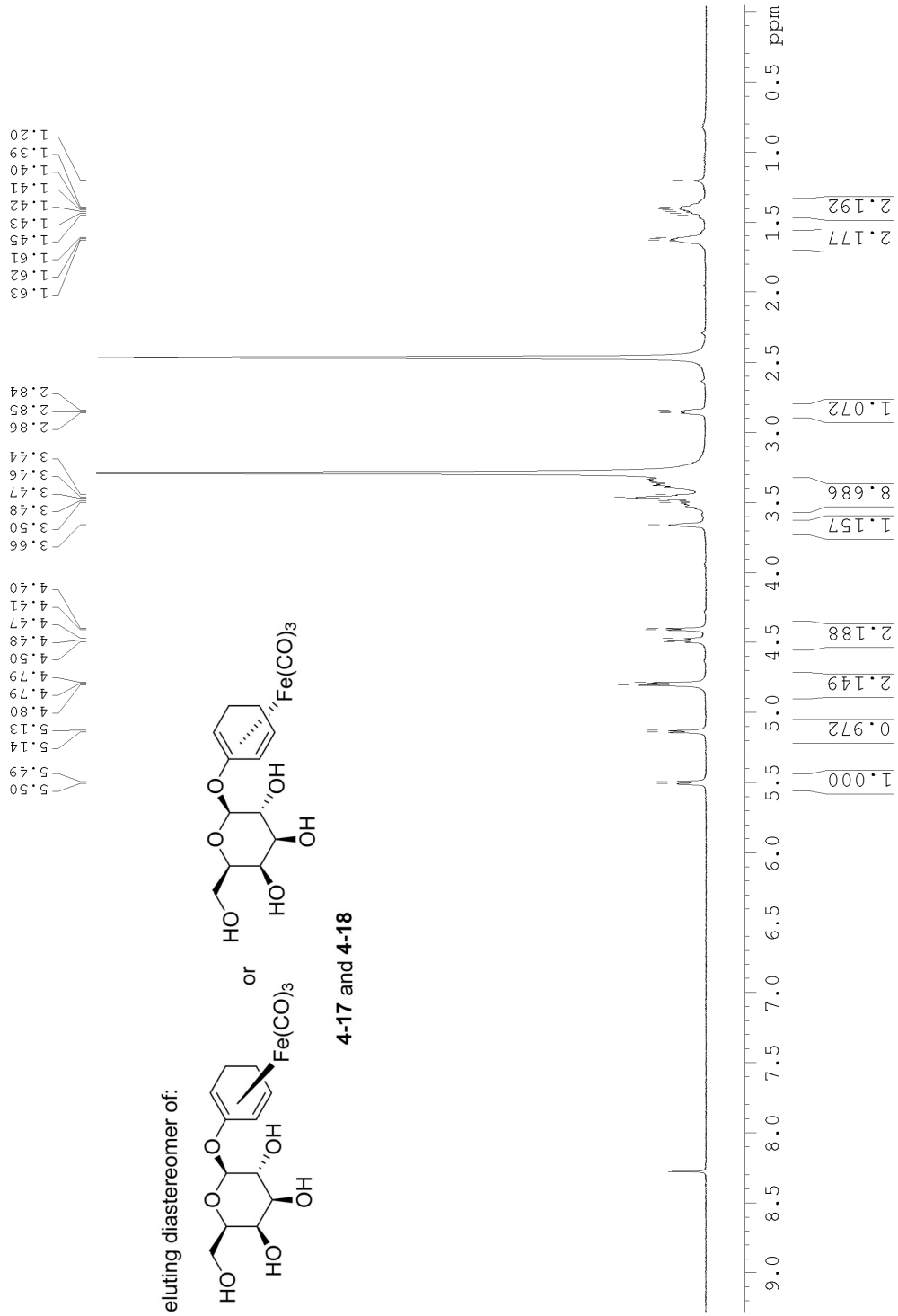


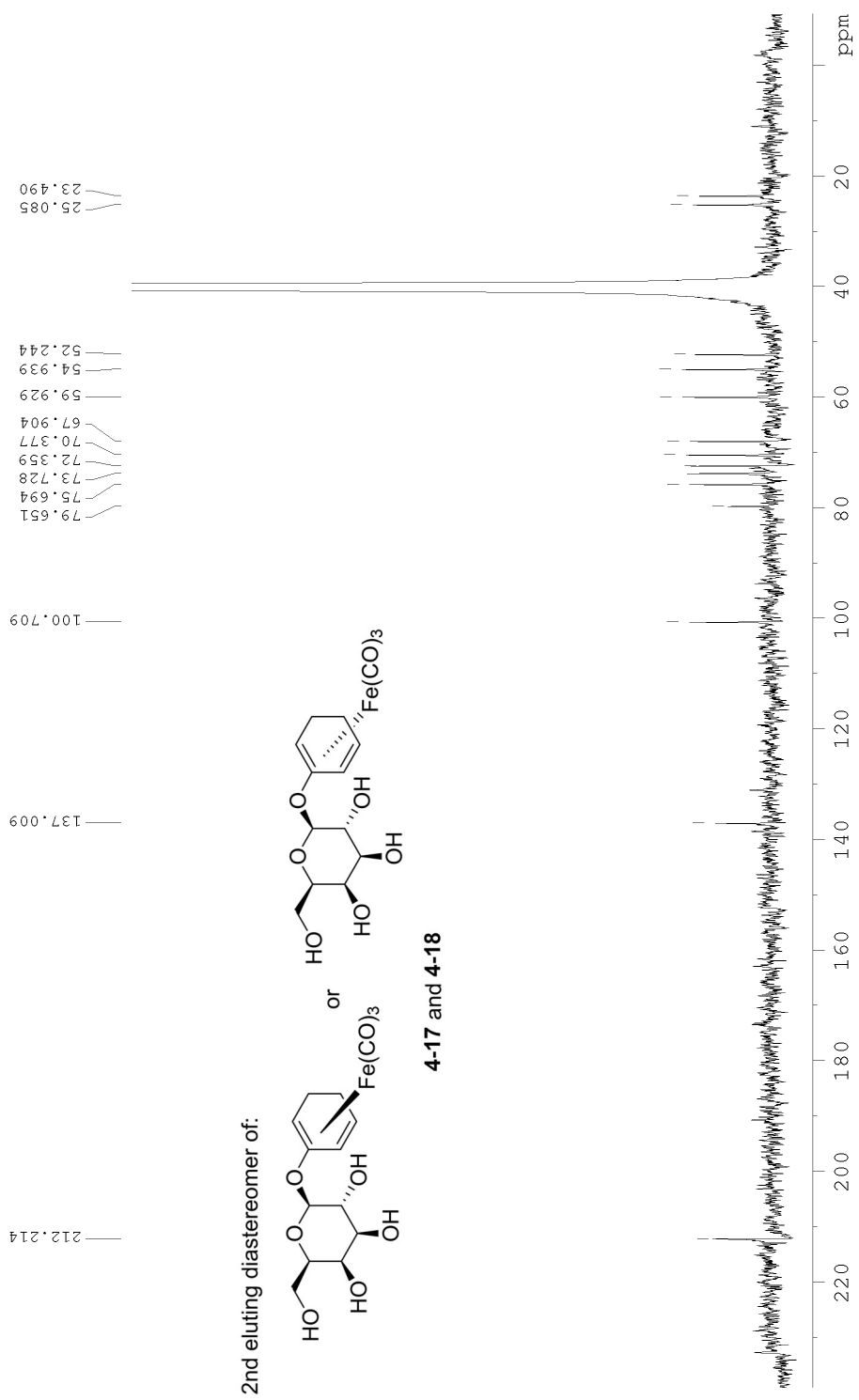


2nd eluting diastereomer of:



4-17 and 4-18





Appendix

Computational Data for Figures 1-3 and 1-4

List of Coordinates and Energy Values

A

C	-2.83888	-0.11124	-0.80837
C	-4.04953	0.16115	-1.46021
C	-4.04139	0.85768	-2.66459
C	-2.81978	1.27054	-3.19393
C	-1.65392	0.98074	-2.48875
N	-1.65863	0.31243	-1.32312
H	-4.97427	1.07207	-3.17817
H	-4.99132	-0.16252	-1.03274
H	-2.76269	1.81110	-4.13336
H	-0.67212	1.28714	-2.83682
C	-1.38030	-1.77629	2.10073
C	-2.44251	-2.42765	2.71962
C	-3.71748	-2.29381	2.17074
C	-3.87608	-1.52967	1.01947
C	-2.76310	-0.89486	0.45032
N	-1.53546	-1.00904	1.00896
H	-4.57318	-2.78947	2.62011
H	-0.36059	-1.87531	2.45621
H	-2.26565	-3.03296	3.60276
H	-4.85489	-1.44422	0.56230
Ir	0.21432	-0.05809	-0.04939
B	1.68594	0.71612	-1.21586
B	0.68642	-1.87034	-0.84254
B	1.70629	-0.38932	1.27844
O	0.10138	-3.07054	-0.39865
O	1.56067	-2.14238	-1.90154
O	1.40308	1.63154	-2.26936
O	3.06432	0.51286	-1.16050
O	2.32172	0.62002	2.04082
O	2.19803	-1.64233	1.69053
C	3.19994	0.03081	2.99633
C	3.31010	-1.44487	2.56297
C	2.59856	1.89095	-3.00971
C	3.72885	1.31384	-2.12970
C	0.76626	-4.16715	-1.02147
C	1.51851	-3.53375	-2.20884
H	4.16517	0.55046	2.98664

H	2.77003	0.13286	4.00451
H	4.24111	-1.64074	2.01393
H	3.25424	-2.14621	3.40418
H	2.70027	2.96882	-3.18531
H	2.53795	1.38869	-3.98462
H	4.30029	2.10420	-1.62271
H	4.43298	0.69820	-2.70164
H	2.53765	-3.92085	-2.32438
H	0.98671	-3.68304	-3.16019
H	1.45590	-4.63034	-0.30172
H	0.03397	-4.92275	-1.33109
C	-0.55190	2.13493	2.23542
C	-0.80103	3.35588	2.85779
C	-0.74043	4.52269	2.09681
C	-0.42787	4.41589	0.74234
C	-0.19388	3.15347	0.20020
H	-0.57574	1.20552	2.79343
H	-1.03119	3.38374	3.91841
H	-0.92581	5.49250	2.55055
H	-0.35695	5.29444	0.10835
H	0.08256	3.02301	-0.84127
N	-0.26140	2.02475	0.92869

ENERGIES IN HARTREE:

SCF:	-1609.547098
SCF + ZPVE:	-1609.083678
Delta H:	-1609.050478
Delta G:	-1609.152323

1,2-B

C	2.42163	0.61259	-1.29172
C	3.59069	0.49705	-2.05469
C	3.72773	-0.56215	-2.94684
C	2.69584	-1.49295	-3.05336
C	1.56385	-1.32680	-2.25901
N	1.42575	-0.29967	-1.40426
H	4.62877	-0.65729	-3.54605
H	4.38810	1.22416	-1.95738
H	2.75999	-2.33566	-3.73412
H	0.73612	-2.02867	-2.27099
C	0.71095	2.69321	1.18043
C	1.56737	3.76607	1.41139
C	2.78464	3.80408	0.73435
C	3.09413	2.77881	-0.15452

C	2.18685	1.72790	-0.33795
N	1.01715	1.69226	0.34120
H	3.48163	4.62304	0.88661
H	-0.26022	2.62089	1.65647
H	1.27810	4.55003	2.10336
H	4.02941	2.80616	-0.70111
Ir	-0.38804	-0.02395	-0.05655
B	-1.52246	-1.65095	-0.53081
B	-1.57631	1.11721	-1.18566
B	-1.77918	0.24651	1.39126
O	-1.45271	2.51142	-1.20289
O	-2.54659	0.69736	-2.09060
O	-0.94586	-2.83116	-1.06908
O	-2.89318	-1.84635	-0.37514
O	-1.90815	-0.62142	2.49114
O	-2.64451	1.33934	1.55580
C	-2.80099	-0.04442	3.44589
C	-3.49866	1.09278	2.67555
C	-1.98600	-3.75692	-1.40238
C	-3.24472	-3.18262	-0.71881
C	-2.52867	3.04443	-1.97635
C	-3.05222	1.83875	-2.78423
H	-3.49911	-0.80712	3.80813
H	-2.22570	0.33140	4.30389
H	-4.49143	0.79374	2.31367
H	-3.60857	2.00894	3.26701
H	-1.72024	-4.75747	-1.04229
H	-2.09404	-3.80222	-2.49464
H	-3.50593	-3.73640	0.19367
H	-4.11976	-3.17892	-1.37880
H	-4.14606	1.79217	-2.82329
H	-2.67010	1.83581	-3.81498
H	-3.29424	3.44678	-1.29925
H	-2.16253	3.86019	-2.61018
C	3.58990	-1.17221	2.65433
C	3.90965	-2.13140	1.68834
C	2.86743	-2.81331	1.06279
C	1.55405	-2.51591	1.43316
H	4.38168	-0.61966	3.15980
H	4.94799	-2.33289	1.43934
H	3.07114	-3.56351	0.30284
H	0.71057	-3.01033	0.96183
C	1.34244	-1.54379	2.41760
N	2.33927	-0.87221	3.02090
H	0.33095	-1.29806	2.73414

ENERGIES IN HARTREE:

SCF: -1609.531838
SCF + ZPVE: -1609.069219
Delta H: -1609.035255
Delta G: -1609.142072

2,3-B

C	2.56811	0.49059	-1.05374
C	3.80080	0.29725	-1.69043
C	4.00035	-0.83672	-2.47177
C	2.96517	-1.76136	-2.59498
C	1.76857	-1.51715	-1.92510
N	1.57068	-0.41861	-1.17729
H	4.95146	-0.99341	-2.97260
H	4.59981	1.02022	-1.57810
H	3.07567	-2.65996	-3.19336
H	0.93149	-2.20745	-1.95960
C	0.67292	2.80999	1.04308
C	1.51558	3.90023	1.23769
C	2.78820	3.86688	0.67003
C	3.16212	2.75689	-0.08079
C	2.26481	1.69246	-0.23458
N	1.04191	1.72549	0.34359
H	3.47806	4.69569	0.79934
H	-0.33794	2.78898	1.43383
H	1.17402	4.75233	1.81609
H	4.14103	2.72745	-0.54412
Ir	-0.34609	-0.01461	-0.00743
B	-1.48443	-1.64428	-0.47553
B	-1.39914	1.03586	-1.34446
B	-1.86576	0.39928	1.26815
O	-1.27679	2.42579	-1.45491
O	-2.27173	0.54124	-2.31043
O	-0.93175	-2.83432	-1.01234
O	-2.86165	-1.81295	-0.32672
O	-2.07019	-0.31818	2.46353
O	-2.78387	1.45748	1.20113
C	-3.10139	0.30862	3.22700
C	-3.74357	1.31391	2.24977
C	-1.99181	-3.71804	-1.39061
C	-3.24098	-3.13411	-0.69933
C	-2.27163	2.89049	-2.36786
C	-2.71223	1.62401	-3.13145
H	-3.80840	-0.44765	3.58591

H	-2.65898	0.80701	4.10166
H	-4.68351	0.93232	1.82952
H	-3.94212	2.29005	2.70729
H	-1.75782	-4.73857	-1.06576
H	-2.09010	-3.71930	-2.48471
H	-3.51721	-3.70194	0.20036
H	-4.11318	-3.09791	-1.36189
H	-3.79732	1.56430	-3.27010
H	-2.23412	1.54937	-4.11846
H	-3.10079	3.33480	-1.80091
H	-1.84597	3.66014	-3.02187
C	3.57417	-1.99262	1.83919
C	2.66944	-2.95734	1.39098
C	1.31101	-2.76199	1.64000
H	4.64168	-2.11579	1.65834
H	3.02438	-3.83328	0.85542
H	0.57017	-3.46887	1.28066
C	0.91601	-1.61753	2.33957
H	-0.12564	-1.42853	2.58391
N	3.21687	-0.88180	2.49885
C	1.90892	-0.71662	2.74105
H	1.63499	0.18542	3.28557

ENERGIES IN HARTREE:

SCF:	-1609.536226
SCF + ZPVE:	-1609.073620
Delta H:	-1609.039737
Delta G:	-1609.145460

3,4-B

C	2.46625	0.59048	-1.23990
C	3.66126	0.44549	-1.95533
C	3.80656	-0.61704	-2.84210
C	2.75499	-1.51892	-2.99214
C	1.59909	-1.32744	-2.23882
N	1.45504	-0.29999	-1.38556
H	4.72941	-0.73763	-3.40195
H	4.47471	1.14836	-1.82135
H	2.82372	-2.36222	-3.67164
H	0.75694	-2.01043	-2.28245
C	0.71062	2.72296	1.15653
C	1.56674	3.79560	1.38791
C	2.80198	3.81229	0.74225
C	3.12699	2.76839	-0.11854

C	2.21831	1.71874	-0.30514
N	1.03250	1.70188	0.34694
H	3.49980	4.63038	0.89538
H	-0.27389	2.66679	1.60673
H	1.26331	4.59690	2.05358
H	4.07462	2.78049	-0.64370
Ir	-0.37195	-0.01381	-0.05301
B	-1.51098	-1.63590	-0.54065
B	-1.54945	1.11844	-1.20217
B	-1.78231	0.26531	1.37485
O	-1.43796	2.51319	-1.22077
O	-2.50321	0.68727	-2.11934
O	-0.95503	-2.79125	-1.14694
O	-2.87366	-1.84388	-0.33356
O	-1.89007	-0.55952	2.51227
O	-2.69953	1.32180	1.48132
C	-2.84485	-0.00090	3.41601
C	-3.57127	1.07546	2.58643
C	-2.00593	-3.70487	-1.47972
C	-3.23804	-3.16444	-0.72378
C	-2.50839	3.03478	-2.00992
C	-3.01069	1.82273	-2.82199
H	-3.51657	-0.78701	3.77827
H	-2.32150	0.42960	4.28218
H	-4.53915	0.71803	2.21071
H	-3.73901	2.00552	3.14161
H	-1.72475	-4.71901	-1.17376
H	-2.15605	-3.70249	-2.56772
H	-3.46509	-3.75900	0.17200
H	-4.13714	-3.13205	-1.34960
H	-4.10345	1.76601	-2.87430
H	-2.61565	1.82097	-3.84772
H	-3.28637	3.43152	-1.34383
H	-2.14105	3.85221	-2.64077
C	2.96637	-2.67342	1.04175
C	1.59365	-2.59075	1.29498
H	3.33640	-3.30079	0.23153
H	0.88492	-3.13228	0.67607
C	1.15822	-1.77386	2.34199
H	0.10091	-1.67258	2.57283
C	2.12135	-1.08146	3.08261
H	1.83356	-0.43635	3.90807
N	3.89798	-2.01323	1.74124
C	3.46579	-1.23440	2.74440
H	4.23833	-0.70844	3.30469

ENERGIES IN HARTREE:

SCF: -1609.533480
SCF + ZPVE: -1609.070755
Delta H: -1609.036799
Delta G: -1609.143736

o-C

Ir	0.22866	0.09973	-0.19981
B	1.25776	-1.23011	1.09830
O	0.62374	-1.81712	2.19507
O	2.58015	-1.66395	1.02304
C	1.58568	-2.55302	2.95755
C	2.81869	-2.64357	2.03673
B	1.81910	-0.57371	-1.36394
O	1.70506	-1.69288	-2.19996
O	3.09356	-0.03728	-1.45125
C	2.93528	-1.86186	-2.91283
C	3.92570	-0.94867	-2.16677
B	1.53110	1.50620	0.49425
O	2.16420	2.51123	-0.23793
O	1.86138	1.64305	1.85759
C	3.10493	3.18414	0.59777
C	2.68849	2.79820	2.03034
C	-2.38895	-0.60129	1.24498
C	-2.41243	-1.50525	0.06977
N	-1.29598	0.18405	1.39467
N	-1.32055	-1.48617	-0.72608
C	-3.42261	-0.56609	2.19123
C	-3.32580	0.27575	3.29239
C	-2.18376	1.06087	3.44062
C	-1.19065	0.97955	2.47112
C	-3.48939	-2.35813	-0.20493
C	-3.43957	-3.18943	-1.31860
C	-2.30837	-3.15843	-2.13044
C	-1.27024	-2.29237	-1.79494
C	-1.08127	1.60972	-1.24359
H	0.27750	0.76134	-1.69876
H	-0.26590	1.54005	2.54292
H	-2.05492	1.72345	4.29008
H	-4.12561	0.30893	4.02659
H	-4.29569	-1.19587	2.07344
H	-4.36370	-2.37165	0.43456
H	-4.27186	-3.85000	-1.54454
H	-2.22170	-3.79030	-3.00844

H	-0.35561	-2.23548	-2.37401
H	2.91427	-3.63229	1.56788
H	3.75731	-2.41579	2.55347
H	1.17395	-3.53350	3.22140
H	1.80201	-2.00810	3.88599
H	2.10747	3.59196	2.52081
H	3.53988	2.54871	2.67267
H	3.06060	4.26351	0.41427
H	4.11564	2.83152	0.35478
H	4.59005	-0.39488	-2.83874
H	4.53746	-1.51122	-1.44946
H	2.79264	-1.55361	-3.95771
H	3.22715	-2.91753	-2.89919
C	-0.75948	2.97584	-1.36151
H	0.24613	3.30654	-1.13046
C	-1.73293	3.87927	-1.78202
H	-1.49747	4.93796	-1.86975
C	-3.00806	3.40669	-2.09654
H	-3.79844	4.07240	-2.43216
C	-3.23255	2.03661	-1.98428
H	-4.20655	1.61520	-2.23448
N	-2.30241	1.15957	-1.58104

ENERGIES IN HARTREE:

SCF:	-1609.498181
SCF + ZPVE:	-1609.039449
Delta H:	-1609.006857
Delta G:	-1609.105779

m-C

Ir	0.22958	0.13586	-0.18783
B	1.29117	-1.06136	1.21117
O	1.90581	-0.60374	2.36712
O	1.37816	-2.45283	1.12604
C	2.38832	-1.71905	3.12259
C	2.21815	-2.93169	2.18237
B	1.85227	-0.64844	-1.21153
O	1.68937	-1.39709	-2.38779
O	3.19519	-0.59482	-0.86379
C	2.94927	-1.98010	-2.74156
C	3.97370	-1.19723	-1.89900
B	1.43301	1.70613	0.32537
O	2.40001	2.29254	-0.48562
O	1.31211	2.43311	1.51927

C	3.07078	3.32183	0.23983
C	2.18125	3.56943	1.47620
C	-2.36169	-0.64396	1.35025
C	-2.28792	-1.67741	0.28880
N	-1.34551	0.25221	1.39964
N	-1.22903	-1.60217	-0.54816
C	-3.40989	-0.58721	2.27788
C	-3.40669	0.39248	3.26524
C	-2.34773	1.29566	3.31115
C	-1.33579	1.19154	2.36066
C	-3.24105	-2.69688	0.15545
C	-3.09557	-3.64480	-0.85169
C	-1.99597	-3.55900	-1.70313
C	-1.08514	-2.52248	-1.51397
C	-1.09187	1.44576	-1.42559
C	-1.95450	0.96073	-2.42001
C	-2.93926	1.78929	-2.96093
C	-3.03110	3.10134	-2.49918
H	0.39427	0.80084	-1.67349
H	-0.48051	1.85815	2.34756
H	-2.29680	2.07393	4.06534
H	-4.21783	0.44428	3.98567
H	-4.22494	-1.29886	2.23068
H	-4.08750	-2.75673	0.82893
H	-3.82898	-4.43798	-0.96460
H	-1.83796	-4.27849	-2.49996
H	-0.20406	-2.40354	-2.13603
H	1.74281	-3.79003	2.67020
H	3.17462	-3.26316	1.75764
H	1.79354	-1.81634	4.04067
H	3.43127	-1.54369	3.40754
H	1.57819	4.48217	1.37809
H	2.75112	3.63009	2.40959
H	3.17807	4.20987	-0.39271
H	4.07388	2.97254	0.51830
H	4.46999	-0.40909	-2.48018
H	4.74354	-1.83810	-1.45610
H	3.10923	-1.87928	-3.82006
H	2.93668	-3.04869	-2.48803
H	-3.78732	3.77887	-2.89519
H	-3.61798	1.42723	-3.72963
H	-1.85805	-0.06193	-2.77643
C	-1.26753	2.79678	-1.07162
H	-0.61923	3.25005	-0.32429
N	-2.21115	3.60823	-1.57002

ENERGIES IN HARTREE:

SCF: -1609.497053
SCF + ZPVE: -1609.038475
Delta H: -1609.005576
Delta G: -1609.106494

p-C

Ir	0.22915	0.13584	-0.19897
B	1.31254	-1.00327	1.22965
O	1.99592	-0.48422	2.32014
O	1.35265	-2.39800	1.24198
C	2.48977	-1.55897	3.12631
C	2.23704	-2.82743	2.28335
B	1.80864	-0.71503	-1.23904
O	1.60195	-1.42629	-2.43122
O	3.15035	-0.75435	-0.88787
C	2.82733	-2.06566	-2.80901
C	3.89498	-1.38210	-1.93276
B	1.46562	1.70145	0.24915
O	2.53595	2.15769	-0.51271
O	1.27083	2.55578	1.34725
C	3.19471	3.22022	0.17436
C	2.20912	3.63490	1.28690
C	-2.32332	-0.59576	1.42964
C	-2.28404	-1.65012	0.38732
N	-1.31261	0.30847	1.42266
N	-1.24893	-1.59749	-0.48006
C	-3.33796	-0.52658	2.39327
C	-3.30891	0.47464	3.35795
C	-2.25858	1.38866	3.34375
C	-1.28013	1.27110	2.36048
C	-3.24937	-2.66295	0.29770
C	-3.14137	-3.62812	-0.69753
C	-2.06704	-3.56449	-1.58229
C	-1.14297	-2.53298	-1.43628
C	-1.11400	1.41065	-1.44789
C	-1.98789	0.89507	-2.41834
C	-2.98304	1.70624	-2.96672
H	0.36426	0.76670	-1.70331
H	-0.43602	1.94908	2.30202
H	-2.18818	2.18494	4.07735
H	-4.09354	0.53478	4.10653
H	-4.14677	-1.24664	2.39203
H	-4.07806	-2.70256	0.99409

H	-3.88495	-4.41581	-0.77695
H	-1.93933	-4.29621	-2.37336
H	-0.28317	-2.43022	-2.09004
H	1.76792	-3.63641	2.85432
H	3.16003	-3.21371	1.83200
H	1.94341	-1.57479	4.07882
H	3.55096	-1.39586	3.34280
H	1.67522	4.56369	1.04459
H	2.69089	3.75753	2.26285
H	3.41362	4.03366	-0.52612
H	4.14470	2.85165	0.58325
H	4.45452	-0.61576	-2.48464
H	4.61079	-2.08962	-1.50082
H	2.99577	-1.92644	-3.88188
H	2.75120	-3.14209	-2.60480
H	-3.66404	1.30110	-3.71622
H	-1.89946	-0.13345	-2.75715
C	-1.29537	2.76643	-1.12766
H	-0.65709	3.25614	-0.39817
C	-2.32547	3.49256	-1.72794
H	-2.47730	4.53978	-1.46368
N	-3.17215	2.99020	-2.63683

ENERGIES IN HARTREE:

SCF:	-1609.497638
SCF + ZPVE:	-1609.038958
Delta H:	-1609.006151
Delta G:	-1609.106074

***o*-D**

Ir	0.20752	0.18964	-0.25337
N	-1.27228	-1.42454	-0.86527
N	-1.06319	-0.09212	1.46725
C	-2.28359	-1.59661	0.01237
C	-2.14993	-0.89096	1.30686
C	-3.06116	-1.06801	2.35599
C	-2.87004	-0.40556	3.56159
C	-1.75463	0.41688	3.70544
C	-0.87308	0.54362	2.63800
C	-3.36704	-2.43174	-0.29283
C	-3.40216	-3.08451	-1.51949
C	-2.34696	-2.90329	-2.41241
C	-1.29972	-2.06427	-2.04226
B	1.87876	-0.64678	-1.20368
O	1.73244	-1.59321	-2.22851

O	3.22426	-0.33443	-1.02239
C	3.03267	-2.04986	-2.60588
C	3.97891	-0.96551	-2.05914
B	1.42177	-1.21577	0.87335
O	1.31095	-2.60088	0.80537
O	2.16853	-0.83001	1.97317
C	1.94955	-3.17530	1.95308
C	2.69849	-1.99598	2.61174
B	1.34672	1.76969	0.37068
O	1.41713	2.25733	1.67970
O	2.11514	2.56855	-0.47464
C	2.19134	3.45925	1.70083
C	2.84437	3.51712	0.30363
C	-1.29275	1.59654	-0.89001
C	-3.55441	2.15792	-0.97891
C	-3.33315	3.29836	-1.74478
H	0.86279	0.59633	-1.68056
H	-0.43871	-1.89992	-2.67864
H	-2.32854	-3.39861	-3.37765
H	-4.24078	-3.72754	-1.77110
H	-4.18136	-2.56434	0.40915
H	-3.91722	-1.71914	2.23064
H	-3.57866	-0.53445	4.37475
H	-1.55899	0.95583	4.62641
H	0.00902	1.17023	2.68900
H	-4.16137	3.92997	-2.05481
H	-4.56704	1.88411	-0.67869
H	3.90171	3.22319	0.33076
H	2.77309	4.50795	-0.15885
H	2.92387	3.40892	2.51383
H	1.52672	4.31390	1.88502
H	2.52897	-1.93125	3.69201
H	3.78064	-2.03865	2.43431
H	1.18204	-3.60244	2.61133
H	2.61626	-3.98375	1.63439
H	3.22015	-3.02936	-2.14488
H	3.08386	-2.15979	-3.69428
H	4.90758	-1.37055	-1.64377
H	4.23462	-0.22017	-2.82433
C	-2.01237	3.59035	-2.09262
H	-1.77966	4.46943	-2.69089
C	-0.99567	2.74226	-1.66308
H	0.03798	2.96080	-1.91071
N	-2.57762	1.33649	-0.56846

ENERGIES IN HARTREE:

SCF: -1609.519518
SCF + ZPVE: -1609.058560
Delta H: -1609.025944
Delta G: -1609.123815

m-D

Ir	0.21428	0.21732	-0.25248
N	-1.51859	-1.06777	-1.02055
N	-1.13243	-0.04874	1.43853
C	-2.45627	-1.37464	-0.09844
C	-2.23413	-0.82685	1.25987
C	-3.11838	-1.06169	2.32017
C	-2.88234	-0.48677	3.56334
C	-1.75667	0.31695	3.72585
C	-0.90495	0.50893	2.64321
C	-3.57814	-2.14370	-0.43668
C	-3.73099	-2.58924	-1.74503
C	-2.76002	-2.25842	-2.68817
C	-1.66774	-1.49737	-2.28070
B	1.67896	-0.89965	-1.25342
O	1.33248	-1.70768	-2.34422
O	3.05690	-0.90682	-1.06079
C	2.50488	-2.39859	-2.78197
C	3.66362	-1.60475	-2.15074
B	1.11499	-1.46601	0.78307
O	0.66117	-2.77847	0.68803
O	1.97702	-1.31496	1.85474
C	1.18457	-3.53014	1.79199
C	2.24320	-2.60088	2.42360
B	1.61663	1.47482	0.53775
O	1.65209	1.90284	1.86908
O	2.62502	2.09785	-0.19043
C	2.65515	2.91282	2.01526
C	3.45614	2.84512	0.69834
C	-0.88203	1.99599	-0.78383
C	-2.39610	4.22325	-1.51271
H	0.99535	0.61105	-1.61123
H	-0.86845	-1.23437	-2.96111
H	-2.83953	-2.58028	-3.72126
H	-4.59796	-3.18201	-2.02166
H	-4.32987	-2.38808	0.30401
H	-3.99165	-1.68513	2.17435
H	-3.56880	-0.66271	4.38629
H	-1.52987	0.79358	4.67357

H	-0.00883	1.11473	2.71237
H	-3.01794	5.07726	-1.78296
H	4.41179	2.31982	0.82385
H	3.65801	3.83367	0.27162
H	3.26492	2.69861	2.89966
H	2.16758	3.88645	2.15545
H	2.16679	-2.54236	3.51451
H	3.26653	-2.90016	2.16375
H	0.36588	-3.76247	2.48560
H	1.60255	-4.47377	1.42602
H	2.46982	-3.43469	-2.41869
H	2.53735	-2.41344	-3.87648
H	4.47084	-2.24206	-1.77499
H	4.09304	-0.87572	-2.85085
C	-1.04727	4.18133	-1.86032
H	-0.59452	5.00487	-2.40847
C	-0.29484	3.06545	-1.49030
H	0.76163	3.03193	-1.74290
N	-3.00069	3.23834	-0.83973
C	-2.24934	2.17664	-0.50184
H	-2.80296	1.41076	0.03912

ENERGIES IN HARTREE:

SCF:	-1609.516473
SCF + ZPVE:	-1609.055442
Delta H:	-1609.022649
Delta G:	-1609.121845

***p*-D**

Ir	0.20384	0.21758	-0.24914
N	-1.47209	-1.12784	-1.02799
N	-1.11929	-0.12227	1.44218
C	-2.40897	-1.45992	-0.11370
C	-2.20037	-0.92622	1.25246
C	-3.07291	-1.20556	2.31213
C	-2.84652	-0.64814	3.56493
C	-1.74265	0.18348	3.73831
C	-0.90137	0.41924	2.65620
C	-3.51537	-2.24571	-0.46510
C	-3.65186	-2.68372	-1.77781
C	-2.68007	-2.32961	-2.71187
C	-1.60453	-1.55159	-2.29218
B	1.72023	-0.82200	-1.25861
O	1.40985	-1.63552	-2.35593

O	3.09651	-0.76991	-1.06427
C	2.61216	-2.27166	-2.79671
C	3.73368	-1.42983	-2.16099
B	1.18690	-1.42950	0.77218
O	0.80815	-2.76389	0.66229
O	2.02722	-1.23836	1.85466
C	1.35947	-3.49316	1.76798
C	2.36064	-2.51269	2.41507
B	1.54735	1.53986	0.54374
O	1.55426	1.97400	1.87307
O	2.53091	2.20135	-0.18136
C	2.51115	3.02798	2.02157
C	3.31728	2.99791	0.70568
C	-0.97621	1.94371	-0.75741
C	-2.33538	2.09632	-0.42580
C	-0.44975	3.02041	-1.50243
C	-3.05607	3.22506	-0.82284
C	-1.24764	4.10821	-1.85806
H	0.96368	0.65439	-1.60724
H	-0.80545	-1.26852	-2.96491
H	-2.74665	-2.64611	-3.74750
H	-4.50639	-3.28950	-2.06479
H	-4.26735	-2.50886	0.26898
H	-3.92783	-1.85239	2.15903
H	-3.52320	-0.85968	4.38765
H	-1.52479	0.64795	4.69411
H	-0.02344	1.05071	2.73140
H	-2.86890	1.34072	0.14614
H	0.59474	3.02431	-1.80009
H	-0.82029	4.92756	-2.43825
H	-4.10945	3.31978	-0.55224
H	4.30061	2.52751	0.83483
H	3.46416	3.99402	0.27431
H	3.12837	2.84017	2.90681
H	1.97983	3.97818	2.16190
H	2.27385	-2.46780	3.50578
H	3.40057	-2.75248	2.15971
H	0.54690	-3.77165	2.45169
H	1.83022	-4.41143	1.40182
H	2.62303	-3.30978	-2.43779
H	2.64524	-2.27976	-3.89118
H	4.57055	-2.03141	-1.79144
H	4.12659	-0.67539	-2.85541
N	-2.54230	4.23522	-1.53418

ENERGIES IN HARTREE:

SCF: -1609.517731
SCF + ZPVE: -1609.056648
Delta H: -1609.023888
Delta G: -1609.122976

***o*-E**

Ir	0.19246	-0.04501	-0.44633
C	-1.90684	-0.71072	1.66720
C	-2.62802	-0.85351	0.38097
N	-0.60657	-0.34177	1.58768
N	-1.91828	-0.58503	-0.74011
C	-2.52220	-0.92050	2.90660
C	-1.79254	-0.72941	4.07547
C	-0.46339	-0.32616	3.97772
C	0.09202	-0.14329	2.71390
C	-3.97559	-1.22845	0.29186
C	-4.58550	-1.32329	-0.95340
C	-3.84010	-1.03696	-2.09717
C	-2.50819	-0.67118	-1.94186
B	0.50555	-2.11952	-0.74508
O	-0.37273	-3.05596	-0.19448
O	1.46767	-2.75906	-1.51932
C	-0.04740	-4.35812	-0.69251
C	1.32254	-4.17482	-1.37693
B	2.17425	-0.51597	-0.05077
O	3.28123	-0.33089	-0.86724
O	2.55078	-1.13418	1.15180
C	4.38428	-1.03606	-0.29966
C	3.97591	-1.25714	1.16790
C	-0.62522	2.03962	-0.45023
C	-2.47077	4.10281	-0.62402
B	1.37251	1.67961	-0.15026
O	2.03446	2.40757	-1.13913
O	1.81439	2.06724	1.12539
C	3.06254	3.17175	-0.51697
C	2.65620	3.21179	0.96808
H	0.63364	0.10700	-1.97228
H	-3.20390	4.90483	-0.63988
H	0.14306	-0.15305	4.86063
H	-2.25923	-0.88760	5.04345
H	1.11830	0.16750	2.57618
H	-3.56075	-1.22370	2.96403
H	-5.62904	-1.61482	-1.02855
H	-4.27509	-1.09406	-3.08936

H	-1.87356	-0.43726	-2.78853
H	-4.54563	-1.44547	1.18699
H	5.29976	-0.44474	-0.40965
H	4.51469	-1.98591	-0.83497
H	4.39767	-0.49111	1.83373
H	4.25754	-2.24336	1.55262
H	4.02598	2.66383	-0.66193
H	3.11762	4.16570	-0.97487
H	3.50798	3.14071	1.65349
H	2.08601	4.11873	1.21349
H	-0.02045	-5.07317	0.13676
H	-0.82512	-4.67927	-1.39881
H	2.14582	-4.56092	-0.76146
H	1.37828	-4.64954	-2.36230
C	-0.84732	2.68908	-1.68378
H	-0.26567	2.38893	-2.54808
H	-1.96265	4.21678	-2.72452
C	-1.78097	3.71734	-1.77516
H	-2.68541	3.70676	1.48816
N	-1.29322	2.43122	0.65598
C	-2.17958	3.43051	0.56243

ENERGIES IN HARTREE:

SCF:	-1609.516266
SCF + ZPVE:	-1609.055850
Delta H:	-1609.023969
Delta G:	-1609.120181

m-E

Ir	0.17635	-0.00588	-0.43365
C	-1.95980	-0.71145	1.64520
C	-2.69353	-0.68991	0.35853
N	-0.64435	-0.38705	1.59190
N	-1.96442	-0.39660	-0.74371
C	-2.57388	-1.03039	2.86255
C	-1.82805	-1.00349	4.03622
C	-0.48069	-0.65492	3.96821
C	0.07325	-0.35625	2.72635
C	-4.06923	-0.93442	0.25433
C	-4.68798	-0.87725	-0.98935
C	-3.92236	-0.56880	-2.11336
C	-2.56280	-0.33347	-1.94318
B	0.32278	-2.09911	-0.82650
O	-0.53644	-2.99286	-0.18701

O	1.10855	-2.76073	-1.75828
C	-0.25659	-4.32432	-0.63310
C	0.74307	-4.14359	-1.79845
B	2.09318	-0.72816	-0.08790
O	3.19963	-0.64285	-0.91966
O	2.41996	-1.41246	1.09409
C	4.23098	-1.47177	-0.38549
C	3.82804	-1.67059	1.08611
C	-0.46596	2.10845	-0.36123
C	-0.95853	2.74424	0.79034
C	-1.70748	3.91877	0.68579
C	-1.95232	4.43807	-0.58381
B	1.56404	1.53811	-0.10921
O	2.26626	2.24786	-1.07424
O	2.02414	1.85710	1.18073
C	3.30686	2.97720	-0.42865
C	2.90335	2.98035	1.05851
H	0.61549	0.18352	-1.95086
H	-2.09373	4.42099	1.56989
H	-2.54327	5.34551	-0.70897
H	0.14028	-0.61542	4.85705
H	-2.29412	-1.24980	4.98578
H	1.11522	-0.09048	2.60945
H	-3.62243	-1.30055	2.89752
H	-5.75390	-1.06542	-1.07737
H	-4.36272	-0.50588	-3.10266
H	-1.91500	-0.08534	-2.77547
H	-4.65608	-1.16126	1.13610
H	5.20245	-0.98121	-0.50698
H	4.24620	-2.42175	-0.93627
H	4.32992	-0.95419	1.75127
H	4.01989	-2.68315	1.45688
H	4.26373	2.46250	-0.59205
H	3.37447	3.98352	-0.85576
H	3.75198	2.86051	1.74061
H	2.36001	3.89537	1.33243
H	0.16998	-4.89856	0.19886
H	-1.18857	-4.81084	-0.94291
H	1.64094	-4.76170	-1.68842
H	0.29365	-4.36582	-2.77438
H	-0.74498	2.33254	1.77302
N	-1.48091	3.87994	-1.70750
C	-0.75068	2.76418	-1.57761
H	-0.35107	2.35907	-2.50488

ENERGIES IN HARTREE:

SCF: -1609.518042
SCF + ZPVE: -1609.057259
Delta H: -1609.025255
Delta G: -1609.122168

***p*-E**

Ir	0.18196	-0.02042	-0.44021
C	-1.93218	-0.77221	1.64437
C	-2.66424	-0.79587	0.35653
N	-0.62708	-0.40937	1.58676
N	-1.94649	-0.48516	-0.74818
C	-2.53816	-1.08682	2.86673
C	-1.79546	-1.01498	4.04067
C	-0.45928	-0.62715	3.96774
C	0.08750	-0.33520	2.72107
C	-4.02805	-1.10002	0.25412
C	-4.64629	-1.08602	-0.99099
C	-3.89213	-0.76194	-2.11819
C	-2.54428	-0.46606	-1.94893
B	0.41972	-2.09846	-0.80984
O	-0.45768	-3.02121	-0.23730
O	1.31435	-2.74167	-1.65570
C	-0.20594	-4.31748	-0.79209
C	1.12712	-4.15651	-1.55111
B	2.14156	-0.60471	-0.07635
O	3.24734	-0.45142	-0.89895
O	2.49820	-1.27116	1.10643
C	4.32080	-1.22262	-0.36030
C	3.91803	-1.45449	1.10668
C	-0.53957	2.08954	-0.37719
C	-1.08606	2.68747	0.77167
C	-1.92770	3.79670	0.65853
B	1.46490	1.62395	-0.13112
O	2.13669	2.35384	-1.10429
O	1.92644	1.96034	1.15440
C	3.17410	3.09691	-0.46915
C	2.77920	3.10246	1.01982
H	0.61909	0.16962	-1.95940
H	-2.35216	4.25318	1.55379
H	0.15851	-0.55129	4.85642
H	-2.25586	-1.25631	4.99423
H	1.12105	-0.04018	2.59976
H	-3.57867	-1.38574	2.90609
H	-5.70303	-1.32067	-1.07776

H	-4.33282	-0.73376	-3.10900
H	-1.90527	-0.20405	-2.78376
H	-4.60626	-1.34102	1.13778
H	5.26301	-0.67534	-0.46979
H	4.39620	-2.16599	-0.91706
H	4.37666	-0.71881	1.78190
H	4.16039	-2.45868	1.47056
H	4.13405	2.58914	-0.63536
H	3.22921	4.10160	-0.90188
H	3.63417	3.00594	1.69760
H	2.21730	4.00716	1.29052
H	-0.15443	-5.05791	0.01324
H	-1.03425	-4.59119	-1.45943
H	1.97124	-4.59018	-0.99917
H	1.10821	-4.59764	-2.55309
H	-0.84853	2.30668	1.76039
C	-0.87418	2.71658	-1.59254
H	-0.45402	2.35511	-2.52623
N	-2.26821	4.36424	-0.50502
C	-1.72985	3.81756	-1.60551
H	-1.99612	4.29177	-2.55072

ENERGIES IN HARTREE:

SCF:	-1609.518503
SCF + ZPVE:	-1609.057586
Delta H:	-1609.025727
Delta G:	-1609.121915

***o*-F**

Ir	0.27897	-0.16859	0.26638
N	2.03488	0.34677	-0.92064
N	0.43179	2.06752	0.34324
C	2.35528	1.66198	-1.04105
C	1.42620	2.61867	-0.39497
C	3.51876	2.06340	-1.70943
C	4.36733	1.10659	-2.25562
C	4.04090	-0.24119	-2.10527
C	2.87394	-0.57695	-1.42784
C	1.55108	4.00896	-0.51128
C	0.64941	4.83569	0.15236
C	-0.36483	4.25637	0.91307
C	-0.44079	2.86720	0.97465
H	3.77010	3.11464	-1.78890
H	5.27222	1.40874	-2.77464

H	2.58512	-1.60719	-1.25045
H	2.33708	4.44486	-1.11698
H	0.73722	5.91530	0.07095
H	-1.09216	4.86245	1.44310
H	-1.22297	2.35808	1.52237
B	1.42156	-0.71980	1.80966
O	2.80866	-0.49909	1.85384
O	0.99552	-1.34421	2.98351
C	3.33827	-1.14441	3.01155
C	2.09997	-1.45940	3.87722
H	4.05452	-0.48236	3.51245
H	3.86944	-2.05747	2.70772
H	1.98043	-0.74041	4.70056
H	2.12643	-2.46717	4.30779
B	0.14539	-2.16568	-0.04181
O	-1.02436	-2.84319	-0.43815
O	1.21325	-3.08911	-0.00575
C	-0.77921	-4.24927	-0.46770
C	0.75772	-4.37683	-0.42217
H	-1.25612	-4.71852	0.40322
H	-1.21746	-4.68699	-1.37271
H	1.10103	-5.13978	0.28572
H	1.18195	-4.61345	-1.40890
H	-0.98349	-0.40036	1.23053
B	-2.66933	-0.13602	-1.42763
O	-1.39427	0.35119	-1.67836
O	-3.08515	-1.04596	-2.36317
C	-0.99118	-0.17677	-2.96378
C	-1.96935	-1.33704	-3.21874
H	-1.08908	0.62466	-3.70600
H	0.05180	-0.49198	-2.90700
H	-2.31261	-1.39030	-4.25619
C	-3.63281	0.31980	-0.28000
C	-4.67646	-0.53229	0.11583
C	-4.32202	1.92165	1.22641
C	-5.55559	-0.12762	1.11869
C	-5.37723	1.13056	1.68911
H	-4.78174	-1.50081	-0.36248
H	-4.16231	2.91485	1.64647
H	-6.36229	-0.77837	1.44628
H	-6.03483	1.49684	2.47247
H	4.68056	-1.02586	-2.49630
H	-1.54641	-2.29845	-2.91518
N	-3.46389	1.54228	0.27626

ENERGIES IN HARTREE:

SCF: -1609.530617
SCF + ZPVE: -1609.069199
Delta H: -1609.036124
Delta G: -1609.139274

m-F

Ir	-0.54999	-0.18186	-0.40519
N	-1.36190	0.84397	1.33116
N	0.50416	1.80835	-0.32056
C	-0.84548	2.05826	1.65631
C	0.21357	2.57710	0.75858
C	-1.33813	2.78127	2.75044
C	-2.38330	2.26373	3.50767
C	-2.93151	1.03456	3.14014
C	-2.39686	0.36228	2.04686
C	0.86169	3.80227	0.96503
C	1.79875	4.24933	0.03885
C	2.06864	3.46417	-1.08130
C	1.40097	2.25031	-1.21721
H	-0.91969	3.74860	3.00231
H	-2.77140	2.81799	4.35711
H	-2.79704	-0.58222	1.69377
H	0.63902	4.40544	1.83751
H	2.30570	5.19798	0.18964
H	2.78558	3.77317	-1.83457
H	1.58251	1.59655	-2.06175
B	-2.10285	0.33440	-1.54958
O	-3.03818	1.30650	-1.16130
O	-2.41699	-0.16602	-2.81192
C	-4.09073	1.34027	-2.12588
C	-3.53842	0.54641	-3.33001
H	-4.33409	2.38015	-2.37410
H	-4.98841	0.87074	-1.70012
H	-3.20589	1.20836	-4.14206
H	-4.26713	-0.15980	-3.74428
B	-1.48996	-1.97373	-0.28229
O	-0.85933	-3.22912	-0.31608
O	-2.86747	-2.15952	-0.03268
C	-1.84577	-4.26133	-0.29472
C	-3.14651	-3.55072	0.13422
H	-1.93014	-4.70182	-1.29701
H	-1.54268	-5.05337	0.40047
H	-4.00889	-3.83267	-0.48034
H	-3.39940	-3.74902	1.18599

H	0.09417	-0.81245	-1.73517
B	2.81521	-1.34723	1.06269
O	1.45272	-1.11748	1.10280
O	3.27223	-2.03117	2.16280
C	0.92242	-1.88108	2.21325
C	2.16497	-2.22867	3.05570
H	0.19312	-1.26717	2.74582
H	0.42249	-2.75961	1.79898
H	2.28690	-1.56464	3.92052
C	3.77778	-0.88255	-0.06372
C	5.15577	-0.75025	0.17568
C	5.99405	-0.31927	-0.84930
C	5.42433	-0.03167	-2.09155
H	5.55904	-0.98267	1.15808
H	7.06333	-0.20433	-0.69565
H	6.04750	0.31967	-2.91364
H	-3.76440	0.60057	3.68391
H	2.16537	-3.26462	3.40703
N	4.11897	-0.16391	-2.36046
C	3.32932	-0.58836	-1.36375
H	2.27566	-0.70933	-1.60866

ENERGIES IN HARTREE:

SCF: -1609.530605
SCF + ZPVE: -1609.068646
Delta H: -1609.035486
Delta G: -1609.139068

***p*-F**

Ir	-0.53655	-0.23841	-0.36662
N	-1.50969	1.03236	1.10205
N	0.41036	1.79489	-0.59159
C	-1.08387	2.31798	1.21943
C	0.02863	2.71807	0.32577
C	-1.70711	3.20694	2.10446
C	-2.78613	2.77736	2.86943
C	-3.23475	1.46513	2.71709
C	-2.57575	0.63086	1.82146
C	0.64787	3.97370	0.38393
C	1.65408	4.28645	-0.52490
C	2.02268	3.33788	-1.47835
C	1.37611	2.10516	-1.47064
H	-1.36557	4.23244	2.18341
H	-3.27619	3.45961	3.55767

H	-2.89584	-0.38852	1.63764
H	0.35429	4.69975	1.13314
H	2.14140	5.25633	-0.48745
H	2.79921	3.53803	-2.20905
H	1.63037	1.32443	-2.17738
B	-2.09017	-0.10966	-1.61509
O	-3.21896	0.68200	-1.35251
O	-2.21879	-0.74548	-2.84926
C	-4.20117	0.41810	-2.35490
C	-3.42225	-0.30310	-3.47484
H	-4.65731	1.35845	-2.68580
H	-4.99076	-0.21736	-1.93033
H	-3.17439	0.37384	-4.30493
H	-3.96412	-1.16217	-3.88631
B	-1.31391	-2.04988	0.09739
O	-0.54893	-3.16859	0.47389
O	-2.68195	-2.36624	0.21701
C	-1.40725	-4.29574	0.65590
C	-2.83116	-3.70128	0.70386
H	-1.27901	-4.98804	-0.18670
H	-1.13567	-4.82667	1.57610
H	-3.54168	-4.24814	0.07383
H	-3.23512	-3.67357	1.72599
H	0.20080	-1.04998	-1.54105
B	2.85524	-0.87457	1.30693
O	1.49306	-0.64430	1.31299
O	3.34190	-1.22020	2.54223
C	0.99184	-1.06227	2.60567
C	2.25620	-1.16991	3.48113
H	0.27686	-0.31794	2.96230
H	0.48233	-2.01824	2.46443
H	2.39427	-0.29779	4.13198
C	3.79467	-0.75311	0.06899
C	5.16438	-0.49412	0.24135
C	5.99192	-0.39759	-0.87719
H	5.58089	-0.36962	1.23701
H	7.05448	-0.18764	-0.75912
H	-4.08688	1.08970	3.27432
H	2.27167	-2.07307	4.09801
C	3.34434	-0.92400	-1.24989
H	2.29891	-1.14106	-1.45198
H	3.92641	-0.95893	-3.32916
C	4.25797	-0.82001	-2.30071
N	5.56093	-0.55329	-2.13622

ENERGIES IN HARTREE:

SCF: -1609.530064
SCF + ZPVE: -1609.068130
Delta H: -1609.035007
Delta G: -1609.138013

***o*-G**

C	2.58187	-1.20750	0.00006
C	3.35668	-0.04258	0.00001
C	2.70156	1.18675	-0.00005
C	1.30715	1.19509	-0.00005
C	0.60614	-0.02198	-0.00000
N	1.24766	-1.21471	0.00005
H	3.26348	2.11731	-0.00009
H	3.06473	-2.18435	0.00010
H	4.44129	-0.10603	0.00001
H	0.75442	2.12987	-0.00010
B	-0.95894	-0.03321	-0.00001
O	-1.68711	1.13429	-0.00027
O	-1.73145	-1.16166	0.00025
C	-3.10835	-0.76202	-0.00042
C	-3.08004	0.79135	0.00043
H	-3.55292	1.22256	0.88947
H	-3.55413	1.22362	-0.88742
H	-3.59924	-1.17531	0.88726
H	-3.59804	-1.17432	-0.88924

ENERGIES IN HARTREE:

SCF: -501.497771
SCF + ZPVE: -501.347956
Delta H: -501.337862
Delta G: -501.384603

***m*-G**

C	-3.33469	-0.08863	-0.00001
C	-2.71568	1.16349	0.00021
C	-1.32407	1.21131	0.00020
C	-0.58989	0.01421	-0.00001
H	-3.31325	2.07060	0.00036
H	-4.42155	-0.16428	-0.00002
H	-0.80267	2.16512	0.00035
B	0.96208	0.00477	-0.00001

O	1.71710	1.15255	0.00122
O	1.71242	-1.14472	-0.00123
C	3.09894	-0.77590	0.00189
C	3.10232	0.77791	-0.00187
H	3.58223	1.19658	-0.89292
H	3.58767	1.20109	0.88401
H	3.58242	-1.20118	-0.88396
H	3.57695	-1.19664	0.89294
C	-1.33052	-1.18079	-0.00020
N	-2.66694	-1.25016	-0.00021
H	-0.80817	-2.13623	-0.00035

ENERGIES IN HARTREE:

SCF: -501.502808
SCF + ZPVE: -501.352635
Delta H: -501.342527
Delta G: -501.389677

p-G

C	-2.71496	1.14223	0.00001
C	-1.32102	1.19522	0.00002
C	-0.58553	0.00000	0.00000
H	-3.30100	2.06041	0.00002
H	-0.81174	2.15476	0.00003
B	0.97168	0.00000	0.00000
O	1.72211	-1.14830	-0.00006
O	1.72211	1.14830	0.00006
C	3.10880	0.77695	-0.00010
C	3.10880	-0.77695	0.00010
H	3.58953	-1.19924	0.88875
H	3.58980	-1.19946	-0.88831
H	3.58981	1.19946	0.88830
H	3.58953	1.19924	-0.88876
C	-1.32102	-1.19522	-0.00001
H	-0.81174	-2.15476	-0.00003
C	-2.71497	-1.14223	-0.00001
N	-3.41515	0.00000	-0.00000
H	-3.30100	-2.06041	-0.00002

ENERGIES IN HARTREE:

SCF: -501.501380
SCF + ZPVE: -501.351208
Delta H: -501.341140

Delta G: -501.387729

H

Ir	0.14463	-0.65655	-0.34331
N	-0.74518	1.32859	-0.20524
N	-2.04961	-1.00106	-0.14815
C	-2.09872	1.40554	-0.10149
C	-2.82466	0.11282	-0.12618
C	-2.74616	2.63801	0.04093
C	-1.99541	3.80897	0.07875
C	-0.60788	3.71788	-0.02075
C	-0.02187	2.46326	-0.15866
C	-4.22156	0.00984	-0.11636
C	-4.81840	-1.24753	-0.11663
C	-4.01024	-2.38441	-0.12855
C	-2.62945	-2.21299	-0.14875
H	-3.82502	2.68612	0.13273
H	-2.48674	4.77105	0.18979
H	1.05133	2.32809	-0.23510
H	-4.84041	0.89932	-0.11437
H	-5.90086	-1.33609	-0.10914
H	-4.43424	-3.38299	-0.12693
H	-1.94454	-3.05322	-0.16439
B	1.19358	-0.48866	1.33936
O	1.04467	0.60978	2.19786
O	2.10103	-1.40620	1.86603
C	2.01609	0.49894	3.23925
C	2.48336	-0.96955	3.17000
H	1.56120	0.76063	4.20150
H	2.83912	1.20031	3.04324
H	1.98469	-1.59444	3.92448
H	3.56621	-1.08108	3.29528
B	2.00249	-0.20170	-1.01931
O	2.67756	-0.92047	-2.00578
O	2.75104	0.94654	-0.67687
C	3.94810	-0.32303	-2.25546
C	3.89576	1.03843	-1.52747
H	4.73763	-0.97345	-1.85560
H	4.10545	-0.22049	-3.33557
H	4.78975	1.23575	-0.92474
H	3.76349	1.87660	-2.22605
H	0.65170	-2.17904	-0.41812
H	0.02015	4.60230	0.00972

ENERGIES IN HARTREE:

SCF: -1108.015207
SCF + ZPVE: -1107.704925
Delta H: -1107.682602
Delta G: -1107.759337

B2eg2 for S1

B	0.00000	0.00000	-0.83785
O	-0.81381	0.81968	-1.62153
O	0.81381	-0.81968	-1.62153
C	0.54646	-0.54995	-3.05532
C	-0.54646	0.54995	-3.05532
B	0.00000	0.00000	0.83785
O	-0.81381	-0.81968	1.62153
O	0.81381	0.81968	1.62153
C	-0.54646	-0.54995	3.05532
C	0.54646	0.54995	3.05532
H	-0.21714	1.48313	-3.51672
H	-1.48193	0.22634	-3.51612
H	1.48193	-0.22634	-3.51612
H	0.21714	-1.48313	-3.51672
H	1.48193	0.22634	3.51612
H	0.21714	1.48313	3.51672
H	-1.48193	-0.22634	3.51612
H	-0.21714	-1.48313	3.51672

ENERGIES IN HARTREE:

SCF: -507.835696
SCF + ZPVE: -507.695586
Delta H: -507.684999
Delta G: -507.732080

HBeg for S2

B	0.00000	0.00000	1.22860
O	0.00000	1.14827	0.48712
O	0.00000	-1.14827	0.48712
C	0.00043	-0.77639	-0.90220
C	-0.00043	0.77639	-0.90220
H	0.88946	-1.19950	-1.38134
H	-0.88763	-1.20051	-1.38220
H	0.88763	1.20051	-1.38220
H	0.00000	0.00000	2.41660

H	-0.88946	1.19950	-1.38134
---	----------	---------	----------

ENERGIES IN HARTREE:

SCF:	-254.518686
SCF + ZPVE:	-254.439231
Delta H:	-254.433745
Delta G:	-254.466471

Pyridine BF₃

C	-0.73100	-1.16500	-0.03300
C	-2.11900	-1.20300	0.00500
C	-2.82600	-0.00000	0.02500
C	-2.11900	1.20300	0.00500
C	-0.73100	1.16500	-0.03300
N	-0.06200	0.00000	-0.04100
H	-3.91100	-0.00000	0.05400
H	-0.11200	-2.05300	-0.06400
H	-2.63100	-2.16000	0.01200
H	-2.63100	2.16000	0.01200
H	-0.11200	2.05300	-0.06400
B	1.61700	0.00000	0.00700
F	1.97300	1.15800	-0.64400
F	1.97300	-1.15800	-0.64500
F	1.93100	-0.00000	1.34300

ENERGIES IN HARTREE:

SCF:	-572.865924
SCF + ZPVE:	-572.761246
Delta H:	-572.751999
Delta G:	-572.795592

I

C	2.95000	0.75300	-0.20600
C	4.15800	1.45800	-0.26600
C	4.14500	2.84900	-0.21500
C	2.92300	3.50900	-0.10500
C	1.75400	2.75100	-0.06400
N	1.76500	1.40700	-0.11600
H	5.07700	3.40500	-0.26200
H	5.10000	0.93100	-0.36200
H	2.86500	4.59200	-0.05800
H	0.76800	3.19900	0.01200

C	1.49500	-2.60200	-0.25200
C	2.58000	-3.47100	-0.18500
C	3.86500	-2.93100	-0.13400
C	4.01600	-1.54800	-0.14500
C	2.88100	-0.73100	-0.22100
N	1.63900	-1.26700	-0.28300
H	4.73700	-3.57500	-0.07700
H	0.47100	-2.95800	-0.26700
H	2.41400	-4.54300	-0.16600
H	5.00700	-1.11400	-0.08100
Ir	-0.12600	0.13400	-0.29500
B	-1.59500	1.55400	-0.23500
B	-0.76400	-0.45700	1.49800
B	-1.56900	-1.11200	-0.96100
O	-0.17800	-1.53900	2.16700
O	-1.75500	0.12900	2.28200
O	-1.31300	2.92400	-0.02800
O	-2.97000	1.38800	-0.38500
O	-2.03900	-1.03100	-2.27700
O	-2.12000	-2.23700	-0.32500
C	-2.87300	-2.15700	-2.55100
C	-3.12900	-2.79500	-1.17000
C	-2.53900	3.64500	0.12000
C	-3.62600	2.65200	-0.34600
C	-0.95500	-1.81300	3.33300
C	-1.78900	-0.53300	3.54700
H	-3.79500	-1.82400	-3.04200
H	-2.35100	-2.84300	-3.23300
H	-4.11900	-2.53200	-0.77300
H	-3.04200	-3.88800	-1.17900
H	-2.50600	4.55900	-0.48400
H	-2.66500	3.93100	1.17300
H	-4.00700	2.89700	-1.34700
H	-4.47800	2.60700	0.34200
H	-2.82800	-0.74200	3.82700
H	-1.35000	0.12200	4.31300
H	-1.59200	-2.68900	3.14500
H	-0.29200	-2.04000	4.17700

ENERGIES IN HARTREE:

SCF:	-1362.164493
SCF + ZPVE:	-1361.791875
Delta H:	-1361.764307
Delta G:	-1361.853557

o-J

Ir	-0.32200	-0.17200	-0.15300
B	-2.07700	-0.40700	0.98100
O	-2.33800	0.38700	2.09700
O	-3.13200	-1.28600	0.75400
C	-3.53800	-0.07200	2.72900
C	-4.17300	-1.03300	1.70200
B	-1.63100	-0.92200	-1.56600
O	-2.34800	-0.07400	-2.42700
O	-1.92600	-2.24200	-1.84100
C	-3.09900	-0.88100	-3.34600
C	-3.03800	-2.29300	-2.73300
B	0.04300	-2.08400	0.49600
O	0.49500	-3.12100	-0.29500
O	-0.06600	-2.47800	1.83300
C	0.92300	-4.19200	0.54600
C	0.33700	-3.85300	1.93400
C	0.41700	2.31400	1.65600
C	-0.26200	2.95800	0.50400
N	0.47200	0.96300	1.65400
N	-0.80000	2.13300	-0.42100
C	0.92900	3.05500	2.72800
C	1.48000	2.39300	3.82100
C	1.48800	1.00300	3.82500
C	0.97300	0.32600	2.72300
C	-0.38700	4.35000	0.38900
C	-1.09900	4.89300	-0.67500
C	-1.68200	4.03100	-1.60100
C	-1.50300	2.65900	-1.43600
C	1.54700	0.23200	-1.40600
C	1.29100	1.01400	-2.55100
C	2.31200	1.58300	-3.29900
C	3.63300	1.34900	-2.91600
H	0.45600	-0.94700	-1.36000
H	0.94200	-0.75400	2.68100
H	1.88600	0.43800	4.66100
H	1.88000	2.95900	4.65800
H	0.88900	4.13700	2.72300
H	0.06300	5.00900	1.12100
H	-1.20200	5.97000	-0.77100
H	-2.26400	4.40300	-2.43800
H	-1.93700	1.93800	-2.12000
H	-5.02900	-0.58100	1.18400
H	-4.50000	-1.97900	2.14700

H	-4.17800	0.78500	2.96600
H	-3.27800	-0.58000	3.66600
H	1.06800	-3.95800	2.74300
H	-0.54300	-4.46100	2.17800
H	2.01800	-4.21300	0.54800
H	0.54800	-5.14200	0.14900
H	-2.87900	-3.07800	-3.47900
H	-3.94500	-2.52800	-2.16100
H	-2.62300	-0.83600	-4.33500
H	-4.11700	-0.48800	-3.43100
H	4.47500	1.76800	-3.45700
H	2.08400	2.19200	-4.17200
H	0.25800	1.15400	-2.84800
C	3.85500	0.52700	-1.82800
H	4.85000	0.27300	-1.49000
F	3.41900	-2.35400	-0.70200
F	4.66500	-0.73900	0.35400
F	2.54200	-1.18300	1.07200
N	2.85100	-0.03000	-1.10400
B	3.39700	-1.16100	-0.01500

ENERGIES IN HARTREE:

SCF:	-1934.996456
SCF + ZPVE:	-1934.522447
Delta H:	-1934.485566
Delta G:	-1934.594242

m-J

Ir	-0.55100	-0.20200	-0.18600
B	-2.27600	-0.43400	1.02000
O	-2.61500	0.51600	1.98400
O	-3.21300	-1.46000	1.00100
C	-3.74600	0.04800	2.72800
C	-4.26000	-1.16900	1.93100
B	-1.82900	-1.33100	-1.37600
O	-2.74000	-0.73400	-2.25700
O	-1.91600	-2.70900	-1.44600
C	-3.41700	-1.76900	-2.98400
C	-3.07000	-3.05700	-2.21100
B	0.06900	-1.97000	0.62800
O	0.78600	-2.95200	-0.04100
O	-0.04600	-2.28900	1.98700
C	1.01400	-4.05700	0.83900

C	0.66200	-3.51300	2.24100
C	-0.04700	2.51200	1.22600
C	-0.84600	2.91200	0.04100
N	0.16200	1.18600	1.40200
N	-1.23900	1.91700	-0.78800
C	0.46600	3.44100	2.13900
C	1.18500	2.99900	3.24500
C	1.36400	1.63100	3.42700
C	0.83200	0.75800	2.48300
C	-1.20300	4.24300	-0.21500
C	-1.97000	4.54800	-1.33500
C	-2.37500	3.51300	-2.17500
C	-1.99100	2.21100	-1.86200
C	1.40500	0.18400	-1.20300
C	1.58700	1.18300	-2.17300
C	2.86700	1.59400	-2.55100
C	3.96800	1.00500	-1.94800
H	0.17500	-0.80300	-1.53100
H	0.91500	-0.31800	2.58300
H	1.91000	1.23600	4.27800
H	1.59200	3.71500	3.95300
H	0.31400	4.50300	1.99000
H	-0.89500	5.03600	0.45500
H	-2.25000	5.57700	-1.54000
H	-2.98100	3.70000	-3.05500
H	-2.29900	1.35900	-2.45700
H	-5.18100	-0.94400	1.37700
H	-4.44300	-2.04600	2.56000
H	-4.48700	0.85100	2.81000
H	-3.42100	-0.22600	3.74000
H	1.55700	-3.29300	2.83800
H	0.02100	-4.19000	2.81500
H	2.05600	-4.38000	0.75500
H	0.36200	-4.88800	0.54200
H	-2.83600	-3.90200	-2.86700
H	-3.87500	-3.35200	-1.52700
H	-3.04000	-1.78900	-4.01500
H	-4.49000	-1.55700	-3.00900
H	4.99400	1.27200	-2.17000
H	3.01300	2.36400	-3.30200
H	0.72200	1.64900	-2.63900
N	3.80800	0.03100	-1.03600
C	2.57600	-0.39400	-0.70100
H	2.56000	-1.23200	-0.01700
B	5.11500	-0.57600	-0.22200
F	4.84100	-1.91400	-0.03100

F	6.20000	-0.33600	-1.04200
F	5.16500	0.13300	0.96200

ENERGIES IN HARTREE:

SCF:	-1935.005849
SCF + ZPVE:	-1934.531513
Delta H:	-1934.494468
Delta G:	-1934.60545

***p*-J**

Ir	-0.66200	-0.22300	-0.12400
B	-2.62100	0.23500	0.55100
O	-3.32600	-0.48300	1.50400
O	-3.33100	1.36400	0.15200
C	-4.63800	0.07700	1.63300
C	-4.55500	1.43100	0.89500
B	-1.91100	-0.73300	-1.70400
O	-1.61600	-0.33600	-3.01600
O	-3.12400	-1.39900	-1.66400
C	-2.73300	-0.65500	-3.85800
C	-3.59600	-1.59900	-2.99900
B	-0.99000	-2.09200	0.64700
O	-1.38800	-3.22400	-0.04900
O	-0.72500	-2.42500	1.98500
C	-1.37100	-4.35800	0.82000
C	-1.17600	-3.76300	2.23000
C	0.29800	2.21900	1.56100
C	0.06900	2.81300	0.22100
N	0.00400	0.90300	1.70700
N	-0.35100	1.96800	-0.74700
C	0.78600	2.96500	2.64200
C	0.96000	2.35700	3.88000
C	0.63500	1.01000	4.01800
C	0.16000	0.31800	2.90700
C	0.25800	4.17600	-0.04500
C	0.01500	4.66600	-1.32400
C	-0.41800	3.78400	-2.31200
C	-0.59000	2.44300	-1.97900
C	1.48800	-0.59900	-0.53900
C	2.24900	0.18000	-1.43200
C	3.63300	0.11200	-1.43100
H	0.16100	-1.08800	-1.25300
H	-0.11300	-0.73000	2.95100
H	0.74700	0.49200	4.96400

H	1.34300	2.92800	4.72000
H	1.03800	4.01100	2.51900
H	0.58700	4.85200	0.73400
H	0.16000	5.72000	-1.54100
H	-0.62200	4.12100	-3.32300
H	-0.92900	1.70700	-2.70000
H	-4.50800	2.28200	1.58700
H	-5.39200	1.59500	0.20700
H	-4.89000	0.18100	2.69300
H	-5.36300	-0.60400	1.16900
H	-0.43100	-4.30000	2.82700
H	-2.11600	-3.72300	2.79600
H	-0.54600	-5.02200	0.53200
H	-2.31000	-4.91200	0.72000
H	-3.45500	-2.65300	-3.27200
H	-4.66500	-1.36700	-3.04900
H	-2.37200	-1.12000	-4.78100
H	-3.26400	0.27100	-4.11800
H	4.25600	0.69700	-2.09800
H	1.76400	0.84600	-2.13800
C	2.21900	-1.48000	0.28200
H	1.71000	-2.14100	0.97500
N	4.30100	-0.70100	-0.59200
C	3.60500	-1.49700	0.24000
H	4.20700	-2.14600	0.86500
B	5.95100	-0.65300	-0.52200
F	6.25500	0.31700	0.41000
F	6.33200	-1.91900	-0.12500
F	6.35700	-0.31900	-1.79800

ENERGIES IN HARTREE:

SCF: -1935.005321
SCF + ZPVE: -1934.530955
Delta H: -1934.493956
Delta G: -1934.604521

***o*-K**

Ir	-0.33500	-0.14200	-0.26900
B	-2.10000	0.06500	0.96200
O	-2.28700	1.26900	1.63600
O	-3.07400	-0.85200	1.32300
C	-3.48300	1.18800	2.42100
C	-3.85900	-0.30700	2.38900
B	-2.14400	-0.54000	-1.26600

O	-2.86600	0.49500	-1.87900
O	-2.78800	-1.75700	-1.41900
C	-4.01400	-0.09100	-2.51300
C	-4.11000	-1.49400	-1.88600
B	-0.20500	-2.12900	0.21700
O	0.08100	-3.13000	-0.69700
O	-0.38200	-2.65000	1.49800
C	0.03900	-4.38800	-0.01800
C	0.05300	-4.01600	1.47600
C	0.84600	2.03200	1.47600
C	0.46900	2.79900	0.26700
N	0.55400	0.70700	1.48500
N	-0.25700	2.13100	-0.65600
C	1.41900	2.64400	2.59400
C	1.68000	1.89700	3.73700
C	1.34900	0.54700	3.73900
C	0.79300	-0.01300	2.59400
C	0.80200	4.14800	0.08000
C	0.34800	4.81400	-1.05300
C	-0.43900	4.12400	-1.97400
C	-0.71200	2.78000	-1.73500
C	1.57500	-0.22600	-1.37500
C	1.44500	0.16000	-2.73300
C	2.49000	0.11900	-3.64300
C	3.74000	-0.32400	-3.20900
H	-0.75600	-0.78500	-1.71600
H	0.52400	-1.05900	2.53900
H	1.52400	-0.08100	4.60600
H	2.12400	2.36700	4.60900
H	1.64400	3.70300	2.58100
H	1.41400	4.67200	0.80300
H	0.60100	5.85900	-1.20900
H	-0.83200	4.60900	-2.86200
H	-1.33200	2.19300	-2.40300
H	-4.92200	-0.48000	2.18700
H	-3.59600	-0.82300	3.32100
H	-4.25400	1.82300	1.96400
H	-3.28500	1.56000	3.43200
H	1.06200	-4.07100	1.90000
H	-0.62700	-4.62500	2.08100
H	0.90200	-4.99400	-0.31400
H	-0.87800	-4.92000	-0.30400
H	-4.40800	-2.26800	-2.60100
H	-4.80000	-1.51400	-1.03300
H	-3.84400	-0.13300	-3.59700
H	-4.89400	0.53200	-2.32200

H	4.59600	-0.39000	-3.87100
H	2.33400	0.42100	-4.67600
H	0.47300	0.49300	-3.07900
C	3.86100	-0.68600	-1.88400
H	4.79600	-1.03300	-1.46600
F	2.30100	-1.83400	1.07600
F	4.49600	-1.60800	0.49000
F	3.32900	0.23200	1.20100
N	2.82900	-0.63400	-1.00200
B	3.25700	-0.98500	0.53200

ENERGIES IN HARTREE:

SCF:	-1935.019624
SCF + ZPVE:	-1934.542071
Delta H:	-1934.505826
Delta G:	-1934.610923

m-K

Ir	-0.61300	-0.17500	-0.31800
N	-0.65200	2.10800	-0.61100
N	0.32600	0.67600	1.45100
C	0.06100	2.79700	0.30700
C	0.55800	2.01600	1.46400
C	1.21900	2.61200	2.54400
C	1.64700	1.83400	3.61300
C	1.39000	0.46700	3.59100
C	0.72400	-0.07400	2.49600
C	0.29200	4.17100	0.15900
C	-0.23300	4.83800	-0.94300
C	-0.98700	4.12000	-1.86900
C	-1.17100	2.75500	-1.66400
B	-2.52800	-0.52000	-1.09400
O	-3.14000	0.43600	-1.91400
O	-3.32600	-1.65100	-0.97800
C	-4.47300	-0.00500	-2.19300
C	-4.44500	-1.50800	-1.85900
B	-2.28200	-0.19700	1.06500
O	-3.17600	0.84100	1.29200
O	-2.37200	-1.16300	2.05200
C	-3.87000	0.59400	2.52400
C	-3.47000	-0.84500	2.91500
B	-0.29300	-2.17500	-0.02200
O	0.34700	-2.69800	1.10100
O	-0.57700	-3.17800	-0.93400

C	0.38600	-4.12800	1.00000
C	-0.06400	-4.42200	-0.44900
C	1.33800	-0.13500	-1.20000
C	1.55900	0.21200	-2.54800
C	2.50200	-0.43100	-0.48200
C	2.84500	0.26800	-3.09100
H	-1.02000	-0.75200	-1.77500
H	-1.76600	2.14700	-2.33500
H	-1.42500	4.60100	-2.73800
H	-0.05700	5.90200	-1.07100
H	0.88100	4.71700	0.88600
H	1.40100	3.68000	2.55100
H	2.17300	2.29100	4.44600
H	1.70500	-0.18600	4.39800
H	0.50900	-1.13300	2.41700
H	0.71300	0.44100	-3.19100
H	2.48200	-0.76400	0.54800
H	3.00500	0.52700	-4.13300
H	-0.84700	-5.18600	-0.50200
H	0.77100	-4.73700	-1.08600
H	-0.29700	-4.55500	1.74500
H	1.40100	-4.47900	1.21400
H	-3.15100	-0.93200	3.95900
H	-4.27900	-1.56500	2.73900
H	-3.54900	1.33600	3.26600
H	-4.94700	0.71200	2.36400
H	-5.17500	0.54600	-1.55400
H	-4.71600	0.20100	-3.24100
H	-5.35300	-1.85600	-1.35700
H	-4.28000	-2.12700	-2.75100
C	3.93300	-0.01600	-2.28000
N	3.74900	-0.35300	-0.99300
B	5.03800	-0.56800	0.00600
F	4.67700	-1.58600	0.87000
F	6.10000	-0.89100	-0.81800
F	5.21200	0.63900	0.65800
H	4.96200	0.00800	-2.61500

ENERGIES IN HARTREE:

SCF: -1935.025497
SCF + ZPVE: -1934.548765
Delta H: -1934.511729
Delta G: -1934.622156

p-K

Ir	-0.52300	-0.27500	-0.17400
N	-0.57900	1.82700	-1.06800
N	-0.47200	1.08500	1.51900
C	-0.55700	2.83000	-0.16300
C	-0.51700	2.42100	1.26100
C	-0.50900	3.34700	2.31100
C	-0.44300	2.90500	3.62800
C	-0.39000	1.53500	3.87300
C	-0.41100	0.65700	2.79500
C	-0.55300	4.17100	-0.57100
C	-0.56800	4.47200	-1.92900
C	-0.59100	3.42700	-2.85100
C	-0.59900	2.11900	-2.37600
B	-1.94300	-1.06100	-1.51000
O	-2.20100	-0.42400	-2.72700
O	-2.66800	-2.24000	-1.40600
C	-3.26900	-1.12100	-3.37700
C	-3.31500	-2.48300	-2.65900
B	-2.62300	-0.16000	0.37400
O	-3.47900	0.86200	-0.01600
O	-3.16600	-0.90500	1.40300
C	-4.63200	0.85000	0.84000
C	-4.51300	-0.47300	1.62700
B	-0.34900	-2.09000	0.76400
O	-0.36300	-2.28300	2.14500
O	-0.10500	-3.28900	0.10900
C	-0.04100	-3.64900	2.43600
C	-0.09500	-4.35500	1.06400
C	1.62000	-0.23100	-0.21500
C	2.39800	0.85000	0.25200
C	2.38000	-1.29100	-0.76300
C	3.78300	0.84800	0.16900
C	3.76400	-1.24100	-0.82400
H	-0.28600	-1.20700	-1.47700
H	-0.64600	1.26800	-3.04300
H	-0.60200	3.61400	-3.91900
H	-0.56000	5.50600	-2.25800
H	-0.53100	4.97400	0.15600
H	-0.55000	4.40900	2.10300
H	-0.43100	3.62100	4.44400
H	-0.33400	1.14000	4.88200
H	-0.38500	-0.41900	2.92400
H	1.93700	1.73000	0.68700
H	1.88700	-2.18100	-1.13800
H	4.36500	-2.03500	-1.25100

H	4.39700	1.67400	0.50900
H	-1.00600	-4.95300	0.94100
H	0.77100	-5.00000	0.88300
H	-0.76700	-4.05000	3.15200
H	0.95700	-3.69300	2.88900
H	-4.68400	-0.35000	2.70200
H	-5.19900	-1.24300	1.25200
H	-4.59800	1.73100	1.49400
H	-5.53900	0.90900	0.23000
H	-4.20100	-0.55500	-3.24500
H	-3.05700	-1.20300	-4.44700
H	-4.33300	-2.84500	-2.48200
H	-2.76000	-3.25700	-3.20500
N	4.46000	-0.18700	-0.35700
B	6.10400	-0.19400	-0.35800
F	6.47300	1.13500	-0.46200
F	6.48900	-0.76100	0.84000
F	6.46500	-0.95700	-1.45300

ENERGIES IN HARTREE:

SCF: -1935.023851
SCF + ZPVE: -1934.546787
Delta H: -1934.509842
Delta G: -1934.619664

***o*-L**

Ir	-0.43800	0.01100	-0.50700
C	0.75600	2.03000	1.45100
C	1.29200	2.44500	0.13500
N	0.05300	0.87300	1.47100
N	0.94600	1.67900	-0.92700
C	0.97300	2.76300	2.62000
C	0.48200	2.28300	3.82900
C	-0.20400	1.07200	3.84200
C	-0.39300	0.39500	2.64000
C	2.12900	3.55400	-0.03800
C	2.60000	3.87400	-1.30600
C	2.23100	3.07600	-2.39000
C	1.40300	1.98700	-2.15100
B	-1.93200	1.43200	-0.77600
O	-1.78200	2.73900	-0.31800
O	-3.13200	1.28700	-1.46100
C	-2.87800	3.52900	-0.79400
C	-3.88900	2.49400	-1.33100

B	-2.24700	-0.86700	0.01300
O	-3.04300	-1.71800	-0.74100
O	-2.88600	-0.54000	1.21600
C	-4.33500	-1.78200	-0.13600
C	-4.10100	-1.29000	1.30300
C	1.40200	-1.44200	-0.84200
C	3.86400	-1.83800	-2.15100
B	-0.23800	-2.13300	-0.13600
O	-0.52300	-3.17100	-1.03800
O	-0.34900	-2.59900	1.17800
C	-1.02600	-4.28000	-0.30000
C	-0.55000	-4.01300	1.13900
H	-0.83800	-0.39200	-1.99800
H	4.84000	-1.98000	-2.60400
H	-0.58600	0.64600	4.76300
H	0.64400	2.84300	4.74600
H	-0.91500	-0.54900	2.58900
H	1.52100	3.69700	2.59300
H	3.25000	4.73300	-1.44500
H	2.57600	3.28700	-3.39600
H	1.08000	1.32600	-2.94700
H	2.42200	4.15700	0.81200
H	-4.72000	-2.80600	-0.18700
H	-5.01800	-1.12200	-0.68700
H	-3.96200	-2.12200	2.00700
H	-4.90500	-0.64900	1.67900
H	-2.12100	-4.29200	-0.37500
H	-0.63200	-5.21200	-0.72100
H	-1.28300	-4.30000	1.90000
H	0.40000	-4.51900	1.36300
H	-3.27800	4.13300	0.02600
H	-2.51900	4.20600	-1.58000
H	-4.71700	2.32500	-0.63000
H	-4.31000	2.76800	-2.30400
C	1.47700	-1.74800	-2.22400
H	0.54500	-1.86700	-2.75700
H	2.69700	-2.14400	-3.95000
C	2.68100	-1.92600	-2.88500
H	4.64000	-1.53300	-0.16200
N	2.58700	-1.38200	-0.15800
C	3.76700	-1.58400	-0.79700
B	2.84200	-0.95200	1.43700
F	1.76100	-1.31200	2.18900
F	3.06200	0.42100	1.38600
F	3.98900	-1.62900	1.82000

ENERGIES IN HARTREE:

SCF: -1935.001820
SCF + ZPVE: -1934.525592
Delta H: -1934.489809
Delta G: -1934.594223

m-L

Ir	-0.77500	-0.02500	-0.49100
C	0.78100	1.80800	1.41400
C	0.90700	2.46100	0.09000
N	0.04000	0.67200	1.45700
N	0.28200	1.85400	-0.94600
C	1.39700	2.30800	2.56600
C	1.24100	1.63800	3.77500
C	0.46800	0.48100	3.80700
C	-0.11500	0.03000	2.62600
C	1.63400	3.64200	-0.11500
C	1.70400	4.19600	-1.38700
C	1.04700	3.56200	-2.44100
C	0.34900	2.39000	-2.17400
B	-2.45700	1.25000	-0.32700
O	-2.35300	2.47100	0.33700
O	-3.72100	1.10100	-0.88200
C	-3.56400	3.21400	0.14900
C	-4.54600	2.19700	-0.46900
B	-2.41100	-1.08600	0.22800
O	-3.24700	-1.94200	-0.46900
O	-2.82800	-0.96500	1.56100
C	-4.37600	-2.24100	0.35200
C	-3.92000	-1.86700	1.77400
C	1.18100	-0.96300	-1.00400
C	2.23900	-0.91600	-0.09300
B	-0.41300	-2.10500	-0.41500
O	-0.60600	-3.01700	-1.44900
O	-0.15000	-2.76600	0.79400
C	-0.64100	-4.32700	-0.88300
C	0.01700	-4.15900	0.50000
H	-1.33000	-0.35900	-1.94700
H	0.32100	-0.07800	4.72500
H	1.72400	2.01300	4.67200
H	-0.72400	-0.86200	2.58900
H	2.00500	3.20300	2.52300
H	2.26800	5.11000	-1.55200

H	1.07500	3.95900	-3.45100
H	-0.18100	1.84900	-2.94800
H	2.14600	4.12200	0.71000
H	-4.64100	-3.29900	0.24700
H	-5.22800	-1.63300	0.02100
H	-3.56100	-2.73900	2.33700
H	-4.69800	-1.37000	2.36300
H	-1.68600	-4.65400	-0.80100
H	-0.10400	-5.02600	-1.53300
H	-0.45600	-4.75900	1.28400
H	1.08900	-4.39600	0.47800
H	-3.90400	3.60800	1.11200
H	-3.36600	4.06200	-0.52000
H	-5.28100	1.83600	0.26100
H	-5.08700	2.59200	-1.33500
H	2.07900	-0.86200	0.97600
C	1.55400	-1.13200	-2.35200
H	0.77800	-1.23300	-3.10400
C	3.87500	-1.05800	-1.75000
H	4.93900	-1.06100	-1.95400
C	2.89700	-1.18400	-2.72700
H	3.18900	-1.31400	-3.76500
B	4.67100	-0.62300	0.70200
N	3.53800	-0.92700	-0.45600
F	4.34300	-1.43400	1.76800
F	5.88800	-0.91900	0.12300
F	4.52200	0.72200	0.99800

ENERGIES IN HARTREE:

SCF: -1935.019581
SCF + ZPVE: -1934.543048
Delta H: -1934.506861
Delta G: -1934.615069

p-L

Ir	-0.74600	-0.09000	-0.43000
C	-0.09200	2.04600	1.67100
C	0.44200	2.60400	0.40500
N	-0.65300	0.81300	1.59800
N	0.28500	1.84200	-0.70300
C	-0.02000	2.73100	2.89000
C	-0.52200	2.13600	4.04300
C	-1.08600	0.86500	3.95400

C	-1.13500	0.23900	2.71100
C	1.09600	3.84000	0.32800
C	1.58100	4.28900	-0.89500
C	1.40700	3.49400	-2.02600
C	0.75300	2.27500	-1.88300
B	-2.46800	1.02300	-0.91900
O	-2.64100	2.31800	-0.43300
O	-3.51600	0.67300	-1.76000
C	-3.80000	2.89800	-1.04500
C	-4.50200	1.71000	-1.73500
B	-2.41700	-1.29300	-0.14800
O	-2.91900	-2.27400	-0.98700
O	-3.23700	-1.13700	0.97800
C	-4.22600	-2.62900	-0.53200
C	-4.26700	-2.13200	0.92400
C	1.34100	-0.90800	-0.20600
C	2.07600	-0.78000	0.98900
C	3.46100	-0.69300	0.96800
B	-0.22500	-2.11500	-0.05800
O	-0.02500	-3.10700	-1.01100
O	-0.34300	-2.67200	1.22900
C	-0.20100	-4.37300	-0.37700
C	-0.03500	-4.06800	1.12400
H	-0.79200	-0.56800	-1.94900
H	4.06300	-0.58300	1.86200
H	-1.48700	0.36000	4.82700
H	-0.47000	2.65800	4.99400
H	-1.57500	-0.74000	2.57500
H	0.42100	3.71800	2.94300
H	2.09400	5.24400	-0.96100
H	1.77400	3.80100	-3.00000
H	0.58900	1.61100	-2.72300
H	1.23400	4.44700	1.21500
H	-4.37000	-3.71100	-0.62600
H	-4.96900	-2.12000	-1.15900
H	-4.03300	-2.93100	1.64100
H	-5.22600	-1.68400	1.20300
H	-1.20600	-4.75100	-0.60800
H	0.54000	-5.08300	-0.75700
H	-0.71300	-4.64300	1.76300
H	0.99500	-4.23700	1.46500
H	-4.41800	3.37600	-0.27900
H	-3.48100	3.66600	-1.76200
H	-5.37500	1.36100	-1.16700
H	-4.82200	1.93300	-2.75800
H	1.56800	-0.75500	1.94600

C	2.10900	-1.01900	-1.38300
H	1.61900	-1.19300	-2.33500
N	4.15200	-0.73400	-0.18400
C	3.49100	-0.91900	-1.34300
H	4.11800	-0.98300	-2.22500
B	5.78000	-0.45700	-0.18700
F	5.91900	0.91000	-0.32600
F	6.22900	-0.92000	1.03400
F	6.26800	-1.16000	-1.26900

ENERGIES IN HARTREE:

SCF:	-1935.017124
SCF + ZPVE:	-1934.540688
Delta H:	-1934.504586
Delta G:	-1934.612023

***o*-M**

Ir	-0.75000	-0.22200	-0.25500
N	-2.23100	0.97400	0.82300
N	-0.31500	1.91200	-0.79800
C	-2.21000	2.31900	0.62700
C	-1.08200	2.84300	-0.17800
C	-3.21600	3.14100	1.14800
C	-4.25300	2.58100	1.88600
C	-4.26900	1.20000	2.07600
C	-3.24700	0.43400	1.52400
C	-0.79300	4.20700	-0.29400
C	0.30300	4.61400	-1.05200
C	1.09000	3.64900	-1.67400
C	0.74100	2.30900	-1.52100
H	-3.20000	4.20900	0.96200
H	-5.03900	3.21100	2.29200
H	-3.22700	-0.64700	1.60900
H	-1.39900	4.94500	0.21900
H	0.54400	5.66900	-1.13900
H	1.97300	3.91200	-2.24500
H	1.32800	1.51800	-1.96900
B	-2.12600	-0.78100	-1.59400
O	-3.38800	-0.17500	-1.69900
O	-1.99600	-1.79100	-2.55200
C	-4.17100	-0.90100	-2.64600
C	-3.15100	-1.79000	-3.38800
H	-4.69400	-0.20300	-3.31000
H	-4.92500	-1.49800	-2.11300
H	-2.88800	-1.37900	-4.37400

H	-3.50600	-2.81700	-3.53300
B	-1.08700	-2.06400	0.51300
O	-0.08600	-2.98400	0.89900
O	-2.34300	-2.60200	0.86600
C	-0.68700	-4.19600	1.36000
C	-2.17400	-3.83800	1.56000
H	-0.55300	-4.97900	0.60200
H	-0.19900	-4.52700	2.28400
H	-2.85300	-4.59200	1.14700
H	-2.42500	-3.69900	2.62100
H	0.31400	-0.96900	-1.19400
B	2.25500	-0.58400	1.37000
O	1.17000	0.27400	1.37900
O	2.50800	-1.16300	2.57800
C	0.86300	0.50400	2.77500
C	1.50200	-0.69600	3.49400
H	1.32300	1.45400	3.06700
H	-0.22000	0.56200	2.89200
H	1.97400	-0.42600	4.44300
C	3.02700	-1.06700	0.07200
C	2.75100	-2.31500	-0.49900
C	4.72000	-0.70700	-1.52400
C	3.47800	-2.74800	-1.60500
C	4.48400	-1.93100	-2.12600
H	1.94200	-2.90400	-0.08200
H	5.49100	-0.02300	-1.85800
H	3.26100	-3.71100	-2.05800
H	5.07900	-2.23500	-2.98100
H	-5.06300	0.71400	2.63300
H	0.78600	-1.50800	3.66200
N	4.00200	-0.29200	-0.46200
B	4.30500	1.20300	0.12300
F	3.59600	2.08800	-0.67100
F	3.83600	1.17400	1.43700
F	5.66500	1.38800	0.03600

ENERGIES IN HARTREE:

SCF: -1935.048850
SCF + ZPVE: -1934.571767
Delta H: -1934.534699
Delta G: -1934.645741

m-M

Ir	0.79300	-0.09500	0.26400
----	---------	----------	---------

N	2.20500	1.14300	-0.84400
N	-0.20200	1.90000	0.04100
C	1.81500	2.40500	-1.16900
C	0.45000	2.79500	-0.74300
C	2.68600	3.28000	-1.83000
C	3.97200	2.86200	-2.15300
C	4.36900	1.57400	-1.79300
C	3.46000	0.75200	-1.13600
C	-0.14800	4.01200	-1.09200
C	-1.42400	4.31300	-0.62100
C	-2.07600	3.39600	0.20300
C	-1.42100	2.20600	0.51100
H	2.36800	4.28700	-2.07400
H	4.65400	3.53500	-2.66400
H	3.71800	-0.24900	-0.80500
H	0.36800	4.71600	-1.73500
H	-1.90000	5.24900	-0.89700
H	-3.07300	3.56300	0.59200
H	-1.88900	1.46500	1.14600
B	1.78800	0.13700	1.97900
O	2.79500	1.09900	2.14100
O	1.60200	-0.58000	3.15900
C	3.39600	0.92100	3.42400
C	2.42900	-0.01900	4.17800
H	3.51800	1.89300	3.91600
H	4.39100	0.47200	3.29900
H	1.80100	0.52600	4.89700
H	2.94700	-0.82000	4.71700
B	1.71800	-1.90000	0.26100
O	1.09500	-3.13600	-0.00400
O	3.10200	-2.11900	0.43500
C	2.02900	-4.19700	0.20300
C	3.40500	-3.50100	0.24000
H	1.79900	-4.70100	1.15100
H	1.94300	-4.93300	-0.60500
H	4.04200	-3.86000	1.05600
H	3.95700	-3.62500	-0.70300
H	-0.32200	-0.86800	1.12400
B	-1.35300	-1.83400	-1.72600
O	-0.56600	-0.73500	-2.02100
O	-1.02700	-2.95200	-2.43500
C	0.29800	-1.12900	-3.11500
C	0.19000	-2.66600	-3.14900
H	-0.08000	-0.66000	-4.03100
H	1.30800	-0.76800	-2.91400
H	0.11400	-3.07000	-4.16200

C	-2.58400	-1.78300	-0.76800
C	-3.05900	-2.92600	-0.10900
C	-4.16500	-2.83600	0.73700
C	-4.78300	-1.60500	0.90500
H	-2.55300	-3.87500	-0.25400
H	-4.54700	-3.70500	1.26200
H	-5.64900	-1.45400	1.53800
H	5.36900	1.20900	-2.00600
H	1.01500	-3.14600	-2.61600
N	-4.33600	-0.50700	0.27000
C	-3.27200	-0.59000	-0.54800
H	-2.98700	0.33700	-1.03000
B	-5.04100	0.96200	0.54900
F	-4.95400	1.64600	-0.64600
F	-4.27700	1.55900	1.54400
F	-6.32600	0.68400	0.95400

ENERGIES IN HARTREE:

SCF: -1935.051750
SCF + ZPVE: -1934.573857
Delta H: -1934.536869
Delta G: -1934.648120

***p*-M**

Ir	1.08600	-0.16400	0.38300
N	2.46500	0.87800	-0.92700
N	0.16800	1.86200	0.01600
C	2.12000	2.11800	-1.36500
C	0.81700	2.63800	-0.88700
C	2.98500	2.86300	-2.17700
C	4.22300	2.33800	-2.53200
C	4.58100	1.08000	-2.04700
C	3.67900	0.38900	-1.24600
C	0.28100	3.86600	-1.29700
C	-0.92300	4.30700	-0.75400
C	-1.56800	3.51400	0.19400
C	-0.98600	2.29900	0.54500
H	2.70300	3.85300	-2.51600
H	4.90000	2.90900	-3.16000
H	3.91300	-0.57800	-0.81600
H	0.79300	4.47300	-2.03400
H	-1.34700	5.25600	-1.06600
H	-2.50300	3.81900	0.65100
H	-1.44400	1.63800	1.27200

B	2.20600	0.21200	1.99500
O	3.38500	0.96700	1.94100
O	1.94000	-0.19300	3.30000
C	4.01800	0.90700	3.22100
C	2.92100	0.37700	4.16800
H	4.38300	1.90200	3.50200
H	4.87800	0.22600	3.16800
H	2.46000	1.18300	4.75700
H	3.28800	-0.38600	4.86300
B	1.92200	-2.00700	0.47000
O	1.27600	-3.18500	0.04700
O	3.24400	-2.31400	0.84100
C	2.11000	-4.31200	0.33000
C	3.49500	-3.70600	0.63900
H	1.69900	-4.85800	1.18900
H	2.12300	-4.99100	-0.53100
H	3.95500	-4.13300	1.53700
H	4.19800	-3.83200	-0.19700
H	0.02200	-0.80100	1.40800
B	-1.65700	-1.31900	-2.02900
O	-0.36500	-0.94500	-1.74700
O	-1.78800	-1.99800	-3.20800
C	0.48900	-1.57200	-2.73900
C	-0.49000	-2.07000	-3.82500
H	1.20100	-0.83000	-3.10700
H	1.02200	-2.38100	-2.23700
H	-0.49400	-1.43400	-4.71800
C	-2.91100	-0.98500	-1.15100
C	-4.17000	-0.84500	-1.75800
C	-5.27900	-0.52300	-0.98900
H	-4.28500	-0.98500	-2.82800
H	-6.27300	-0.39500	-1.40000
H	5.54500	0.63800	-2.27600
H	-0.29700	-3.10200	-4.12900
C	-2.84500	-0.83000	0.24300
H	-1.90100	-0.94700	0.76800
H	-4.01400	-0.40200	2.03100
C	-3.99800	-0.52200	0.95500
N	-5.18100	-0.35000	0.34000
B	-6.50100	0.18200	1.21000
F	-6.33100	-0.34900	2.46900
F	-6.41000	1.55600	1.18000
F	-7.59200	-0.30800	0.52700

ENERGIES IN HARTREE:

SCF: -1935.040980
SCF + ZPVE: -1934.563546
Delta H: -1934.526166
Delta G: -1934.640547

***o*-N**

B	1.20700	-0.54700	0.01100
O	1.89200	-0.16700	1.13000
O	1.99300	-0.89700	-1.05100
C	3.26100	0.01800	0.73200
C	3.35800	-0.64000	-0.66900
H	3.46900	1.09200	0.69900
H	3.91500	-0.45000	1.47300
H	3.81800	0.01500	-1.41400
C	-0.34500	-0.87300	0.03100
C	-0.81500	-2.18700	0.08800
C	-2.56200	-0.08700	-0.00000
C	-2.18400	-2.44500	0.11700
C	-3.07600	-1.37400	0.07400
H	-0.09900	-3.00300	0.10500
H	-3.18700	0.79500	-0.06800
H	-2.55100	-3.46600	0.16500
H	-4.15000	-1.52600	0.08500
H	3.90000	-1.59300	-0.65400
N	-1.23800	0.14500	-0.01100
B	-0.71600	1.71200	-0.07600
F	-0.70500	2.18200	1.20900
F	0.56100	1.60700	-0.63300
F	-1.61200	2.36000	-0.89400

ENERGIES IN HARTREE:

SCF: -826.280364
SCF + ZPVE: -826.115167
Delta H: -826.101092
Delta G: -826.156632

***m*-N**

B	2.19100	0.02400	-0.00300
O	2.43600	-1.32000	-0.02500
O	3.31700	0.80100	0.02600
C	3.86200	-1.51100	-0.01400
C	4.45800	-0.07700	0.02600
H	4.13000	-2.10700	0.86400

H	4.14900	-2.06500	-0.91300
H	5.04700	0.11200	0.92900
C	0.75400	0.62600	-0.00800
C	0.52500	2.01100	0.01200
C	-0.77900	2.50600	-0.00400
C	-1.83500	1.60400	-0.03600
H	1.37000	2.69300	0.03700
H	-0.98100	3.57200	0.00300
H	-2.87500	1.90500	-0.06200
H	5.07700	0.14900	-0.84800
N	-1.62200	0.27600	-0.04400
C	-0.36900	-0.20500	-0.04000
H	-0.29000	-1.28600	-0.07000
B	-2.92700	-0.77400	0.01300
F	-3.16100	-0.97800	1.35100
F	-2.49000	-1.89900	-0.64900
F	-3.93900	-0.09300	-0.62500

ENERGIES IN HARTREE:

SCF: -826.285574
SCF + ZPVE: -826.119882
Delta H: -826.105654
Delta G: -826.163029

p-N

B	-2.52700	-0.00000	-0.00200
O	-3.26800	-1.14900	0.00700
O	-3.26800	1.14900	0.00700
C	-4.65800	-0.77700	0.02500
C	-4.65800	0.77700	0.02500
H	-5.14700	-1.20100	-0.85800
H	-5.12400	-1.20100	0.91900
H	-5.14700	1.20100	-0.85800
C	-0.96300	-0.00000	-0.02200
C	-0.23400	1.19900	-0.03300
C	1.15400	1.16500	-0.05100
H	-0.74600	2.15600	-0.03300
H	1.77200	2.05400	-0.07300
H	-5.12400	1.20100	0.92000
C	-0.23400	-1.19900	-0.03300
H	-0.74600	-2.15600	-0.03300
H	1.77200	-2.05400	-0.07300
C	1.15400	-1.16500	-0.05100
N	1.82400	0.00000	-0.05000
B	3.49900	0.00000	0.02400

F	3.86900	-1.15800	-0.62300
F	3.86900	1.15800	-0.62300
F	3.79500	-0.00000	1.36400

ENERGIES IN HARTREE:

SCF:	-826.284091
SCF + ZPVE:	-826.118425
Delta H:	-826.104212
Delta G:	-826.161423

O

Ir	0.14500	-0.65700	-0.34300
N	-0.74500	1.32900	-0.20500
N	-2.05000	-1.00100	-0.14800
C	-2.09900	1.40600	-0.10100
C	-2.82500	0.11300	-0.12600
C	-2.74600	2.63800	0.04100
C	-1.99500	3.80900	0.07900
C	-0.60800	3.71800	-0.02100
C	-0.02200	2.46300	-0.15900
C	-4.22200	0.01000	-0.11600
C	-4.81800	-1.24800	-0.11700
C	-4.01000	-2.38400	-0.12900
C	-2.62900	-2.21300	-0.14900
H	-3.82500	2.68600	0.13300
H	-2.48700	4.77100	0.19000
H	1.05100	2.32800	-0.23500
H	-4.84000	0.89900	-0.11400
H	-5.90100	-1.33600	-0.10900
H	-4.43400	-3.38300	-0.12700
H	-1.94500	-3.05300	-0.16400
B	1.19400	-0.48900	1.33900
O	1.04500	0.61000	2.19800
O	2.10100	-1.40600	1.86600
C	2.01600	0.49900	3.23900
C	2.48300	-0.97000	3.17000
H	1.56100	0.76100	4.20200
H	2.83900	1.20000	3.04300
H	1.98500	-1.59400	3.92400
H	3.56600	-1.08100	3.29500
B	2.00200	-0.20200	-1.01900
O	2.67800	-0.92000	-2.00600
O	2.75100	0.94700	-0.67700
C	3.94800	-0.32300	-2.25500
C	3.89600	1.03800	-1.52700

H	4.73800	-0.97300	-1.85600
H	4.10500	-0.22000	-3.33600
H	4.79000	1.23600	-0.92500
H	3.76300	1.87700	-2.22600
H	0.65200	-2.17900	-0.41800
H	0.02000	4.60200	0.01000

ENERGIES IN HARTREE:

SCF: -1108.745666
SCF + ZPVE: -1108.435383
Delta H: -1108.413061
Delta G: -1108.489796

B2eg2 for S2

B	-0.85200	-0.00000	-0.00000
O	-1.60900	0.81100	-0.80900
O	-1.60900	-0.81100	0.80900
C	-2.99900	0.54800	-0.54800
C	-2.99900	-0.54800	0.54800
H	-3.47900	1.47600	-0.21900
H	-3.47800	0.22000	-1.47600
H	-3.47800	-0.22000	1.47600
H	-3.47900	-1.47600	0.21900
B	0.85200	-0.00000	-0.00000
O	1.60900	0.81200	0.80900
O	1.60900	-0.81200	-0.80900
C	2.99900	0.54800	0.54700
C	2.99900	-0.54800	-0.54700
H	3.47900	1.47600	0.21800
H	3.47800	0.22100	1.47600
H	3.47800	-0.22100	-1.47600
H	3.47900	-1.47600	-0.21800

ENERGIES IN HARTREE:

SCF: -507.996734
SCF + ZPVE: -507.855489
Delta H: -507.844910
Delta G: -507.894472

HBeg for S2

B	1.22900	-0.00000	0.00000
O	0.48800	1.14800	-0.00000

O	0.48700	-1.14800	0.00000
C	-0.90200	0.77700	0.00000
C	-0.90300	-0.77600	-0.00000
H	-1.38100	1.20000	0.89000
H	-1.38200	1.20100	-0.88700
H	-1.38300	-1.20000	0.88700
H	-1.38200	-1.19900	-0.89000
H	2.41700	-0.00100	0.00000

ENERGIES IN HARTREE:

SCF:	-254.595910
SCF + ZPVE:	-254.516455
Delta H:	-254.510969
Delta G:	-254.544350